Bio(molecular) control of selective ion transport, gas separation and catalytic enzyme-based reactions using functionalized membranes

Mohamed Yahia Marei Abdelrahim

THESIS
To obtain the grade of Doctor

Issued by:

University of Montpellier (France)
University Nova de Lisboa (Portugal)
University of Calabria (Italy)

Prepared in the graduate school
Science Chimiques Balard (ED 459)
and research unit (UMR 5635)
Institut Européen des Membranes (IEM)

Specialty:

Chemistry and Physico-Chemistry of Materials

Presented by:

Mohamed YAHIA MAREI ABDELRAHIM

(Bio)Molecular control of selective ion transport, gas separation and catalytic enzyme-based reactions using functionalized membranes

Defended on 21th December 2015 in front of the esteemed jury comprising

Mr. Mihai BARBOIU	Dr, Université de Montpellier, Montpellier, France.	Thesis director
Mr. Antony SZYMCZYK	Prof, Institut des Sciences Chimiques Rennes, France.	Reviewer
Mrs. Cristiana BOI	Dr, Università di Bologna, Bologna, Italy.	Reviewer
Mr. Andre AYRAL	Prof, Université de Montpellier, Montpellier, France.	Examiner
Mr. Joao CRESPO	Prof, Universidade Nova de Lisboa Lisbon, Portugal.	Examiner
Mr. Thomas SCHAFER	Prof, POLYMAT, Basque Research Center, San Sebastián, Spain.	Examiner
Mrs. Lidietta GIORNO	Dr, Institute on Membrane Technology, Calabria, Italy.	Examiner

Erasmus Mundus Doctorate in Membrane Engineering–EUDIME

Doctorate in Chemical Sciences, University of Montpellier (France)

Erasmus Mundus Doctorate in Membrane Engineering, University Nova de Lisboa (Portugal)

Erasmus Mundus Doctorate in Membrane Engineering, University of Calabria (Italy)

[(Bio)Molecular control of selective ion transport, gas separation and catalytic enzyme-based reactions using functionalized membranes]

[Thesis defense on Monday 21th December 2015]

Supervisor

Dr. Mihai BARBOIU

Doctoral candidate

Mohamed YAHIA MAREI ABDELRAHIM

Co-supervsiors

Prof. Joao CRESPO

Dr. Lidietta GIORNO

ACADEMIC YEAR 2014-2015

This thesis is dedicated to

My family

My father, who taught me that the best kind of knowledge to have is that which is learned for its own sake. My mother, who taught me that even the largest task can be accomplished if it is done one step at a time, also supports me by encouragement and happiness usually and prays to God (Allah) to help and guide me to the right way. My wife, brothers, and sister, who usually give me the guides, supporting and advices when I need it.

ACKNOWLEDGEMENTS

Words are often too less to reveal one's deep regards. An understanding of the work like this is never the outcome of the efforts of a single person. I take this opportunity to express my profound sense of gratitude and respect to all those who helped me through the duration of this doctoral thesis.

EUDIME: Erasmus Mundus Doctoral in Membrane Engineering is not a doctoral degree of any kind. It is a special doctoral that makes the students special too. EUDIME program gave me the chance to study my doctoral at three different research institutions (Institute Europeen des membranes, University of Montpellier (IEM-UM) France, (Faculty of science and technology, University Nova de Lisboa (FCT-UNL) Portugal, and (Institute on Membrane Technology, University of Calabria (ITM-CNR, UNICAL) Italy. On one end as this PhD was more challenging than a normal PhD and had faced a lot of problems and difficulties but on the other end I got the pleasure of working with so many amazing people and I can't write enough to thank them for all the support, encouragement, and motivation that they gave to me.

Before I start to present my thesis, I would like to give special thanks to all the people who in one way or another have helped me get to this final stage of the master.

I would like to express my sincere gratitude to the thesis supervisors **Prof. Mihai Barboiu** (IEM, France), **Prof. Joao Crespo** (FCT-UNL, Portugal), and **Prof. Lidietta Giorno** (ITM-CNR, Italy) for their continuous support, motivation and outstanding scientific guidance and patience throughout this research work, beside supporting me in the research work and giving me their opinion and directives every time I needed such. Moreover, I have learnt from the best experts researchers in the field of membranes during PhD studies. In additional too, I would like to thanks the European Union and EUDIME consortium for selecting me to be a part of this challenging and amazing PhD adventure. Special and worthy thanks for **Prof. Enrico Diroli, Prof. Efrem Curcio, Prof. Isabel Coelhoso, Prof. Andre Ayral, and Dr. Maria-Elena Vallejo** for all the support, encouragement, and motivation that they gave to me during the EUDIME doctoral studies at the three research institutions.

Moreover, I would like to express the gratitude to my colleagues (Dr. Yves-marie Legrand, Dr. Sophie Cerneaux, Dr. Arnaud Gilles, Dr. Florina Dumitru, Arie Van Der Lee, Nathalie Masquelez, Eddy Petit, Dan Dumitrescu, Alina Cristian, Romina Catana, Yan Zhang, Weixu Feng, Istvan Kocsis, Maria Pascanu, Zhanhu Sun, Erol Licsandru , Sana Gassara, Mikhael Bechelany, Christelle Floutier, Abdeslam El-Mansouri, Fabienne Biondi, Dominique Diamante, Florence Leroy, Didier Cot, Christophe Charmette, Abderrahmane Mouhtarim, Gamal Elghazaly, Mohamed Boushaki, and Others) at (IEM, UMII University,

France) for their kind assistance, great interest and help for me since the moment I arrived to Montpellier, France.

In additional too, I would like to express the gratitude to my colleagues (Dr. Luisa Neves, Dr. Carla Portugal, Carla Daniel, Carla Martins, Rita Ferreira, and others) at (FCT-UNL, Portugal) for their kind assistance and a great interest and help for me since the moment I arrived to Lisbon.

Furthermore, great thanks for my colleagues (Prof. Giuseppe Barbieri, Dr. Alessandra Criscuoli, Dr. Alberto Figoli, Dr. Rosalinda Mazzei, Dr. Emma Piacentini, Leo D'Agostino, Giuseppe Vitola, Giuseppe Ranieri, Fabio Bazzarelli, Francesca Militano, Paolo Miraglia, Valentina Tortelli, Ahmed Elbadri, Arsanios Ayoub, and other) at (ITM-CNR, UNICAL University, Italy) for their kind assistance and a great interest and help for me since the moment I arrived to Calabria, Italy.

Worthy thanks all EUDIME colleagues, especially (Abaynesh Yihdego, Ramto Ashu, Usman Sayed, Nayan Nayak, Veysi Altun, Mariella Bau Polino, Airama Albs, Sergio Santoro, Sushumna Shukla, Lakshmeesha Upadhyaya, Shazia Ilyas, Aamir Ali, Alessio Fuoco, Salman Shahid, Ming Zhou, Parashuram Kallem, Jenny Evtimova, and others) for those enjoyable moments and for being such good friends during EUDIME doctoral studies.

Also, great thanks to all the staff, professors, and friends at the Department of Chemistry, Faculty of Science, Helwan University, Cairo, Egypt, for their helping and supporting me since I have started to put my feet at the road of scientific research by working as a research and teacher assistant at the Department of Chemistry, Faculty of Science, Helwan University.

Worthy thanks to my wonderful parents, my father **(Mr. Yahia Marei)** and my mother **(Mrs. A. Selim)** for giving my education and being behind me all this time. I know it is too hard to be far from both of you, but I know you are usually beside me giving support and help. I will never forget your praying to Allah (God) asking him usually to save, help and support me during my life and studies. Great thanks for my great brothers **(Kahled, Mahmoud, Ahmed)** and my sister **(Mrs. S. Yahia)** and her husband **(Mr. Abdo Mohamed)** for being beside me giving me encouragement, Advices and helping during all my life.

The life in Europe would never been so enjoyable without my wife (**Dalia Refaat**). Her tolerance of my occasional mood shifts during writing this dissertation is a testament in itself of her unyielding devotion and love. **Dalia (داليا)**, your help and support has been instrumental during my doctoral studies and you support and encouragement was in the end what made this dissertation possible. From writing scientific articles to doctoral thesis and preparing and delivering presentations, you have always been there to motivate and support me. Thanks you for your love, support, patience and prayers.

Finally, I would like also to thank the secret soldier my great country **(Egypt)** for supporting, encouraging and helping me to be at this level of Education. I will never forget the best moments that I have spent at its streets and cities with my friends, also the best places at it such as (Pyramids, Cairo tower, Alexandria, Hurghada, Luxor, and Aswan). I wish that God support and help it for much progress and democracy at the future. The studying at European countries gave me the chance to see what they always hear about the culture, civilization, and hospitality of Egypt. By studying abroad I can get a better understanding of the other's culture as well as giving a good example of our culture. I hope that all my Professors and friends from outside Egypt can visit it at the future to enjoy their time there.

Résumé de la Thèse

Différents travaux de recherche ont été décrits dans cette thèse. Les travaux de recherche peuvent être résumés comme suit. Le premier chapitre a porté sur l'identification d'inhibiteurs puissants efficaces vis-à-vis de de l'isoenzyme anhydrase carbonique humaine I (hCAI). Considérant l'importance pharmacologique de trouver des inhibiteurs (CAIs) et des activateurs (AACs) sélectifs aux isoformes de l'anhydrase carbonique), l'anhydrase carbonique humaine I (hCAI) a été confrontée en parallèle à diverses bibliothèques dynamiques constitutionnelles (CDL). Dans le deuxième chapitre, des réseaux constitutionnels dynamiques ont été préparés sous forme de systèmes membranaires liquides et solides agissant comme un réseau pour le transport spécifique des ions lanthanides. Le transport est basé sur la capacité de complexation des lanthanides (La^{+3}, Lu^{+3}, Eu^{+3}) avec les groupes polyéther fonctionnels situés dans les matériaux membranaires. Dans le troisième chapitre, l'approche proposée consiste en l'utilisation de membranes liquides ioniques supportées (SILMs) comprenant deux enzymes différentes de l'anhydrase carbonique, l'enzyme thermo-résistante SspCA et l'enzyme bovine-CA, qui catalysent la réaction de conversion réversible du CO_2 en bicarbonate en favorisantla force motrice vers le transport de CO_2. La stabilité des membrane, leur perméabilité vis-à-vis de CO_2 et de N_2 ainsi que la selectivité idéale (CO_2/N_2) ont été déterminées pour les membranes développées. Le quatrième chapitre porte sur la synthèse et la caractérisation de membranes polymères denses pour une application en séparation de gaz. Les mesures de perméabilité aux gaz des membranes polymères synthétisées ont montré que la perméabilité de CO_2 est supérieure à celle des autres gaz testés (CH_4 et N_2). Dans le dernier chapitre, des membranes de PVDF ont été fonctionnalisées avec une enzyme, la phosphotriestérase (PTE), selon deux méthodes différentes pour construire un réacteur à membrane biocatalytique (BMR) avec pour finalité la bioconversion et la séparation sélective du substrat paraoxon. La première méthode met en œuvre une dispersion réversible de nanoparticules magnétiques de PTE qui estimmobilisée à la surface de la membrane de PVDF sous l'effet d'un champ magnétique externe . A l'inverse, la seconde méthode porte sur le greffage chimique de l'enzyme PTE, après modification de la surface de la membrane de PVDF native (DAMP-GA-enzymatique). Les deux techniques d'immobilisation d'enzymes ont montré une bonne efficacité et une sensibilité à l'égard de la bioconversion du paraoxon dans les différentes conditions appliquées dans un réacteur à membrane biocatalytique (BMR).

De façon globale, les concepts développés dans ce travail de thèse permettront d'ouvrir de nouvelles pistes de recherche allant vers le développement d'une membrane polymère sélective au transport d'ions, de gaz mais aussi active dans les réactions catalytiques enzymatiques grâce à un contrôle bio-moléculaire au niveau des matériaux membranaires.

Mots clés:

Membrane polymère; Fonctionnalisées; Séparation de gaz; Contrôle bio-moléculaire; Réactions catalytiques enzymatiques ; Transport sélectif d'ions ; Bioconversion du paraoxon ; Membranes liquides ioniques supportées (SILMs) ; L'anhydrase carbonique (CA) enzyme ; Phosphotriestérase (PTE) enzyme ; Un réacteur à membrane biocatalytique (BMR).

Abstract

Different research works have been described in this thesis. The research works can be summarized as the following. The first chapter deals with the identification of effective potent inhibitors for the human carbonic anhydrase I (hCAI) isozyme. Considering the pharmacological importance to find selective CA inhibitors (CAIs) and CA activators (CAAs), human carbonic anhydrase I (hCAI) has been subjected to a parallel screening of various constitutional dynamic libraries (CDL). In the second chapter, constitutional dynamic networks have been used in liquid and solid membrane systems as a carrier network for transporting lanthanides. The transport is based on the complexing ability of lanthanides metals (La^{+3}, Lu^{+3}, Eu^{+3}) with the functional polyether groups in the membrane materials. In the third chapter, the proposed approach consists in using supported ionic liquid membranes (SILMs) comprising two different carbonic anhydrase enzymes, the thermo-resistant SspCA enzyme and the Bovine-CA enzyme, which catalyze the reaction of reversible conversion of CO_2 to bicarbonate, enhancing the driving force for CO_2 transport. Membrane stability, CO_2 and N_2 permeability and (CO_2/N_2) ideal selectivity were determined for the membranes developed. In the fourth chapter, the research work consists in the synthesis and characterization of dense polymeric membranes for gas separation application. The gas permeability measurements for the synthesized polymeric membranes showed that the permeability of CO_2 is higher than other used gases (N_2 and CH_4). In the last chapter, two different methods of PVDF membrane functionalization with a phosphotriesterase (PTE) enzyme have been developed to construct biocatalytic membrane reactor (BMR) for bioconversion and selective separation of paraoxon substrate. The first method employs reversible dispersion of magnetic nanoparticle immobilized with PTE using an external magnetic field on the surface of native PVDF membrane. On the contrary, the second method comprises chemical grafting of the PTE enzyme after surface modification of the native PVDF membrane (DAMP-GA-Enzyme). Both methods of enzyme immobilization showed good efficiency and sensitivity towards the bioconversion of paraoxon substrate at different conditions applied in a biocatalytic membrane reactor (BMR).

In general, the concepts developed in this thesis research work will help bring new tracks on the way to the development of a polymeric membrane for selective ion and gas separation but also for selective catalytic reaction under bio(molecular) control.

Keywords:

Polymeric membrane; Functionalized; Gas separation; Bio-molecular control; Enzymatic catalytic reactions; Selective ion transport; Bioconversion of paraoxon; Supported ionic liquid membranes (SILMs); Carbonic anhydrase (CA) enzyme; Phosphotriesterase (PTE) enzyme; Biocatalytic membrane reactor (BMR).

Table of contents

General Introduction

Different research works have been described in this research thesis, the general introduction of the research thesis can be summarized as the following:

Constitutional Dynamic Chemistry (CDC) and its application Dynamic Combinatorial Chemistry (DCC) are new evolutional approaches to obtain chemical diversity. By virtue of the reversible interchanges, a Dynamic Combinatorial Library (DCL), virtually forming all possible combinations of building components, can adapt to a biotarget that can be used to select an active ligand. Carbonic Anhydrases (CAs) are one of the early addressed biotargets for DCC. The pioneering work of Lehn et al. demonstrated that a known inhibitor of the bovine CA (bCA II, EC4.2.1.1) was amplified from a DCL and the feasibility has been further proven by other groups. Various DCLs generated under thermodynamic control have been evaluated by our groups for their relative inhibition toward the physiologically relevant human CAs, hCA I and hCA II, the most active isoforms and studied as drug targets. They are able to differentiate amplified binders, under the specific binding effect of the two isozymes. The literature survey allows the following conclusions to be made: (a) important progress has been achieved in the past two decades for identifying CAIs by using DCLs; (b) no DCL studies were dedicated to the chemistry of CAAs so far; (c) the use of DCC for the discovery of CAIs/CAAs might provide insights into the discovery of efficient classes of active compounds, against 16 CA isoforms known nowadays in humans. In the first part of this manuscript, we report DCLs of components susceptible to selective binding to the hCA I, both as inhibitors or as activators, subjected to a parallel screening by using aminocarbonyl–imine reversible chemistry. We investigate whether the competitive generation of potent CAIs and CAAs could be selectively expressed as an independent (linear), an interfering (crossover) or a dominant behaviour of the above-mentioned events.

On the other hand, supramolecular chemistry is by nature a dynamic chemistry in view of the reversibility of the non-covalent interactions connecting the molecular components of a supramolecular system. The dynamic self-assembly of the components may allow the flow of structural information from the molecular level toward nanoscale dimensions.

Understanding and controlling such upscale propagation of structural information might offer the possibility of imposing a further precise order at the mesoscale and new routes to obtain highly ordered ultradense arrays over macroscopic distances. DYNAMERS (dynamic polymers) are polymeric materials exhibiting reversible formation and component exchange. They comprise both the supramolecular polymers that are dynamic by nature and molecular polymers that are dynamic by intent, due either to the presence of a non-covalent or to the introduction of a covalent reversibility cassette. Their formation and dynamic character result either from recognition-directed reversible poly-association of components through complementary interactional groups (supramolecular, non-covalent, physical, interactional recognition) or from reversible polycondensation of components through complementary functional groups (molecular, covalent, chemical, functional recognition), respectively. In view of the ability of dynamers to build up by self-assembly and to select in principle their components in response to external stimuli or to environmental factors, they behave as adaptive materials.

Membrane-mediated separations are an attractive alternative to other chemical methods for purification, recovery (i.e., ion exchange, extraction, or chromatographic processes), etc. Numerous artificial membrane systems using molecular components have been developed in the past decades. The supramolecular design and application of receptors for recognition of cations, anions, or molecular species have attracted a great deal of interest as these systems have many potential functions such as solubilization, extraction, and membrane transport. For all these reasons, functional dynamic polymers “dynamers” may be used to conceive novel membrane materials. Our efforts in the second part of the manuscript, involve the synthesis and the fabrication of novel “dynameric” membranes designed to transport ionic salts of lanthanides metal ions (La^{3+}, Lu^{3+}, Eu^{3+}) based on encoded molecular features of the monomeric subcomponents. Their transport performances (permeability and selectivity) are evaluated by using the solution-diffusion model. The membrane performances are exploited *via* dynamic reversible covalent exchange processes of variable composition of subcomponents in solution during the membrane synthesis. The resulting polymeric membranes are stable and are conserved during and after the membrane transport experiments.

Membrane is a semi-permeable active or passive barrier which, under a certain driving force, permits preferential passage of one or more selected species or mixtures of components (molecules, particles or polymers) in a gaseous phase and /or liquid solution. Membranes have been investigated for over 150 years, and since 1980 gas separation membranes have been used commercially. Gas separation membranes are used in a number of industrial processes; such as the production of oxygen enriched air, separation of CO_2 and H_2O from natural gas or of CO_2 from N_2 in flue gas streams, purification of H_2, and recovery of vapors from vent gases. Different strategies towards the construction of more efficient membranes have suggested. Polymeric membranes perform their process by different mechanisms which are based upon the properties of membrane means physical and chemical structure, also interaction between membrane, components and nature of gas.

In spite of the large number of different membrane materials and operating conditions described for the separation of CO_2 from flue gas and natural gas, the performance of existing processes to effectively separate CO_2 are not yet satisfactory. The applications developed so far have been compromised mainly by the CO_2 permeability and membrane selectivity. For this specific application, it is therefore mandatory to develop membranes with a high CO_2 permeability, a high (CO_2/N_2) selectivity, thermally and chemically resistant to be used at high temperatures. They should also be resistant to plasticization effects which normally occur due to absorption of CO_2 and may have negative implications on process selectivity.

One possible approach for enhancing the flux is the use of liquid membranes, due to the high diffusivity of gases when compared with solid membranes, which will lead to higher permeability values. In particular, supported liquid membranes (SLM) in which a solvent is immobilized inside the porous structure of the supporting membrane by capillary forces, have been considered one of the most attractive membrane configurations to be used in gas separation applications. However, operating conditions such as high temperature and moderate pressure, as well as lack of differentiated selectivity towards specific gases is still limiting its application. High temperatures may lead to the

evaporation of the solvent contained within the membrane pores and moderate pressures may lead to the displacement of the liquid from the membrane pores. The properties of ionic liquids such as viscosity and non-volatility can stop the membrane solvent flowing out from porous membrane, which prolongs the life of the SILM greatly without diminishing the ability and selectivity of separation. The high-thermal stability and non-flammation of IL is suitable for capturing CO_2 from the flue-gases at high temperature, and SILM can enhance the contact area between gas and ionic liquids. There are several works available in the literature where supported ionic liquid membranes (SILMs) were studied for potential applications in gas separations. The pure gas permeability of N_2, CH_4 and CO_2 and the corresponding ideal selectivities through a porous hydrophilic polyethersulfone support with different immobilized RTILs showed that the permeabilities/selectivities of SILMs were competitive or even superior to other membrane materials. The facilitated transport of CO_2 and SO_2 through SILMs showed that SILMs can be very selective to CO_2 and SO_2.

An important potential avenue for improvement in CO_2 capture is based on biologically assisted membrane systems, with the use of a Carbonic anhydrase enzyme. This enzyme catalyzes the reversible reaction of carbon dioxide with water to produce bicarbonate. The first proposed for this approach, where the carbon dioxide presents in the flue gas stream contacts with carbonic anhydrase aqueous solution and produces bicarbonate. The bicarbonate diffuses across the liquid membrane and it is converted back to carbon dioxide upon desorption in the presence of vacuum or a sweep gas in the permeate side. The main problem with this technology is water management, since water evaporates even at relatively low temperatures. Therefore, in order to prevent liquid loss, the feed and sweep gases have to be humidified. Although enzymes in ionic liquids (ILs) have presented enhanced activity, stability, and selectivity, the practical obstacle of using ILs is that many enzymes do not dissolve readily in most ILs, which has ruled out many potential biotechnological applications. In fact, enzymes that show catalytic activities in ILs normally do not dissolve in ILs. When enzymes become active in ILs, they remain suspended as a powder. Although some ILs can dissolve enzymes through the weak hydrogen bonding interactions, they often induce enzyme conformational changes

resulting in deactivation of enzyme. To improve the enzyme solubility as well as activity in ILs various attempts have been made by modifying the form of enzymes in which it is used, including immobilized enzymes, the use of microemulsions, and the use of whole cells. According to that many research groups have modified the enzymes through the immobilization to improve the enzyme solubility as well as activity in ILs. All these strategies provide more robust, more efficient, and more enantioselective biocatalyst suitable for biotransformation with ionic liquids. Luisa Neves et al. 2012 provided an innovative concept for the removal of CO_2 from flue gas streams using supported liquid membranes with non-volatile ionic liquids (or solvents), comprising an enzyme that enhances the selective transport of CO_2.

The approach proposed in this research work consists on using supported ionic liquid membranes (SILMs) comprising two different carbonic anhydrase enzymes, the thermo resistant SspCA enzyme and the Bovine-CA enzyme, which catalyze the reaction of reversible conversion of CO_2 to bicarbonate, enhancing the driving force for CO_2 transport. Membrane stability, CO_2 and N_2 permeability and CO_2/N_2 ideal selectivity were determined for the membranes developed. To validate this hypothesis, the present work proposes to investigate the following aspects: 1- Design of supported liquid membranes by immobilization of an ionic liquid in a polymeric hydrophobic support; 2- Evaluation of the stability of the SLMs at high temperatures; 3- Determination of CO_2 and N_2 pure gas permeabilities and assessment of the potential of the membranes for the CO_2/N_2 separation; 4- Determination of the effect of water activity present in the selected solvent on the improvement of CO_2 transport and selectivity. To validate this hypothesis, the present work proposes to investigate the following aspects: 1- Design of supported liquid membranes by immobilization of an ionic liquid in a polymeric hydrophobic support; 2- Evaluation of the stability of the SLMs at high temperatures; 3- Determination of CO_2 and N_2 pure gas permeabilities and assessment of the potential of the membranes for the CO_2/N_2 separation; 4- Determination of the effect of water activity present in the selected solvent on the improvement of CO_2 transport and selectivity.

Numerous polymeric membranes that have excellent physical and chemical bulk properties do not possess the appropriate surface properties required for particular applications. For this reason, surface modification of polymeric membranes has been of prime importance in various applications from the advent of membrane-involving industries. Incorporation of novel functionalities is a versatile means for surface modification of polymeric membranes. Functionalized membranes are used for immobilization of enzymes, for improvement of biocompatibility, preparation of biosensors and application in membrane bioreactors due to their interesting properties of high specific surface area and the possibility to combine separation with chemical reaction. For example, biocatalytic membrane reactors (BMR) combine selective mass transport with chemical reactions. The selective removal of products from the reaction site increases the conversion of product-inhibited or thermodynamically unfavourable reactions. Membrane reactors using biological catalysts can be used in production, processing and treatment operations.

The recent trend towards environmentally friendly technologies makes these membrane reactors particularly attractive because they do not require additives, are able to function at moderate temperature and pressure, and reduce the formation of by-products. The catalytic action of enzymes is extremely efficient and selective compared with chemical catalysts; Enzymes demonstrate higher reaction rates, milder reaction conditions and greater stereo specificity. Their potential applications have lead to a series of developments in several technology sectors: (1) the induction of microorganisms to produce specific enzymes; (2) the development of techniques to purify enzymes; (3) the development of bioengineering techniques for enzyme immobilization; and (4) the design of efficient productive processes. In this research work, two different kind of modified membranes with a phosphotriesterase (PTE) enzyme have been developed for bioconversion of paraoxon substrate to P-nitro phenol as a product. One of these membranes was modified with MNPs-Enzyme, while the other one was modified with DAMP-GA-Enzyme. Both of these two membranes showed good efficiency and sensitivity towards the bioconversion of paraoxon substrate to p-nitrophenol product at different conditions applied to the biocatalytic membrane reactor (BMR).

There are various parameters that had significant effect on the efficiency and performance of the developed polymeric membranes with immobilized PTE enzyme. There parameters are the loaded amount of Enzyme, paraoxon concentration, pressure applied to BMR reactor, and the residence time between the paraoxon substrate and enzyme.

In general, the concepts developed in this research thesis will help bring new tracks on the way to the development of polymeric membrane with bio(molecular) materials to create membrane materials for different application (Ion selective membranes, gas separation, and biological applications). Indeed, it is quite possible to translate these principles to other traditional membrane systems to improve their properties and make them more efficient and selective towards membrane industrial applications.

Chapter (1)

Carbonic anhydrase towards Dynamic Combinatorial Libraries (DCLs).

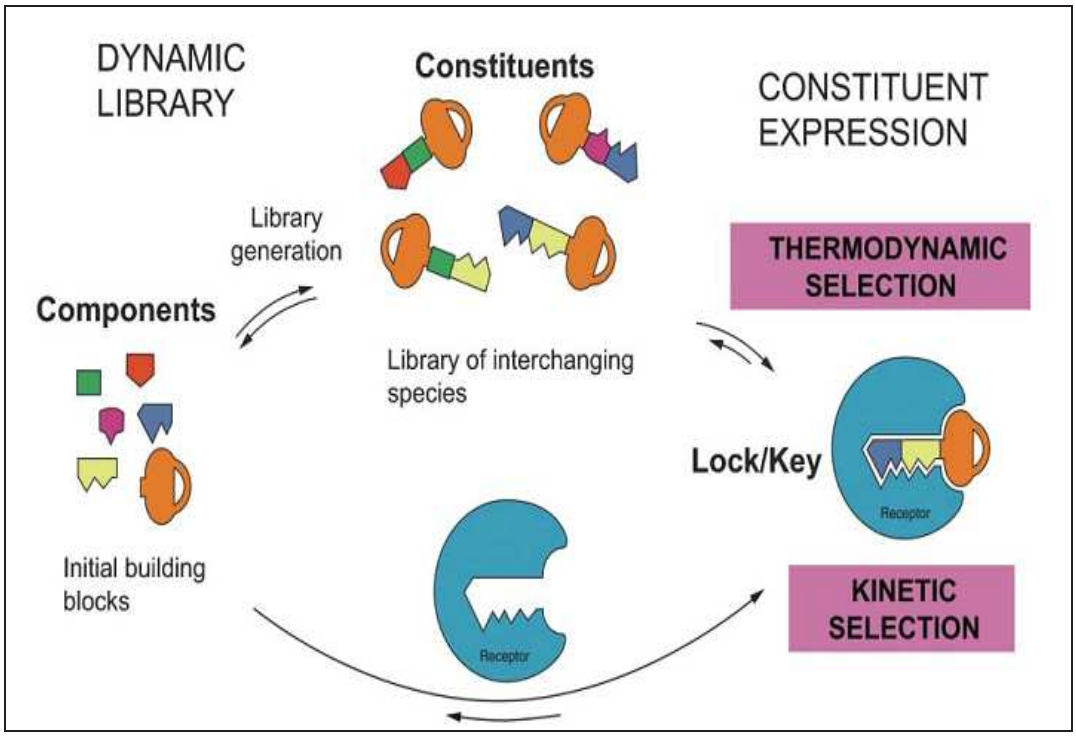

Abstract

Here we describe the screening via Dynamic Deconvolution of constitutional dynamic libraries (DCLs) of inhibitors (CAIs) and activators (CAAs) of human carbonic anhydrase I (hCAI) isozyme. The inhibitory effects dominate over the activating ones, while the CAAs may be identified in the absence of CAIs. Our findings show that the DCL-Carbonic Anhydrase story may hold novel surprises, relevant to the general drug design research, especially with enzyme families like CAs with a multitude of members. The present study revealed a new paradigm: if compounds of agonistic inhibitor and activator activities are formed, the Dynamic Deconvolution may lead to the discovery of the inhibitory set of components expressed at the expense of the activator ones. This sheds light on the dominant mechanistic inhibition behaviours. Moreover the simplicity of the Dynamic Deconvolution strategy and of its analysis can easily lead to valuable simple mechanistic insights into inhibitory–activatory relative synergistic affinities toward the hCAs. This contribution adds several new behaviours to the systematic rationalization and prediction of novel CA active compounds.

Keywords:

Constitutional dynamic libraries (DCLs); Inhibitors; Activators; Dynamic Deconvolution; Synergistic affinities; Human carbonic anhydrase I (hCAI).

The Aim of the research work

The goal of the work described in this chapter is the identification of effective potent inhibitors for the human carbonic anhydrase I (hCAI) isozyme. Considering the pharmacological importance to find isoform-selective CA inhibitors (CAIs), human carbonic anhydrase I (hCAI) has been subjected to a parallel screening of various constitutional dynamic libraries (CDL). The use of parallel constitutional screening of CDL chemistry for the discovery of enzyme inhibitors is straightforward and it might provide initial insights toward the generation of efficient classes of selective and high affinity inhibitors. The originality of this work depend on using human isozymes than the studies described in Dynamic Combinatorial Libraries-DCL for bovine isozyme, as human isozyme may have better specificity with respect to certain inhibitors.

The introductory bibliographic part is divided into two parts: The first part provides an introduction to Supramolecular and Dynamic combinatorial chemistries and their various aspects and the methods used for the identification of the active components of biological interest. We define subsequently the role of Carbonic Anhydrase as a target potential for inhibitors such sulfonamides. The last part focuses on the synthesis and the screening of four DCLs to assess their inhibitions properties with human isozymes CAI by spectrophotometric studies using UV-Vis Spectrophotometer to identify the best inhibitors of each library.

1. Introduction

1.1. Supramolecular Chemistry toward Constitutional Dynamic Chemistry

Supramolecular chemistry has developed over the last forty years as “chemistry beyond the molecule”. Starting with the investigation of the basis of molecular recognition, it has explored the implementation of molecular information in the programming of chemical systems towards self-organization processes that may occur either on the basis of design or with selection of their components. Supramolecular chemistry deals with the complex entities formed by the association of two or more chemical species held together by non-covalent intermolecular forces, whereas molecular chemistry concerns the entities constructed from atoms linked by covalent bonds. Subsequently, the area developed into the chemistry of "self-organization" processes and more recently into "constitutional dynamic chemistry" as represented in

Fig.1. Molecular chemistry has, over about two centuries, developed a wide range of very powerful procedures for creating ever more sophisticated molecules and materials from atoms linked by covalent bonds. Beyond molecular chemistry, supramolecular chemistry aims at constructing highly complex, functional chemical systems from components held together by intermolecular forces [1].

Supramolecular entities are by nature constitutionally dynamic by virtue of the liability of non-covalent interactions. Importing such features into molecular chemistry, through the introduction of reversible bonds into molecules, leads to the emergence of a Constitutional dynamic chemistry, covering both the molecular and supramolecular levels. It considers chemical objects and systems capable of responding to external solicitations by modification of their constitution through component exchange or reorganization. It thus opens the way towards an adaptive and evolutive chemistry, a further step towards the chemistry of complex matter [1].

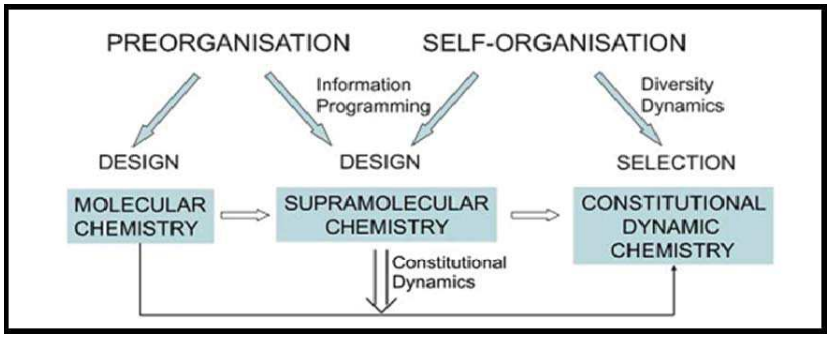

Fig.1: From molecular, to Supramolecular and to Constitutional Dynamic Chemistry under Preorganisation and Self-organisation by design and with selection [1].

Supramolecular chemistry has thus progressed over the years along three overlapping phases. The first is that of molecular recognition and its corollaries, supramolecular reactivity, catalysis, and transport; it relies on design and preorganization and implements information storage and processing. The second concerns self-assembly and self-organization, i.e., self-processes in general; it relies on design and implements programming and programmed systems, which involve messages in molecules controlling the generation of specific entities in complex mixtures. The third concerns constitutional dynamics of both molecular and supramolecular entities, defining constitutional dynamic chemistry as a unifying concept; it allows for adaptation and evolution; it relies on self-organization with selection in addition to design, and implements chemical diversity and' informed dynamics [2]. However, most biological phenomena do not involve formation or destruction of covalent bonds Biological structures are usually made from simple molecular aggregates that are associated with weak non - covalent interactions. These interactions are responsible for most processes in living systems, recognition antibody / antigen, ion transport across cell membranes, Recognition RNA / DNA, etc...). Located at the interface of chemistry, physics and biology, chemistry supramolecular can be defined as "chemistry beyond the molecule" in based on poly - organized molecular entities with a level of complexity growing. It results from the combination of several molecular species maintained together by non-covalent interactions and intermolecular forces [3].

Inspired by biological models and controlling non- interactions covalent artificial supramolecular systems highly structured and functionalized have been developed and used in the field of biology and medicine. Nature teaches us that the "molecular recognition" is a step important of all biological process: it is the property of a molecule to recognize and restrain or hold a substrate, by structural complementarily. Paul Ehrlich (Nobel Medicine in 1908) introduced the concept of studying receptor affinity between dyes according to body tissues and the immune response between antigens and antibodies. Then the concept of selectivity was stated by Emil Fischer [4] through the image "Lock and key ", that represented in (Fig. 2). Selectivity involves geometric and functional complementarity wherein based on molecular recognition. The selective binding also requires interaction between partners in coordination made by Alfred Warner (Nobel Prize 1913). Fixation, recognition and coordination are the basis of chemistry supramolecular [3].

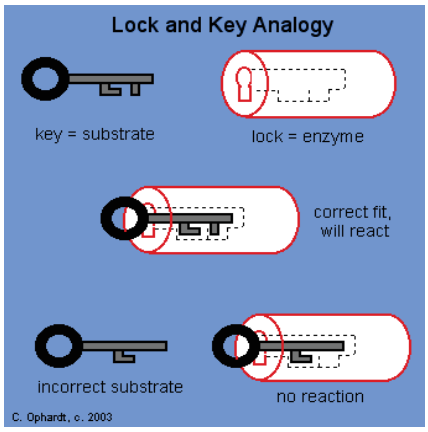

Fig.2: Concept of complementarity schematically represented by Image (key and lock) [3].

Molecular recognition involves the energy and information in molecular fixing a substrate with a receptor. The molecular information is incorporated in the architecture of a receptor and its functional groups that will interact selectively with a substrate that will read the information by structural complementarity. The molecular receptors are organic structures or metal-organic compounds (e.g. protein zinc: the carbonic anhydrase), by which the intermolecular interactions occur with the binding site of the substrate. Binding sites involve various interactions (hydrogen bonding, ion dipole, dipole-dipole, ionic Van der Waals, etc.). Recognition may be coupled with other chemical processes such as oxidation / reduction, and protonation/deprotonation [3].

The substrate is adapted to be set by a receptor through a coupling site for potential recognition it is necessary that the two species are functionally and compatible. This leads to the principle of double complementarity covers the energy and geometrical properties always represented by the concept “lock and key”. Another important idea is to consider the supramolecular syntheses are appeal to non-covalent associations which means that the construction of entities supramolecular itself, based on the creation and destruction of non-links covalent. These routes programmed and incorporated into the "design" of molecular components may also be subject to change and adapt in relation with their relative, so as to obtain the properties and effects entities environment remarkable. However they can also be stabilized by fixing and / or immobilization with cross functional groups present in the supramolecular architectures, this is carried out by conventional chemical means (crystallization, polymerization, absorption, and precipitation) while introducing the concept of supramolecular material. The concentration and fixing of supramolecular nanoscale systems can be the development of a new material organized from the microscopic level to macroscopic objects.

1.2. Dynamic combinatorial libraries (DCLs) concepts

1.2.1. Aspects of Dynamic Combinatorial Chemistry (DCC)

Combinatorial chemistry has been extensively used in drug-discovery processes as a powerful tool to explore functional compounds, individually synthesized in parallel through high-throughput methods [5]. Dynamic combinatorial chemistry (DCC) is a new paradigm in drug discovery, that gives access to rapid ligand identification based on simultaneous implementation of reversible molecular assembly and supramolecular recognition processes [6-9]. The DCC screening is based on a shift of chemical equilibrium in mixtures of reversibly connected components driven by a biomolecular target, resulting in the preferred amplification of one or a few components. DCC has been used in a variety of biomolecular systems, non-exhaustively including lectins [10,11] , acetylcholine-esterase [12], neuramidase [13], galactosyltransferase [14], glycosidase [15], DNA [16], etc.

The lines of the search for bioactive substances, including molecules with properties targeted for a specific therapeutic application, are based on the synthesis series of individual molecules to test their potential activities with given biological target [17]. The aim to obtain quick and efficient molecules with useful properties, combinatorial chemistry has been initiated [18-23]. During the past 20 years, several publications and reviews have appeared demonstrating the success of this multidisciplinary field. Currently, pharmaceutical companies are certainly interested in this powerful and efficient tool to find molecules with a biological activity. The combinatorial approach is characterized by two main steps: the synthesis of library and identification of the active component by screening [24].

1.2.2. The synthesis of combinatorial libraries

The basic idea of combinatorial chemistry is to carry out reactions with several starting reagents or with small libraries, or with mixtures (high Library > 10000 components). Thus, all possible combinations are formed each step, generating a library with a wide variety of components from a limited number of starting reagents. The number of components increases so exponentially with the number of initial reagents and steps put in. The synthesis combinatorial synthesis also called high-capacity (high –throughput synthesis), has stimulated the development of powerful new tools, including heterogeneous synthesis solid support [25]. It boasts of new synthetic methods such as “divided couple and recombine” (split method) [26], (Fig. 3).

Isolation and purification of products, and thereby generate libraries with statistical distribution. Synthesis of defined mixtures requires procedures that deliver a large number of structurally defined compounds in equal molar amounts with as few reaction steps as possible. Thus mixtures of reactants could be used in each reaction step so that many reaction products are formed in one reaction vessel at the same time. This is the usual procedure for combinatorial synthesis of mixtures in solution. Combinatorial chemistry requires small amounts of reagents, and methodologies for efficient synthesis selectivity, and it's possible for using the automatic robots synthesis to increase productivity [27].

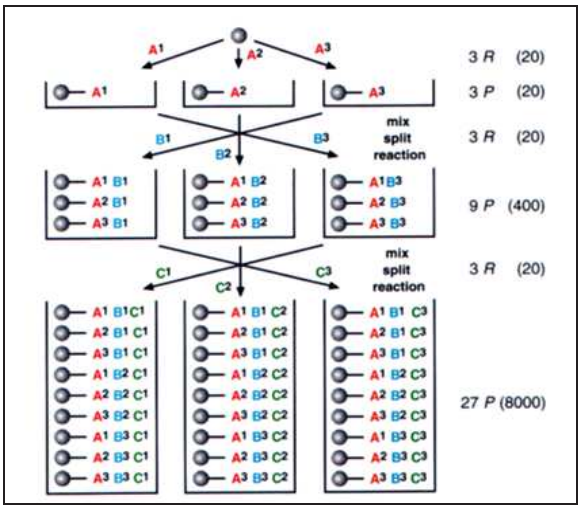

Fig.3: Split method, Sphere = polymeric support; R gives the number of reactions performed in parallel; P is the number of different products [26].

1.2.3. Design of Dynamic combinatorial libraries-DCLs and generation of diversity

The choice of the components of the DCLs is made with respect to the initial reactants supposed to lead to active products. The probability of finding an active compound increases with diversity and the dissimilarity of the components of the library. There is a difference between diversity variety and library in the expense variety of critically molecular site interaction. A combinatorial library can have a wide range for a given target, but no variety to another target [27].

Know the structural information on the active site of the target, the modeling computer-aided design can effectively targeted library rational design and structure based combinatorial synthesis. Unfortunately, information structural are not yet available for majority biological targets, thus the trial and error methods (random design) become interesting.

The success of such an approach requires a good balance between the number and diversity of compounds tested. The composition of the libraries varies depending on the purpose: looking for a track (active), or optimization of a track that represented at table 1.

Table 1: Features of combinatorial libraries [28].

Search track	Optimization track
1. Random libraries. 2. Several targets 3. Synthesis on a solid support: (synthesis of libraries of small molecules) 4. Syntheses "split" Mixtures of individual components ("One-bead, one compound"). 5. >>10000 components, <1 mg product 6. Screening mixtures (with convolution)	1. Targeted libraries. 2. A target / A target family 3. Synthesis in solution/ solid support (the structure of the track determines the chemistry). 4. Automated parallel synthesis individual components. 5. << 10000 components, 1 mg product. 6. Screening of individual components (with decoding)

1.2.4. Principles of dynamic combinatorial chemistry

Dynamic combinatorial chemistry (DCC) exploits reversible covalent chemistry to generate combinatorial libraries that are under thermodynamic control [29,30]. The use of DCC has enabled combinatorial pools of candidates to be established through reversible connections, either by using covalent or noncovalent chemistry. Such a collection of molecules is termed a dynamic combinatorial library (DCL) [31-38] and may be viewed as a collection of reversible combinations of a series of building blocks which undergo thermodynamic exchange with each other as represented in (Fig. 4).

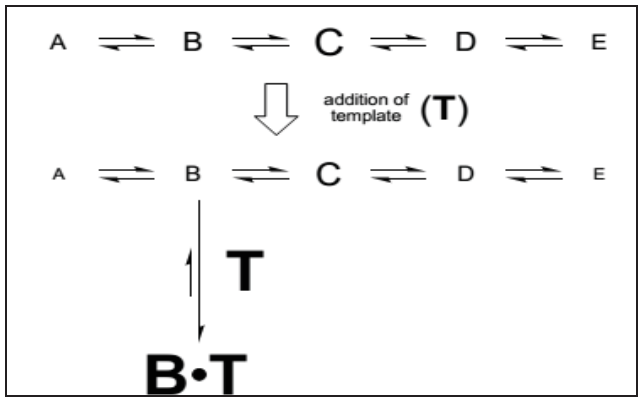

Fig.4: Schematic representation of the interconversion of library members by equilibrium processes. The letter sizes are representative of product concentration [29].

Since the library members interconvert by equilibrium processes, any stabilization of a given member of the library will result in the thermodynamic redistribution of the equilibrium to yield a new thermodynamic equilibrium. The result, which is in accordance with the Le Chatelier principle, is amplification of the stabilized library member, whose formation is, favored above all other possible members that might co-exist in solution. Indeed, those other possible members are "proof-read" and consumed to produce more of the favored member. Stabilization of a library member may be achieved by introducing a template into the DCL. Templating methods for DCLs has been considered [39] into two classes (Fig. 5) "casting" and "molding". In casting, a macromolecule provides a cavity within which the optimum ligand may be trapped, whereas, in moulding, the ligand collects the optimum receptor around itself.

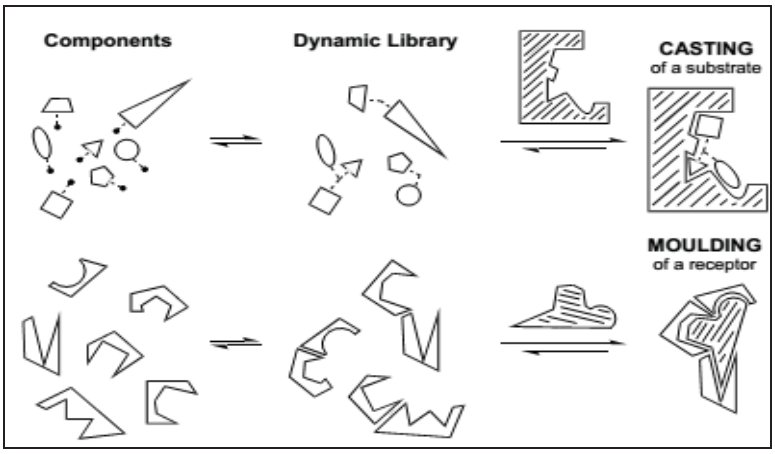

Fig.5: Diagrammatic representation of casting and moulding in DCLs [39].

Dynamic combinatorial/covalent chemistry (DCC), that relies on the dynamic generation of interconverting "keys" resulting from all the possible combinations of "fragments of keys", with the goal that this virtual set of potential keys may contain one (or more) that fits the lock, under either thermodynamic selection, expressing the constituent/key that presents the strongest interaction with the target/lock, or kinetic selection, giving the key that forms fastest within the lock. In both cases, the supramolecular lock/key recognition interactions direct the process (Fig. 6). A dynamic library of constituent keys is generated from reversibly connecting fragments of the keys. The receptor/lock amplifies/favours the expression of the constituent/key that binds best to it (thermodynamic selection) or that forms fastest within it (kinetic selection). The library constituents/keys do not need to be formed before the addition of the receptor/lock, illustrating the notion of virtual dynamic library.

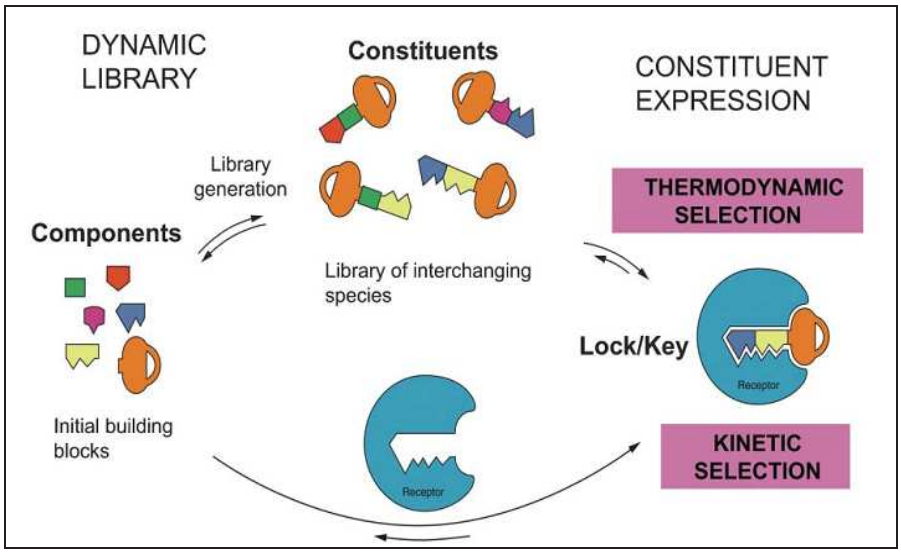

Fig.6: Schematic representation of the principle of dynamic combinatorial/covalent chemistry (DCC) as applied in particular to the discovery of leads for bioactive compounds [40].

Supramolecular chemistry as previously defined as the chemistry of non-covalent interactions is a part of a dynamic chemistry. Indeed, its principles are based on the recognition and assembly natural or synthetic molecular entities through reversible interactions covalent or non-covalent. The dynamic materials, as materials whose components are linked through reversible covalent or noncovalent connections and undergo spontaneous and continuous change in constitution by assembly/dis-assembly processes in a given set of conditions via recognition directed association and self-organization processes, supramolecular chemistry has opened new perspectives in materials science towards the design and engineering of supramolecular materials. These, again, are dynamic by nature, whereas molecular materials must be rendered dynamic by introduction of reversible covalent connections between building blocks. Because of their intrinsic ability to exchange their components, they may in principle select them in response to external stimuli or environmental factors and therefore behave as adaptive materials of either molecular or supramolecular nature [1, 4, 41, 42].

1.2.5. The Peculiarities of DCLs and VCLs

The reversibility is the fundamental characteristic of the CCD, allowing the approach dynamic and allows the creation of VCLs through continuous and spontaneous interconversion these components ensure the adaptive nature of libraries thus formed. The VCLs are dependent on the mechanism of formation and connections. i.e. if the process assembly occurs *via* reversible covalent connections, Molecular recognition resulting in a VCL, if such interactions are non-

covalent, the VCL is called supramolecular. The dynamic process is conducted in the presence of a target. This target allows direct the system to the highest molecular recognition, and thus towards the highest system thermodynamically stable. The development of supramolecular from dynamic combinatorial libraries therefore rests on two foundations of supramolecular chemistry. On the one hand, the recognition Molecular selective pre-arranged and the other self-assembly via their species intermolecular connections. Stability and evolution of these structures can be modulated not only by the dynamics of weak connections in play , that is to say, the existing reversibility between molecular building blocks, but also by external factors such as temperature, concentration , or solvents. The comparative features between Virtual Combinatorial Libraries (VCL) and Dynamic Combinatorial Chemistry (DCL) can be represented in Table 2.

Table 2: Static and dynamic combinatorial chemistry; comparative basic features of real and dynamic virtual combinatorial libraries.

Dynamic Combinatorial Library (DCL).	Virtual Combinatorial Library (VCL).
1. Molecular constitutions	1. Molecular or supramolecular constituents
2. Real set	2. Virtual set
3. Collection of molecules	3. Collection of components
4. Covalent	4. Covalent or non-covalent
5.Non reversible	5. Reversible
6. Neutral, uninformed	6. Instructed
	a) Internally (self-recognition)
	b) Externally (species binding)
	⇨ Adaptive
7. Systematic	7. Recognition-Directed
8. Preformed by synthesis	8. self assembled
9. In absence of the target	9. In presence of the target.

1.3. Definition and role of carbonic anhydrase

Carbonic anhydrases (CA) represent an important class of ubiquitously expressed zinc metallo-enzymes, catalyzing the reversible hydration of carbon dioxide to bicarbonate and a proton [43-45].

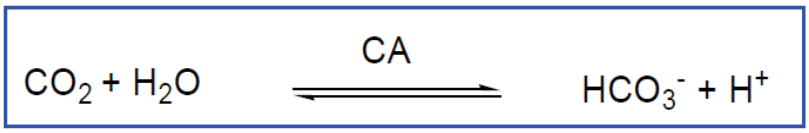

Equation 1: Hydration of CO_2 in the presence of CA

The active form of the enzyme is the basic one, with hydroxide bound to Zn(II). This strong nucleophile attacks the CO_2 molecule bound in a hydrophobic pocket in its neighborhood leading to formation of bicarbonate coordinated to Zn(II).

As represented in (Fig. 8), the bicarbonate ion is displaced by a water molecule and liberated into solution, leading to the acid form of the enzyme, then coordinated with water to Zn(II), which is catalytically inactive [44-46].

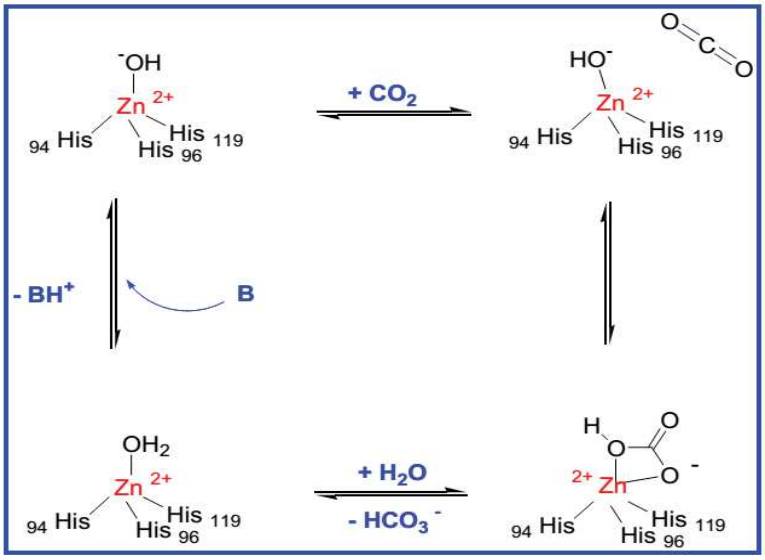

Fig.8: Schematic representation of the catalytic mechanism for the CA catalyzed CO_2 hydration [47].

In order to regenerate the basic form, a proton transfer reaction from the active site to the environment takes place, which may be assisted either by active site residues (such as His 64) or by buffers present in the medium. The process may be schematically represented by equation (2) and equation (3).

$$EZn^{2+}\text{-}OH^{-} + CO^{2-} \Leftrightarrow EZn^{2+}\text{-}HCO^{3-} \Leftrightarrow EZn^{2+}\text{-}OH_2 + HCO^{3-} \quad (2)$$

$$EZn^{2+}\text{-}OH_2 \Leftrightarrow EZn^{2+}\text{-}HO^{-} + H^{+} \quad (3)$$

In addition to the physiological reaction, the reversible hydration of CO_2 to bicarbonate (reaction 1), CAs catalyze a variety of other reactions, such as: the hydration of cyanate to carbamic acid, or of cyanamide to urea (reactions 2 and 3); the aldehyde hydration to gem-diols (reaction 4); the hydrolysis of carboxylic, sulfonic or phosphoric acids esters (reaction 5-7), as well as other less investigated hydrolytic processes, such as those described by reactions 8-10 (Fig. 9) [48-51].

$O=C=O + H_2O \Leftrightarrow HCO_3^- + H^+$	(1)
$O=C=NH + H_2O \Leftrightarrow H_2NCOOH$	(2)
$HN=C=NH + H_2O \Leftrightarrow H_2NCONH_2$	(3)
$RCHO + H_2O \Leftrightarrow RCH(OH)_2$	(4)
$RCOOAr + H_2O \Leftrightarrow RCOOH + ArOH$	(5)
$RSO_3Ar + H_2O \Leftrightarrow RSO_3H + ArOH$	(6)
$ArOPO_3^{2-} + H_2O \Leftrightarrow HPO_3^{2-} + ArOH$	(7)
$ArF + H_2O \Leftrightarrow HF + ArOH$ (Ar = 2,4-dinitrophenyl)	(8)
$PhCH_2OCOCl + H_2O \Leftrightarrow PhCH_2OH + CO_2 + HCl$	(9)
$RSO_2Cl + H_2O \Leftrightarrow RSO_3H + HCl$ (R = Me; Ph)	(10)

Fig.9: Reactions catalyzed by α-CAs [48-51].

1.3.1. Catalytic and inhibition mechanisms of carbonic anhydrase

The clinically available pharmacological agents known to date, present weak inhibition selectivity toward of different CA isoforms, inducing important side effects. Thus, the development of isozyme-specific inhibitors is currently a great challenge for obtaining novel types of drugs acting in specific physiologic/pathologic processes [43]. Much progress has been achieved in the past decade for identifying selective CA inhibitors (CAIs) by means of rational drug design [44,45]. The emergence of numerous families of selective CA inhibitors against several pharmacologically relevant isozymes is based on specific strategies including X-ray crystal structures for some enzyme-inhibitor complexes [51]. They mostly address major basic structural elements such as the zinc coordinating function [52,53] or the nature of the hydrophobic residue [54-56] lying to the hydrophobic pocket standing above active metal ion binding site. Among the 13 catalytically active R-CA isozymes currently known and studied as the drug targets, human carbonic anhydrases hCA I and hCA II are considered the most selective isoforms. Their inhibition has already offered important biomedical options in the development of antiglaucoma, antiepileptic, antiobesity, or anticancer drugs. The Zn(II) ion of CAs is essential for catalysis [43-46]. X-ray crystallographic data showed that the metal ion is situated at the bottom (Fig.10), being coordinated by three histidine residues (His 94, His 96 and His119) and a water molecule/ hydroxide ion [44, 46, 56]. The zinc-bound water is also engaged in hydrogen bond interactions with the hydroxyl moiety of Thr 199, which in turn is bridged to the

carboxylate moiety of Glu 106; these interactions enhance the nucleophilicity of the zinc-bound water molecule, and orient the substrate (CO_2) in a favorable location for the nucleophilic attack [56-58].

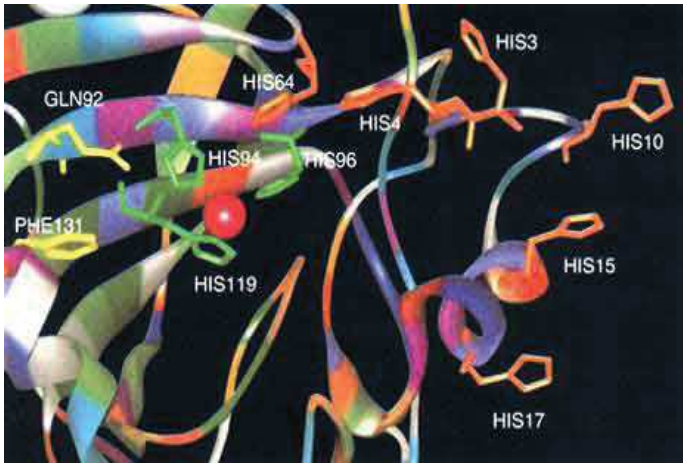

Fig.10: hCA II active site, with the Zn(II) ion (pink sphere), its three histidine ligands (His 94, His 96 and His 119, in green), the proton shuttle residue His 64 as well as the histidine cluster extending from the rim of the active site to the surface of the protein, comprising residues 3, 4, 10, 15 and 17 – in orange) [56].

Table 3: CA isozymes, their catalytic activity in CO_2 affinity for sulfonamides, and their subcellular localization [60].

Isozyme	Catalytic activity (CO2 hydration)	Affinity for sulfonamides	Sub-cellular localization
CA I	low (10 % of that of CA II)	medium	Cytosol
CA II	high	very high	Cytosol
CA III	very low	(0.3% of that of CA II) very low	Cytosol
CA IV	high	high	membrane-bound
CA V	moderate-high #	high	Mitochondria
CA VI	moderate	medium-low	secreted into saliva
CA VII	high	very high	Cytosol
CARP VIII	a catalytic	**	probably cytosolic
CA IX	high	high	membrane-bound
CARP X	a catalytic	**	unknown
CARP XI	a catalytic	**	Unknown
CA XII	active (no quantitative data)	unknown	membrane-bound
CA XIII*	probably high	unknown	Unknown
CA XIV	low	unknown	membrane-bound

Notes: # Moderate at pH 7.4, high at pH 8.2 or higher.
* CA XIII has not been isolated as a protein but has been identified from an expressed sequence tag (EST) derived from a mouse mammary gland cDNA library.
** The native CARP isozymes do not contain Zn(II), so that their affinity for the sulfonamide inhibitors has not been measured. By site-directed mutagenesis it is possible to modify these proteins and transform them in enzymes with CA-like activity which probably is inhibited by sulfonamides, but no studies on this subject are available presently.

The CA is mainly involved in different processes, linking the breathing and transfer between CO_2/bicarbonate tissues and lungs and pH homeostasis and CO_2. It also occurs during the secretion of electrolytes in various tissues and organs and also plays a role in different biosynthetic reactions such as triglyceride synthesis (lipogenesis), but also the formation of urea

and calcification [59]. In mammals, at least fourteen different isoforms of CA have been described. Table 3 represents different isozymes of carbonic anhydrase: catalytic activity (hydration CO_2), the affinity inhibitors sulfonamides types and their subcellular localization and tissue distribution [59, 60]. The crystallographic structures of these seven isozymes (CA I, II, III, IV, V, XII and XIV) were determined in the presence and absence of inhibitors [61-68].

The enzyme inhibition is also a physiological approaches used in the treatment and prevention of many diseases such as osteoporosis, ulcers, altitude sickness, epilepsy, neurological disorders, Parkinson disease, neuromuscular diseases, and treatment of glaucoma [60,68]. The use of carbonic anhydrase inhibitors in the treatment of certain cancers is also the focus of attention particular [69,70]. Recently, a study showed that the activation of isozymes I and II represents a new treatment for Alzheimer's disease, as the rate of hCA I and hCA II in the patient's brains has low affect by Alzheimer's disease. The dysfunction activity of hCA I and hCA II causes extra pH imbalance and intracellular protein aggregation and contribute to the progression of disease [63].

$$\mathbf{E\text{-}Zn^{2+}\text{-}OH_2 + I \Leftrightarrow E\text{-}Zn^{2+}\text{-}I + H_2O} \quad \textbf{(Tetrahedral adduct)} \quad \textbf{(substitution)} \quad (4)$$

$$\mathbf{E\text{-}Zn^{2+}\text{-}OH_2 + I \Leftrightarrow E\text{-}Zn^{2+}\text{-}OH_2\,(I)} \quad \textbf{(Trigonal-bipyramidal adduct)} \quad \textbf{(addition)} \quad (5)$$

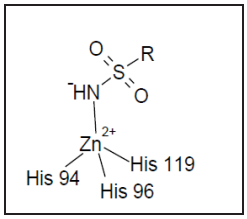

Tetrahedral adduct (sulfonamide) (A)

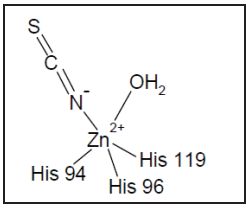

Trigonal-bipiramidal adduct (thiocyanate) (B)

Fig.11: CA inhibition mechanism by sulfonamide and anionic inhibitors [60].

Two main classes of CA inhibitors (CAIs) are known: the metal complexing anions, and the unsubstituted sulfonamides, which bind to the Zn(II) ion of the enzyme either by substituting the non-protein zinc ligand (equation 4 in Fig. 11), or add to the metal coordination sphere (equation 5 in Fig. 11) generating trigonal-bipyramidal species [46,47,71,72]. Sulfonamides, which are the most important CAIs bind in a tetrahedral geometry of the Zn(II) ion (Fig. 11A), in deprotonated state, with the nitrogen atom of the sulfonamide moiety coordinated to Zn(II); anions may bind either in tetrahedral geometry of the metal ion, or as trigonal-bipyramidal adducts, such as for instance the thiocyanate adduct shown in (Fig. 11B) [73].

1.3.2. Sulfonamides as carbonic anhydrase inhibitors: Sample application in the treatment of glaucoma.

Sulfonamides ($R\text{-}SO_2\text{-}NH_2$) are a class of important pharmacological agents for the inhibition of carbonic anhydrase (Fig. 12). Heterocyclic sulfonamides have been operating for many years in medicine, mainly as a diuretic, and in the treatment of neurological disorders and glaucoma.

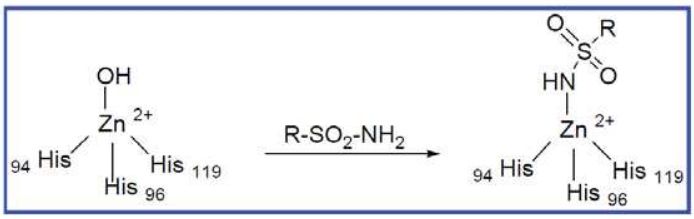

Fig.12: CA inhibition mechanism with sulfonamides [47].

The glaucoma poses a significant public health problem, this chronic disease and degenerative affects 1% of the French population and represents 10 to 15% of cases of blindness in industrialized countries. The open-angle glaucoma is an eye disease that causes impaired visual field, optic nerve damage, and loss of visual acuity leading to blindness. This disease is characterized by high elevated intraocular pressure (IOP), and it depends on the balance between two factors: The secretion of aqueous humor, and the resorption of aqueous humor through the trabecular meshwork scleral pores. Four systemic sulfonamide drugs have been used clinically mainly as antiglaucoma agents, for a long time: acetazolamide, methazolamide , ethoxzolamide and dichlorophenamide [44,59]. Systemic inhibitors are useful in reducing elevated intraocular pressure (IOP) characteristic of this disease, as they represent the most physiological treatment of glaucoma, since by inhibiting the ciliary process enzyme (the sulfonamide susceptible isozymes CA II and CAIV), a reduced rate of bicarbonate and aqueous humor secretion is achieved, which leads to a 25 –30 % decrease of IOP, but the inhibition of various CA isozymes present in other tissues than the eye, leads to an entire range of side effects [35,50]. The first sulfonamides used as anti-glaucoma are the Acetazolamide, and Methazolamide represented in (Fig. 13). These drugs administered Oral cause many side effects (gastrointestinal irritation, fatigue, malaise, decreased libido, kidney stones, etc.) due to their action on different carbonic anhydrase present in other tissues and organs.

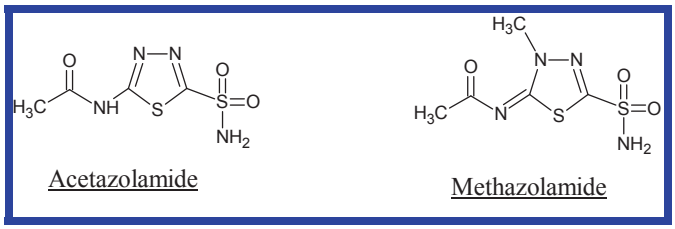

Fig.13: Antiglocaumes drugs administered orally [47].

It appeared an interest to try for administering such sulfonamide CAIs topically, directly into the eye [44,59]. Still, none of the clinically used inhibitors or other structurally related investigational agents proved to be effective when administered topically in reducing elevated IOP, and thus, for a long period, it was considered that sulfonamide CAIs cannot be administered via topical route. In a classical study, Maren's group showed that this is principally due to the un appropriate physicochemical properties of the existing CAIs available at that moment, and put the basis for the discovery of the topically acting sulfonamides: the first such drug dorzolamide [67] entered in clinics in 1995, and the second one related to brinzolamide [68] entered in clinics in 1999. Thus drug represented in (Fig. 14). In addition to the systemically acting inhibitors, the clinical antiglaucoma armamentarium comprises these two new drugs, which show much less side effects as compared to the first drugs mentioned above, which also basically inhibit all the physiologically relevant CA isozymes.

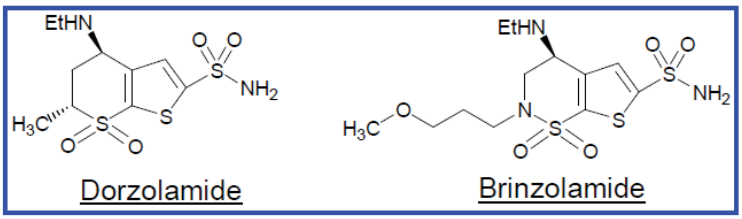

Fig.14: Drugs administered topically [47].

Although these two sulfonamides cause the lowering of intraocular pressure acting mainly on the CA II and CA IV, they often lead to tingling, burning in eye level or blurred vision and that due to the acidity (pH = 5.5) of the administered ophthalmic solution in the form of molecules hydrochlorides [70]. In addition, more serious problems may occur such as allergies, depression, and see dementia. While conventional sulfonamide inhibitors types were the most used, other types of inhibitors also showed good affinity to carbonic anhydrase as: sulfamate, sulfamate phosphorylated, sulfonamides base Schiff, ureas, hydroxyureas.

Two main approaches were used for the drug design of effective antiglaucoma sulfonamides. **The ‘‘ring’’ approach**, used for the discovery of dorzolamide and brinzolamide, consisted in exploring a great variety of ring systems on which the sulfonamide group (and eventually other moieties) have been attached. This approach was really beneficial for the chemistry of this class of derivatives as a very large number of new ring systems was explored in this way, but generally led to few effective in vivo IOP lowering agents, and the largest majority of the obtained derivatives were potent allergens [70]. **The ‘‘tail’’ approach**, consisted in attaching water solubilizing tails to different scaffolds of well-known aromatic/heterocyclic sulfonamides possessing affinity for the CA active site, assuring in this way the possibility to modulate in greater details the physico-chemical properties of these pharmacological agents. This approach did not lead for the moment to a clinically used drug, but led to the development of a very large number of much more effective antiglaucoma sulfonamides as compared to dorzolamide and brinzolamide at least in animal models of the disease) in comparison with the ring approach. One must also mention that these two approaches are both valuable and complementary, since it was proved for example that dorzolamide may also be further derivatized by the tail strategy, leading to even more effective IOP lowering compounds [70].

The discovery and development of novel water-soluble CA inhibitors, potentially more active and less toxic, still represent an important issue. Professor Claudiu T. Supuran group contributed to the discovery and development of good inhibitors known so far. Inhibitors must have essentially two distinct parts: 1. A pattern (eg: sulfonamide) capable of binding to the catalytic site of the carbonic anhydrase and 2. A group (substituted or unsubstituted aromatic) providing interactions with amino in the enzyme pocket acid residues. In the laboratory of Dr. JeanYves Winum, new series of potential inhibitor of carbonic anhydrase were synthesized: N-alkyl-N'-hydroxysulfamides. The inhibition constants of this series have been determined for the human isozymes (hCAII , hCAIX , hCAXII , hCAI).

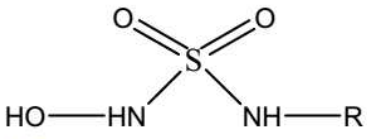

R = Octadecyl, decyl, dodecyl, benzyl, phenyl methyl.

The hydroxysulfamide unsubstituted showed a higher affinity (K_i= 473 nM to 4.05 μM) for isozymes tested against those of their counterparts, sulfonamides and sulfamic acids. Hydroxysulfamides the substituted derivatives of n-decyl, n-dodecyl, benzyl, biphenyl or methyl showed smaller affinity for HCAI for the hCAII. In fact, affinity for HCAI has decreased from decyl drifted biphenyl methyl derivative having larger steric genes. The group hydroxysulfamides deprotonated "ZBF" (Zinc Binding Function) engages in an affair with the

Zn^{2+} and participates in hydrogen bonds with threonine and glutamate residues (Fig.15). The R group or "Scaffold" interacts with the hydrophobic and hydrophilic part of enzyme (amino acid residues) as represented in (Fig. 15).

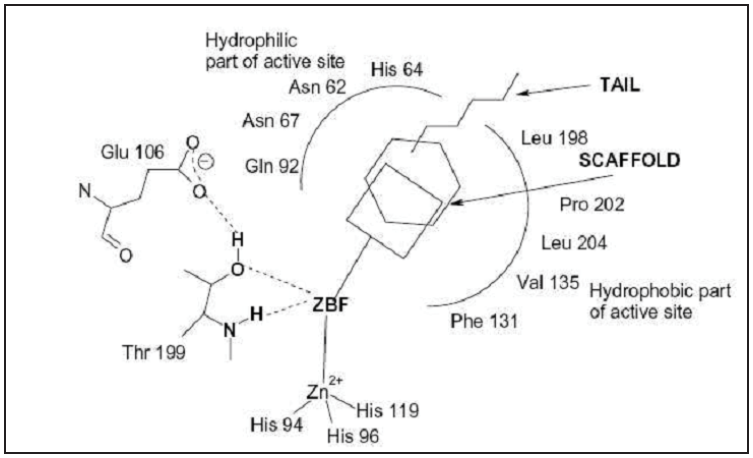

Fig.15: Schematic representation of CAI interacting with inhibitor. This presentation shows hydrophilic and hydrophobic interactions of the inhibitor with the active site of the enzyme, the ZBF "zinc binding function" interacts with the Zn^{2+} ion and with threonine and glutamate residues [74].

1.3.3. Carbonic anhydrase and Dynamic combinatorial chemistry (DCC)

Carbonic anhydrases (CA) have been one of the early addressed biological targets for which the DCC [75-79] may offer a complementary route to high-throughput combinatorial methods [80]. The first example in this field has been pioneered by Lehn et al., who reported a library of 12 constituents containing different Zn(II) complexing groups and various aromatic moieties connected by the reversible imino-bond, generating thus a hydrophobic sulphonamide inhibitor possessing high affinity toward the bovine carbonic anhydrase (bCA II, EC 4.2.1.1) [75]. Then, the feasibility of this concept has been extended by Nguyen et al. [76] and Poulsen et al. [77-79] including a kinetic approach and a thermodynamic approach based of cross-metathesis reversible reaction, all of which addressing the same challenge: discovery of small molecule inhibitors of bCA II, an easily accessible and inexpensive enzyme. One major advantage with reversible dynamic combinatorial libraries (DCLs) over their irreversible counterparts is their potential adaptability to express the sorting constituent in response to an external selection pressure [80,81]. Change in the output constituents of a DCL under the pressure of internal and external factors (stimuli) based on constitutional dynamics 31express the system adaptation to a given situation [82,83]. Barboiu et al. reported a such CDL that is susceptible to change its composition (output expression) through component selection driven by the selective binding to human hCAI and hCA II isozymes [84].

Considering the pharmacological importance to find selective CAIs isozymes for a specific inhibitor, the human hCAI and hCA II isozymes, known to be more selective (specific) than bovine carbonic anhydrase (bCA II), are subjected to a parallel screening of the same CDL [85-90] by using the aminocarbonyl/imine interconversion as reversible chemistry. In particular, the use of CDL chemistry for the inhibitors discovery might provide initial insights toward the strategy of generation of efficient classes of selective active compounds, against human carbonic anhydrases, for instance our group have developed a Dynamic combinatorial library (DCL) of 20 initial constituents that are susceptible to binding to hCA II isozyme using aminocarbonyl/imine interconversion [91]. The high affinity of hCA II isozyme towards some sulfonamide inhibitors obtained was used to select from the dynamic library specific inhibitors of this isoform. These results point out to the possibility of identifying sulfonamide amplified compounds presenting potent inhibition and high yield of formation in the presence of the isoform(s) towards which the inhibitors were designed [92].

1.3.4. Esterase activity of Carbonic Anhydrase

It is hard to measure the activity of free enzyme with gas phase substrate such as CO_2. For this reason, in this research work carbonic anhydrase activity could also be measured in aqueous phase by using nitrophenyl esters. Carbonic anhydrase catalyses the hydrolysis of nitrophenyl esters with different efficiencies depending on the structure of the acyl part of substrate. But, as shown in Table 4, most efficient ester substrate for Bovine CA and Human CAII is para-nitrophenyl acetate (p-NPA) because of short and few acyl groups. p-NPA is bound as neutral species to the CA active site, allowing the strong nucleophilic ($Zn^{2+}(OH)^-$) attack, without any electrostatic repulsions, thus effectively hydrolyze it [93].

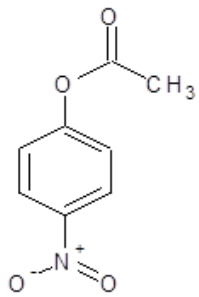

Fig.16: p-Nitrophenyl Acetate.

Table 4: The apparent rate constants for the CA-catalyzed hydrolysis of various esters [94].

Substrate	Rate Constant (kcat/KM, $M^{-1}s^{-1}$)
Phenyl acetate	3
o-nitrophenyl acetate	100
m-nitrophenyl acetate	240
p-nitrophenyl acetate	960
p-nitrophenyl propionate	68
p-nitrophenyl butyrate	6
p-nitrophenyl caproate	2

2. Materials and procedures

Materials: Carbonic anhydrase hCA I isosymes from human erythrocytes (Sigma), p-nitrophenyl acetate 99% (Sigma), Acetaldehyde 99.5% **(1)** (Sigma), Benzaldehyde 99.5% **(2)** (Sigma), 2-hydroxy-4-methoxybenzaldhye 95% **(3)** (Fluka)**,** 2-hydroxy-5-nitrobenzaldehyde 99% **(4)** (Sigma)**,** 3-formylbenzoic acid 97% **(5)** (Sigma), 2-fluorobenzaldhyde 97% **(6)** (Sigma), 3,4-difluorobenzaldhyde 97% **(7)** (Sigma), 2-formylbenzoic acid 97% **(8)** (Sigma), 2-formyl benzenesulfonic acid sodium salt 95% **(9)** (Sigma), 2-hydroxy-5-methoxybenzaldhye 95% **(10)** (Fluka), 4-amino benzenesulfonamide 98% **(A)** (Sigma), Methyl 4-aminobenzoate 98% (B) (Sigma), 5-sulfamoyl-1,3,4-thiadiazol-2-aminium chloride 97% (**C)** (Fluka), 3-methyl-5-sulfamoyl-1,3,4-thiadiazol-2(3H)-iminium chloride 97% (**D**) (Fluka) , 4-(2-aminoethyl)aniline 97% **(E)** (Sigma), benzylamine 99% **(F)** (Sigma), 4-(aminomethyl)benzenesulfonamide 98% (**G**) (Sigma), 4-(2-aminoethyl) benzenesulfonamide 98% (**H)** (Sigma) , Histamine 96% **(I)** (Sigma), 2-phenylethanamine 98% (**J)** (Sigma), propan-1-amine 98% **(K)** (Sigma), 4-(aminomethyl)aniline 98% (**L)** (Sigma).

Methodology: The reactions between DCLs members were performed in water at pH 6.5. A10-fold excess of the starting amines was used to limit side reactions between the aldehydes and the terminal amino residues groups of CA. Two reactions were performed with and without enzyme (hCAI, 0.1 mM) in a sodium phosphate solution at pH 6.5 (20 mM phosphate buffer). Stock solution in DMSO of 5 aldehydes (5 mM) and the 5 amines (50 mM) were added to aqueous solutions in order to reach the final concentration of 0.05 mM for aldehydes and 0.5 mM for amines, respectively. The clear mixture was incubated at 25 ^{0}C for 3 days before addition 0.1 mM of p- NPA. Then the absorbance of the generated product (p-NP) measured at using UV-Vis Spectrophotometer at 400 nm, the measurements recorded each min for ½ hr. The slope of absorbance versus time was defined as the activity gradient. The experimental steps were performed as the following:

1. Different dynamic combinatorial libraries (DCLs) have been prepared by adding different mixtures from the aldehydes and amines as the following: 0.05 ml of hCA (I), 0.76 ml phosphate buffer solution (pH = 6.5), and 0.01 ml from each aldehyde or amine.
2. The prepared solution stored at room temperature for period 3 days minimum, and then 0.1 ml from Para-nitro phenyl acetate was added to each mixture for measuring the enzyme activity by the generation of Para-nitro phenol product with time.

3. Stock solutions of (6.25 x 10^{-4}) g/mL p-NPA were prepared in acetonitrile, which was used to prevent spontaneous decomposition of p-NPA in air or in water. 10% (v/v) was added into each sample solution.

4. The absorbance intensity at 400 nm for the yellow product, p-nitrophenol, was followed versus time with Double Beam UV-Vis Spectrophotometer, the slope of absorbance versus time was defined as the activity gradient. (See appendix 6.1).

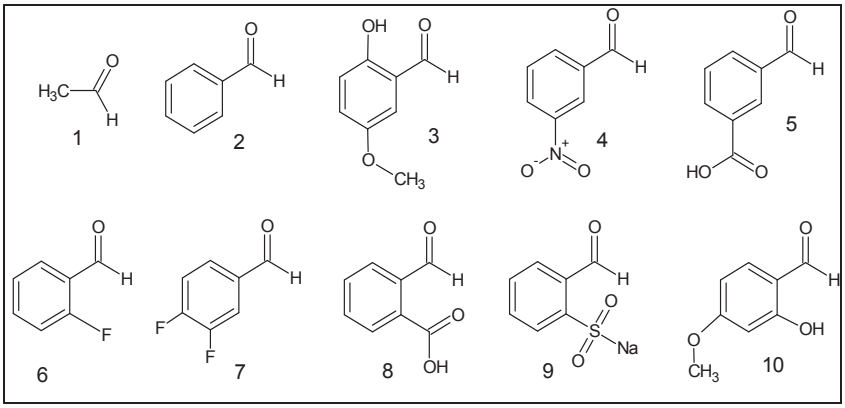

Fig.17: The chemical structures of the Aldehydes that used for the construction of the Dynamic combinatorial Libraries (DCLs).

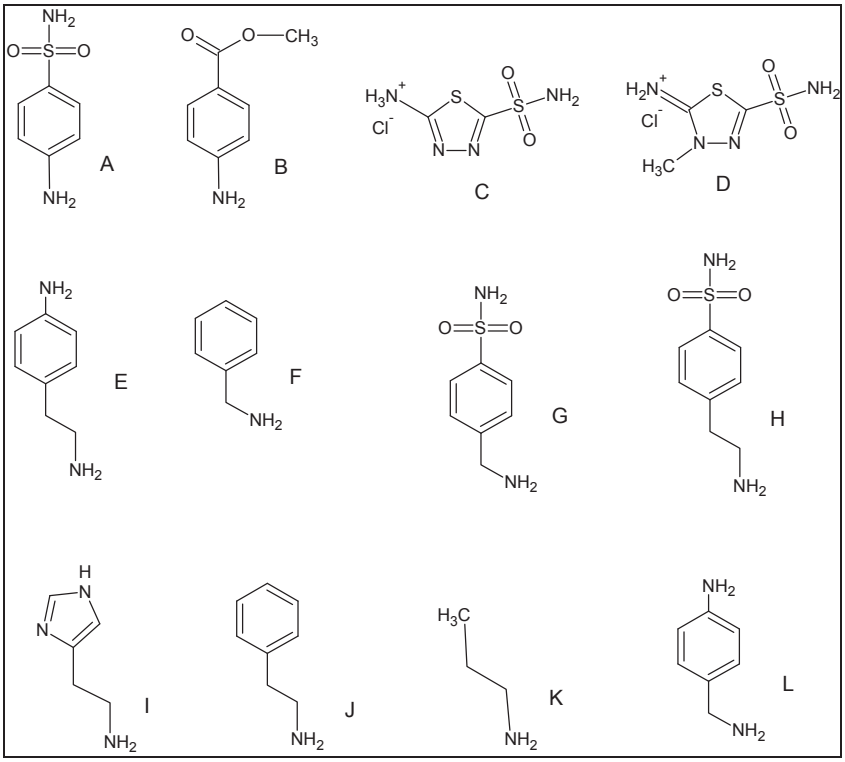

Fig.18: The chemical structures of the Amines that used for the construction of the Dynamic combinatorial Libraries (DCLs).

Instrumental analysis: A UVIKON 923, Double Beam UV-Vis Spectrophotometer has been used to measure the activity of Carbonic anhydrase enzyme with different dynamic combinatorial library (DCL).

The principle of UV-visible spectroscopy technique: Ultra-Violet and visible spectroscopy (UV-vis) is a reliable and accurate analytical laboratory assessment procedure that allows for the analysis of a substance. Specifically, ultraviolet and visible spectroscopy measures the absorption, transmission and emission of ultraviolet and visible light wavelengths by matter. Ultraviolet and visible spectroscopy (UV-vis spectroscopy) is used to study molecules and inorganic ions in solution. In UV/visible spectroscopy, a beam of light is split into a sample and reference beams. As its name implies, the sample beam is allowed to pass through the target sample. Alternately, the reference beam passes through the control solvent or a portion of the solvent that does not contain the actual target. Once the light passes through the target sample of interest it is measured by a special meter termed a spectrometer designed to compare the difference in the transmissions of the sample and reference beams. Double beam UV-visible spectroscopy instruments allow for simultaneous measures of transmissions through the target sample and solvent. The diagram for the typical UV-vis molecular absorption spectrophotometer represents in (Fig. 19).

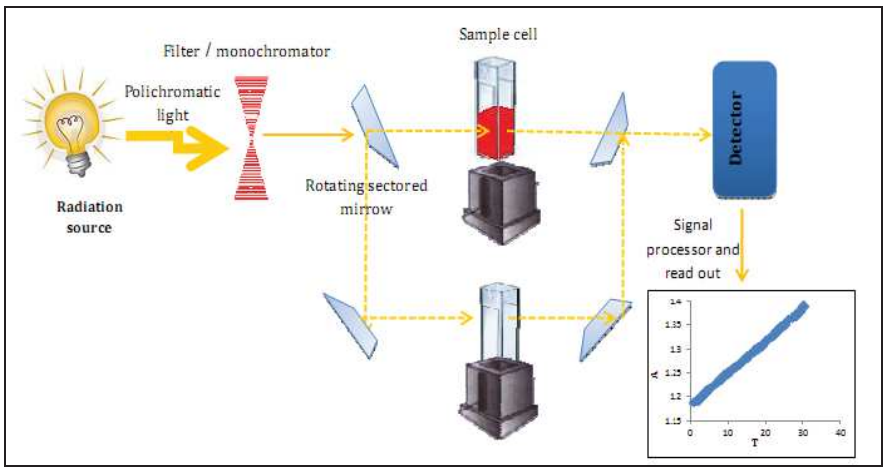

Fig.19: Diagram for a UV- visible molecular absorption spectrophotometers.

Special instrumentation is used in UV-vis spectroscopy. Hydrogen or deuterium lights provide the source of light for ultraviolet measurements. Tungsten lamps provide the light for visible measurements. These light sources generate light at specific wavelengths. The wavelengths of ultraviolet or visible light absorbed by a substance result in a unique ultraviolet-visible spectroscopic signature for each substance and can be used as analytical tool.

3. Results and Discussion

Here we describe the screening via Dynamic Deconvolution of DCLs of inhibitors (CAIs) and activators (CAAs) of hCA I. The inhibitory effects dominate over the activating ones, while the CAAs may be identified in the absence of CAIs. We report DCLs of components susceptible to selective binding to the hCA I, both as inhibitors or as activators, subjected to a parallel screening by using the amino-carbonyl/imine reversible chemistry. We investigate whether the competitive generation of potent CAIs and CAAs could be selectively expressed as an independent (linear), an interfering (crossover) or a dominant behaviour of the above mentioned events. The reversible formation of a Schiff's base is an advantageous reaction for generating DCLs, because the formation and component interchange processes are faster in slightly acidic aqueous solutions (PBS buffer, pH=6.5) as represented in Fig. (20).

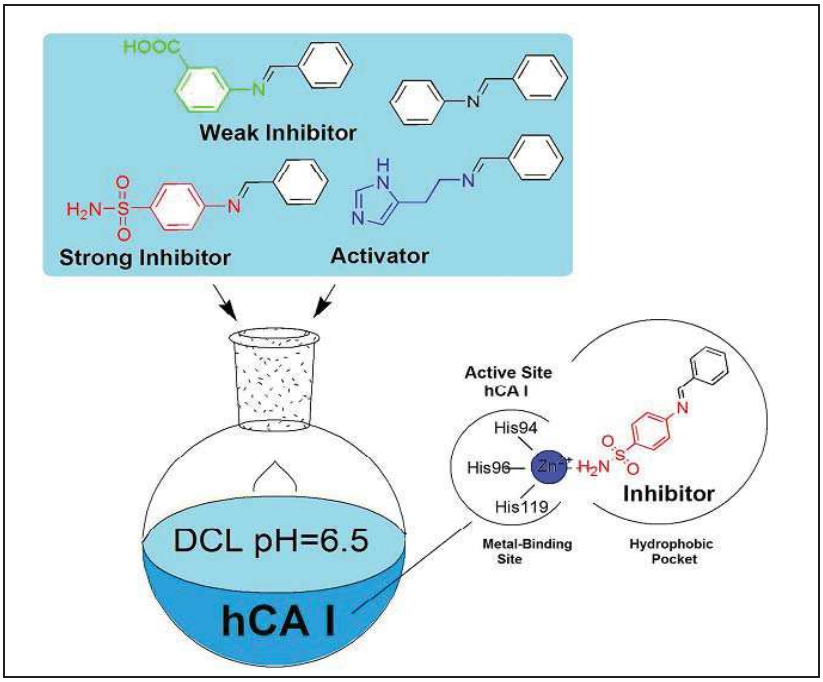

Fig.20: Dynamic Deconvolution of DCLs of inhibitors (CAIs) and activators (CAAs) of hCA(I) show that the inhibitory effects dominate over the activating ones.

However, the quantitative analysis of the final DCL mixture became very complicate and time-consuming, when using large numbers of building blocks [91, 92]. One more efficient way is the Dynamic Deconvolution procedure reported by Ramström and Lehn [11,12] based on the sequential, one by one removal of the starting components of a given DCL, followed by the determination of the enzyme activity.

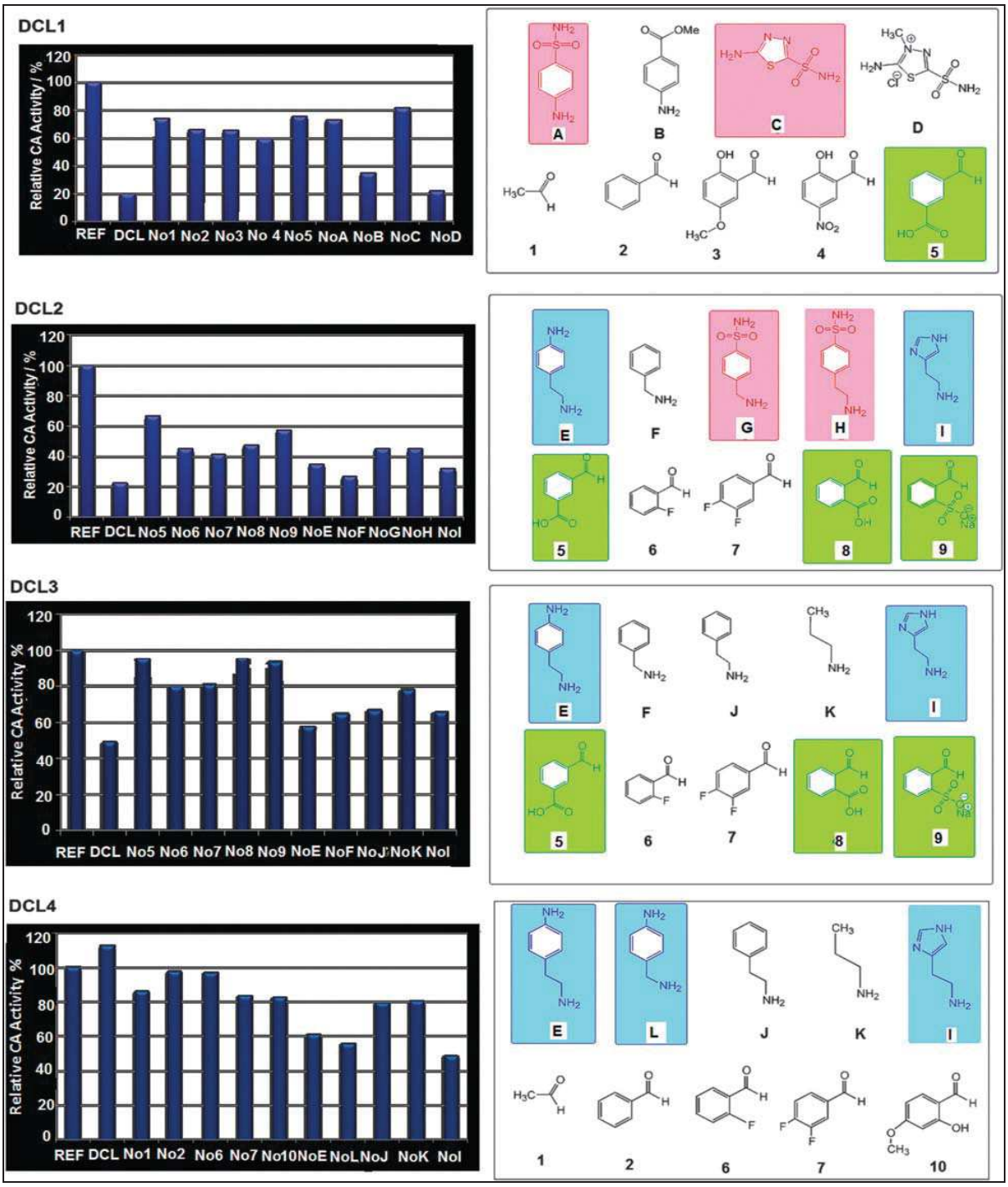

Fig.21: Dynamic Deconvolution of the DCL (1–4), containing mixtures of: active strong-inhibitor-components (pink)-DCL1; active strong-inhibitor (pink) and activator (blue) components-DCL (2); active low-inhibitor (green) and activator (blue) components-DCL3and activator (blue) components-DCL (4). All libraries contain inactive components represented in black supposed to not bind the active metal site but interact with the hydrophobic pocket of the enzyme. In the presence of strong metal binding site inhibitors, the low-inhibitors might be located in the hydrophobic pocket of the enzyme.

A decrease in the inhibition– activation effects compared with the presence of all components of the DCL indicates that the removed component is an important part of an active molecule that can be generated from the DCL. According to that in each library, one aldehyde or one amine were sort out from the DCL solution one by one to understand the effect of each amine and aldehyde and compare with the solutions which includes all aldehydes and amines also with blank. So, the DCL1–4 and the corresponding deconvoluted libraries have been generated in the presence of hCA I, from all building components and from all except one component, respectively, and then we measured the enzymatic activity. The choice of the DCL components has been related to the presence in their structure of various functional moieties such as: strong and low zinc coordinating function [52, 95, 96] or the nature of the residues [84] lying via donor and acceptor H-bonding, or hydrophobic interactions within the hydrophobic pocket of the enzyme [97-98]. The resultant relative activities to the reference samples of hCA I without any component are presented in Fig. 21. The DCL1, containing active strong-inhibitor-components, showed 80% relative inhibition of the reference hCA I activity, indicating the presence of active CAIs in the equilibrated mixture (Fig. 21). Upon removal of a specific building block from the DCL1, a decrease in inhibition indicates that the component omitted contributed to the inhibition of hCA I. For the DCL1 all the aldehyde counterparts showed important effects, but the largest effects were observed when either 1 or 5 have been removed from the pool. Conversely, the amine counterparts A or C showed important effects, so that the most active combinations as CAIs are 1A, 5A, 1C or 5C.

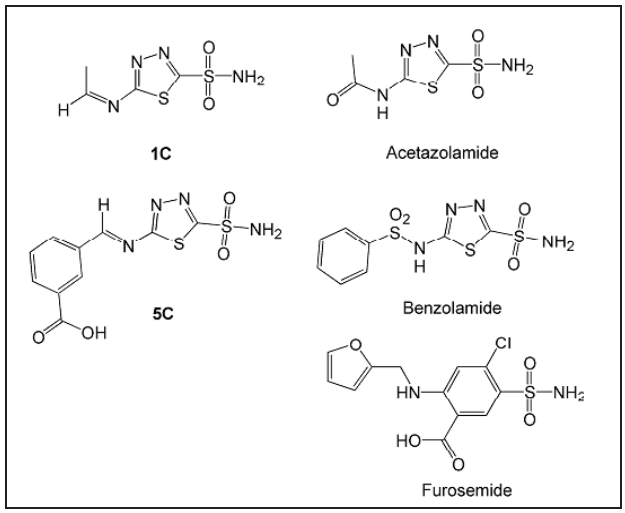

Scheme 1: Structural similarity between the potent inhibitors discovered herein and clinically used drugs as inhibitors of hCA I.

In fact, compounds 1C and 5C have a structural similarity to two clinically used compounds, acetazolamide AAZ and benzol-amide BZA (an orphan drug), (Scheme 1) which are highly effective inhibitors of hCA I [43]. Then, by mixing strong inhibitor-type (G, H) and activator-type (E, I) components together with hydrophobic (6, 7) and H-bonding (5, 8, 9) counterparts within DCL2, the hCA I activity showed 78% relative inhibition when compared with the reference one (Fig. 21). As previously observed, most hydrophobic components proved to be active but the largest effect arises upon removal of the H-bonding components 5 and 9 binding the hydrophobic pocket. The fluorinated components 6 and 7 are less active, in accordance with their low inhibition activity towards hCA I (KI = 620 nM) [92]. More importantly, the inhibitor-components G and H showed, when removed from the pool, dominant effects at the expense of the activator-ones E and I, see the detailed discussion below (Scheme 2) about mechanistic behaviours governing this assumption. The most active inhibitors of DCL2 are: 5G, 9G, (KI = 65 nM, for the amino reduced analogue) [92] 5H and 9H (KI = 35 nM for a similar 5-propylaminofuran-2- sulfonate inhibitor) [92,93].

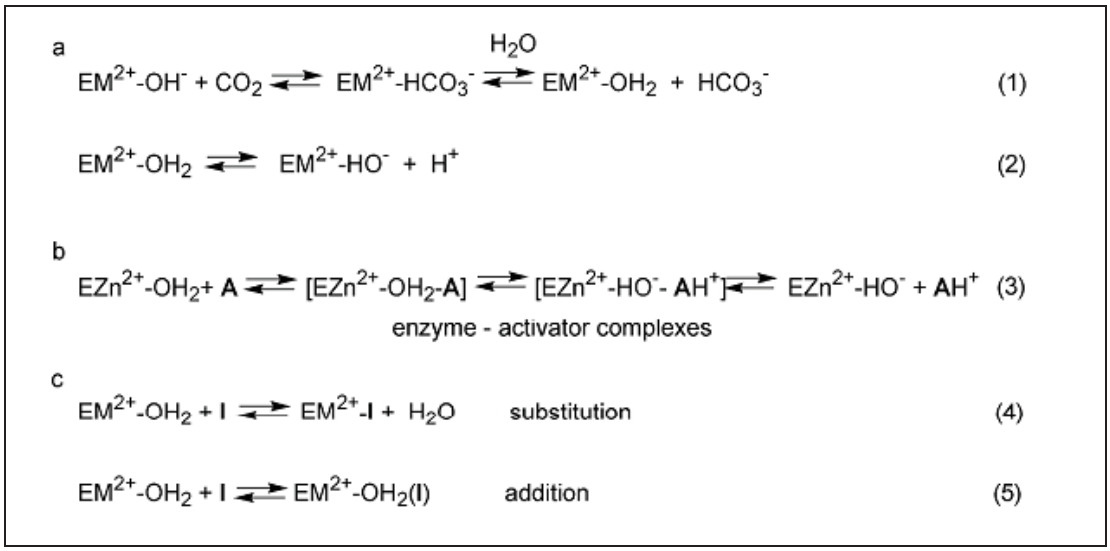

Scheme 2: (a) The CO_2 hydration mechanism with carbonic anhydrase – CA; (b) the activation and (c) the inhibition CA mechanisms in the presence of activator (A) and inhibitor (I) molecules respectively.

These compounds confirm the strong inhibitory power of the $–SO_2NH_2$ group combined to H-bonding interactions of the –COOH and $–SO_3H$ groups in the hydrophobic pocket. Amazingly, upon removal of the strong-inhibitor components G and H, in the DCL3, the data show less effective, but still inhibition (50%) of the hCA I activity compared to DCL1 and DCL2 (20%) (Fig.21). Within the DCL3 the carboxylic-type 5, 8 and sulfonic-type (9) used as

hydrophobic components show multiple expression and exhibit within this context differently low-inhibitory effects, as proved by almost recovery of the reference activity when these components have been removed from the pool. Moreover their inhibitory activity is still dominant at the expense of the activator E and I components. Some reports described the low-inhibition of CAs with carboxylate, acetate or salicylic acid, with inhibition constants in the range of mM [97]. There are also several cases of compounds containing –COOH moieties the best studied being furosemide (Scheme 1), which acts as a very effective hCA I (KI of 62 nM) and hCA II (KI of 65 nM) inhibitor [98]. Upon complete removal of both strong- (G and H in DCL2) and low-inhibitor (5, 8 and 9 in DCL3) components within DCL4, 10% relative activation activity of hCA I has been observed (Fig. 21). This is reminiscent of the fact that components E and I are effective activators of hCA I, only in the absence of the inhibitor-type components. Upon removal of a component from the DCL4, a decrease in activation indicates that the omitted component contributed to the activation of hCA I. For the DCL4 all the aldehyde counterparts show some effects but the largest effects were observed when components 1, 7 or 8 have been removed from the pool. Similar to the amine counterparts E or I, the fragment L shows important effects, so that the most active derivatives 1E, 7E, 10E, 1L, 7L, 10L, 1I, 7I or 10I combine the activation power of the amine [99] and imidazole [63] groups for which both hydrophobic and H-bonding effects lead to interactions with the active site as shown by means of X-ray crystallography for the adduct of hCA I with L-His [63].

The physiological reaction catalysed by the CAs involves the nucleophilic attack of the metal-bound hydroxide on the CO_2, optimally positioned and orientated in a hydrophobic binding pocket of the enzyme. Bicarbonate formed in this way is then replaced by a water molecule, with generation of the catalytically inactive (acidic) form of the enzyme $EM^{2+}–OH_2$ (eqn (1)), where M^{2+} is Zn^{2+} for hCA I (α-CAs), the isoform discussed here (Scheme 2a). In order to regenerate the catalytically active form, a proton transfer reaction occurs from the water bound to Zn^{2+} within the enzyme active site, to the external medium. In most α-CAs this step (eqn (2)) is assisted by an active site amino-acid residue (e.g. His 64), placed in the middle of the cavity or at the entrance of the active site [99]. In the presence of activators eqn (2) becomes (3), it has been demonstrated that they participate in the proton transfer processes (Scheme 2b). The activator-binding site is placed at the entrance of the active site cavity, in a region exposed to the solvent. Most CAAs investigated so far showed mM affinity (although some nM CAAs were also reported) [49, 56, 100]. Differently, the inhibitors bind deep within the active site and coordinate

to the Zn^{2+} ion (Scheme 2c, eqn (4) and (5)) [101,102]. This explains why many strong CAIs have low nM affinity. Such a difference in the binding sites of the CAAs compared to the CAIs also explain our present findings why the inhibitory effects dominate over the activating ones in DCLs containing both inhibitors and activators of the hCA I.

4. Conclusion

In this research work, our findings show that the DCL-Carbonic Anhydrase story may hold novel surprises, relevant to the general drug design research, especially with enzyme families like CAs with a multitude of members. The present study revealed a new paradigm: if compounds of agonistic inhibitor and activator activities are formed, the Dynamic Deconvolution may lead to the discovery of the inhibitory set of components expressed at the expense of the activator ones. This sheds light on the dominant mechanistic inhibition behaviours. Moreover the simplicity of the Dynamic Deconvolution strategy and of its analysis can easily lead to valuable simple mechanistic insights into inhibitory–activatory relative synergistic affinities toward the hCAs. This contribution adds several new behaviours to the systematic rationalization and prediction of novel CA active compounds.

5. References

[1] J.-M. Lehn, "From supramolecular chemistry towards constitutional dynamic chemistry and adaptive chemistry" , Chem. Soc. Rev., 2007, 36,151-160.

[2] A. Marquis A., V. Smith, J. Harrowfield, J.-M. Lehn, H. Herschbach, R. Sanvito, E. Leize- Wagner and A. Van Dorsselaer, "Messages in Molecules: Ligand/Cation Coding and Self-Recognition in a Constitutionally Dynamic System of Heterometallic Double Helicates", Chem. –Eur. J., 2006, 12, 5632.

[3] J.-M. Lehn, "Supramolecular Chemistry: Concepts and perspectives", Wiley-VCH: Weinheim, 1995.

[4] E. Fisher, "Synthesen in der Zuckergruppe II", Ber. Dtsch. Chem. Ges., 1894, 27, 3189–3232.

[5] S. R. Wilson, A. W. Czarnik, "Combinatorial Chemistry-Synthesis and Applications", Eds., Wiley: New York, 1997.

[6] J.-M. Lehn, "Toward complex matter: Supramolecular chemistry and self-organization", Proc. Natl. Acad. Sci. U.S.A, 2002, 99, 4763-4768.

[7] O. Ramstrom, J.-M. Lehn, "Drug discovery by dynamic combinatorial libraries", Nat. Rev. Drug Disc, 2002, 1, 26-36.

[8] Lehn, J.-M.,"Dynamic Combinatorial Chemistry and Virtual Combinatorial Libraries", Chem. Eur. J., 1999, 5, 2455–2463.

[9] P.T. Corbett, J. Leclaire, L. Vial, K. R. West, J.-L. Wietor, J. K. M. Sanders, S. Otto, "Dynamic combinatorial chemistry", Chem. Rev., 2006, 106, 3652.

[10] O. Ramstrom, J.-M. Lehn, " In situ generation and screening of a dynamic combinatorial carbohydrate library against Concanavalin A", ChemBioChem, 2000, 1, 41.

[11] O. Ramstrom, S. Lohman, T. Bunyapaiboonsri, J.-M. Lehn, "Dynamic Combinatorial Carbohydrate Libraries: Probing the Binding Site of the Concanavalin A Lectin" , Chem Eur. J., 2004, 10, 1711.

[12] T. Bunyapaiboonsri, O. Ramström, S. Lohman, J.-M. Lehn, " Dynamic deconvolution of a pr-equilibrated dynamic combinatorial library of acetylcholinesterase inhibitors", ChemBioChem, 2001, 2, 438.

[13] M. Hochgurtel, H. Kroth, D. Piecha, M. W. Hofmann, C. Nicolau, S. Krause, O. Schaaf, G. Sonnenmoser, A. V. Eliseev, "Target-induced formation of neuraminidase inhibitors from in vitro virtual combinatorial libraries", Proc. Natl. Acad. Sci. U.S.A. 2002, 99, 3382-3387

[14] A. Vlade, D. Urban, J.-M. Beau, " Target-assisted selection of galactosyltransferase binders from dynamic combinatorial libraries. An unexpected solution with restricted amounts of the enzyme", ChemBioChem 2006, 7, 1023-1027.

[15] S. Gerber-Lemaire, F. Popowycz, E. Rodriguez-Garcia, A. T. Asenjo, I. Robina, P. Vogel, "An Efficient Combinatorial Method for the Discovery of Glycosidase Inhibitors", ChemBioChem , 2002, 3, 466-470.

[16] A. M. Whitney, S. Ladame, S. Balasubramanian, " Templated Ligand Assembly by Using G-Quadruplex DNA and Dynamic Covalent Chemistry ", Angew. Chem., Int. Ed., 2004, 43, 1143-1146.

[17] J. Sadowski, M. Wagener, J. Gasteiger, "Assessing Similarity and Diversity of Combinatorial Libraries by Spatial Autocorrelation Functions and Neural Networks ", Angew. Chem., Int. Ed. Engl. 1995, 34, 2674–2677.

[18] P. J. Edwards, M. Gardner, W. Klute, G. F. Smith, N. K. Terrett, "Applications of combinatorial chemistry to drug design and development ", Curr Opin Drug Disc Devel, 1999, (4), 321-331.

[19] S. H. DeWitt, A. W. Czarnik, " Combinatorial organic synthesis using Parke-Davis' DIVERSOMERS™ method ", Acc. Chem. Res. 1996, 29, 114.

[20] J. W. Szostak, " Introduction: Combinatorial Chemistry, Chemical Reviews (Washington, D. C.) ", 1997,97, (2), 347-348.

[21] F. Balkenhohl, C. von dem Bussche-Huennefeld, A. Lansky, C. Zechel, " Combinatorial synthesis of small organic molecules ", Angewandte Chemie, International Edition in English 1996,35, (20), 2288-2337.

[22] N. K. Terrett, M. Gardner, D. W. Gordon, R. J. Kobylecki, J. Steele, " Combinatorial synthesis - the design of compound libraries and their application to drug discovery ", Tetrahedron 1995, 51, (30), 8135-73.

[23] M. Famulok, E. L. Winnacker, C. H. Wong, " Combinatorial Chemistry in Biology ", In: Curr. Top. Microbiol. Immunol., 1999,5, 195-243.

[24] B. Volker, Aspects structuraux, " combinatoires et dynamiques, d'auto-assemblages organiques ", Thesis 2000.

[25] R. B. Merrifield, " Solid phase peptide synthesis. I. The synthesis of a tetrapeptide ", Journal of the American Chemical Society, 1963, 85, (14), 2149-54.

[26] A. Furka, M. Sebestyen, G. Dibo, Abstr., 14th Congr. Biochem, Prague 1988, 47.

[27] B. Volker, " Aspects structuraux, combinatoires et dynamiques, d'auto-assemblages organiques ", Thesis 2000.

[28] F. Balkenhohl, C. Von dem Bussche-Huennefeld, A. Lansky, C. Zechel, " Combinatorial synthesis of small organic molecules ", Angewandte Chemie, International Edition in English 1996,35, (20), 2288-2337.

[29] Gihane Nasr, "Matériaux polymères dynamiques pour membranes adaptatifs ", Thesis 2007.

[30] S. J. Rowan, S. J. Cantrill, G. R. L. Cousins, J. K. M. Sanders, J. F. Stoddart ," Dynamic Covalent Chemistry", Angew. Chem. Int. Ed. 2002, 41(6), 898 – 952.

[31] P. A. Brady, J. K. M. Sanders, " Selection approaches to catalytic systems ", Chem. Soc. Rev. 1997, 26(5), 327 - 336.

[32] S. J. Rowan, J. K. M. Sanders, " Enzyme models: design and selection ", Curr. Opin. Chem. Biol. 1997, 1(4), 483 – 490.

[33] A. Ganesan, " Strategies for the Dynamic Integration of Combinatorial Synthesis and Screening ", Angew. Chem. 1998, 37(20) ,2828 – 2831.

[34] P. Timmerman, D. N. Reinhoudt, " A Combinatorial Approach to Synthetic Receptors ", Adv. Mater. 1999, 11(1), 71 – 74.

[35] B. Klekota, B. J. Miller," Dynamic diversity and small-molecule evolution: a new paradigm for ligand identification", Trends Biotechnol. 1999, 17(5), 205 -209.

[36] G. R. L. Cousins, S.-A. Poulsen, J. K. M. Sanders, " Molecular evolution: dynamic combinatorial libraries, autocatalytic networks and the quest for molecular function ", Curr. Opin. Chem. Biol. 2000, 4(3), 270 – 279.

[37] J.-M. Lehn, A. V. Eliseev, " Dynamic Combinatorial Chemistry",Science, 2001, 291(5512), 2331 -2332.

[38] S. Otto, R. L. E. Furlan, J. K. M. Sanders," Dynamic combinatorial chemistry:review", Drug Discovery Today 2002, 7(2), 117 - 125.

[39] P. A. Brady, J. K. M. Sanders,"Thermodynamically-controlled cyclisation and interconversion of oligocholates: metal ion templated ‘living’ macrolactonisation", J. Chem. Soc. Perkin Trans. 1 1997, 21, 3237 - 3254.

[40] I. Huc, J.-M. Lehn," Virtual combinatorial libraries: Dynamic generation of molecular and supramolecular diversity by self-assembly", Proc. Natl. Acad. Sci. USA 1997, 94(6), 2106 - 2110.

[41] J.-M. Lehn, "Supramolecular Chemistry/Science – Some Conjectures and Perspectives", in Supramolecular Chemistry: Where It Is and Where It Is Going (R. Ungaro, E. Dalcanale, eds.), Kluwer, Dordrecht, 1999, 287-304.

[42] J.-M. Lehn," Dynamers: dynamic molecular and supramolecular polymers" Prog. Polym. Sci., 2005, 30(8-9),814-831.

[43] C.T. Supuran, " Carbonic anhydrases: novel therapeutic applications for inhibitors and activators", Nat. Rev. Drug. Discovery 2008, 7, 168–181.

[44] C.T. Supuran, A. Scozzafava, J. Conway, " Carbonic Anhydrase: Its Inhibitors and Activators", Eds.; CRC Press: Boca Raton, FL, 2004, 1-376, and references cited therein.

[45] C.T. Supuran, J.Y. Winum, " Selectivity issues in the design of CA inhibitors. In Drug Design of Zinc-Enzyme Inhibitors: Functional, Structural, and Disease Applications", Eds. Wiley: New York, 2009.

[46] D.W. Christianson, J.D. Cox, " Catalysis by metal-activated hydroxide in zinc and manganese metalloenzymes ", Annu. Rev. Biochem., 1999, 68, 33-57.

[47] C.T. Supuran, A. Scozzafava, " Carbonic anhydrase inhibitors and their therapeutic potential", Exp. Opin. Ther. Patents, 2000, 10(5), 575-600.

[48] C.T. Supuran, C.W. Conroy, T.H. Maren, Is cyanate a carbonic anhydrase substrate? Proteins: Structure, Function and Genetics, 1997, 27, 272–278.

[49] F. Briganti, S. Mangani, A. Scozzafava, G. Vernaglione, C.T. Supuran, " Carbonic anhydrase catalyzes cyanamide hydration to urea: is it mimicking the physiological reaction?", J. Biol. Inorg. Chem., 1999, 4(5), 528-536.

[50] A. Guerri, F. Briganti, A. Scozzafava, C.T. Supuran, S. Mangani, " Mechanism of Cyanamide Hydration Catalyzed by Carbonic Anhydrase II Suggested by Cryogenic X-ray Diffraction", Biochemistry, 2000, 39(40), 12391-12397.

[51] C.T. Supuran, J.-Y. Winum, " De Simone G. X-Ray crystallography of CA inhibitors and its importance in drug design. In Drug Design of Zinc-Enzyme Inhibitors: Functional, Structural, and Disease Applications. ", Eds.; Wiley: New York, 2009.

[52] J.-Y. Winum, J.-L. Montero, A. Scozzafava, C. T. Supuran, " New zinc binding motifs in the design of selective carbonic anhydrase inhibitors ", Mini-Rev. Med. Chem. 2006, 6, 921–936.

[53] A. Guerri, F. Briganti, A. Scozzafava, C.T. Supuran, S. Mangani, " Mechanism of Cyanamide Hydration Catalyzed by Carbonic Anhydrase II Suggested by Cryogenic X-ray Diffraction" Biochemistry, 2000, 39(40), 12391-12397.

[54] S. Mitsuhashi, T. Mizushima, E. Yamashita, M. Yamamoto, T. Kumasaka, H. Moriyama, T. Ueki, S. Miyachi, T. Tsukihara, "X-ray structure of beta-carbonic anhydrase from the red alga, Porphyridium purpureum, reveals a novel catalytic site for CO_2 hydration ", J. Biol. Chem., 2000, 275, 5521-5526.

[55] E.I. Kisker, H. Schindelin, B.E. Alber, J.G. Ferry, D.C. Rees, " A left-hand beta-helix revealed by the crystal structure of a carbonic anhydrase from the archaeon Methanosarcina thermophila", EMBO J., 1996, 15(10), 2323-2330.

[56] F. Briganti, S. Mangani, P. Orioli, A. Scozzafava, G. Vernaglione, C.T. Supuran, " Carbonic Anhydrase Activators: X-ray Crystallographic and Spectroscopic Investigations for the Interaction of Isozymes I and II with Histamine" Biochemistry, 1997, 36(34), 10384-10392.

[57] C.A. Fierke, T. L. Calderone, J.F. Krebs, " Functional consequences of engineering the hydrophobic pocket of carbonic anhydrase II", Biochemistry, 1991, 30(46), 11054-11063.

[58] S. Lindskog, D.W. Silverman, "The catalytic mechanism of mammalian carbonic anhdrases. In The Carbonic Anhydrases – New Horizons", W.R. Chegwidden, Y. Edwards, N. Carter, Eds.; Birkhäuser Verlag, Basel, 2000, 175-196.

[59] D. K. Scrivastava, K. M. Jude, A. L. Banerjee, M. Haldar, S. Manokaran, J. Kooren, S. Mallik, D.W. Christianson, "Structural Analysis of Change Discrimination in the Binding of Inhibitors to Human Carbonic Anhydrases I and II", J. Am. Chem. Soc. 2007, 129, 5528-5537.

[60] C.T. Supuran, A. Scozzafava, A. Casini, "Carbonic Anhydrase Inhibitors", Medicinal Research Reviews 2003, 23, (2), 146-189.

[61] A. Casini, J. Antel, F. Abbate, A. Scozzafava, S. David, H. Waldeck, S. Schäfer, C. T. Supuran, "Carbonic Anhydrase Inhibitors: SAR and X-Ray Crystallographic Study for the interaction of Sugar Sulfamates/Sulfamides with Isozymes I, II and IV", Bioorg. Med. Chem. Lett. 2003, 13, 841-845.

[62] M. Ferraroni, F. Briganti, W. R. Chegwidden, C.T. Supuran, A. Scozzafava, "Crystal analysis of aromatic sulfonamide binding to native and (Zn)2 adduct of human carbonic anhydrase I Michigan1", Inorganica Chimica Acta 2002, 339, 135-144.

[63] C. Temperini, A. Scozzafava, D. Vullo, C.T. Supuran, "Carbonic Anhydrase Activators. Activation of Isoforms I, II, IV, VA, VII, and XIV with L-and D-Phenylalanine and Crystallographic Analysis of Their Adducts with Isozyme II: Stereospecific Recognition within the Active Site of an Enzyme and Its Consequences for the Drug Design", J. Med. Chem. 2006, 49, 3019-3027.

[64] K. K. Kannan, B. Notstrand, K. Fridborg, S. Lövgren, A. Ohlsson, M. Petef, " Crystal Structure of Humain Erythrocyte Carbonic Anhydrase B. Three-Dimensional Structure at a Nominal 2.2-A Resolution", Proc. Natl. Acad. Sci. USA 1975, 72, (1), 51-55.

[65] T. Stams, Y. Chen, P. A. Boriack-Sjodin, J. D. Hurt, J. Liao, J. A. May, T. Dean, P. Laipis, D.N. Silverman, D.W. Christianson, " Structures of murine carbonic anhydrase IV and human carbonic anhydrase II complexed with brinzolamide: Molecular basis of isozymedrug discrimination", Protein Science 1998, 7, 556-563.

[66] D.A. Whitington, J.H. Grubbs, A. Waheed, G.N. Shah, W.S. Sly, D.W. Christianson, " Expression, Assay, and Structure of the Extracellular Domain of Murine Carbonic Anhydrase XIV", J. Biol. Chem 2004, 279, (8), 7223-7228.

[67] D.A. Whitington, A. Waheed, G.N.Shah, J.H. Grubbs, W.S. Sly, D.W. Christianson, " Crystal structure of the dimeric extracellular domain of human carbonic anhydrase XII, a bitopic membrane protein overexpressed in certain cancer tumor cells". Proc. Natl. Acad. Sci. USA 2001, 98, (17), 9545-9550.

[68] C.T. Supuran, A. Scozzafava, " Carbonic Anhydrase Inhibitors and their therapeutic potential", Expert Opinion on Therapeutic Patent 2000, 10, (5), 575-600.

[69] C.T. Supuran, F. Briganti, S. Tilli, R. Chegwidden, A. Scozzafava, " Carbonic Anhydrase Inhibitors: Sulfonamide as antitumor agents? ", Bioorg. Med. Chem. Lett. 2001, 9, 703-714.

[70] A. Casini, A. Scozzafava, A. Mastrolorenzo, C.T. Supuran, " Sulfonamides and Sulfonylated Derivatives as anticancer agents", Current Cancer Drug Target 2002, 2, 55-75.

[71] I. Bertini, C. Luchinat, A. Scozzafava, "Carbonic anhydrase: an insight into the zinc binding site and into the active site through metal substitution", Struct. Bonding, 1982, 48, 45-92.

[72] F. Briganti, A. Pierattelli, A. Scozzafava, C.T. Supuran, " Carbonic anhydrase inhibitors. Part 37. Novel classes of isozyme I and II inhibitors and their mechanism of action. Kinetic and spectroscopic investigations on native and cobalt-substituted enzymes ", Eur.J.Med.Chem., 1996, 31(12), 1001-1010.

[73] M. Lindahl, J. Vidgren, E. Eriksson, J. Habash, S. Harrop, J. Helliwell, A. Liljas, M. Lindeskog, N. Walker, "crystallographic studies of carbonic anhydrase inhibtion. In Carbonic Anhydrase", F. Botrè, G. Gros, B.T. Storey. Eds., VCH, Weinheim, 1991, 111-118.

[74] J.-Y. Winum, A. Innocenti, J. Nasr, J.-L. Montero, A. Scozzafava, D. Vullo, C.T. Supuran, " Carbonic anhydrase inhibitors: synthesis and inhibition of cytosolic/tumor-associated carbonic anhydrase isozymes I, II, IX, and XII with Nhydroxysulfamides - a new zinc-binding function in the design of inhibitors", Bioorg Med Chem Lett FIELD Full Journal Title:Bioorganic & medicinal chemistry letters 2005,15, (9), 2353-8.
[75] I. Huc, J.-M. Lehn, "Virtual combinatorial libraries: dynamic generation of molecular and supramolecular diversity by self assembly", Proc. Natl. Acad. Sci. U.S.A. 1997, 94, 2106–2110.

[76] R. Nguyen, I. Huc, "Using and enzyme's active site to template inhibitors", Angew. Chem., Int. Ed 2001, 40, 1774–1776.

[77] S.-A. Poulsen, L. F. Bornaghi, "Fragment-based drug discovery of carbonic anhydrase II inhibitors by dynamic combinatorial chemistry utilizing cross metathesis", Bioorg. Med. Chem. 2006, 14, 3275– 3284.

[78] S.-A, Poulsen, "Direct screening of a dynamic combinatorial library using mass spectrometry", J. Am. Soc. Mass Spectrom. 2006, 17, 1074–1080.

[79] S.-A Poulsen, R.A. Davis, T.G. Keys, "Screening natural product-based combinatorial library using FTICR mass spectrometry", Bioorg. Med. Chem. 2006, 14, 510–515.

[80] N. Giusepponne, J.-M. Lehn, "Protonic and Temperature Modulation of Constituent Expression by Component Selection in a Dynamic Combinatorial Library of Imines." , Chem. Eur. J. 2006, 12, 1715–1722.

[81] J.-M. Lehn, "Dynamic combinatorial chemistry and virtual combinatorial libraries", Chem. Eur. J. 1999, 5, 2455–2463.

[82] J.-M. Lehn, "Toward complex matter: Supramolecular chemistry and self-organization", Proc. Natl. Acad. Sci. U.S.A. 2002, 99, 4763– 4768.

[83] A. Valade, D. Urban, J.-M. Beau, "Two galactosyltransferases' selection of different binders from the same uridine-based dynamic combinatorial library", J. Comb. Chem. 2007, 9, 1–4.

[84] C.T. Supuran, M. Barboiu, C. Luca, E. Pop, A. Dinculescu, "Carbonic Anhydrase Activators. Part 14. Syntheses of positively charged derivatives of 2-amino-5-(2-aminoethyl) and
2-amino- 5-(2-aminopropyl)-1,3,4 thiadiazole and their interaction with isozyme II. ", Eur. J. Med. Chem. 1996, 31, 597–606.

[85] F. Dumitru, E. Petit, A. van der Lee, M. Barboiu, " Homo- and Heteroduplex Complexes Containing Terpyridine-Type Ligands and Zn^{2+} ", Eur. J. Inorg. Chem. 2005, 21, 4255-4262.

[86] Y.-M. Legrand, A. van der Lee, M. Barboiu, " Self-Optimizing Charge-Transfer Energy Phenomena in Metallosupramolecular Complexes by Dynamic Constitutional Self-Sorting", Inorg. Chem.2007, 46(23), 9540-9547.

[87] M. Barboiu, E. Petit, A. van der Lee, G. Vaughan, " Constitutional Self-Selection of [2 × 2] Homonuclear Grids from a Dynamic Mixture of Copper(I) and Silver(I) Metal Complexes", Inorg. Chem. 2006,45(2), 484-486.

[88] M. Barboiu, J.-M. Lehn, " Dynamic chemical devices: modulation of contraction/extension molecular motion by coupled-ion binding/pH change-induced structural switching", Proc. Natl. Acad. Sci. U.S.A. 2002, 99, 5201.

[89] M. Barboiu, F. Dumitru, Y.-M. Legrand, A. van der Lee, " Self-sorting of equilibrating metallosupramolecular DCLs via constitutional crystallization" Chem. Commun. 2009,(16), 2192-2194.

[90] F. Dumitru, Y.-M. Legrand, E. Petit, A. van der Lee, M. Barboiu, " Constitutional self sorting of homochiral supramolecular helical single crystals from achiral components", Chem. Commun. 2009,(19), 2667-2669.

[91] G. Nasr, E. Petit, C.T. Supuran, J.-Y. Winumc, M. Barboiu, " Carbonic anhydrase II-induced selection of inhibitors from a dynamic combinatorial library of Schiff's bases", Bioorganic & Medicinal Chemistry Letters 19(21), (2009) 6014–6017.

[92] G. Nasr, E. Petit, D. Vullo, J.-Y. Winum, C. T. Supuran, M. Barboiu, " Carbonic Anhydrase-Encoded Dynamic Constitutional Libraries: Toward the Discovery of Isozyme-Specific Inhibitors", J. Med. Chem. 2009, 52(15), 4853–4859.

[93] A. Innocenti, A. Scozzafava , S. Parkkila, L. Puccetti, G.D. Simone, C.T. Supuran, "Investigation of the Esterase, Phosphate, and Sulfatase Activities of the Cytosolic Mammalian Carbonic Anhydrase Isoform I, II and XIII with 4-nitrophenyl Esters as Substrates. ", Bioorganic & Medicinal Chemisry Letters, 2008, 2267-2271.

[94] A. Thorslund, S. Lindskog, " Studies of the Esterase Activity and Anion Inhibition of Bovine Zinc and Cobalt Carbonic Anhydrases. ", Europen J. Biochem.1967, 117-123.

[95] C. Luca, M. Barboiu, C.T. Supuran, "Stability constant of complex inhibitors and their mechanism of action". Rev Roum Chim., 1991, 36(9–10):1169–1173.

[96] M. Barboiu, C. T. Supuran, L. Menabuoni, A. Scozzafava, F. Mincione, F. Briganti and G. Mincione,"Carbonic Anhydrase Inhibitors. Synthesis of Topically Effective Intraocular Pressure Lowering Agents Derived from 5-(ω-Amino-Alkylcarboxamido)-1,3,4-Thia-Diazole-2-Sulfonamide", J. Enzyme Inhib. 2000, 15(1), 23–46.

[97] V. Alterio, A. Di Fiore, K. D'Ambrosio, C. T. Supuran and G. De Simone,"Multiple Binding Modes of Inhibitors to Carbonic Anhydrases: How to Design Specific Drugs Targeting 15 Different Isoforms?", Chem. Rev., 2012, 112(8), 4421–4468.

[98] C. Temperini, A. Cecchi, A. Scozzafava, C. T. Supuran,"Carbonic anhydrase inhibitors. Comparison of chlorthalidone, indapamide, trichloromethiazide, and furosemide X-ray crystal structures in adducts with isozyme II, when several water molecules make the difference",Bioorg. Med. Chem., 2009,17(3), 1214–1221.

[99] C. T. Supuran, "Bacterial Carbonic Anhydrases as Drug Targets: Toward Novel Antibiotics?",Front. Pharmacol., 2011, 2(34), 1–6.

[100] A. Scozzafava, B. Iorga and C. T. Supuran,"Carbonic Anhydrase Activators: Synthesis of High Affinity Isozymes I, II and IV Activators, Derivatives of 4-(4-Tosylureido-Amino Acyl) Ethyl-1H-Imidazole (Histamine Derivatives)",J. Enzyme Inhib., 2000,15(2),139–161.

[101] C. T. Supuran,"Structure-based drug discovery of carbonic anhydrase inhibitors", J. Enzyme Inhib. Med. Chem., 2012, 27(6), 759–772.

[102] C. T. Supuran,"Carbonic anhydrase inhibitors", Bioorg. Med. Chem. Lett., 2010, 20(12), 3467–3474.

6. Appendix

6.1. Appendix I: The estimation of the activity of carbonic anhydrase using Uv- spectroscopy:

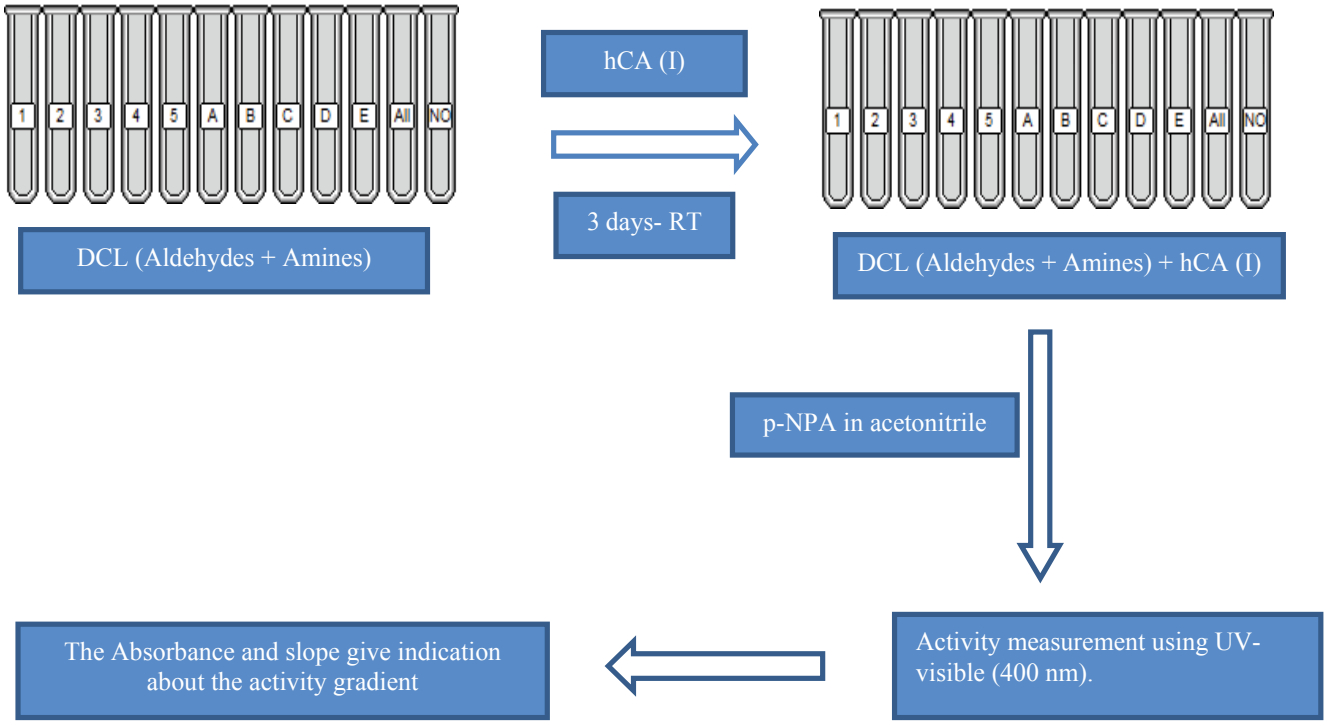

Scheme 3: The determination of human carbonic anhydrase activity using the Uv-Visible spectroscopy at 400 nm.

Chapter (2)

Membrane separation and extraction of lanthanides with constitutional dynamic networks.

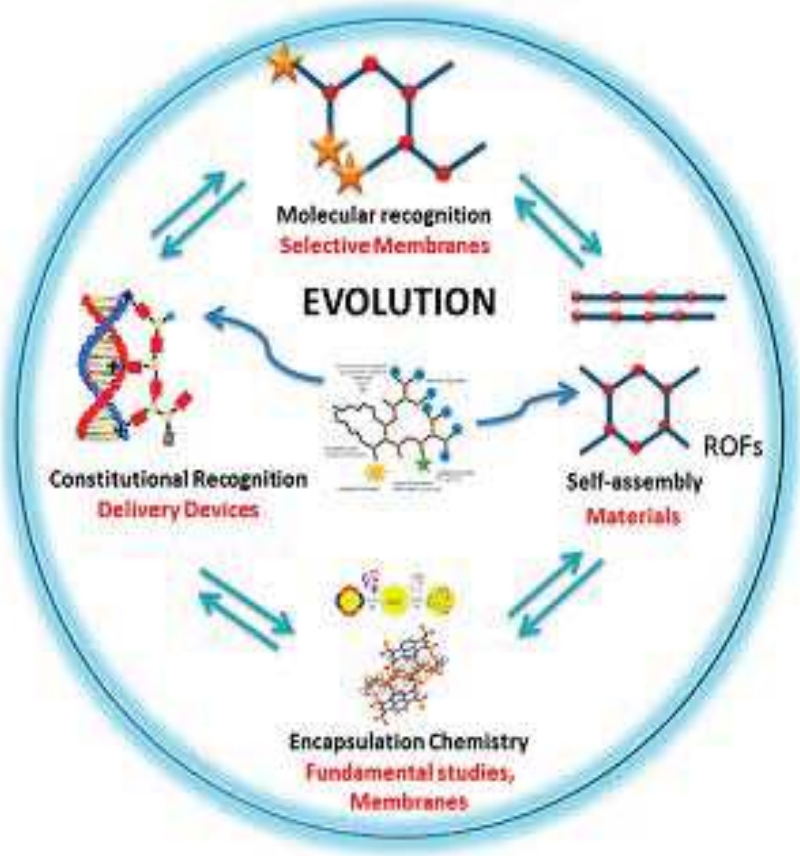

Abstract

Dynamic covalent polymers or dynamers, generated from reversibly interacting monomers, offer the possibility to generate homogeneous molecular networks with addressable domains based on structural relationships different from the former monomers. Constitutional dynamic networks have been used in liquid and solid membrane systems as a carrier network for transporting lanthanides. The transport is based on the complexing ability of lanthanides metals (La^{3+}, Lu^{3+}, and Eu^{3+}) with the functional polyether groups in the membrane materials. Based on corresponding dynamic diffusional domains within the solid and liquid bulk membrane phases, the lanthanides are extracted and selectively transported through the membrane, only in the presence of constitutional networks, while the former monomers did not show any selectivity. This would be explained by the formation of a dynamic self-assembly of low-size and molecularly addressable recognition networks in which the diffusional/selective percolation pathways might exist.

Keywords:
Constitutional dynamic networks; Liquid and Solid membrane; Dynamers; Lanthanides; Complexing ability; Exctraction; Selectivity.

Aims of the research work

The main aims of this research work will be as following:

1. Synthesis, characterization, and application of the constitutional dynamic networks as membrane materials.

2. Selective extraction of lanthanides through the prepared membrane materials.

3. Use of the constitutional dynamic networks (Dynamers) in liquid and solid membrane systems as a carrier network for transporting lanthanide metal ions.

1. Introduction

Nowadays, radioactive wastes that are hazardous to environment and human beings represent one drawback to be overcome since they will still be produced in a near future. These wastes mainly originate from the civil nuclear power programmes, medical, industrial and research uses of radioactive materials and in some cases, from military programmes. Radioactive contaminated residues also result from industrial activities such as oil extraction, where radioactivity is incidental. In all cases, radioactive waste needs to be managed responsibly to ensure public safety, protection of the environment, and security from malicious intervention now and in the future.

1.1. Various Effects of Lanthanides

In this study, some lanthanides are separated and extracted from their aqueous solutions by using polymeric materials (Dynamers). This is due to three important reasons:

- Their effects on the environment.
- Their effects on human health.
- Their importance in many industrial applications.

1.2. Separation and Preconcentration of Elements

The determination of particular elements is usually proceeded by their separation from the major components (matrix) of the sample and from other elements. In the trace analysis of high-purity materials, separation from the matrix involves simultaneous preconcentration of the trace components. Separation methods often enable a particular element to be determined in a sample containing no interfering elements [1]. The present section comprises a discussion of some methods of preconcentration and separation as following [2].

1.2.1. Solvent Extraction

Solvent extraction separation is based on the solubility differences of elements and their compounds in two immiscible liquid phases. Usually, one phase consists in an aqueous solution and the second one is an organic solvent immiscible with water. Shaking both phases in a separating funnel during an extraction or re-extraction must be continued until equilibrium is attained. The time required for the system to reach equilibrium varies from seconds to several minutes, depending on the kinetics of the extraction [3, 4]. When the shaking time recommended

is more than two minutes, it is advisable to use a mechanical shaker. Extraction is equally useful in the preconcentration and separation of small amounts of elements, and in the separation of macro components from traces. Extraction methods generally require less time than precipitation methods. The former also give purer separations of elements owing to the small area of phase contact. Co-extraction has been little explored in separation methods, though it may be useful.

1.2.2. Precipitation

Precipitation methods for the separation of elements are based on the differences in solubility of their compounds in aqueous solutions. Precipitation methods are used for separating trace elements alone, as well as for separating macrocomponents from the traces. Trace elements are separated quantitatively from the solution by using collectors (scavengers or carriers). When macrocomponents are precipitated, the aim is to prevent trace elements from co-precipitation with the large mass of the macrocomponent precipitate. This pre-requisite restricts the application of the method to cases in which co-precipitation of trace elements with the macrocomponent precipitate is negligible.

1.2.3. Floatation

Ions of precipitate particles are adsorbed or attached to the surfaces of bubbles rising through the liquid, and are thereby separated. A substance, which is not surface active itself, can be made so through union with, or adherence to, a surface active agent (surfactant). Froth floatation involves separation (preconcentration) by frothing. If an insoluble product results from interaction between the ion to be separated and a surfactant, the process is called floatation. If the ion is first precipitated and the precipitate is then floated with or without addition of surfactant, the process is called precipitate floatation. Floatation is accomplished in a special cylindrical vessel provided with a sintered-glass disk at the bottom to break the gas (nitrogen, air) stream into small bubbles. Precipitate floatation is applied in the analysis of natural water.

1.2.4. Electrolysis

In an acid solution, the electrolytic deposition of metal on a solid cathode is limited to noble and semi-noble metals. For example, anodic dissolution is used to separate macroquantities of copper in the trace analysis of copper and its compounds. A sample in the form of bar, plate or wire is the anode in the electrolytic system. When current is passed through the electrolyte, copper is

deposited on the graphite cathode, while most trace elements are accumulated in the solution. In the trace analysis of platinum, the matrix was also separated on a cathode.

1.2.5. Volatility

This method for separating elements is based on differences in the vapor pressures of individual elements and their compounds. Covalent compounds are generally fairly volatile whereas ionic compounds are not, though polymeric covalent species (e.g. diamond) are non-volatile. Covalently bonded compounds are also more soluble in non-polar solvents. Therefore, volatile compounds bear certain resemblances to those soluble in non-polar solvents. Gas chromatography may be regarded as a special case.

1.2.6. Ion Exchange

Separation and concentration of trace elements can be achieved by using ion-exchangers. Ion-exchange processes are based on the reversal exchange of ions between the solid ion-exchange resin and a liquid eluent. Separation depends on the differences in stability of complexes, and the associated differences in distribution coefficients. Generally, ion-exchangers consist of a matrix of cross-linked polymerized hydrocarbons, which contains ionizable functional groups. The functional groups in cation-exchangers are $–SO_3H$, –COOH and –OH; those in anion exchangers are $–NR_3^+$, $–NR_2$, –NHR and $–NH_2$. In ion-exchange chromatography, the components retained by the ion-exchanger can often be separated by treatment with suitable eluents, the separation being achieved by pH-control and/or use of a complexing agent. Ion-exchangers serve to retain small and trace amounts of ions from solutions. They are often used to isolate trace elements from matrices (preconcentration of traces).

1.2.7. Adsorption

It is the process in which a specific substance or element is concentrated on a solid stationary phase. Adsorption is the most used way to concentrate materials at the solid-liquid interfaces. This type of adsorption can be distinguished into positive and negative adsorption. Positive adsorption is the concentration of the solute on the adsorbent surfaces. It is also referred to as specific adsorption. The solute usually decreases surface tension. On the other hand, negative adsorption is the concentration of the solvent on the adsorbent surface. The solute is then concentrated in the bulk solution; here, surface tension is increased [5].

Types of Adsorbents

Adsorbents can be classified according to their nature into inorganic and organic adsorbents.

1.2.7.1. Inorganic Adsorbents

Inorganic stationary phases receive a good attention in analytical separation method due to their special physical properties such as high resistance to oxidation and reduction process, high thermal stability and high radiation stability. The most important inorganic stationary phases are clay, zeolite and silica gel.

a) Clays

Clays as a natural sorption phase was used in separation of metal ions. Clays consist of two main units; the first one is a silica matrix in which the silicon atom is surrounded by four oxygen atoms in a tetrahedral structure, the second unit is an aluminum octahedral unit where aluminum atom is surrounded by six hydroxyl ions in an octahedral structure [6].

Clays are characterized by negative charges delocalized on their surfaces, so they are electrically neutral when binding with sodium ions. Thus, clays can be used as ion-exchangers according to the following equation (1):

$$M + X\text{-Clay} \longrightarrow M\text{-Clay} + X \qquad \text{(Eq.1)}$$

Where M and X represent the metal ion in solution and metal ion attached to the clay, respectively.

Clays can be used as adsorbents, catalysts or catalyst supports, ion exchangers, decolorizing agents, etc., depending on their specifc properties. For example, the high surface area and surface polarity of some clays determine high adsorption and water-retention capacities. Clays also play an important role in agriculture, considering that many soils contain large amounts of clay materials, which determine key soil properties (structure, texture, water retention, fertility, etc.). Clays may be divided into two broad groups: cationic clays, widespread in nature, and anionic clays, rarer in nature but relatively simple and inexpensive to synthesize. The cationic clays have negatively charged alumino-silicate layers, which have cations in the interlayer space to balance the charge, while the anionic clays have positively charged metal hydroxide layers with balancing anions and water molecules located interstitially. Cationic clays are generally prepared starting from the minerals, whereas anionic clays used industrially are synthetic [6].

b) Zeolites

Zeolites are crystalline aluminosilicates of alkali or alkali earth elements, such as sodium, potassium, and calcium, that are represented by the general chemical composition below:

$$M_{x/n}[(A1O_2)_x(SiO_2)_y]. zH_2O,$$

Where (x) and (y) are integers with y/x equal to or greater than 1, n is the valence of cation M, and z is the number of water molecules in each unit cell. The primary structural units of zeolites are the tetrahedral of silicon and aluminum, SiO_4 and $A1O_4$. These units are assembled into secondary polyhedral building units such as cubes, hexagonal prisms, octahedral, and truncated octahedral. The silicon and aluminum atoms, located at the corners of the polyhedra, are joined by a shared oxygen. The final zeolite structure consists of assemblages of the secondary units in a regular three-dimensional crystalline framework. Substitution (i.e., isomorphous substitution) of other elements for Al and/or Si in the zeolite framework can yield myriad molecular sieves (which are formally not zeolites). However, the main interest for synthesizing these new molecular sieve materials was in catalysis for developing (1) large pores or channels and (2) catalytic sites other than acid sites [7].

c) Activated Carbon

Activated carbon is the most widely used sorbent. Its usefulness derives mainly from its large specific surface area. The modern manufacturing processes basically involve the following steps: raw material preparation, low-temperature carbonization, and activation. Thermal decomposition of carbonaceous materials such as wood, peat, coals, bones, and coconut shell followed by activation with steam or carbon dioxide at elevated temperature (700-1100°C) results in activated carbon. The activation process involves essentially the removal of tarry carbonization products formed during the pyrolysis, thereby opening the pores [8, 9].

The unique surface property of activated carbon, in contrast to the other major sorbents, is that its surface is non-polar or only slightly polar as a result of the surface oxide groups and inorganic impurities. This unique property gives activated carbon the following advantages [10]:

1. It is the only commercial sorbent used to perform separation and purification processes without requiring prior stringent moisture removal, which is needed in air purification. For the same reason, it is also widely used as a sorbent for processes of treating aqueous solutions.

2. Because of its large, accessible internal surface, it adsorbs more non polar and weakly polar organic molecules than other sorbents do.

3. The heat of adsorption, or bond strength, is generally lower on activated carbon than on other sorbents. This is because only non-specific, van der Waals forces are available as the main forces for adsorption.

d) Activated Alumina

Activated alumina is a porous high-area form of aluminum oxide, prepared either directly from bauxite ($Al_2O_3.3H_2O$) or from the monohydrated alumina by dehydration and recrystallization at elevated temperature. The surface is more strongly polar than that of silica gel and has both

acidic and basic character, reflecting the amphoteric nature of the oxide. The affinity of activated alumina for water at room temperature is comparable to that of silica gel with a lower capacity. At elevated temperatures, the capacity of activated alumina is higher than silica gel and it was therefore commonly used as a desiccant for drying warm air or gas streams. However, for this application it was largely replaced by molecular sieve adsorbents, which exhibit both a higher capacity and a lower equilibrium vapor pressure under most conditions of practical importance [11].

e) Silica Gel

Silica gel is of particular importance as stationary phase especially in high performance liquid chromatography (HPLC), because of no swelling and strain properties as well as good mechanical strength and thermal stability. Silica gel used in purpose of preconcentration of metal ions from aqueous media is too limited due to the weak interaction between metal ions and silica gel surface. The physical loading of chelating agent is a disadvantage for silica gel due to leaching of the loaded reagent. Therefore, the modification of silica gel by chelating agent chemically bonded on its surface improved its collection and selectivity properties. Many chelating agents bonded chemically on the silica gel surface such as ethylenediamine [12] and ninhydrin [13] were prepared.

1.2.7.2. Organic Adsorbents.

Organic adsorbents have received interest because of wide range of application of these phases in metal ions extraction and preconcentration from different aqueous media over wide range of pH. The selectivity and capacity of organic adsorbents are improved by incorporation of chelating reagents. In the last decades, attention has been focused on different types of organic stationary phases such as polyurethane foam and different forms of chelating organic polymers.

a) Polyurethane Foam

Polyurethane foam is the most widely used cellular plastics in separation and preconcentration of organic [14] and inorganic [15] species from aqueous and gaseous media. Polyurethane foam is defined as a plastic material in which a proportion of solid is replaced by gas in the form of numerous small bubbles. Polyurethanes are conventionally the reaction products of an isocyanate with an ether or ester and terminated with hydroxyl groups. While these materials are relatively resistant to hydrolysis, they can be readily cleaved by vigorous hydrolytic reactions. The polyurethane ether materials are more resistant to simple solution hydrolysis than the polyurethane esters.

b) Chelating Polymers

Immobilization of chelating reagent on polymeric materials received special attention for application in analytical chemistry. Immobilized chelating polymer can be investigated in three parts, namely: backbone of polymer, cross-linked degree and chelating reagent immobilized on polymer. In reference [16], authors reported facilitated transport of actinides and lanthanides from nitrate medium through a hollow fiber-supported liquid membrane using a mixture of N,N,N',N'-tetraoctyl diglycolamide (TODGA) and N,N-di-n-hexyl octanamide (DHOA) in normal paraffin hydrocarbon (NPH) as the carrier solvent. Hollow fiber-supported liquid membrane containing TODGA and DHOA in normal paraffin hydrocarbon (NPH) appeared promising for the separation of actinides and lanthanides from high-level waste.

c) Polymer Backbone

The nature of polymer backbone corresponds to the hydrophilic and hydrophobic characters of resin. For example, the polystyrene has low ability to interact with metal ions in aqueous media. In contrary, polyacrylamide has hydrophilic character and is highly interacting with water to adsorb metal ions on its surface.

d) Cross linking Degree in Polymer

The cross linking degree in a polymer is responsible of various properties of the chelating polymer [17, 18]. The lower cross-linking polymers allow faster diffusion especially of large ions; however they are very soft and tend to swell and shrink excessively [19]. The higher cross-linking polymers are harder and less easily deformed. The higher cross-linking degree of polymer renders its structure sufficiently rigid to be used under moderate or high pressure. The degree of cross-linking is controlled by the porous character of the polymer.

e) Chelating Reagent Immobilized on Polymer

In recent years, chelating reagent has been widely used in order to enhance the efficiency of separation of metal ions by polymeric support. An important feature of chelating ion exchanger is the greater selectivity compared with the conventional type of ion exchanger. The affinity of metal ions for a certain chelating resin depends mainly on the nature of chelating group and the selectivity behavior of the resin, which is largely based on the different stabilities of the complexes formed on the resin. The highly selective properties of chelating polymer rather than

ion exchanger are attributed to the higher binding energy in chelation process than in ion exchange process.

Traditional treatment methods employed for separation processes include chemical precipitation and filtration, chemical oxidation or reduction, electrochemical treatment, solvent extraction, ion-exchange and evaporation. They present some disadvantages such as their high price, difficulty of application, incomplete metal removal, low selectivity, high energy requirements and the generation of toxic slurries that are difficult to be eliminated [20,21].

Adsorption is one of the most respective methods that was successfully applied for removal of metal ions from hazardous wastes due to low maintenance costs, high efficiency and ease of operation [22]. According to that, the first objective of this research work will focuse on finding and contracting new adsorbent materials from the polymeric materials called (Dynamers) for the adsorption and extraction of lanthanide metal ions (La^{3+}, Lu^{3+}, Eu^{3+}) from aqueous solution.

1.3. Scope of constitutional dynamic chemistry

The extension of the concepts and features of supramolecular chemistry [23–25] from discrete species to polymolecular entities is opening novel perspectives in materials science. It defines a field of supramolecular materials that rests on the explicit implementation of intermolecular interactions and recognition processes for controlling the build-up, the architecture and the properties of polymolecular assemblies emerging from their components through self-organization [23–26]. Such spontaneous but directed self-assembly is of major interest for the supramolecular design, synthesis and engineering of novel materials presenting novel properties. Supramolecular chemistry is by nature a dynamic chemistry [27] in view of the lability of the noncovalent interactions connecting the molecular components of a supramolecular entity [23–25], which allows incorporation, decorporation, rearrangement of partners in the supramolecular species. Importing such dynamic features into molecular chemistry requires shifting from stable to labile covalent bonds, so as to endow molecular species with the ability to undergo similar dynamic exchange and reorganization processes by virtue of the reversible formation and breaking of covalent connections. This change in outlook amounts to take a standpoint opposite to the traditional one and to consider that the lability resulting from reversible connections rather than being a drawback, gives access both to the richness of constitutional diversity and to the benefits of adaptability.

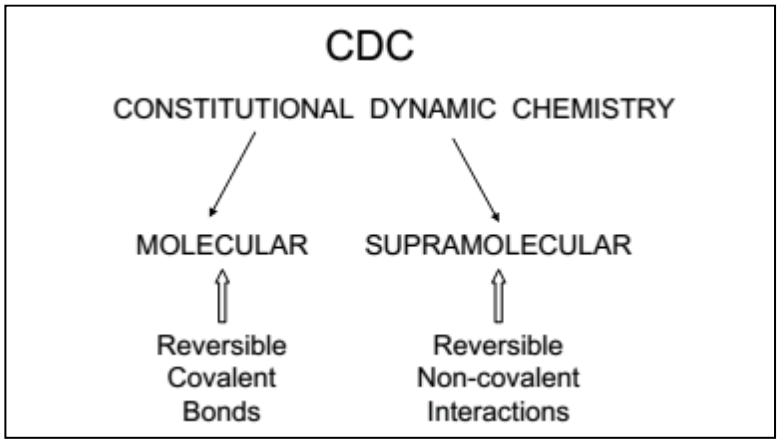

Fig.1: Scope of constitutional dynamic chemistry, covering both molecular and supramolecular entities [28].

One may conjecture that an intriguing line of development of chemistry is thus being fueled by a basic paradigm shift from a constitutionally static to a constitutionally dynamic chemistry (CDC) [25], encompassing both covalent molecular [29, 30] and non-covalent supramolecular entities (Fig.1) [23, 27, 30]. These may be considered as, respectively, chemically dynamic, involving a reversible chemical reaction, and physically dynamic, based on physical non-covalent interactions.

1.3.1. Constitutional dynamic chemistry and materials

Feeding-back the dynamic features, characteristic of supramolecular chemistry, into molecular chemistry implies looking at molecules as labile entities, in contrast to the usual longing for stability, and opens novel perspectives to covalent chemistry. It requires searching for reversible reactions that will allow the making and breaking of covalent bonds, preferentially under mild conditions. These developments are embodied in the recent emergence of dynamic combinatorial chemistry as a powerful means for generating dynamic, responsive molecular diversity [30, 31]. Thus, dynamic chemistry comprises not only motional dynamics, but also constitutional dynamics, changes in constitution concerning the nature, number and arrangement of the components of a molecular or supramolecular entity, generating molecular and supramolecular diversity through reversibility of covalent bonds and of non-covalent interactions. CDC is defined by chemical entities undergoing continuous recomposition, recombination, reorganization, construction and deconstruction by incorporation, decorporation or reshuffling of components, under the pressure of internal or external factors. The system may respond to such

effects through selection of the most suitable components among those available by expressing the constituents presenting best adaptation to a given situation (Fig.2) (28). As supramolecular chemistry is by nature constitutionally dynamic, supramolecular materials are dynamic materials (DYNAMATs) [27]. Extending this notion to covalent species, CDC covers constitutional dynamic materials (CDMs) on both the supramolecular and the molecular levels.

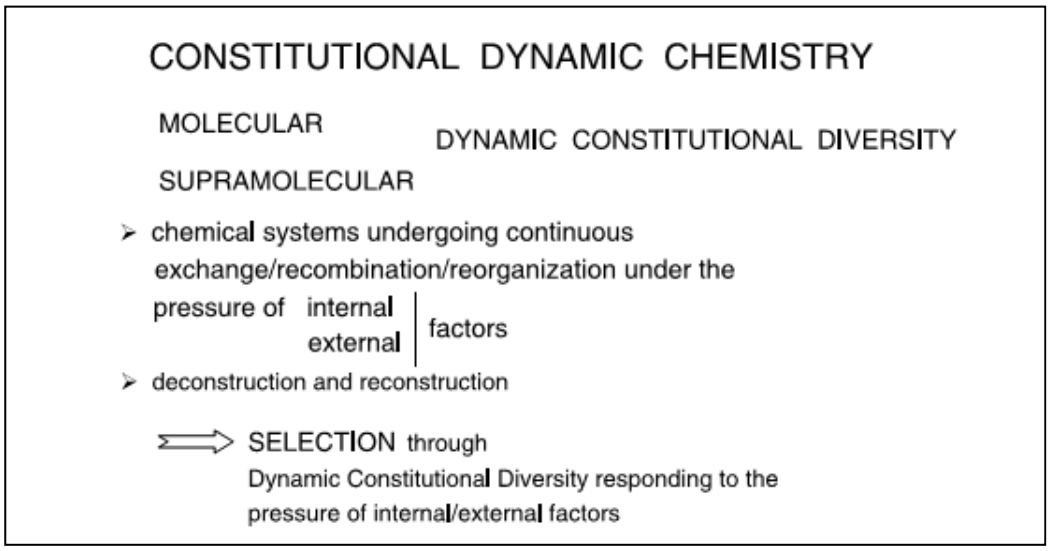

Fig.2: Constitutional dynamic chemistry, constitutional diversity generation and selection [28].

Dynamic materials may be defined as materials whose constituents are linked through reversible connections (non-covalent or covalent) and are able to continuously reorganize through assembly/disassembly processes and exchange of components in a given set of conditions, usually under thermodynamic control [27,30], but eventually involving kinetic bottlenecks or traps.

1.3.2. Dynamers: constitutional dynamic polymers

Focusing on a specific class of materials, polymers, one may designate under the term DYNAMERS, dynamic polymers [32, 33], polymeric materials exhibiting reversible formation and component exchange. They comprise both the supramolecular polymers [33–36] that are dynamic by nature and molecular polymers that are dynamic by intent, due either to the presence of a non-covalent or to the introduction of a covalent reversibility cassette (Scheme 1). Their

formation and dynamic character result either from recognition-directed reversible polyassociation of components through complementary interactional groups (supramolecular, non-covalent, physical, interactional recognition) or from reversible polycondensation of components through complementary functional groups (molecular, covalent, chemical, functional recognition), respectively (Fig.3). In view of the ability of dynamers to build up by self-assembly [23–26] and to select in principle their components in response to external stimuli or to environmental factors, they behave as adaptive materials [27,30,33].

Dynamers may be obtained from hetero- or homo-complementary monomers (Fig.4) by the usual type of polymerization processes (Fig.5). They may be of either main chain type, as those pictured below, or involve reversible side-chain attachment. They display a number of particularly attractive features for polymer chemistry [28].

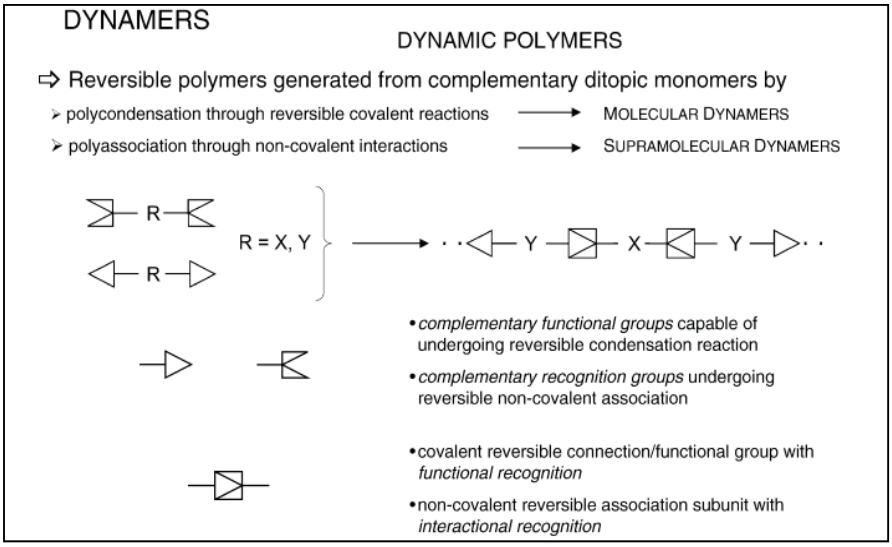

Fig.3: Dynamers: dynamic (reversible) polymers of molecular (covalent) and supramolecular (non covalent) nature [28].

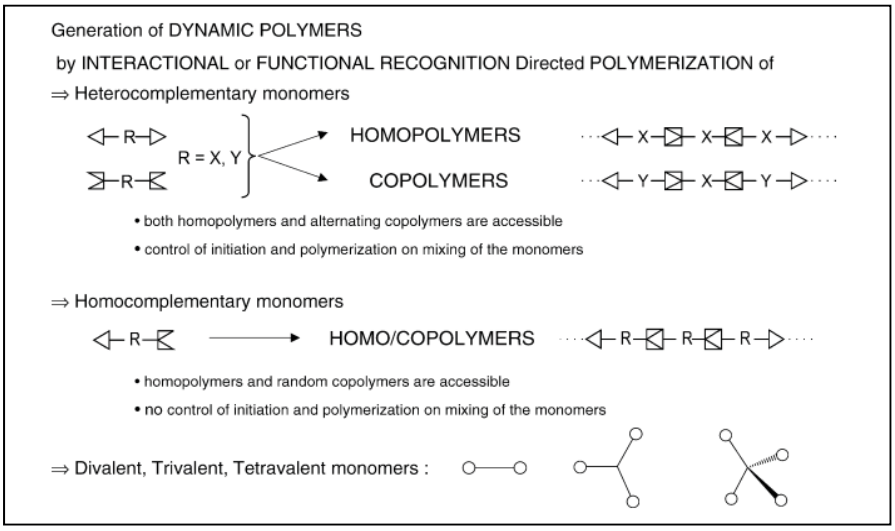

Fig.4: Dynamer chemistry: types of main-chain dynamers [28].

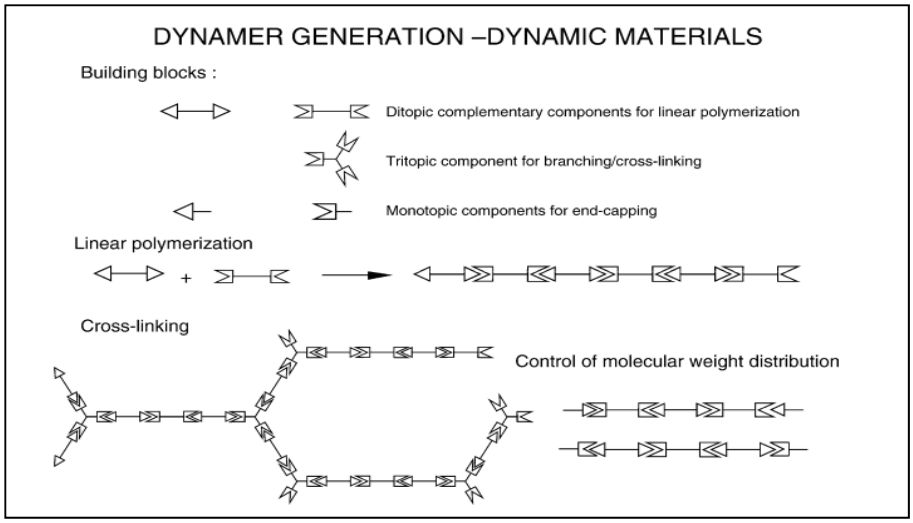

Fig.5: Dynamer generation processes [28].

1.3.3. Molecular dynamers

Molecular dynamers, reversible covalent polymers, open a range of perspectives to polymer chemistry. Even though exchange reactions have long been known in macromolecular chemistry [29] and have been put to use even in large scale industrial processes (involving, e.g. trans esterification), the exploitation of reversible polymerization has been hampered by the difficulties in controlling the process. The primary focus of polymer methodology has been on trying to avoid exchange reactions and to produce chemically as well defined as possible, unique

polymers, in particular for industry. Taking the opposite standpoint consists in deliberately pursuing constitutional diversity rather than emphasizing unicity. It involves exploring the generation of diversity through reversibility, which allows component exchange leading to highly diverse populations, combinatorial libraries of polymeric constituents in dynamic equilibrium (Fig.6). Reversible reactions are presently receiving increasing attention and provide a means for developing new materials exhibiting unusual features. Recent covalent polymers investigated for their reversible properties have included entities based on various reactions such as: transesterification [37–40], transetherification [41], Diels–Alder reaction [42, 43], [2+2] photodimerization [44], radical reaction [45] and boronate ester formation [46].

One may distinguish (1) self-contained reversible reactions (holo reactions), where all atoms present in the starting compounds are also present in the product (e.g. the Diels–Alder reaction and cyclo additions in general, the Michael addition, hemiketal and aldol condensation, etc. and their retro processes); (2) exchange reactions, where isofunctional components are exchanged from starting compounds to products (e.g. transesterification, transimination, etc.); and (3) non-self-contained reversible reactions, where an ancillary molecule (such as water) is formed (e.g. carbonyl-amine condensation, ester and amide formation, etc.).

Exchange and non-self-contained reactions may be manipulated or affected (e.g. their reversibility may be inhibited) by acting upon the ancillary compound or the isofunctional partner, whereas self-contained reactions respond to physico-chemical parameters (temperature, pressure, medium). Among the known reversible covalent reactions [29–31], amino/carbonyl condensations to give C=N products such as imines, hydrazones and oximes (Scheme 2), are particularly attractive in view of the very wide range of structural variations available, the easy synthetic accessibility, the control through conditions of yields, rates and reversibility, as well as their role and potential for application in both biological/medicinal [29,30,46] and materials sciences.

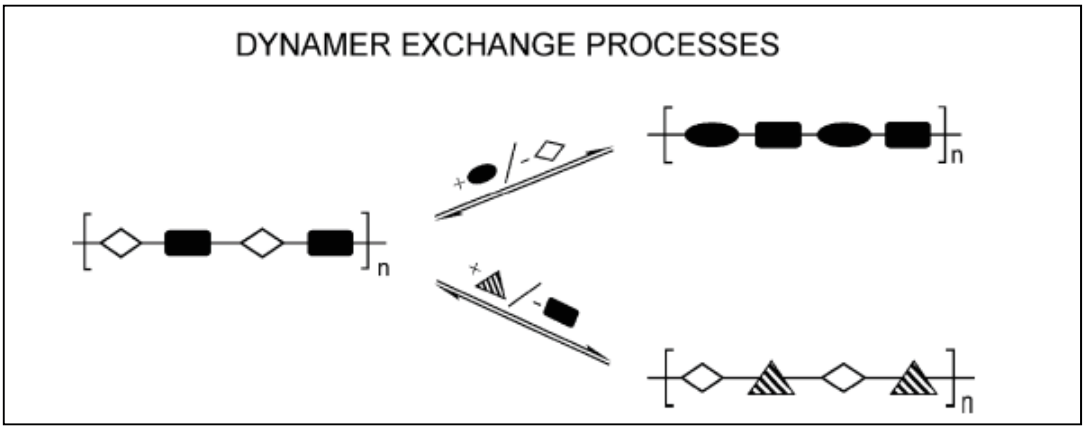

Fig.6: Component exchange in dynamers [28].

1.3.4. Supramolecular dynamers

Supramolecular polymers are defined as the entities generated by the polyassociation of molecular monomers bearing complementary binding groups capable of connecting through the usual non-covalent interactions implemented in supramolecular chemistry: electrostatic, hydrogen bonding, donor–acceptor, Van der Waals as well as metal ion coordination.

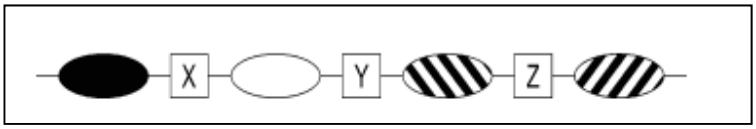

Scheme 1. Schematic representation of main-chain dynamers in which complementary ditopic monomers are linked by either supramolecular or molecular reversibility cassettes X, Y, and Z, conferring dynamic character through reversible connections, non-covalent interactions or reversible covalent bonds, respectively. X,Y, and Z may be the same or different. In conventional polymers, they represent covalent bonds that are not reversible in the conditions considered [28].

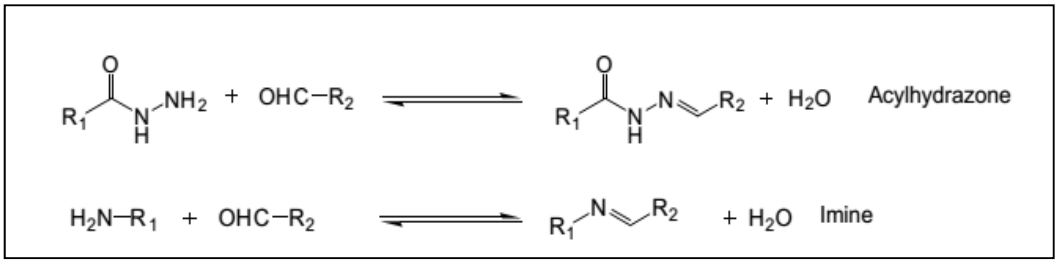

Scheme 2. Reversible condensation reaction in imine and acylhydrazone formation [28].

1.4. Constitutional dynameric networks for membranes

Membrane-mediated separations are an attractive alternative to other chemical methods for purification, recovery (i.e., ion exchange, extraction, or chromatographic processes), etc. [48-50]. Numerous artificial membrane systems using carriers or channel-forming structures have been developed in the past decades. The supramolecular design and application of receptors for recognition of cations, anions, or molecular species have attracted a great deal of interest as these systems have many potential functions such as solubilization, extraction, and membrane transport [49–55]. Concurrently, convergent multidimensional self-assembly strategies have been used for the synthesis of ion-channel self-organized systems, designed to mimic natural ion-channel proteins. Crown ethers [49–55], cyclic peptides [56], barrel-stave structures [57], and bolaamphiphiles [58] illustrate the convergence of molecular recognition and supramolecular self-organization properties with the supramolecular transport functions. They define the field of supramolecular membrane materials. Of particular interest is the potential ability of supramolecular membranes to present multifunctional properties such as molecular recognition [58–61] and generation of directional diffusion pathways by self-assembling [62–65]. It was previously showed that the basic molecular information encoded in the molecular precursors (i.e., crown ethers [58–63], amino acids [64], and nucleobases [63, 65]) results in the generation of isotropic superstructures in solution and in the solid state, which can be "frozen" in a polymeric solid membranes. These systems have been successfully employed to design artificial ion channels and illustrate how a self-organized material performs interesting and potentially useful transport functions. On the other hand, supramolecular chemistry is by nature a dynamic chemistry in view of the reversibility of the non-covalent interactions connecting the molecular components of a supramolecular system [48,66]. During the past decades, constitutional dynamic chemistry (CDC) and its application in dynamic combinatorial chemistry (DCC) served as new evolutional approaches that produced chemical diversity, convergent to molecular and supramolecular systems [66]. The dynamic self-assembly of the components may allow the flow of structural information from the molecular level toward nanoscale dimensions. Understanding and controlling such upscale propagation of structural information might offer the possibility of imposing a further precise order at the mesoscale and new routes to obtain highly ordered ultradense arrays over macroscopic distances. CDC provides an evolutional approach to the generation of chemical diversity at both the molecular and supramolecular levels through the

implementation of reversible covalent reactions and noncovalent intermolecular interactions, respectively. It confers chemical systems a fifth dimension, that of constitution, in addition to the 4D spatial/temporal chemical space. Within this context, during the past decade, the CDC has been expressing more and more interest toward dynamic interactive systems (DIS). Networks of reversibly exchanging and reorganizing connected objects form the core of DIS, operating under a natural selection to allow structural and functional adaptability in response to internal constitutional/affinity or to external stimulant factors. In other words, the CDC implements a dynamic reversible connection between interacting constituents, mediating the self-correlation of different constitutional domains of the system based on the structural affinity between them. Importing such dynamic features into the field of molecular and supramolecular polymers implies looking at dynamic polymers-dynamers [28, 67–71]. Compared with a physical mixture of classical polymers (Fig.7a), a dynameric mixture gives access via dynamic monomeric exchanges to new homogeneous entities presenting controllable modulation of their structure at the molecular level in response to internal structural constraints or to external stimuli and experimental conditions. They are capable of undergoing exchange, incorporation, or decorporation of their monomeric subunits (Fig.7b), linked together by labile non-covalent interactions or reversible covalent bonds. This might play an important role in the ability to more finely mutate the mechanical or functional properties of such new molecularly tunable materials, compared with physical mixtures of polymers [69–71]. Using this strategy, specific recognition domains (e.g., the AAAA signature in Fig.7c) would be more easily generated, giving access to molecularly controlled membrane materials. With all these in mind, the novel constitutional concepts previously described might open interesting perspectives for the generation of membrane materials in which selective transport occurs through molecularly controlled domains. The more significant challenge is to minimize the size of nanoscopic domains of the membrane material, which would give the possibility of achieving the molecular limit control for percolated conductive domains of high diffusional behaviors, specifically of interest in membrane science (Fig.8) [72,73]. In this context, the dynamic covalent polymers or dynamers (67, 68), generated from reversibly interacting monomers, offer the possibility of generating homogeneous systems with addressable domains based on structural relationships within the former monomers. In dynamers, the components self-assemble reversibly in such a manner that their external hyper surfaces might be able to maximize all structure/energy combinations via their constitutional

affinity. In such a scenario, the adaptive self-assembly might override defects and use the topography only as a guide to the formation/orientation of the segregated domains of different behaviors. The internal driving force is related to the pressure of internal structural stabilization: the constitution of or affinity between components. This would mediate the dynamic self-assembly of low size and molecularly addressable domains toward the macroscopic membrane films in which the diffusional/selective percolation pathways might exist (Fig.8).

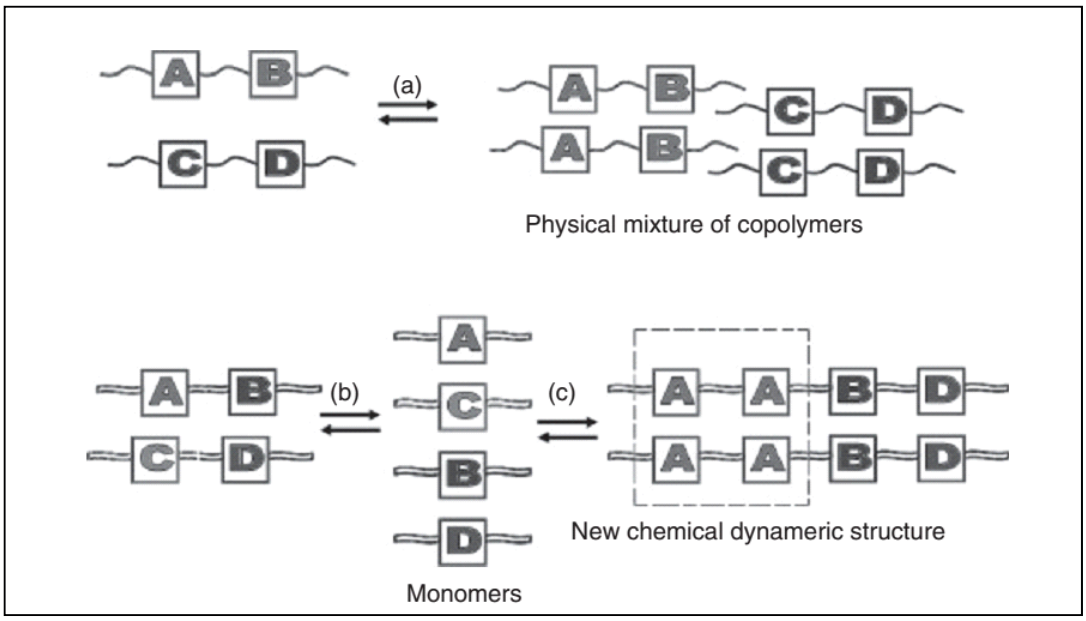

Fig.7: Structural comparative features between classical mixtures of (a) polymers in which the monomers are irreversibly connected and of (b) dynamers capable of undergoing reversible exchange of their monomeric subunits, giving more easy access to specific constitutional superstructures (e.g., the AAAA signature in (c) based on the enhanced constitutional affinity between the components A)[71,73].

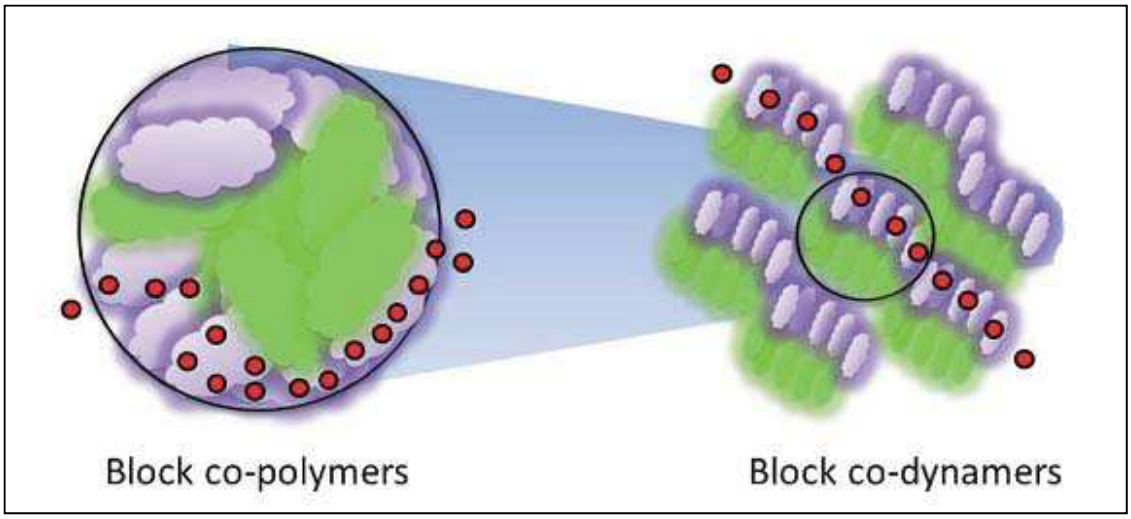

Fig.8: Converging the structural behaviors of block copolymers and of ultradense block codynamers controlled at the molecular level. The different iso-structural domains are represented in light grey and grey; the diffusing molecules are represented by black circles. The circled area details part of diffusion area within the respective materials [72,73].

For all these reasons, functional dynamic polymers "dynamers" may be used to conceive novel membrane materials. Our efforts involve the synthesis and the fabrication of "dynameric" polymeric membranes. Then, their transport performances (permeability and selectivity) are evaluated by using the solution-diffusion model. The membrane performances designed to transport ionic salts of lanthanides metal ions (La^{3+}, Lu^{3+}, Eu^{3+}) depend and are based on encoded molecular features of the monomeric subcomponents.

In the present study, we are exploiting the dynamic reversible covalent exchange processes of the constituent dynameric subcomponents in solution during the membrane synthesis. The resulting polymeric membranes are stable and are conserved during and after the membrane transport experiments.

2. Materials and procedures

2.1. Materials

In our experiments, benzene-1,3,5–tricarbaldehyde (TCA) (98%, Manchester Organics Ltd) , Jeffamine D-2000 and Jeffamine T-3000 were used to prepare the dynameric membranes. TCA was used as the core connectors of the membrane structures. Jeffamine D-2000 and Jeffamine T-3000 were used as monomers and purchased from Huntsman Holland BV. All the products were used as recieved without modifications. For all the solutions, chloroform was used as a solvent and purchased from Sigma Aldrich. Lanthanide (III) chloride (99%, Alfa Aesar), Lutetium (III) chloride (99%, Sigma Alrdich), and Europium (III) chloride hexahydrate (99%, Janssen chimica) have been used as the source of the lanthanides ions. Also Ascorbic acid (98%, Sigma), and Arsenazo III (98%, Fluka) were used for the UV-spectroscopy determination of lanthanides.

2.2. The synthesis of the polymeric materials

A series of polymeric materials has been prepared by using three main substances (polyoxypropylenediamine) Jeffamine D-2000, (polyetheramine) Jeffamine T-3000, and Benzene-1,3,5-tricarbaldehyde (TCA) as reactants. The cross-linking degree of the polymerwas varied by changing the molar fraction of Jeffamine material (J-D2000 and J-T3000) incorporated, while the molar fraction of TCA reactant was held constant as shown in the table (1). The structures and stability of the prepared series (P1-P7) were confirmed by Nuclear Magnetic Resonance spectrophotometry using a BRUKER NMR ADVANCE 300MHz spectrophotometer. In addition, the polymeric materials were characterized by ThermoGravimetric Analysis (Hi-Res TGA 2950,TA Instruments), Differential Scanning Calorimetry (DSC 2920 Modulated DSC, TA Instruments), FTIR Spectrometry (model Nicolet 710), and UV-visible Spectroscopy (A UVIKON 923, Double Beam UV-Vis Spectrophotometer), contact angle, Scanning Electron microscopy (SEM) (Hitachi S4800 Field effect microscope detector), and Energy Dispersive X-ray Spectroscopy (EDX) (Hitachi S4500 Field microscope).

Polymer	Mass TCA, g	Mass Jeffamine-D2000, g	Mass Jeffamine-T3000, g
P1	0.1 (mol. frac. 1)	1.86 (mol. frac. 1.5)	0
P2	0.1 (mol. frac. 1)	1.55 (mol. frac. 1.25)	0.32 (mol. frac. 0.17)
P3	0.1 (mol. frac. 1)	1.24 (mol. frac. 1)	0.61 (mol. frac. 0.33)
P4	0.1 (mol. frac. 1)	0.93 (mol. frac. 0.75)	0.93 (mol. frac. 0.5)
P5	0.1 (mol. frac. 1)	0.62 (mol. frac. 0.5)	1.25 (mol. frac. 0.67)
P6	0.1 (mol. frac. 1)	0.31 (mol. frac. 0.25)	1.54 (mol. frac. 0.83)
P7	0.1 (mol. frac. 1)	0	1.86 (mol. frac. 1)

Table1: Composition of the various prepared polymeric materials P1 to P7

-The polymeric materials were synthesized according to the following procedure

1. Weigh the suitable amount of reactant substances according to the above table.
2. Dissolve the reactant substances in 50 mL of chloroform.
3. Place the dissolved reactants in 100 mL round bottom flask and then reflux the reaction mixture at 70°C under stirring at around 450 rpm. For how long???
4. Keep the reaction running until it is completed. The reaction time for each synthesis was followed by ^{1}H NMR analysis.
5. Use the rotary evaporator at 40°C and 200 rpm to decrease the amount of chloroform solvent.
6. Cast the resulting polymeric materials by putting it in a Teflon plate then place it inside an oven successively at 60°C and 120°C overnight.
7. Leave the produced polymeric material inside the oven at 120 °C for more than two days, to allow the conversion into a very sticky material that do not swell during the extraction process of lanthanides.

- The chemical structures of the polymeric materials

Figs. (9, 10, and 11) represent the chemical structure of the prepared polymeric materials that have been used in the extraction and transportion process of lanthanides metal ions.

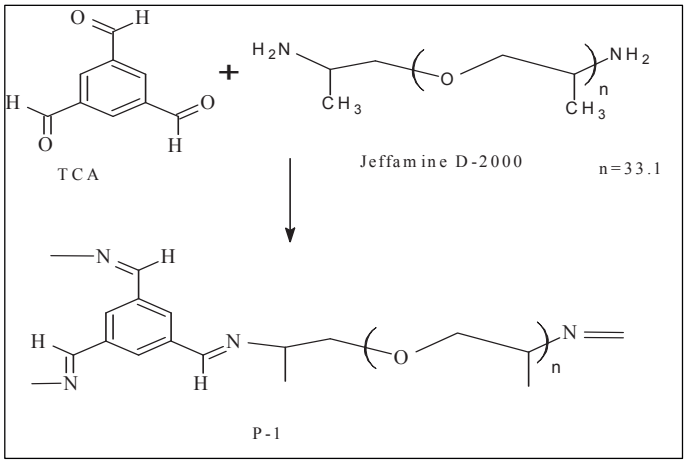

Fig.9: Scheme representing the chemical reaction between TCA and Jeffamine D-2000 leading to the synthesis of (P1).

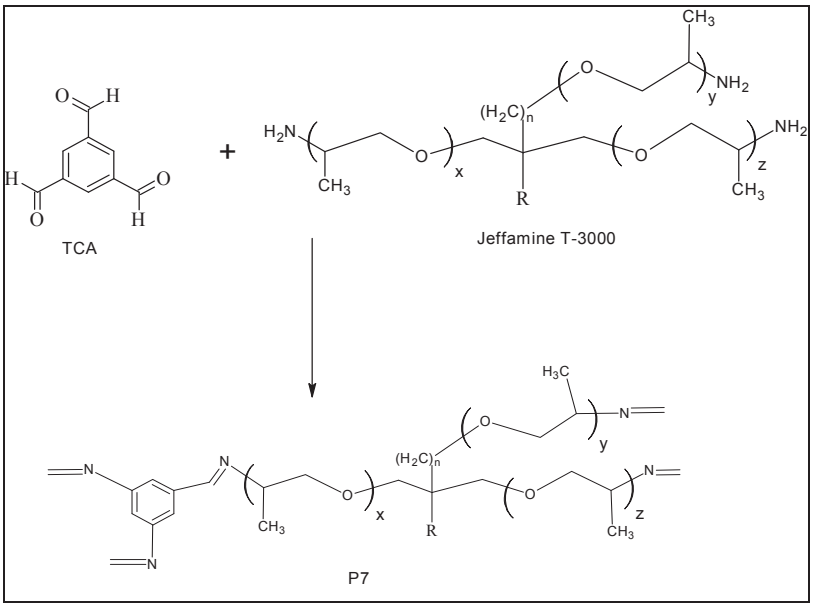

Fig.10: Scheme representing the chemical reaction between TCA and Jeffamine T-3000 leading to the synthesis of (P7).

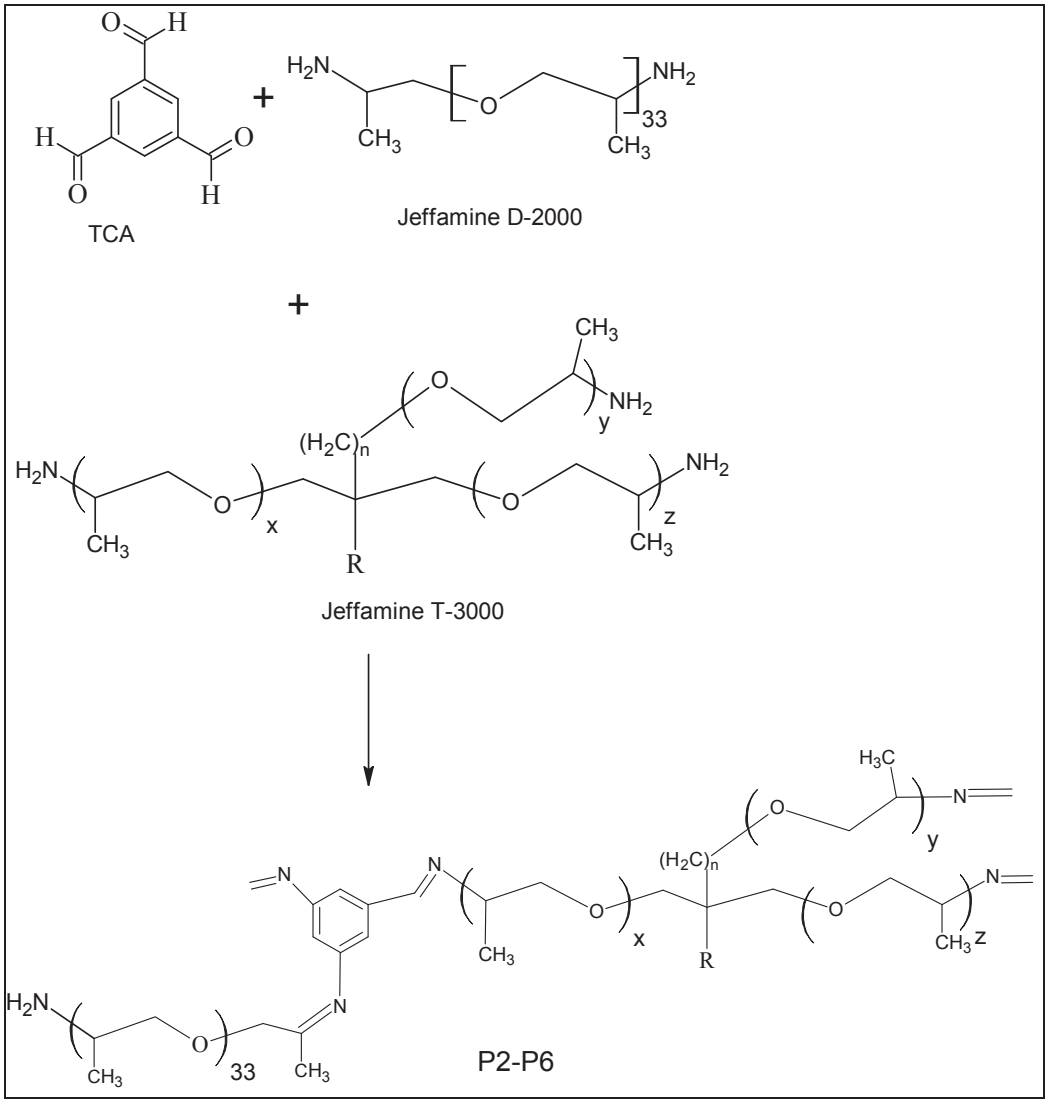

Fig.11: Scheme representing the chemical reaction between TCA, Jeffamine D-2000 and Jeffamine T-3000 leading to the synthesis of (P2 to P6).

2.3. Adsorption and extraction experiments

The solvent extraction and adsorption techniques are used with the prepared polymers for the separation processes of lanthanides. Firstly, a trial experiment was performed using a definite amount of the polymer dissolved in chloroform mixed with the aqueous phase containing the lanthanide ion. A sample from the aqueous phase was taken and analyzed by UV-Spectrophotometry using Arsenazo III as coloring agent to determine the remaining amount of the metal ion in the aqueous solution. On the other hand, adsorption technique can also be carried

out with the same conditions of the solvent extraction. The lanthanides determination was carried out according to the procedure proposed by Z. Marczenco (Analytical Spectroscopy Library, Vol. 10) as following: 1 mL (1% molar, 1 gm dissloved in 100 ml distilled water) of Ascorbic acid was added to a sample containing lanthanides metal ion, then 1 mL of formate Buffer was added to the mixture (28 g sodium hydroxide + 60 mL of formic acid/1L distilled water). Finally, 2 mL (0.05 % molar, Dissolve 0.05 g Arzenazo (III) in 100 ml of double-distilled water) of Arsenazo III solution was added and the total volume of the mixture was completed to 25 mL with distilled water. The UV absorbance was measured at 655 nm in the presence of the blank (Marczenko and Balcerzak, 2000).

Three lanthanide (La^{3+}, Lu^{3+}, Eu^{3+}) standard solutions of the same concentration (200 ppm) were prepared by dissolving the appropriate amounts of the corresponding chloride forms into distilled water. Dffernet amounts of the prepared polymeric materials were used for the adsprotion process for three lanthanide solutions seperatlly as the following (5 mL of lanhainde solutions were shaked over night with the certain amount of the polymeric materials). Then each sample was analyzed by spectrophotometry, and the uptake percentage can be calculated from the absorbance values using the following equation:

$$\% \text{ uptake} = (\text{Abs.}_{\text{int.}} - \text{Abs.}_{\text{fin.}}) / \text{Abs.}_{\text{int.}}$$

Where: (Abs. int.) is the absorbance of the standard solution before contact with polymer, while (Abs. fin.) is the same but after the sorption experiment.

2.4. Instrumental techniques

2.4.1. UV-visible spectroscopy

The uptake(%) of lanthanides was measured by UV spectrophotometry using the polymeric materials and Arsenazo III as coloring agent to determine the remaining amount of the lanthanide metal ions after the adsorption and extraction process. The detection process has been done at a wavelength of 655 nm to determine the solution colour. The principle of the UV-visible spectroscopy has been illustrated, see chapter (1).

2.4.2. Infrared spectroscopy (FTIR)

FTIR is a very useful tool for the analysis of the chemical structure of a polymer. Vibrational energies of chemical bonds measured identify the nature of these functional groups in the sample. The apparatus used in this study is a spectrometer Nicolet Nexus Fourier transform (speed of mirror = 0.6329 cm s^{-1}, iris aperture = 100, detector DTGS) equipped with a diamond ATR accessory Golden Gate whose resolution is 4 cm^{-1}. The swept frequency range covers the area of the mid-infrared 400 - 4000 cm^{-1}. The acquisition of the spectra is performed in transmittance mode (64 scans). FTIR technique has been used to confirm the complexation interaction between the polymeric materials and lanthanides metal ions by seeing the possibility of changes in functional groups of the polymeric materials due to the attachement of metal ions to the functional groups at the polymeric materials. The FTIR spectra have been taken for different configurations of the prepared polymeric materials containing different molar fractions of Jeffamine T-3000 (0, 50, 70 and 100%). The obtained results have been compared before and after extraction process to see if there were any differences in spectra, which will give indication about the complexation reaction occuring between the polymers and the lanthanides metal ions. See Appendix1 for FTIR measurements on other formed polymers.

2.4.3. Proton nuclear magnetic resonance spectroscopy (^{1}H NMR)

1H NMR spectra of the solutions were taken using a BRUKER NMR ADVANCE 300MHz spectrophotometer. Deuterated chloroform ($CDCl_3$) EURISO-TOP was used as solvent. Based on the NMR analysis, we could determine if the reaction was complete by comparing the integration of the aldehyde group R-CHO (present in TCA) at about 10ppm with that of the secondary aldimine group formed -RC=N-R due to the reaction between the aldehyde group in TCA and the amine group in Jeffamine, present at about 8ppm. Another alternative method was to compare the integration of the aldehyde group at 10ppm with that of the hydrocarbon group in the long chain of the Jeffamine present at about 1ppm. As will be seen in ^{1}HNMR figure analysis, the aldehyde group at 10ppm was seen to be insignificant in comparison with the integration at 8ppm and even too small compared to the one at 1ppm.

2.4.4. Thermogravimetric analysis (TGA)

Thermogravimetric analysis (TGA) involves heating a sample in an oven gradually and recording its weight loss function by the elevation of its temperature. Thermogravimetric profiles of polymeric materials have been made on a heat-balance type TGAQ50 Thermal Analysis under flow of inert gas (nitrogen). A region of 5-15 mg of polymer material was placed in a platinum crucible, then heated from -80°C to 500°C at a temperature gradient of 10°C/min. TA Universal Analysis software has enabled us to record and calculate the evolution of the mass and its derivative as a function of temperature. The plot of the derivative of the weight loss versus temperature allowed us to distinguish the begining of successive mass loss. Based on samples analysis, we can observe the thermograms, which represent the dehydration, the denaturation and degradation of the polymeric materials.

2.4.5. Differential Scanning Calorimetric Analysis (DSC)

This technique was used to determine the temperature of transition of the first order, (melting and crystallization), the specific heat, the degree of crystallinity in the polymers and their thermal conductivity. The principle consists in analyzing the recorded enthalpy differences between a sample and an inert reference each undergoes the same heat treatment. The sample, mass of about 2-5 mg was placed in an aluminum crimped and sealed vial so that the measurement is more accurate because the mass of the sample is constant. The measurements were performed on a TA Instruments DSC2920 machine equipped with a module between 150°C and 400°C at a heating rate of 10 °C/ min. The exploitation of the results was performed using the TA Universal Analysis software, marketed by TA Instruments.

2.4.6. Scanning electron microscopy (SEM)

The surface structure of the polymeric membranes prepared was analyzed using a Hitachi S4800 Field effect microscope detector secondary and backscattered electron. The acceleration voltage ranges from 0.1 kV to 30 kV. The maximum magnification is 800000x. The scanning electron microscope is operated with an electron beam intensity of 10kV. This microscope allows the observation and characterization of the membrane surface morphology at the scale of micro (10^{-6}) to nano (10^{-9}) meters. Cross section imaging can also be done by using the “tilt” facility, which

allows the sample to be held at an angle of 45° for analysis. The principle of SEM involves the incidence of an electron beam on the sample surface producing secondary electrons, backscattered electrons or retro-diffused X-rays that can be analyzed to obtain an image that is magnified over 200,000 times. $2cm^2$ pieces of the sample were cut in a liquid nitrogen environment to avoid distorting the material surface or cross section. The sample was then coated with a thin layer of gold or platinum particles to make it a good conductor.

2.4.7. Energy Dispersive X-ray Spectroscopy (SEM-EDX)

The surface structure and chemical composition of the polymeric membranes prepared were analyzed using a Hitachi S4500 Field microscope equipped with secondary electron detector and backscattered. The acceleration voltage ranges from 0.5 kV to 30 kV. The maximum magnification is 500000x. The resolution obtained is 1.5 nm at a voltage of 15 kV. This microscope also has a Thermo fisher EDX detector for chemical analysis of samples from the boron element. In addition to the analysis at a point or globally, concentration profiles can be achieved as well as maps showing the distribution of a chemical element in the observed area. During EDX analysis, the specimen is bombarded with an electron beam inside the scanning electron microscope. The bombarding electrons collide with the specimen atoms' own electrons, knocking some of them off in the process. A position vacated by an ejected inner shell electron is eventually occupied by a higher-energy electron from an outer shell. To be able to do so, however, the transferring outer electron must give up some of its energy by emitting X-ray, to balance the energy difference between the two electrons states. The amount of energy released by the transferring electron depends on from which energy level it has been transferred, as well as to which level it is transferred. Furthermore, the atom of every element releases X-rays with unique amounts of energy during the transferring process. Thus, by measuring the amounts of energy present in the X-rays being released by a specimen during electron beam bombardment, the identity of the atom from which the X-ray was emitted can be established.

2.4.8. Contact Angle

The contact angle (Θ) of a liquid drop on a solid surface is defined by the mechanical equilibrium of the drop under the action of three interfacial tensions: solid-vapour (γ_{SV}), solid-liquid (γ_{SL}) and liquid-vapour (γ_{LV}) (Fig.12).

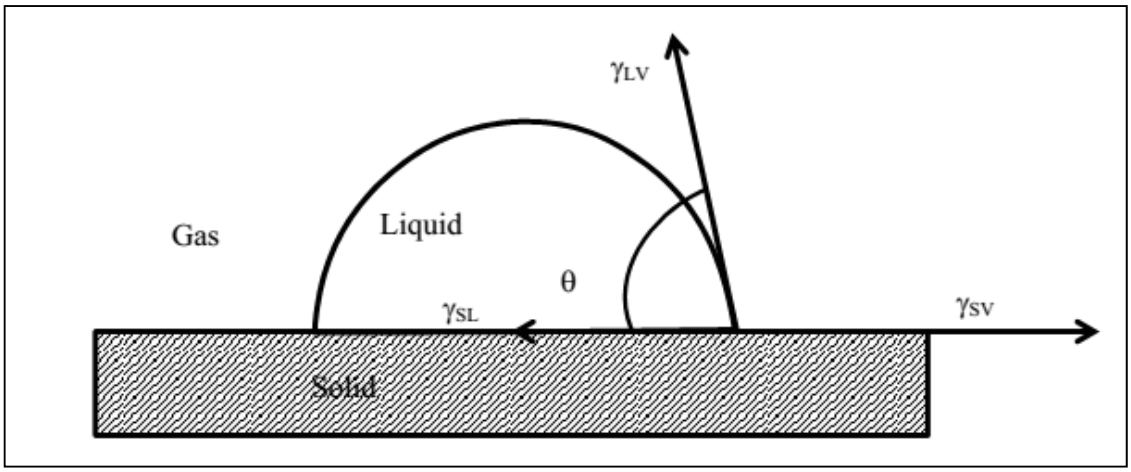

Fig.12: Schematic of a sessile drop, contact angle and the three interfacial tensions are shown [74].

The contact angle (Θ) was measured by sessile drop method. A drop of distilled water is deposited manually on the membrane surface by a Pasteur pipette. Various photographs are acquired by the software and the tangent is determined by fitting the drop shape to known mathematical functions. The measurements are performed immediately after the drop falls on the surface using the software called Imagei. Multiple replicates are performed and the mean contact angle is reported with its standard deviation.

2.5. Facilitated transport procedures through the polymeric membranes

The lanthanides metal ions have been transported through the polymeric membranes through two different ways (solid membranes and liquid membranes). In case of solid membranes, the membrane transport experiments were performed with a bi-compartmental device, magnetically stirred at room temperature (Fig.13). It consisted of two PTFE cell devices separated by the solid membrane oriented with the active dense film facing the feed phase. Nitrogen permeation measurements were performed to ensure that they were dense and defect free. While in case of liquid membranes, the membrane transport experiments were performed under magnetic stirring using a conventional U-tube glass cell, at room temperature. In both cases, the feed phase was an aqueous solution with a volume of 50 mL and a concentration of 200 ppm of lanthanides metal ions ($LaCl_3$. $(H_2O)_6$ / $LuCl_3$.$(H_2O)_6$ / $EuCl_3$.$(H_2O)_6$) solution for the competitive cation transport experiments. The membrane consisted of supported "dynamer" dense material (S= 5.32 cm^2) while the receiving phase consisted of 50 mL of deionized water. The La^{3+}, Lu^{3+}, and Eu^{2+} concentrations were monitored at different time intervals using UV- spectrophotometry. The permeabilities (P) and the partition coefficient ratio of ions have been determined from experimental concentration versus time profiles using the solution-diffusion model [59-64].

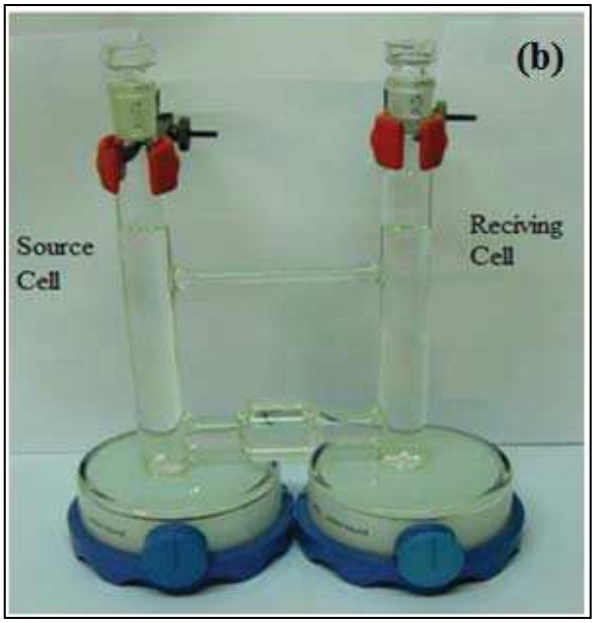

Fig.13: Experimental devices used in membrane transport experiments, (a) Solid membrane, (b) Liquid membrane.

3. Results and Discussion

3.1. Uptake(%) of lanthanides for the Jeffamine polymers

Fig.14 represents the uptake(%) of lanthanides metal ions (La^{3+}, Lu^{3+}, Eu^{3+}) using Jeffamine polymers as absorbing agents of lanthanides. The experimental work has been done at room temperature under shaking overnight. The absorption and extraction of lanthanides depend on the complexing and chelating properties between the amine groups present in these polymers and the different metal ions. It has been observed that the uptake(%) is higher in case of J-T3000 than J-D2000 due to the increment in the number of amino groups in J-T3000 compared to J-D2000.

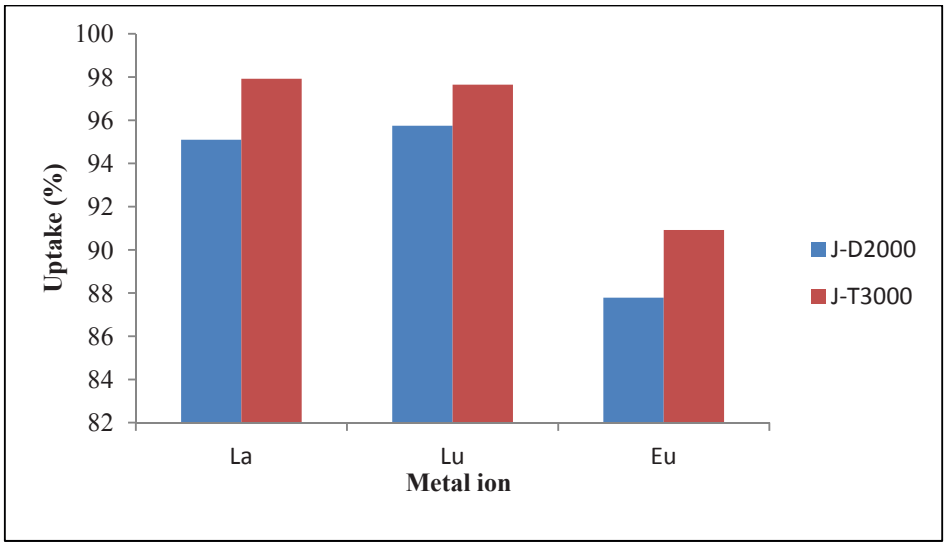

Fig.14: The uptake(%) of lanthanides for the Jeffamine polymers.

3.2. Effect of contactor towards the Jeffamine structure

The polymerization of TCA cross-linker with both Jeffamine polymers (J-T3000 and J-D2000) lead to a series of dynameric polymeric materials. These dynameric networks have been used for the extraction of lanthanide metal ions, and the uptake of lanthanides are shown in (Fig.14) representing the variation percentage of J-T3000 with the uptake (%) of lanthanide metal ions (La^{3+}, Lu^{3+}, Eu^{3+}).

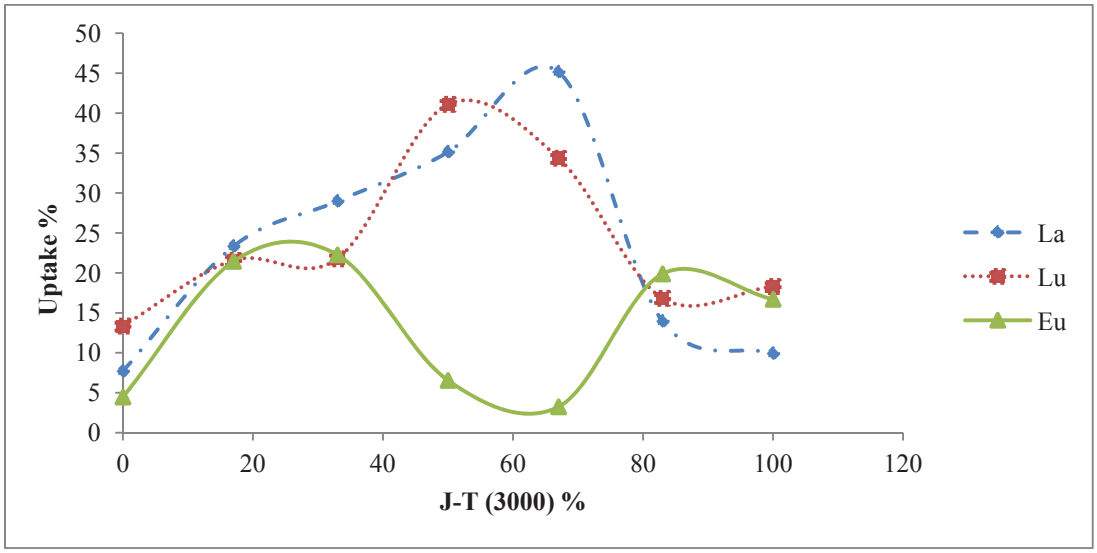

Fig.15: The variation of J-T3000 (%) in the synthesized polymers with the uptake (%) for lanthanides.

The above figure shows that there is a different uptake(%) of lanthanides by using different polymeric materials (P1-P7); this might be related to the difference in the cross-linking degrees of each polymer used in the extraction process. The separation by such polymers may be depending on the availability of the electrons lone pairs of both nitrogen and oxygen atoms present in the Jeffamine substrates. These free electrons can be donated to the empty orbital of the metal ions through a coordination bond. Another aspect for the separation mechanism might be the size of pores of the polymer materials that are suitable for a specific metal ion over the other one. Additionally, it is obvious from (Fig.15) that Europium ion can be separated from the other two lanthanides by using P5 or/and P4, this might give indication about the selectivity of P5 and P4 towards lanthanide metal ions. Fig.16 represents the uptake(%) of lanthanides by polymer P5 when using different amounts of polymer, and also shows that the uptake(%) of lanthanides is increasing when the amount of P5 is increasing until the maximum amount of P5 around (400-500)mg, to finally reach a constant value above this amount of uptake(%).

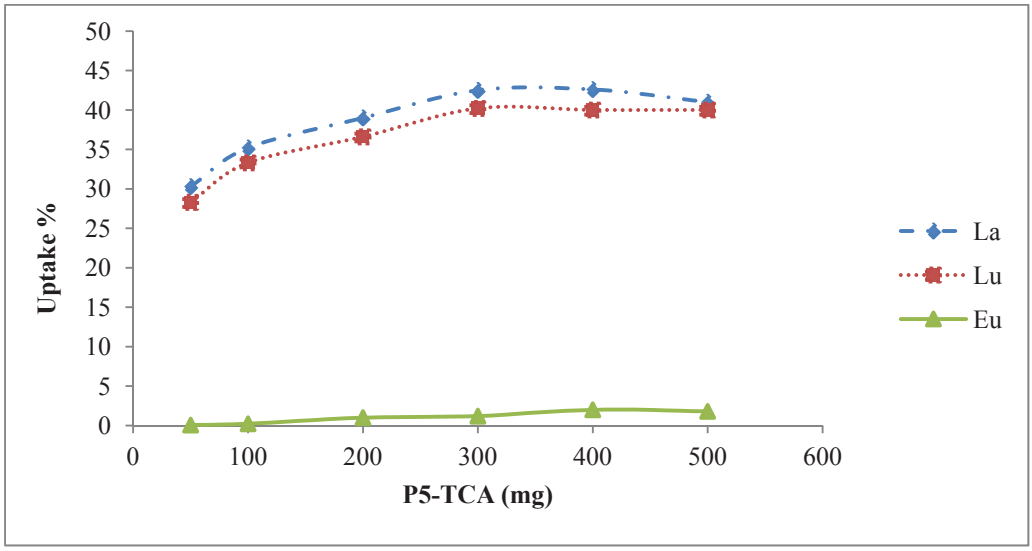

Fig.16: The variation of P5 dose with the uptake(%) of lanthanides under shaking overnight.

From (Fig. 15) and (Fig.16), we can conclude that changing the J-T3000 (%) in the used polymeric materials has an effect on the lanthanides uptake(%). The higher uptakes of La^{3+} and Lu^{3+} have been observed with polymers P5 and P4 and the lower uptake of Eu^{3+} has been observed with the same polymers. This might be giving an indication about the selectivity of these two polymers (P4, P5) towards (La^{3+}, Lu^{3+}) than (Eu^{3+}). This selectivity may be related to the stability of lanthanides in the acidic media (ascorbic acid) during the extraction process, as most of lanthanides metal ions are stable in the hydrated form $[Ln(H_2O)_6]^{3+}$. The most stable oxidation state of La and Lu is the oxidation state (+3), while the most stable oxidation state of Eu is oxidation state (+2). Additionally, the atomic radius of lanthanides metal ions has an effect on the selectivity as the atomic radius of Eu metal ion is 0.204 nm that is higher than both La (0.187 nm) and Lu (0.174 nm) metal ions radii.

3.3. Characterization of the polymeric materials

The polymeric membranes have been synthesized by reflux method, and were casted in a Teflon plate inside an oven at 60 $^{\circ}$C overnight. After the membranes were dried at room temperature, the membrane materials and their metal complexes were characterized by FTIR spectroscopy, TGA, DSC, and ^{1}H NMR. Nitrogen permeation measurements were performed to ensure that they were dense and defect free. SEM analysis allowed the thickness and the quality of the active deposited

layer to be determined, whereas EDX analysis gave indication on the chemical compositions of the polymeric materials and their metal ions. In addition, the hydrophilic character of the used membranes has been measured by contact angle method before and after the transportation of lanthanides. The results and discussion obtained from these characterizations of polymeric materials are summarized below.

3.3.1. FTIR analysis technique

FTIR technique has been used to confirm the complexation interaction between the polymeric materials and lanthanides metal ions by observing the changes in functional groups of the polymeric materials due to the attachement of metal ions to the functional groups in the polymeric materials. (Fig.17) represents the FTIR measurements of the P5 polymer and its metal ions (La^{3+}, Lu^{3+}, Eu^{3+}). It is obvious that in case of polymers complexed with metal ions, shifting of the peaks are encountered in the wavelength area of 3400-3700 cm^{-1}. Indeed, this range is related to the amine groups in the Jeffamine compounds present in the polymeric structures. We also observed a small shift of the wavelength around 1600-1800 cm^{-1} that is related to the aldehyde groups in the aromatic structure. Both shifts might be due to the interactions between the functional groups in the polymeric structures after complexation with the metal ions. Furthermore, the broadness of the shifting might be due to the lanthanides ions interacting in their hydrated forms with the functional groups in the polymeric structures. Therefore, FTIR analysis represents a powerful tool to characterize the effect of lanthanides metal ions complexation with the polymeric materials. See the Appendix (6.1) for the FTIR analysis for the other selected polymeric materials (P1, P4, and P7).

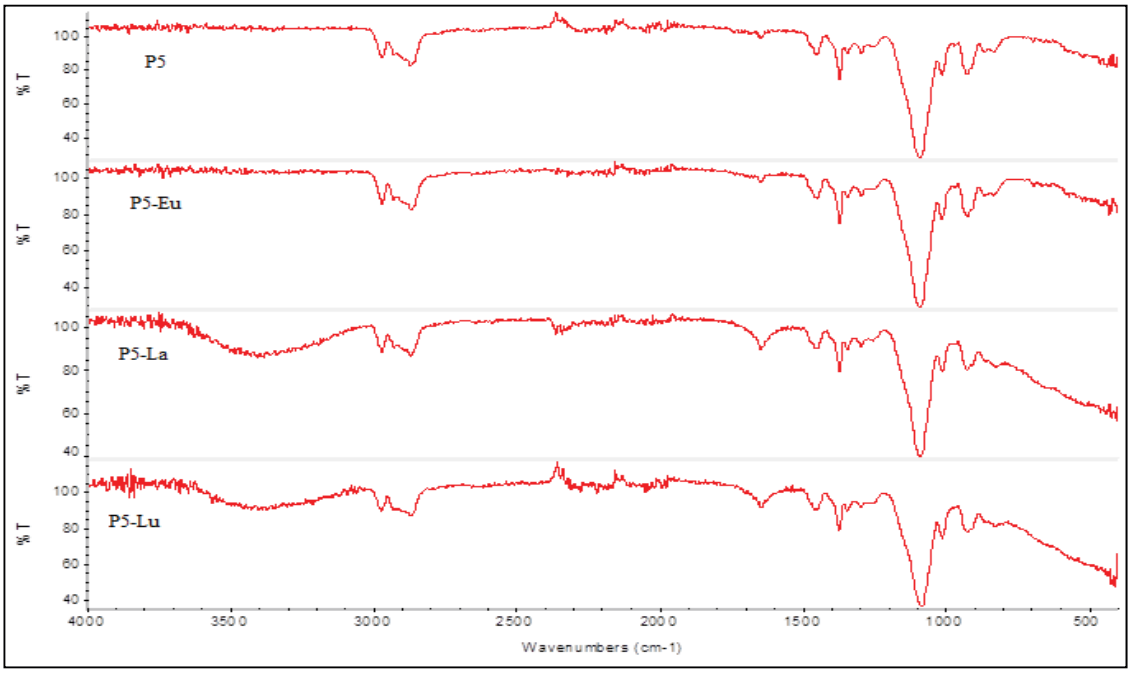

Fig.17: The FTIR spectra obtained for P5 upon complexation with lanthanide metal ions (La^{3+}, Lu^{3+}, Eu^{3+}).

3.3.2. ^{1}H NMR analysis technique

The composition of the polymeric membranes was determined by ^{1}H NMR spectroscopy on the basis of the characteristic bands that appeared in the spectra of P5 and its metal ions (La^{3+}, Lu^{3+}, Eu^{3+}) are illustrated in (Fig.18). The ^{1}H NMR spectra analysis of polymeric membranes after the extraction process showed a reasonable shift for definite peaks from their original chemical shift, which means there is a different electron density occuring due to the presence of the metal ion and thus to to the transfer of some protons from one peak to another one. The spectra showed there is a chemical shift occurring for the peak centered at 8.3 ppm corresponding to aldimine group (-RC=N-R) that are formed upon interaction between the aldehyde groups in TCA contactor and the amine groups in Jeffamine substrates, during the extraction process. Similarly, we notice a chemical shift occurring for the peak centered at 10ppmcorresponding to aldehyde groups from the TCA contactor. Finally, the ^{1}H NMR analysis gives a good evidence for the chelation between P5 and lanthanides metal ions. See the Appendix (6.2) for the ^{1}HNMR analysis for the other selected polymeric materials (P1, P4, and P7).

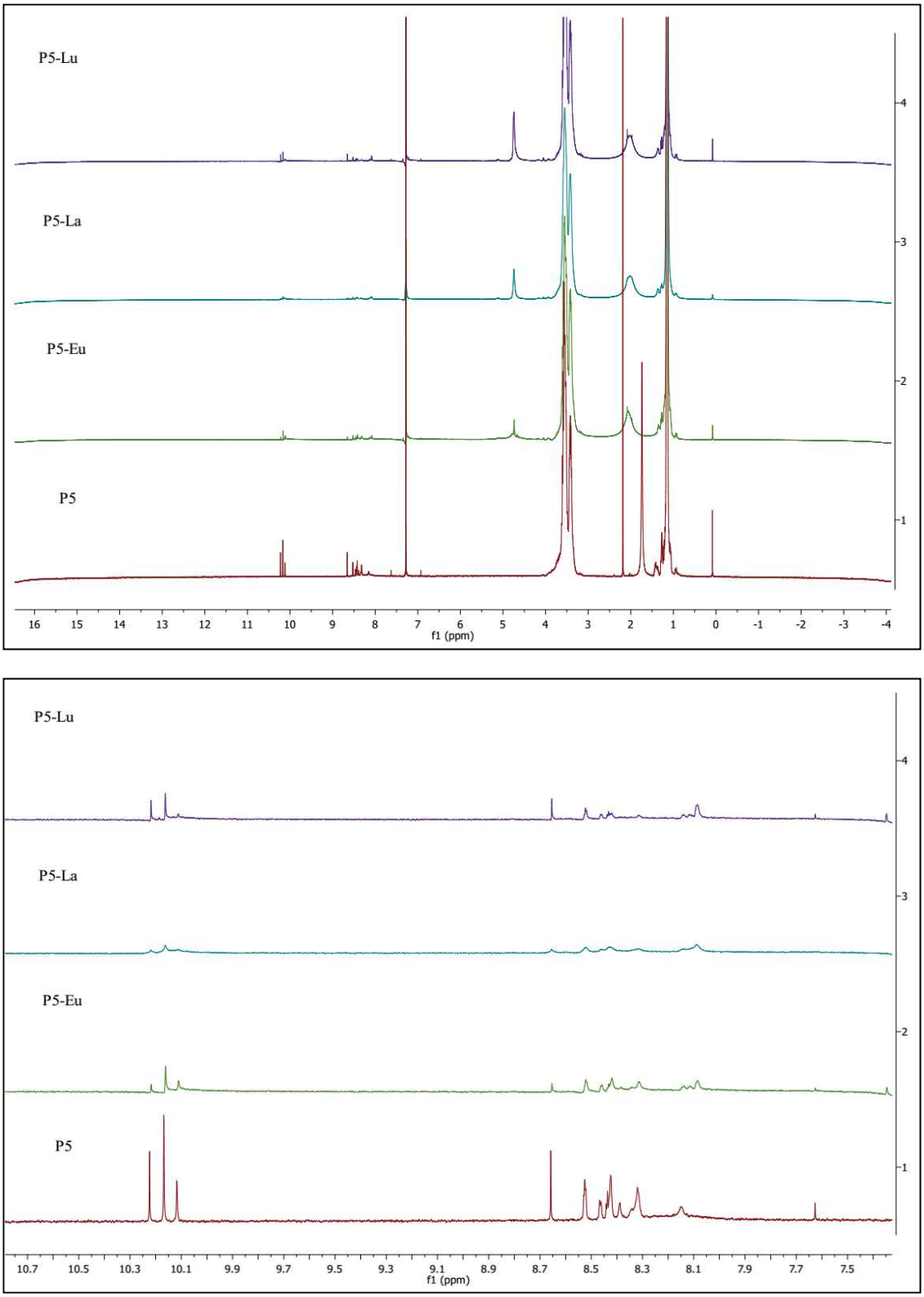

Fig.18: ^{1}H NMR spectra of the membrane P5 after complexation with the lanthanide metal ions (La^{3+}, Lu^{3+}, Eu^{3+}).

3.3.3. DSC measurements

(Fig.19) represents the complete data for glass transition temperatures of all the membranes used (P1, P4, P5, and P7) complexed with their metal ions, extracted from DSC. From the obtained results, we observed that P4 and P5 even in presence of the metal ions have a higher glass transition temperature (Tg) values comparing with other membranes P1 and P7.This might be related to the chemical composition of the used polymeric membranes, which might affect the cross-linking within the membranes. In case of P4 and P5, both Jeffamine substrates (J-D2000 and J-T3000) have been used with the TCA contactor for synthesizing the membranes. In case of P1 and P7, only one Jeffamine substrate (J-D2000 or J-T3000) has been used in the preparation of the polymeric membranes, respectively. Additionally, Figure 20 represents the DSC measurements of P5 and its complexes with lanthanides metal ions (La^{3+}, Lu^{3+}, and Eu^{3+}). We see that the glass transition temperatures of P5-La > P5-Lu > P5-Eu > P5, which may be attributed to the complexation interaction between P5 and Lanthanides metal ions that is stronger than other used polymeric membranes. In general, the DSC showed a good trend of glass transition temperature and thermal stability of the used membranes. See the Appendix (6.3) for the DSC measurements for the other selected polymeric materials (P1, P4, and P7).

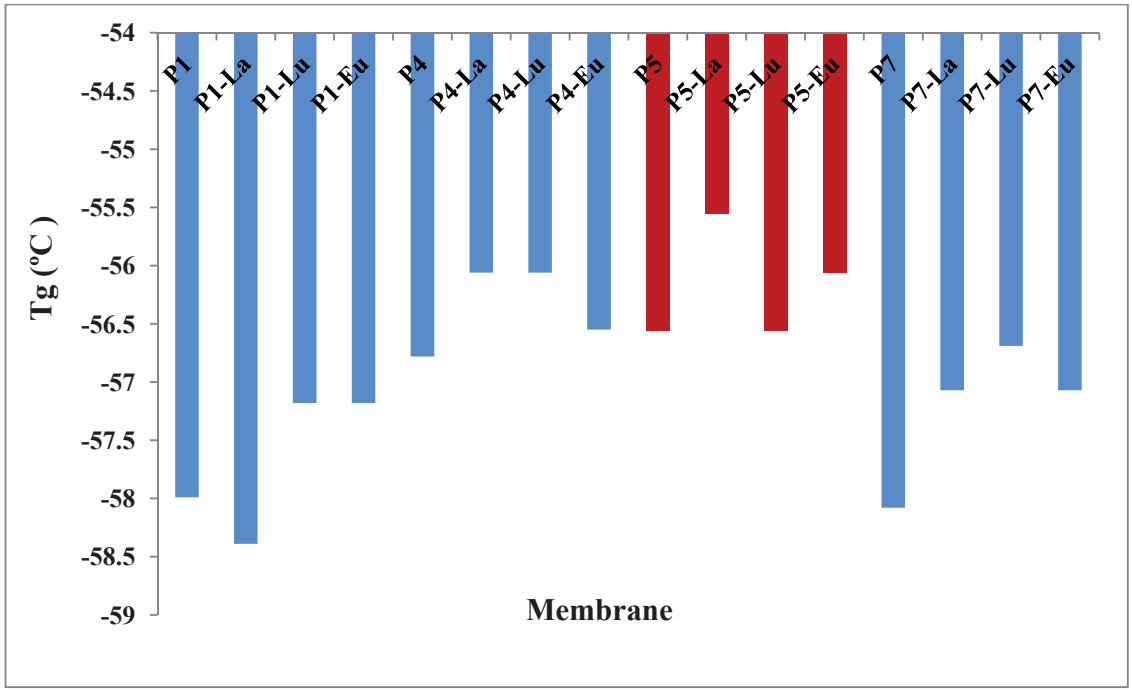

Fig.19: DSC of the used polymeric membranes (P1, P4, P5, and P7) with their metal ions (La^{3+}, Lu^{3+}, Eu^{3+}).

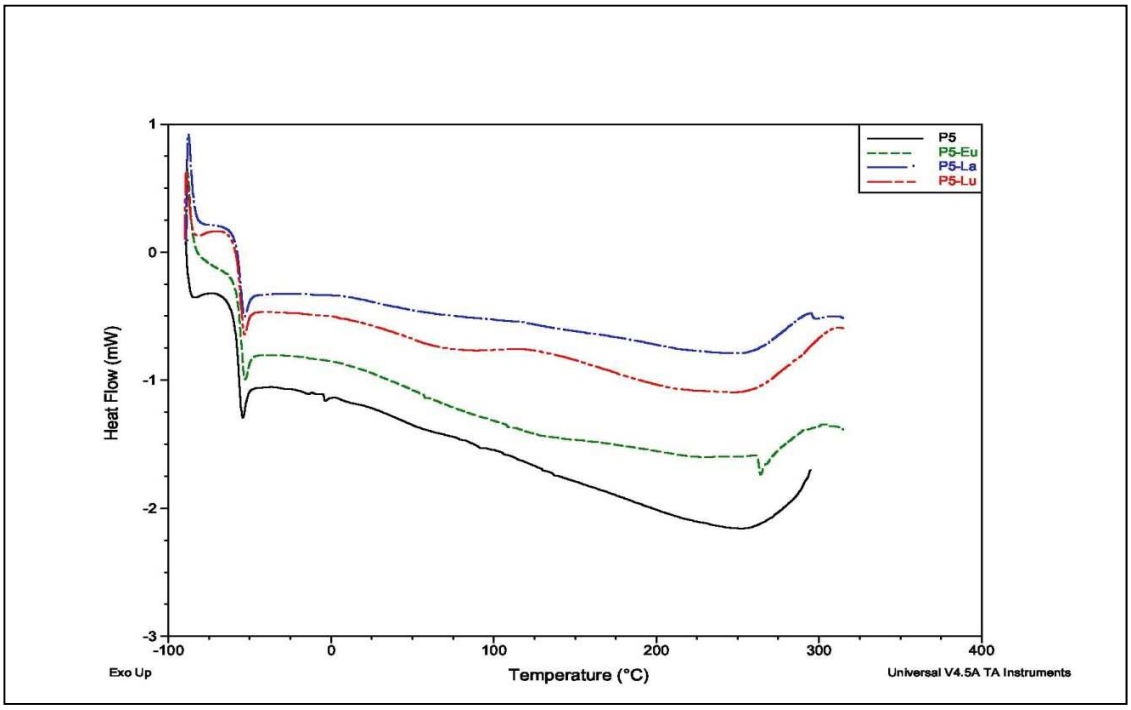

Fig.20: DSC measurements of the membrane P5 with its metal ions (La^{3+}, Lu^{3+}, Eu^{3+}).

3.3.4. TGA measurements

The TGA measurements were done for all membranes (P1, P4, P5, and P7), as shown in (Fig.21). The higher thermal stability has been observed in case of P5 and its metal ions, this might indicate that the higher cross-linking of polymer (P5) structure compared with others. This may be attributed to the complexation interaction between P5 and Lanthanides metal ions, which is higher than other used polymeric membranes. (Fig.22) represents the TGA measurements for P5 and its metal ions complexes with (La^{3+}, Lu^{3+}, Eu^{3+}). From this figure, a common trend can be drawn with one big drop in weight loss around (296.74^0C- 303.91^0C). The other peaks were insignificant because the Jeffamines polymers are dominant in the membranes. They make up a major portion of the polymeric structures in comparison with TCA. Therefore, the big drop in weight loss can be accounted for the presence of Jeffamines, and the rest of the components are not significant on the TGA spectra. See the Appendix (6.4) for the DSC measurements for the other selected polymeric materials (P1, P4, and P7).

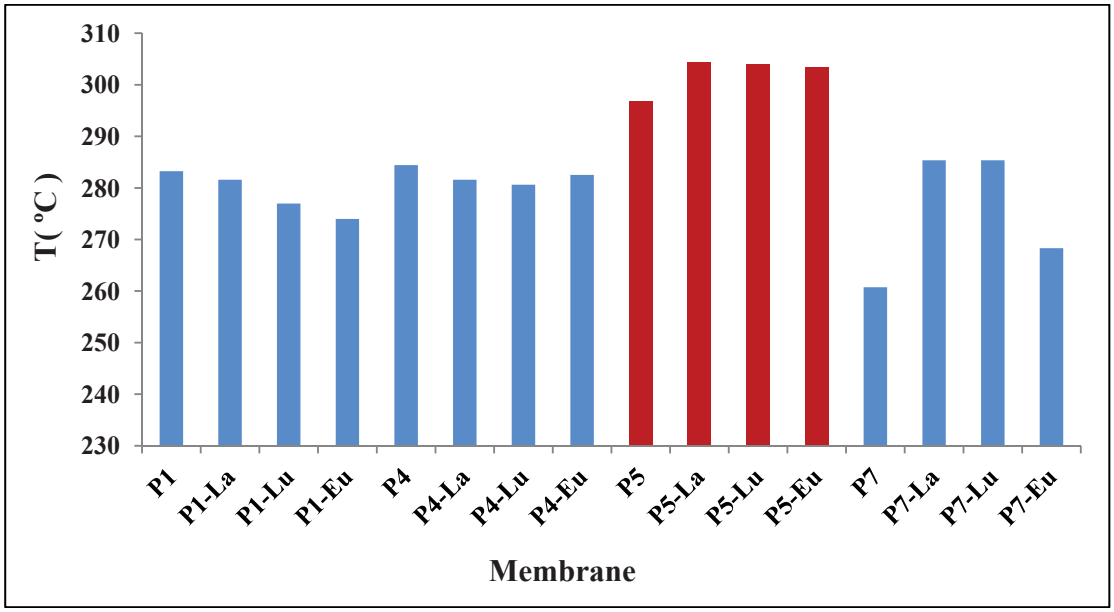

Fig. 21: TGA measurements of the used polymeric membranes (P1, P4, P5, and P7) with their metal ions (La^{3+}, Lu^{3+}, Eu^{3+}).

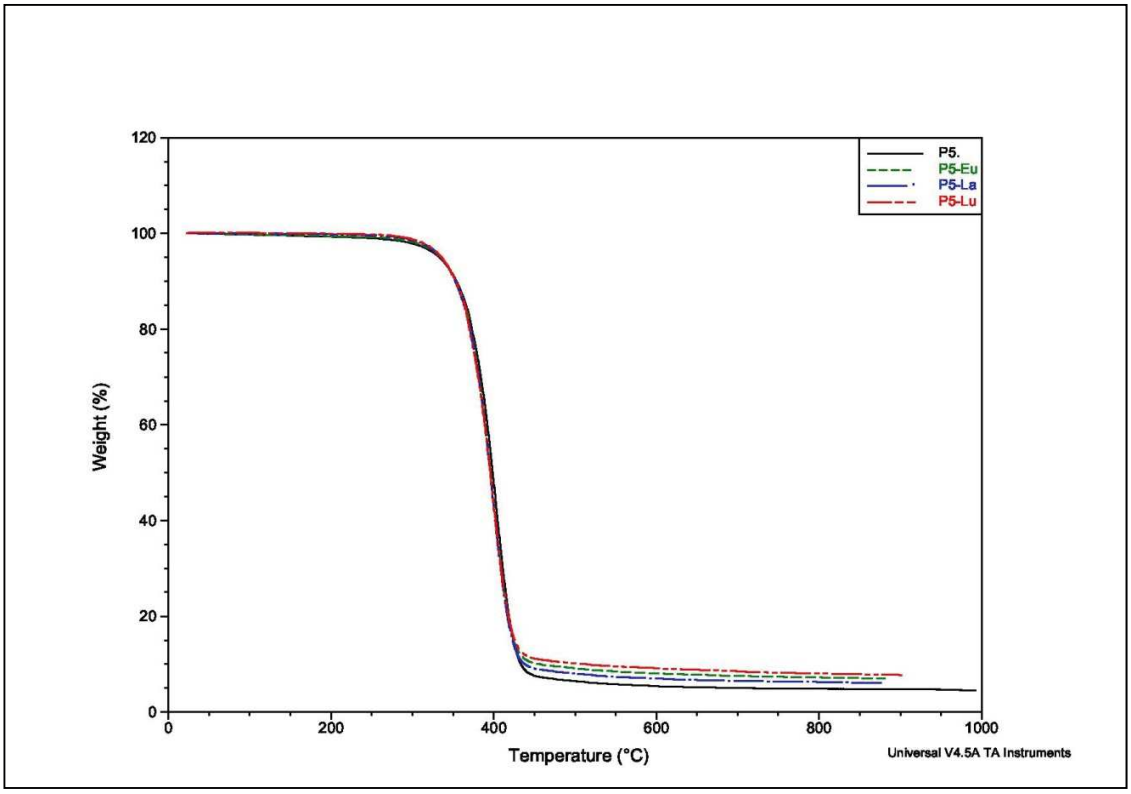

Fig.22: TGA measurements of the membrane P5 with its metal ions (La^{3+}, Lu^{3+}, Eu^{3+}).

3.3.5. Scanning electron microscopy (SEM)

(Fig.23) represents the Scanning Electron Microscopy (SEM) analysis of P5, in cross section view and top view, to evidence the thickness of the membranes, and the quality of the active deposited layer.

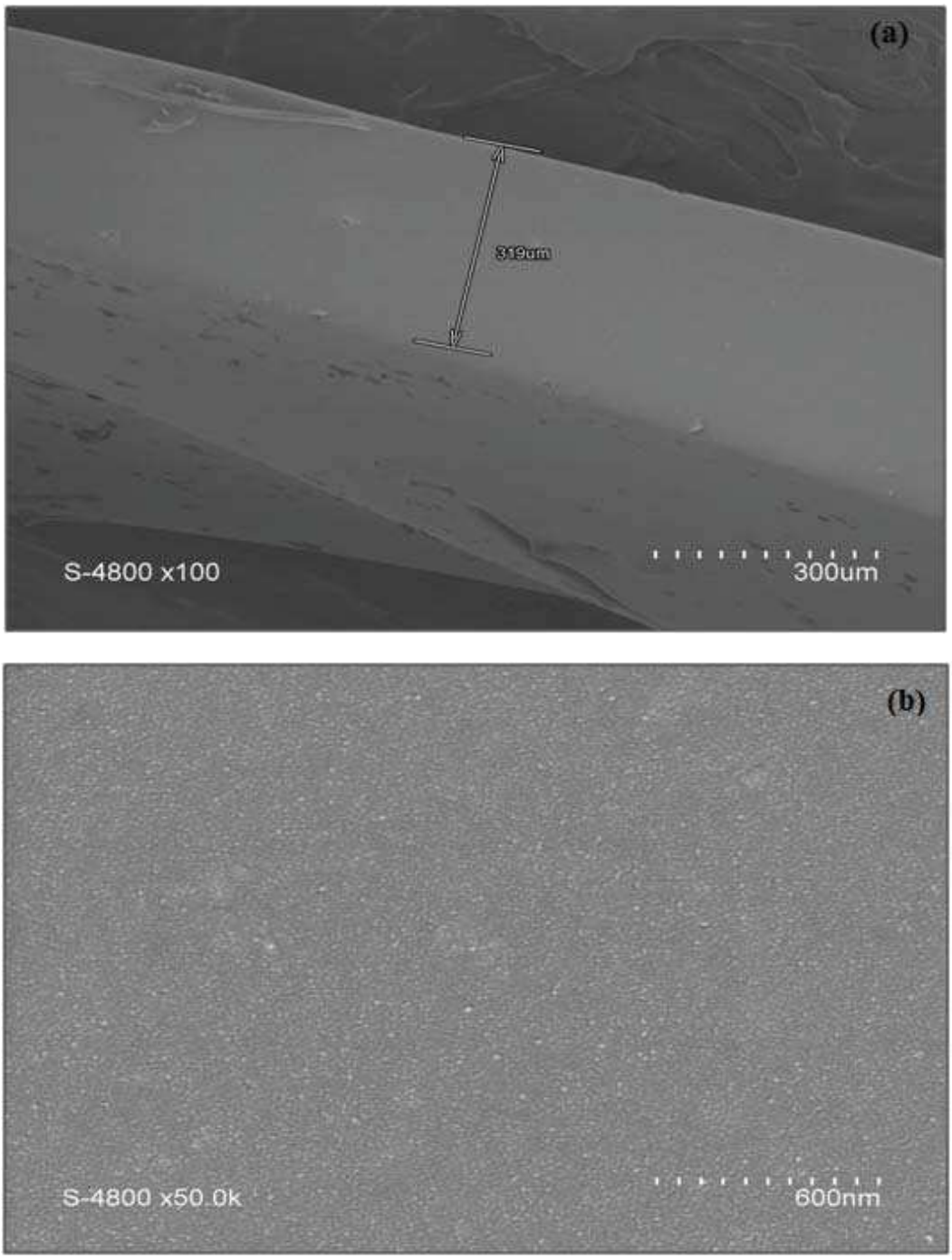

Fig.23: SEM images of the P5 membrane (a) cross section view and (b) surface section view.

3.3.6. SEM-EDX Analysis

Scanning electron microscopic examination of P5 before and after lanthanides metal ions extraction and adsorption was undertaken in order to locate the active adsorptive sites of the polymeric materials to form its metal complexes as seen in (Fig.24). The energy dispersive X-ray analysis (EDX) of polymeric material P5 before and after interaction with lanthanides metal ions is shown in (Fig.25). SEM image of the P5 without metal (Fig.24a) shows that the major elements present are C, O, Al, Si, and Cl inside the polymeric matrix. C and O elements are present from the raw materials used for the synthesis of the polymeric materials, while the other metals like (Al, Si, and Cl) might be contamination elements from the surrounding environment. Meanwhile, the EDX spectrum of P5 presented in (Fig. 24) and (Fig.25) showed that the major elements present are C, O, Al, Si, Cl, in addition to the presence of lanthanides metal ions. The interaction between the selected polymer P5 with lanthanides metals ions (La^{3+}, Lu^{3+}, Eu^{3+}) is depicted in (Fig. 25b), (Fig. 25c), and (Fig.25d) respectively. EDX spectra gave indication about the interaction of lanthanides metal ions with imines and polyether groups that are present in the polymeric materials P5. Also, the EDX spectra show that the lanthanides metal ions might be interrupted inside the polymeric porous structure as represented in the figures.

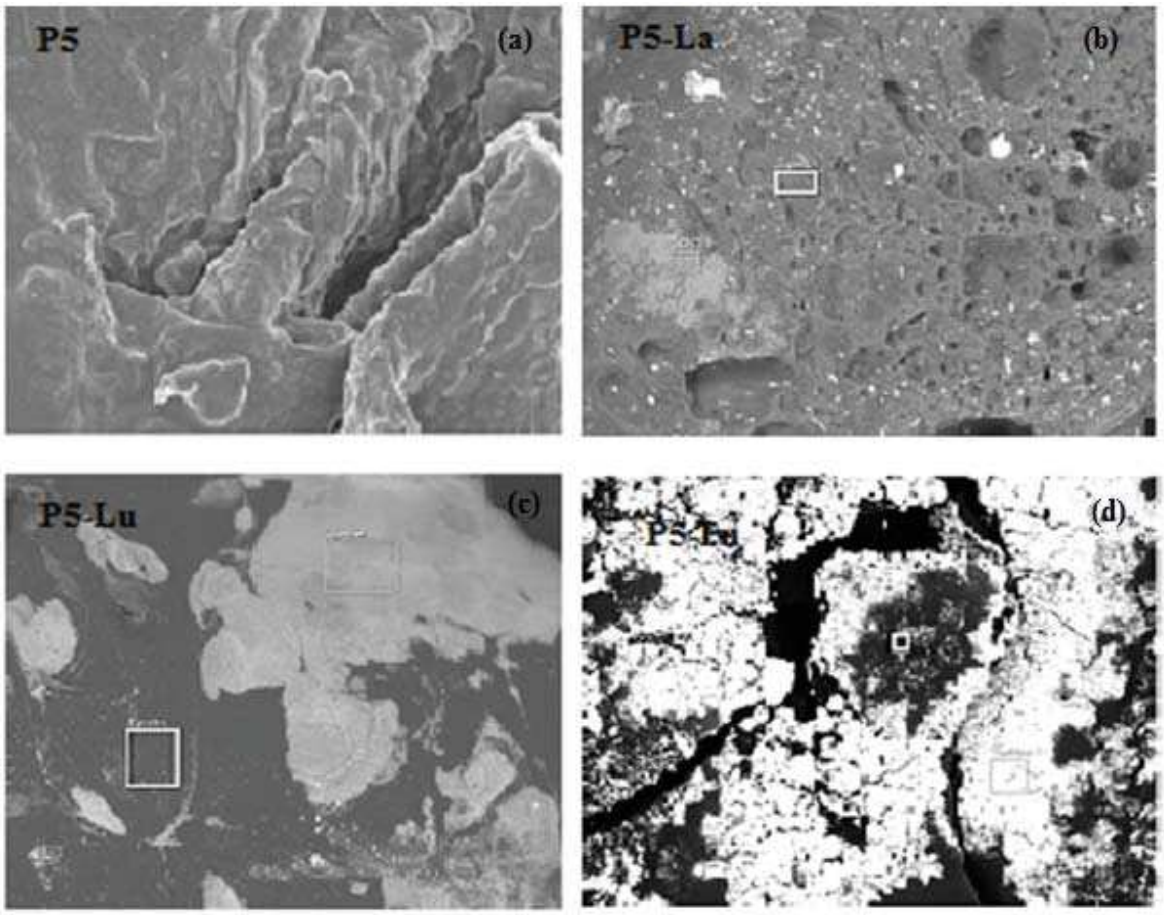

Fig.24: SEM micrographs of P5 before and after metal adsorption and extraction, indicating morphological and structural changes (a) P5 before metal adsorption; (b) P5-La complex; (c) P5-Lu complex; (d) P5-Eu complex, respectively.

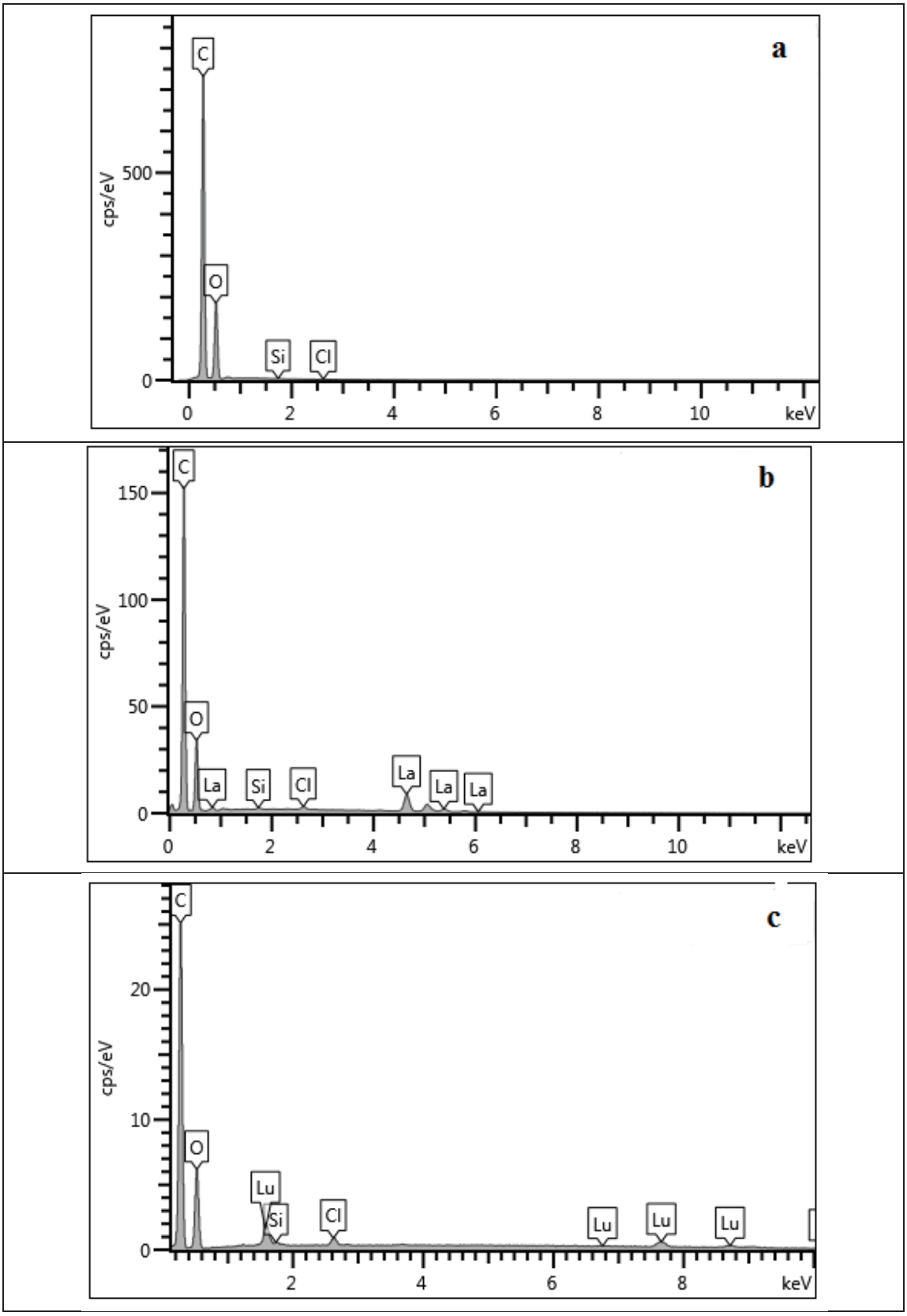
a
C
O
Si
Cl
cps/eV
500
0
0
2
4
6
8
10
keV
b
C
O
La
Si
Cl
La
La
La
150
100
50
0
cps/eV
0
2
4
6
8
10
keV
c
C
O
Lu
Si
Cl
Lu
Lu
Lu
20
10
0
cps/eV
2
4
6
8
keV

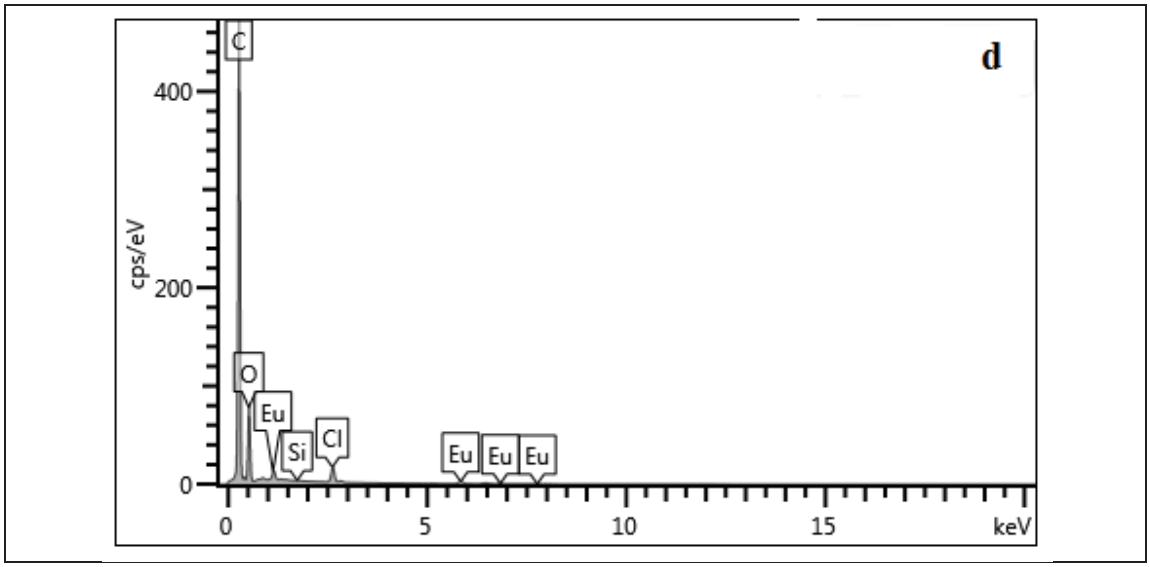

Fig.25: EDX spectrum of P5 before and after metal adsorption and extraction, (a) P5 before metal biosorption; (b) P5-La complex; (c) P5-Lu complex; (d) P5-Eu complex respectively.

3.3.7. Contact angle measurements

Surface properties of a membrane give information about its hydrophilicity. The contact angle increases with increasing surface hydrophobicity. This can help better understand the kinetic interaction of the metal ions with the membrane surface. (Fig.26) and (Fig.27) represent the contact angle measurements for the used polymeric membrane (P5) before and after the transportation of lanthanides metal ions. It is clear that the used membranes materials have hydrophilic and symmetrical characters as the left and right contact angles are almost equal. In addition, the hydrophilic character of the used membranes is increasing after the transportation of the lanthanides metal ions (La^{3+}, Lu^{3+}, Eu^{3+}) through the used membrane. This might be related to the decrease of the contact angle after the transportation process, as the used polymeric membrane might interact with the metal ions through the polymeric function groups in the membrane structure.

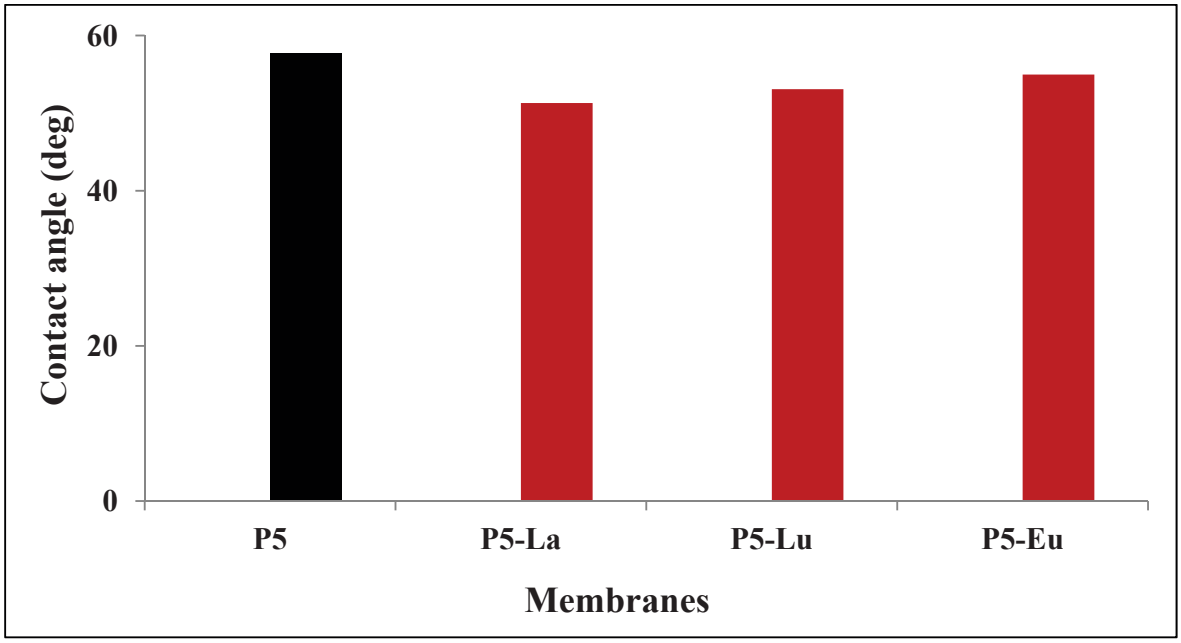

Fig.26: Contact angle for the P5 membranes with and without lanthanides metal ions (La^{3+}, Lu^{3+}, Eu^{3+}).

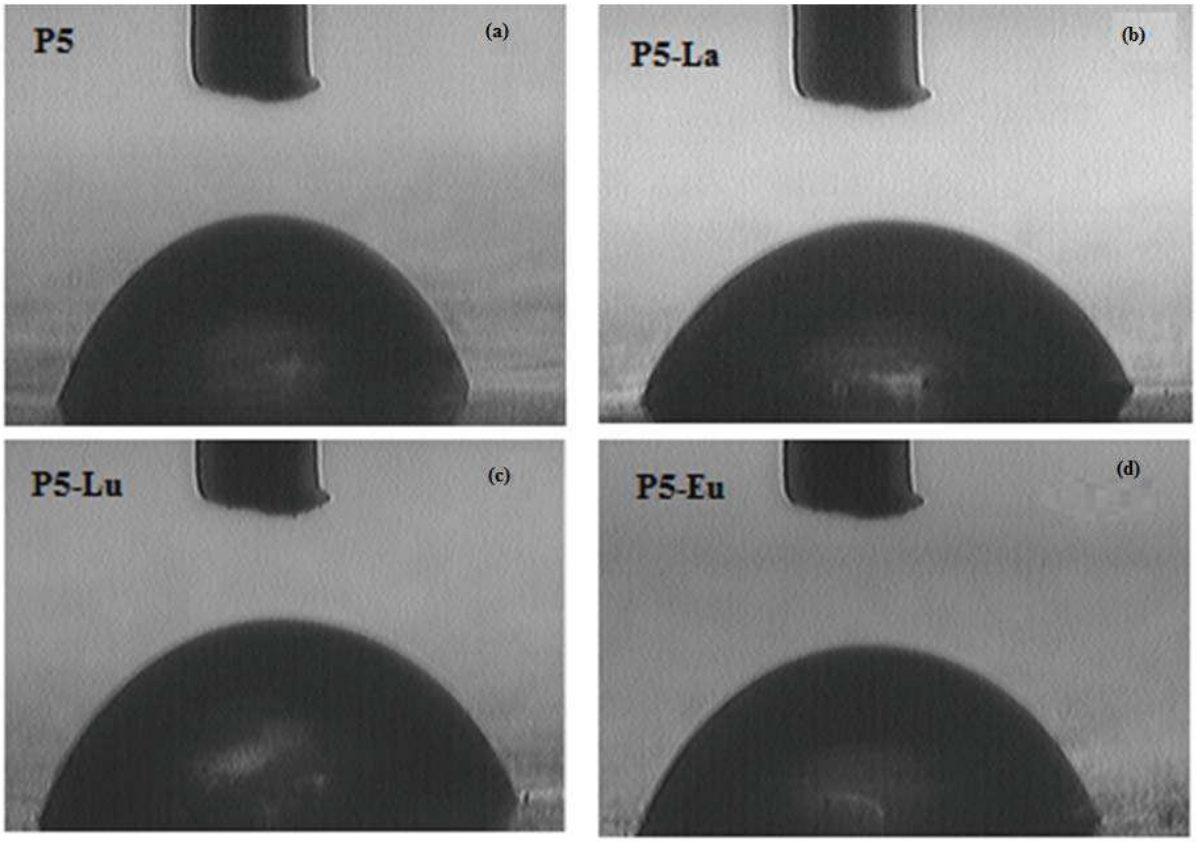

Fig.27: Contact angles of polymeric membrane P5 before and after metal adsorption and extraction (a) P5 before metal adsorption; (b) P5-La; (c) P5-Lu; (d) P5-Eu, respectively.

3.4. Dialysis membrane transport experiments

In order to study the transport properties of the "dynamer" membrane films, we carried out dialysis transport experiments. The competitive transport of La^{3+}, Lu^{3+}, and Eu^{2+} across the membranes P1–P7 occurs according to the solution-diffusion mechanism [59-64] and was evaluated using passive transport conditions. We have recently reported a model based on a solution-diffusion (Fick's law), which can be described for different membrane processes such as dialysis, reverse osmosis, gas permeation, pervaporation, etc.[61]. This model assumes that the chemical potential gradient across the membrane is only due to a concentration gradient. The flux of the solute "i" can be expressed as follows:

$$J_i = -D_i \frac{dc_i}{dx} \quad (3.4.1)$$

By integrating over the thickness *l* of the membrane, the flux J of solute «i» is:

$$J_i = -\frac{D_i}{l}\left(C_i^{m,s} - C_i^{m,f}\right) \quad (3.4.2)$$

While: $C_i^{m,s}$, $C_i^{m,f}$ are the concentrations of the solute in the membrane at the strip and the feed phase interfaces, respectively. The concentration gradient through the membrane can be deduced by assuming thermodynamically equilibrium at the interfaces:

$$C_i^{m,s} = K_i^s x\, C_i^s \quad (3.4.3)$$

$$C_i^{m,f} = K_i^f x\, C_i^f \quad (3.4.4)$$

With C_i^s, C_i^f are the concentrations of the solute «i» in the strip and feed phases, respectively, and $K_i^s$and K_i^f represent the partition coefficients at the strip and feed phase interfaces with the membrane, respectively. By combining Eq. (3.4.2) with Eqs.(3.4.3) and (3.4.4), we obtain the flux J according to the concentrations in the feed and the strip phases:

$$J_i = \frac{D_i}{l}\left(k_i^f c_i^f - k_i^s c_i^s\right) \quad (3.4.5)$$

D_i and K_i, the effective diffusion and partition coefficients of this macroscopic approach, can be correlated with the physical and chemical structures of the dense membrane. If we suppose that the transport rate is governed by diffusion and that the complexation- decomplexation reactions are kinetically rapid, then the accumulation of the solute in the membrane can be neglected. In a quasi-stationary regime (Fig.28), the transport rate across each interface becomes approximately equal to:

$$-J_1 = a\frac{dc_i^f}{dt} = -\frac{D_i}{l}\left(k_i^f c_i^f - k_i^s c_i^s\right) \quad (3.4.6)$$

$$J_2 = a\frac{dc_i^s}{dt} = -\frac{D_i}{l}\left(k_i^f c_i^f - k_i^s c_i^s\right) \quad (3.4.7)$$

With a = V/A the compartment length (we suppose a simple geometry), V the compartment volume, and (A) the active surface of the membrane. The solute flux Jm density across the membrane is then simply:

$$J_m \cong J_1 = J_2$$

with, $\frac{(D_i K_i^f)}{al} = \lambda$, $\frac{(K_i^s)}{K_i^f} = \alpha$ and the initial conditions ($C_{1,t=0} = C_1^0$ and $C_{2,t=0} = 0$), then Eq(6) and Eq (7) yield:

$$C_2(t) = \frac{C_1^0}{1+\alpha}[1 - e^{-\lambda(1+\alpha)t}] \quad (3.4.8)$$

Note that:

as $\alpha \to 0$, $(i.e., K_i^s \ll K_i^f)$, $C_2(\infty) \to C_1^0$ and as $\alpha \gg 1$, $(i.e., K_i^s \gg K_i^f)$, $C_2(\infty) \to 0$

The fitting of experimental data in the strip phase by Marquandt Levenberg non-linear regression allows the permeability P (evaluation of the transport), and the partition coefficient ratio of solute «i» (affinity of the membrane towards the solute), to be determined:

$$P_i = D_i K_i^f = \lambda\, \alpha\, l \quad (3.4.9) \qquad \alpha = \frac{K_i^s}{K_i^f} \quad (3.4.10)$$

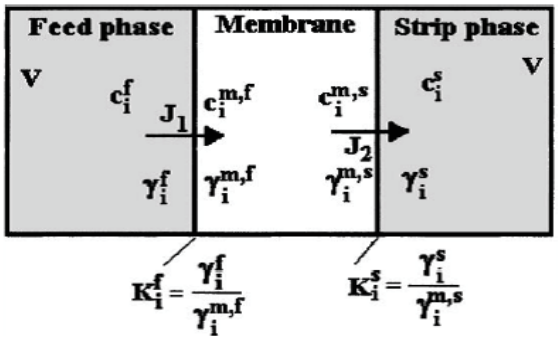

Fig.28: Parameters of transport modeling, (γ_i) activity coefficient.

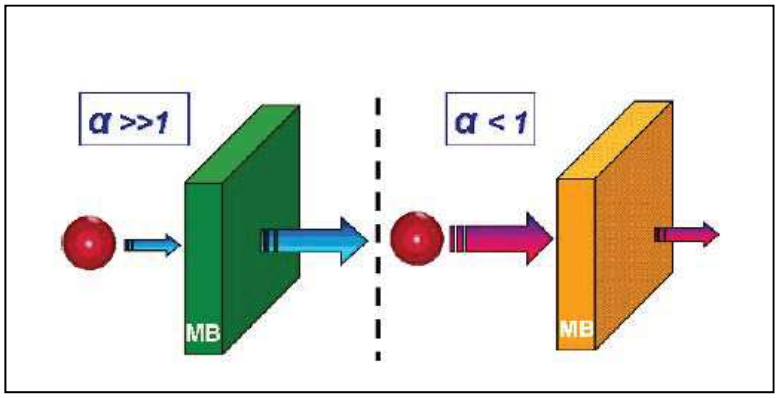

Fig.29: the representation reports of partition coefficients α <1 and α >> 1.

In the present study, the following parameters were adopted for the facilitated transport of lanthanides ions through polymeric membranes:

- The initial concentration of Lanthanides ions: C_1^0= 10^{-2} ppm
- The compartment length, $a = V/A = 9.4$, with (V) compartment volume = 50 cm^3, and (A) active membrane area= 5.32 cm^2 ;
- The membrane thickness (l) =319 µm = 0.0319 cm in case of solid membrane, while in case of liquid membrane = 28.9 cm.

The diffusion coefficient is obtained from Eq. (3.4.11), derived from Eq.(3.4.8) where (c_i^0) is the initial concentration in the feed phase,(c_i^t) the concentration in the strip phase A_m the membrane area, V the volume of the receiving phase, and (D_m) the thickness of the active layer of the membrane.

$$\ln \frac{c_1^0 - (1+\alpha)c_2(t)}{c_1^0} = -(1+\alpha)\frac{A_m . D_m}{V_r . l} t \qquad (3.4.11)$$

The transport parameters, the permeability (P), and the partition coefficient ratio (α) of solutes La^{3+}, Lu^{3+}, and Eu^{3+} are determined for all dialysis transport experiments performed by using P5 solid and liquid membranes (tables (2) and (3)). The novelty of this approach is in interpreting the parameters of the solution-diffusion model in terms of the interactions between the lanthanides ions and the complexing sites at the supramolecular polymeric network, since the transport of lanthanides through the membranes is related to the constitutional dynamic networks. The transport is based on the complexing ability of lanthanides metal ions (La^{3+}, Lu^{3+}, Eu^{3+}) with the functional polyether groups in the membrane materials. Based on corresponding

dynamic diffusional domains within the solid and liquid bulk membrane phases, the lanthanides are extracted and selectively transported through the membranes.

Tables (2) and (3) represent the transport results of lanthanides metal ions (La^{3+}, Lu^{3+}, Eu^{3+}) through both solid membranes (SM) and liquid membrane (LM). We observed that the permeability of lanthanides through Liquid membranes is higher than the solid membranes; even the thickness in case of liquid membranes is higher than solid ones. This might relate to the solubility and diffusivity coefficients of compounds in a liquid medium are higher than those in a solid one. So the liquid membranes contain solvent as a transporting phase, so this helps to increase the diffusion and transporting for the extracted lantahnides metal ions through the liquid membranes comparing with solid ones due to the tunable nature of the solvent for a certain separation task, as the extraction of the lanthaindes metal ions can be easily carried out by a solvent that is totally miscible with the ionic liquid of the membranes. According to that in case of liquid membranes the functional groups in the dynamic network that are acting as a complexing agent and carrier for the lanthanides metal ions will be more free movement than in case of solid membranes, thus will help to accelerate the diffusion process by increasing the extracting ability and transportation of the lanthanides metal ions from the feed phase to the strip (receiving) phase. Moreover, the results show that the permeability of (La^{3+} and Lu^{3+}) is higher than that of (Eu^{3+}), this might relate to the complexing ability of both metal ions with the functional polyether groups and amino groups in the dynamic network, which helping in the extraction and transportation of these metal ions from the feed phase to the strip phase. Additionally, the flow rate values (J) that represent the concentration of ions transported per hour through feed and receiving interfaces, have been calculated from the slope of the initial nearly linear part of the profiles (time 0–140 h) in case of solid membranes and (time 0-40 h) in case of liquid membranes using the solution-diffusion model. Moreover, (Fig.30a) and (Fig.30b) show that the flow rate of lanthanides metal ions through the liquid membranes is higher than the flow rate through the solid membranes. As mentioned before, this might relate to the free movement of the complexing and carrier functional groups in the dynamic network in case of liquid membranes than solid ones, as the solubility and diffusivity coefficients of the extracted compounds are higher in a liquid medium than in a solid one, so the permeability and transportation of lanthanides metal ions in the liquid membranes are higher than solid ones.

According to that, the permeation of a compound in a liquid membrane can be divided into the following steps: 1) Sorption at the feed interface, 2) Complexation reaction with the carrier, 3) Diffusion of the species/carrier complex across the membrane, 4) Decomplexation reaction at the permeate interface and 5) desorption of the species. After completing this cycle, the carrier diffuses back to the feed interface to complex more molecules.

Membrane	α	1/α = Kf/Ks	λ	l	P (cm^2/sec) x 10^{-05}	J(M/h) Strip cell x 10^{-06}	J (M/h) Feed cell x 10^{-06}
TCA-SM-La	0.4306	2.3222	0.0038	0.0319	5.27	4.00	-4.00
TCA-SLM-Lu	0.3834	2.6079	0.0053	0.0319	6.51	4.00	-4.00
TCA-SLM-Eu	0.2917	3.4277	0.0028	0.0319	2.62	5.00	-5.00

Table 2: Transport parameters of the facilitated transport of lanthanides through Solid Membrane (SM).

Membrane	α	1/α = Kf/Ks	λ	l	P (cm^2/sec)	J (M/h) Strip cell x 10^{-05}	J (M/h) Feed cell x 10^{-05}
TCA-LM-La	0.6931	1.4426	0.0175	28.9	0.3515	1.00	-1.00
TCA-LM-Lu	0.6341	1.5771	0.016	28.9	0.2945	1.00	-1.00
TCA-LM-Eu	0.3692	2.7085	0.0095	28.9	0.1012	0.90	-0.90

Table 3: Transport parameters of the facilitated transport of lanthanides through Liquid Membrane (LM).

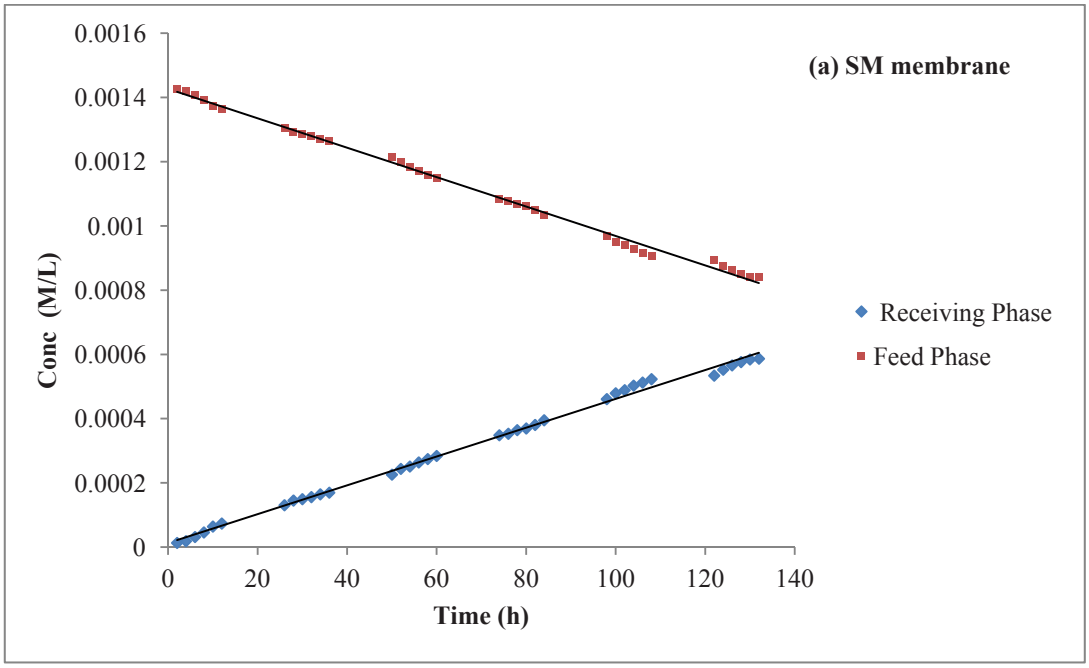

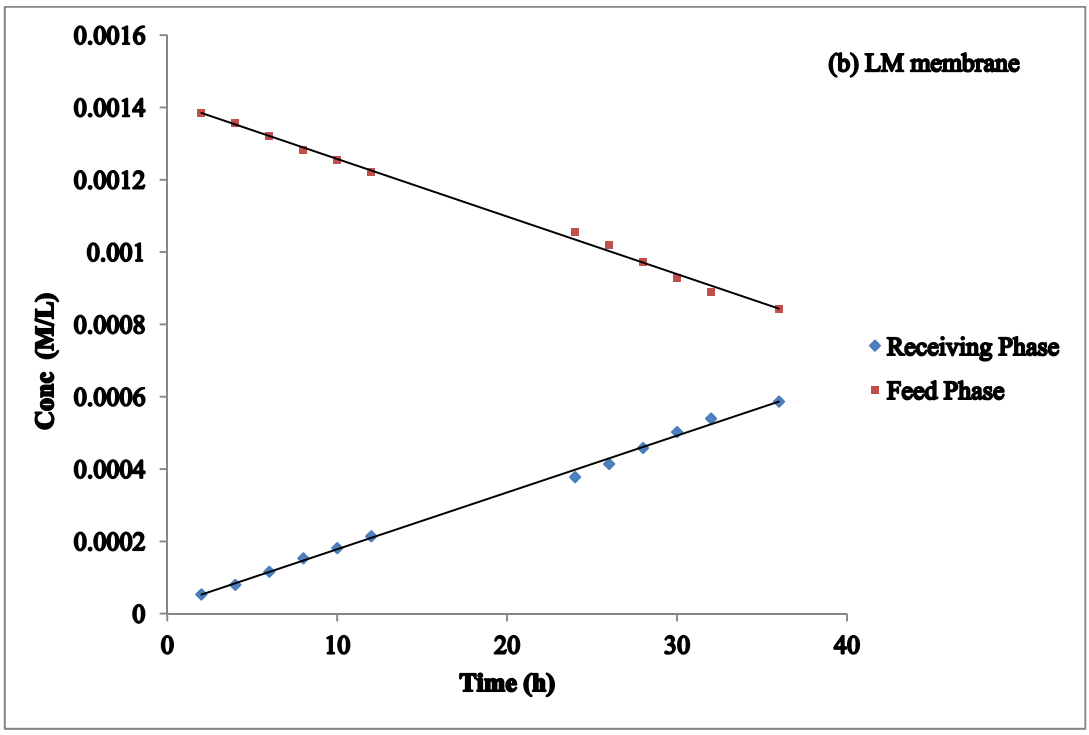

Fig.30: Flow rate of lanthanides through (a) SM membrane and (b) LM membrane.

4. Conclusion

Dynamic covalent polymers or dynamers, generated from reversibly interacting monomers, offer the possibility to generate homogeneous molecular networks with addressable domains based on structural relationships different from the former monomers. Constitutional dynamic networks have been used in liquid and solid membrane systems as a carrier network for transporting lanthanides. The transport is based on the complexing ability of lanthanides metals (La^{3+}, Lu^{3+}, and Eu^{3+}) with the functional polyether and amino groups in the membrane materials. Based on corresponding dynamic diffusional domains within the solid and liquid bulk membrane phases, the lanthanides are extracted and selectively transported through the membranes, only in the presence of constitutional networks, while the former monomers did not show any selectivity. This would be explained by the formation of a dynamic self-assembly of low-size and molecularly addressable recognition networks in which the diffusional/selective percolation pathways might exist. The resulting polymeric membranes and their metals complexes have been characterized by (UV-visible, FTIR and ^{1}H NMR), and the thermal stability by (TGA, and DSC). The physico-chemical characterizations gave a good indication about the complexation and selectivity of selected lanthanides metal ions with the prepared dynameric membranes. Additionally, the Jeffamine T-3000 substrate is better than Jeffamine D-2000 in the Lanthanides uptake(%), because J-3000 bears/contains more amino groups than J-2000. Also, the dynameric membranes have high selectivity towards (La^{3+} and Lu^{3+}) than Eu^{3+}, and this might relate to the stability of the formed complexes in the membrane phase in direct relation with the atomic radius and the hydration behaviors of the used lanthanide metal ions. Moreover, the results showed that the liquid membrane (LM) is better than solid membrane (SM) for the lanthanides transportation, this might relate to the free movement of the complexing and carrier functional groups in the dynamic network in case of liquid membranes than solid ones, as the solubility and diffusivity coefficients of the compounds are higher in a liquid medium than in a solid one, so the permeability and transportation of lanthanides metal ions in the liquid membranes are higher than solid ones. Finally, thanks to the possibility to combine the structural and functional features of different monomers, the heteropolymeric membrane materials can exhibit very different properties from their original homopolymeric components. In the above-developed examples, this strategy revealed itself to be a versatile way for the synthesis of new membranes presenting different permeabilities and preserving their selectivity towards lanthanide metal ions.

5. References

[1] R.P. Budhiraja: "Separation Chemistry", New Age International (P) Ltd., Publishers, New York, Part III, 2004.

[2] S. Pratibha, T. Renu, S. Pankaj, T. Radha, J. Radioanal. Nucl. Chem., 268, 329, 2006.

[3] R. Harjula and J. Lehto:" Effect of sodium and potassium ions on cesium absorption from nuclear power plant waste solutions on synthetic zeolites", Nuclear and Chemical Waste Management., 6 (2),133-137,1986.

[4] P. Misaelides, A. Godelitsas, A. Filippidis, D. Charistos, I. Anousis:" Thorium and uranium uptake by natural zeolitic materials", Science of The Total Environment., Volumes 173–174,237-246, 1995.

[5] D.M. Ruthven:" Principles of adsorption and adsorption processes",1984.

[6] S. Moreno and G. Poncelet:" Dealumination of small- and large-port mordenites: A comparative study", Microporous Materials., 12 (4–6),197-222, 1997.

[7] H. Mimura and T. Kanno:"Ion-exchange properties of zeolites and their application to processing of high-level liquid waste", International Atomic Energy Agency., Vienna (Austria); 282, 237-247, 1985.

[8] C. Fernandez, JC. Faivre, D. Fasching, F. Feinstein:" Measurement of the spin-dependent structure function gl (x) of the proton", Physics Letters B 329., 399-406, 1994.

[9] S. Moreno and G. Poncelet, Micropor. Mater., 12, 197, (1997).

[10] J.A.Moreno and G. Poncelet:" Isomerization of *n*-Butane over Sulfated Al- and Ga-Promoted Zirconium Oxide Catalysts. Influence of Promoter and Preparation Method", Journal of Catalysis., 203(2) , 453–465,2001.

[11] A.B. Farag, A.M.A. Helmy, M.S. El –Shahawi, S. Farag, Talanta., 41(4), 617, 1994.

[12] H.P. Gregor, D.Y. Semnzare, G.H. Yenah, , lnd. Eng. Chem., 44, 2834, (1952).

[13] A.M. Soliman :" Generation of Current Conveyor-Based All-Pass Filters From Op Amp-Based Circuits", IEEE TRANSACTIONS ON CIRCUITS AND SYSTEMS—II: ANALOG AND DIGITAL SIGNAL PROCESSING., 44(4), 1997.

[14] G.S. Franz, B. Vera, P. Burkhard, Applied Geochemistry., 23, 2137, 2008.

[15] J.R. Klaehn, D. R. Peterman, M. K. Harrup, R. D. Tillotson, T. A. Luther, J. D.Law, L. M.Daniels:" Synthesis of symmetric dithiophosphinic acids for “minor actinide” extraction", Inorganica Chimica Acta., 361(8) ,2522-2532,2008.

[16] A.Z. Ansari, G. Badis, E. T. Chan, H.V. Bakel, L. Pena-Castillo, D. Tillo, K. Tsui, C. D. Carlson, A. J. Gossett, M. J. Hasinoff, C. L. Warren, M. Gebbia, Sh. Talukder, A. Yang, S. Mnaimneh, D. Terterov, D. Coburn, A. L. Yeo, Z. X. Yeo, N. D.Clarke, J. D. Lieb, C. Nislow, T. R. Hughes:"A Library of Yeast Transcription Factor Motifs Reveals a Widespread Function for Rsc3 in Targeting Nucleosome Exclusion at Promoters", Molecular cell., 32(6), 878–887, 2008.

[17] J. S. Vrentas, J. L.Dude, A. C. How, J. Appl. Polym. Sci., 29, 399, 1984.

[18] W.M. Mekenzie and O.C. Sherington, J. polym. Sci. Poly. Chem., 20, 431, 1982.

[19] V.K. Gupta and I. Ali, J. Colloid. Interf. Sci., 271, 321, 2004.

[20] B. Volesky, "Removal and recovery of heavy metals by biosorption" in: B. Volesky (Ed.), Biosorption of Heavy Metals, CRC Press, Boca Raton, FL, pp. 7–43, 1990.

[21] B. Volesky, Hydrometallurgy, 59 (2–3), 203, 2001.[22] P.J. Panak, M.A. Kim, J.I. Yuna, J.I. Kim, Colloid Surf. A, 227, 93, 2003.

[23] J-M. Lehn,: "Supramolecular chemistry: concepts and perspectives", Weinheim: VCH., 1995.

[24] JL. Atwood, JED. Davies, DD. MacNicol, F. Vogtle, J-M. Lehn:" Comprehensive supramolecular chemistry", Oxford: Perga-mon., 1996.

[25] J-M. Lehn:" Toward complex matter: supramolecular chemistry and self-organization", Proc Natl Acad Sci USA., 99, 4763–8, 2002.

[26] D. Philp, JF. Stoddart :" Self-assembly in natural and unnatural systems", Angew Chem Int Ed Engl.,35, 1154–96, 1996.

[27] J-M. Lehn:" Supramolecular chemistry/science. Some conjectures and perspectives", In: Ungaro R, Dalcanale E, editors. Supramolecular science: where it is and where it is going. Dordrecht: Kluwer., 287–304, 1999..

[28] J-M. Lehn: "Dynamers: dynamic molecular and supramolecular polymers", Prog Polym Sci., 30, 814–831, 2005.

[29] SJ. Rowan, SJ. Cantrill, GRL.Cousins, JKM. Sanders, JF. Stoddart:" Dynamic covalent chemistry", Angew Chem Int Ed Engl.,41,898–952, 2002.

[30] J-M.Lehn:" Dynamic combinatorial chemistry and virtual combinatorial libraries", Chem Eur J., 5, 2455–63,1999.

[31] GRL. Cousins, SA. Poulsen, JKM.Sanders :"Molecular evolution: dynamic combinatorial libraries, autocatalytic networks and the quest for molecular function", Curr OpinChem Biol., 4, 270–9, 2000.

[32] WG. Skene, J-M. Lehn :"Dynamers: polyacylhydrazone reversible covalent polymers, component exchange, and constitutional diversity", Proc Natl Acad Sci USA., 101, 8270–5, 2004.

[33] J-M.Lehn :"Supramolecular polymer chemistry—scope and perspectives", Polym Int., 51, 825–39, 2002.

[34] A. Ciferri:" Supramolecular polymers", New York: Dekker., 2000.

[35] J-M. Lehn:" Supramolecular chemistry—molecular information and the design of supramolecular materials", Makromol Chem Macromol Symp., 69, 1–17, 1993.

[36] L. Brunsveld, BJB. Folmer, EW. Meijer, RP. Sijbesma:" Supramolecular polymers", Chem Rev., 101, 4071–4097, 2001.

[37] HR. Kricheldorf :"Macrocycles. 21. Role of ring–ring equilibria in thermodynamically controlled polycondensations", Macro-molecules., 36, 2302–8, 2003.

[38] J. Xie, Y-L. Hsieh:" Enzyme-catalyzed transesterification of vinyl esters on cellulose solids", J Polym Sci Polym Chem Ed., 39, 1931–9, 2001.

[39] C. Berkane, G. Mezoul, T. Lalot, M. Brigodiot, E. Marechal:" Lipase-catalyzed polyester synthesis in organic medium. Study of ring-chain equilibrium", Macromolecules., 30, 7729–34, 1997.

[40] A. Lavalette, T. Lalot, M. Brigodiot, E. Marechal,:" Lipase-catalyzed synthesis of a pure macrocyclic polyester from dimethyl terephthalate and diethylene glycol", Biomacromole-cules.,3,225–8, 2002.

[41] HM. Colquhoun, DF. Lewis, A. Ben-Haida, P. Hodge:" Ring- chain interconversion in high-performance polymer systems. 2. Ring-opening polymerization–copolyetherification in the synthesis of aromatic poly(ether sulfones)", Macromolecules., 36, 3775–8, 2003.

[42] X. Chen, MA. Dam, K. Ono, A. Mal, H. Shen, SR. Nutt, K. Sheran, F. Wudl :" A thermally re-mendable cross-linked polymeric material", Science., 295, 1698–702, 2002.

[43] X. Chen, E. Ruckenstein:" Thermally reversible covalently bonded linear polymers prepared from a dihalide monomer and a salt of dicyclopentadiene dicarboxylic acid", J Polym Sci Polym Chem., 38, 1662–72, 2000.

[44] Y.Chen, K-H. Chen:" Synthesis and reversible photo- cleavage of novel polyurethanes containing coumarin dimer components", J Polym Sci Polym Chem., 35, 613–24, 1997.

[45] H. Otsuka, K. Aotani, Y. Higaki, A. Takahara:" Polymer scrambling: macromolecular radical crossover reaction between the main chains of alkoxyamine-based dynamic covalent polymers", J Am Chem Soc., 125, 4064–5, 2003.

[46] I. Nakazawa, S. Suda, M. Masuda, M. Asai, T. Shimizu:" pH- dependent reversible polymers formed from cyclic sugar- and aromatic boronic acid-based bolaamphiphiles", Chem Commun., 881–2, 2000.

[47] O. Ramstrom, J-M. Lehn:" Drug discovery by dynamic combinatorial libraries", Nat Rev Drug Discov.,1, 26–36, 2002.

[48] J-M. Lehn:" Supramolecular Chemistry - Concepts and Perspectives", Weinheim: VCH., 1995.

[49] GW. Gokel, A. Mukhopadhyay :" Synthetic models of cation-conducting channels", Chem SocRev., 30, 274–286, 2001.

[50] N. Voyer :"The development of peptide nanostructures", Top Curr Chem., 184, 1–35, 1996.

[51] J-M. Lehn, J-P.Behr :" Transport of amino acids through organic liquid membranes", J Am Chem Soc., 95, 6108–6110, 1973.

[52] M. Barboiu, G. Vaughan, A. van der Lee,:" Self-organized heteroditopic macrocyclic superstructures", Org Lett., 5, 3073–3076, 2003.

[53] M. Barboiu:" Supramolecular macrocyclic receptors-hybrid carrier vs. Channel transporters in bulk liquid membranes", J Inclusion Phenom Mol Recognit Chem., 49,133–137, 2004.

[54] A. Cazacu, C. Tong, A. van der Lee, TM. Fyles, M. Barboiu:" Columnar self-assembled ureidocrown-ethers—an example of ion-channel organization in lipid bilayers", J Am Chem Soc., 128, 9541–9548, 2006.

[55] DT. Bong, TD. Clark, JR. Granja, MR. Ghadiri :" Self-assembling organic nanotubes", Angew Chem Int Ed., 40, 988–1011, 2001.

[56] S. Matile :" En route to supramolecular functional plasticity: Synthetic β-barrels, the barrel-stave motif, and related approaches", Chem Soc Rev., 30,158–167, 2001.

[57] PK. Eggers, TM. Fyles, KDD. Mitchell, T. Sutherland:" Ion channels from linear and branched bolaamphiphiles", J Org Chem., 68, 1050–1058, 2003.

[58] M. Barboiu, C. Luca, C. Guizard, N. Hovnanaian, L. Cot, G. Popescu:" Hybrid organic-inorganic fixed site dibenzo-18-crown complexant membranes", J Membr Sci., 129,197–207, 1997.

[59] M. Barboiu, C. Guizard, C. Luca, B. Albu, N. Hovnanian, J. Palmeri,:" A new alternative to amino acid transport: Facilitated transport of L-Phenylalanine by hybrid siloxane membrane containing a fixed site macrocyclic complexant", J Membr Sci., 161,193–206, 1999.

[60] M. Barboiu, C. Guizard, C. Luca, N. Hovnanian, J. Palmeri, L.Cot:" Facilitated transport of organics of biological interest II. Selective transport of organic acids by macrocyclic fixed site complexant membranes", J Membr Sci., 174, 277–286,2000.

[61] M. Barboiu, C. Guizard, N. Hovnanian, J. Palmeri, C. Reibel, C.Luca, L. Cot :"Facilitated transport of organics of biological interest I. A new alternative for the amino acids separations by fixed-site crown-ether polysiloxane membranes", J Membr Sci., 172, 91–103, 2000.

[62] M. Barboiu, S. Cerneaux, G. Vaughan, A. van der Lee:" Ion-driven ATP-pump by self-organized hybrid membrane materials", J Am Chem Soc., 126, 3545–3550, 2004.
[63] C. Arnal-Herault, M. Michau, A. Pasc-Banu, M. Barboiu:" Amplification and transcription of the dynamic supramolecular chirality of G-quadruplex", Angew Chem Int Ed., 46, 4268–4272, 2007.
[64] A. Cazacu, M. Michau, R. Caraballo, C. Arnal-Herault, A. Pasc-Banu, A. Ayral, M. Barboiu:" Dynamic supramolecular hybrid and mesoporous membranes", Ann Chem Sci Mater., 32,127–139, 2007.
[65] C. Arnal-Herault, M. Barboiu, A. Pasc, M. Michau, P. Perriat, A. van der Lee:" Constitutional self-organization of adenine-uracil-derived hybrid materials", Chem Eur J., 13, 6792–6800, 2007.
[66] J-M.Lehn:" From supramolecular chemistry towards constitutional dynamic chemistry and adaptative chemistry", Chem Soc Rev., 36,151–160, 2007.
[67] WG. Skene, J-M.Lehn:" Dynamers: polyacylhydrazone reversible covalent polymers, component exchange, and constitutional diversity", Proc Natl Acad Sci USA., 99, 8270–8275, 2002.
[68] T. Ono, T. Nobori, J-M. Lehn:" Dynamic polymer blends-component recombination between neat dynamic polymers at room temperature", Chem Commun., 12, 1522–1524, 2005.
[69] T. Ono, S. Fujii, T. Nobori, J-M. Lehn:" Soft-to-hard transformation of the mechanical properties of dynamic covalent polymers through component incorporation", Chem Commun.,1, 46–48, 2007.
[70] T. Ono, S. Fujii, T. Nobori, J-M.Lehn:" Optodynamers: expression of color and fluores-cence at the interface between two films of different dynamic polymers", Chem Commun., 42,4360–4362, 2007.
[71] G. Nasr, M. Barboiu, T. Ono, S. Fujii, J-M Lehn, "Dynamic polymer membranes displaying tunable transport properties on constitutional exchange", J Membr Sci., 321 (2008) 8–14
[72] G. Nasr, A. Gilles, T.Macron, C. Charmette, J.Sanchez, M. Barboiu:" Tuning gas-diffusion through dynameric membranes: toward rubbery organic frameworks (ROFs)", Isr. J. Chem. 53 (2013) 97 – 101.
[73] M. Barboiu:" Constitutional Dynameric Networks for Membranes", Encyclopedia of Membrane Science and Technology., 2013.
[74] Yuan, Y., and T. R. Lee. Surface Science Techniques. (Eds.) G. Bracco, B. Holst.2013. ISBN: 978-3-642-34242-4.

6. Appendix

6.1. Appendix: FTIR measurements

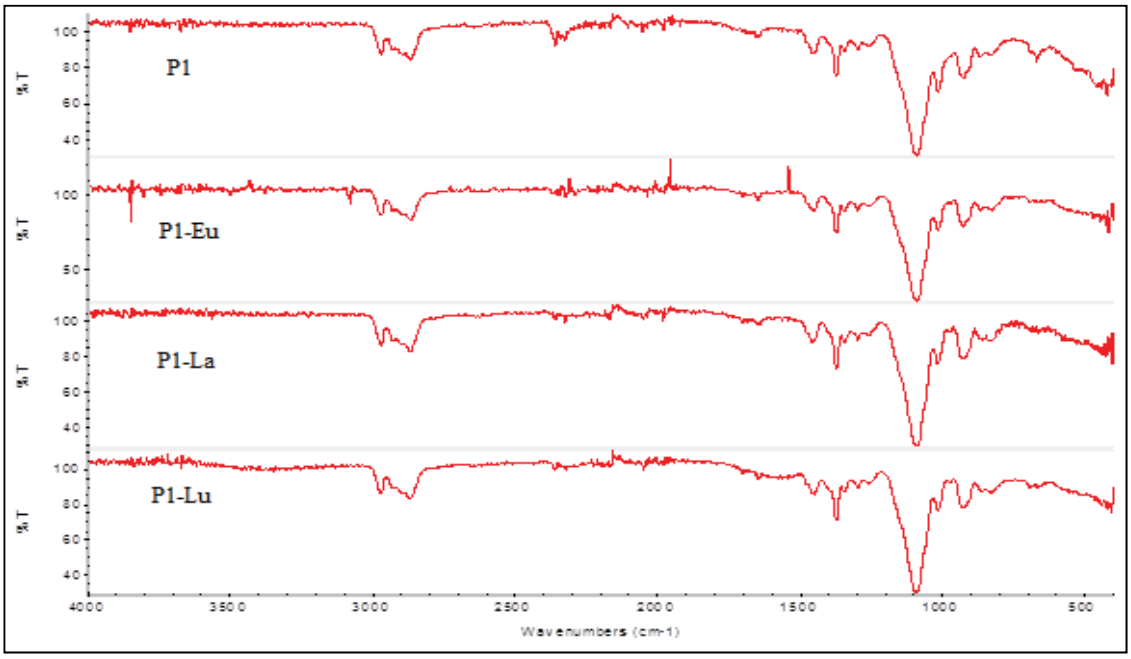

Fig.31: The FTIR measurements for P1 with Lanthanide metal ions (La^{3+}, Lu^{3+}, Eu^{3+}).

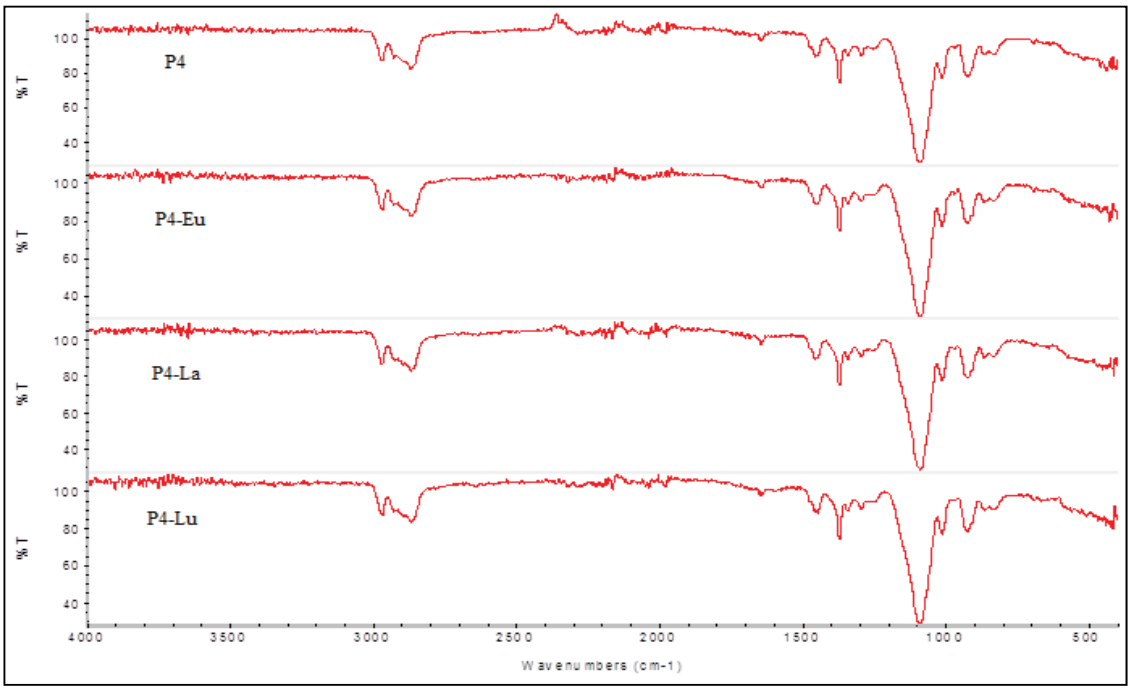

Fig.32: The FTIR measurements for P4 with Lanthanide metal ions (La^{3+}, Lu^{3+}, Eu^{3+}).

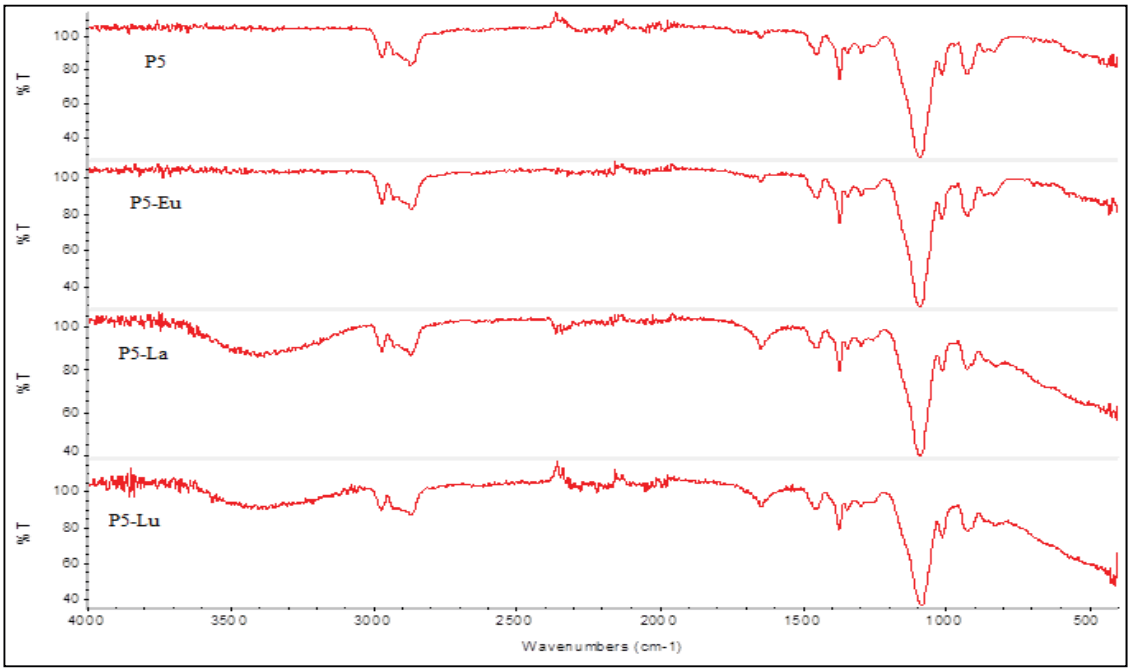

Fig.33: The FTIR measurements for (P5) with Lanthanide metal ions (La^{3+}, Lu^{3+}, Eu^{3+}).

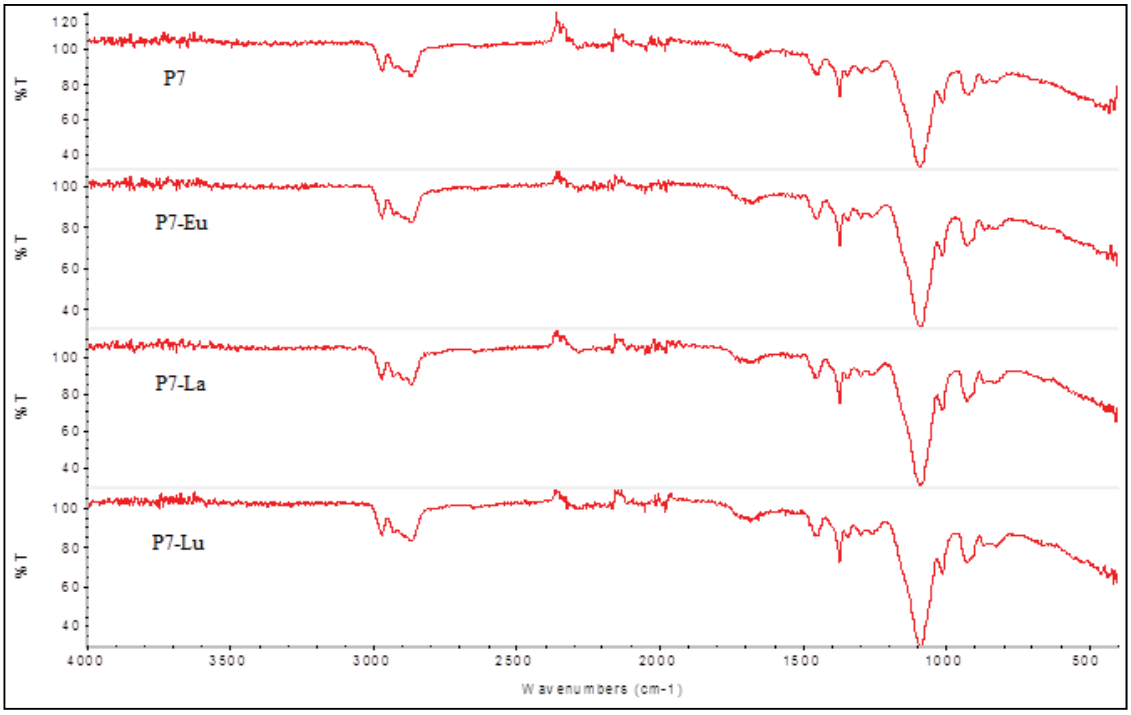

Fig.34: The FTIR measurements for (P7) with Lanthanide metal ions (La^{3+}, Lu^{3+}, Eu^{3+}).

6.2. Appendix: ^{1}H NMR measurements

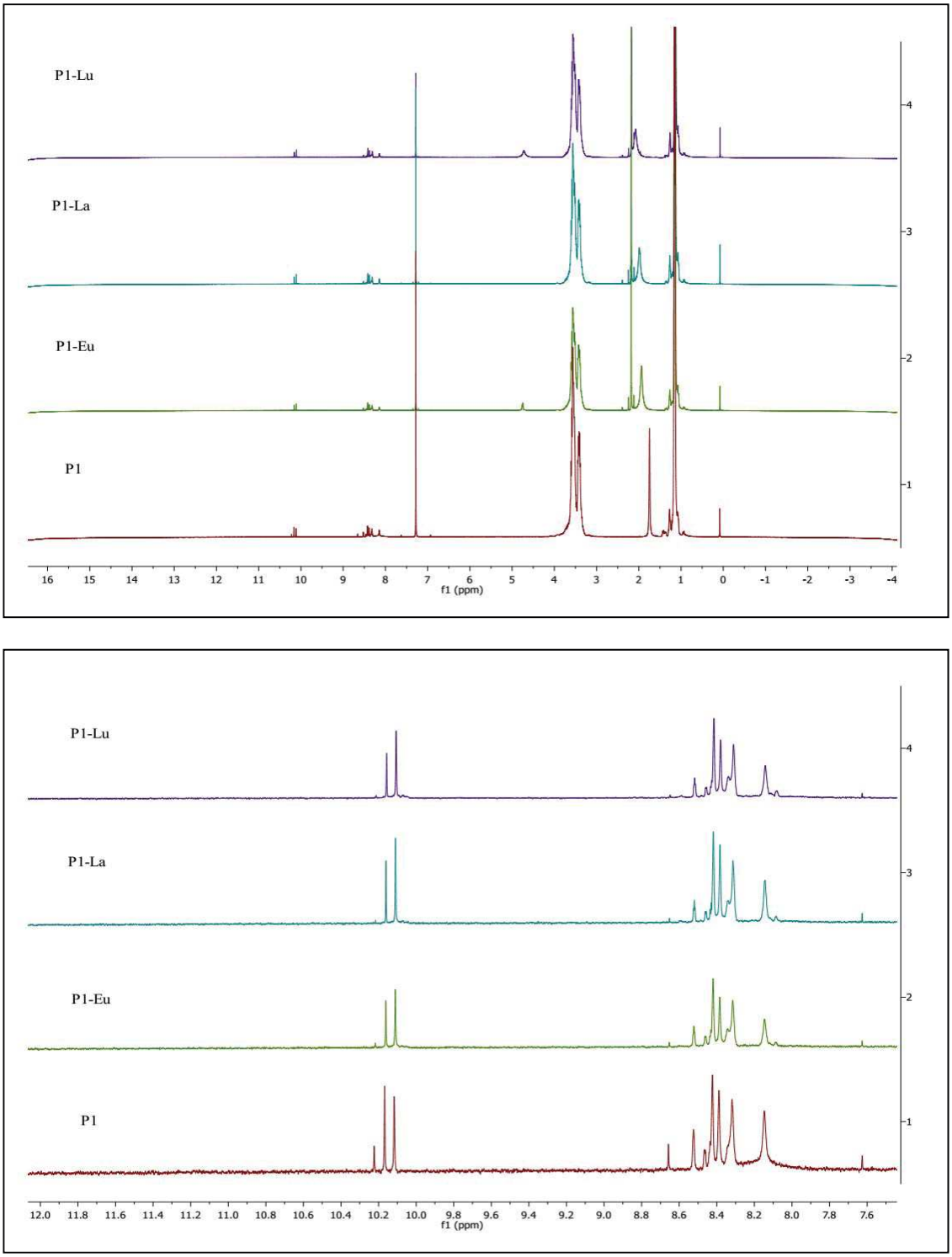

Fig.35: ^{1}H NMR measurements of the membrane (P1) with its metal ions (La^{3+}, Lu^{3+}, Eu^{3+}).

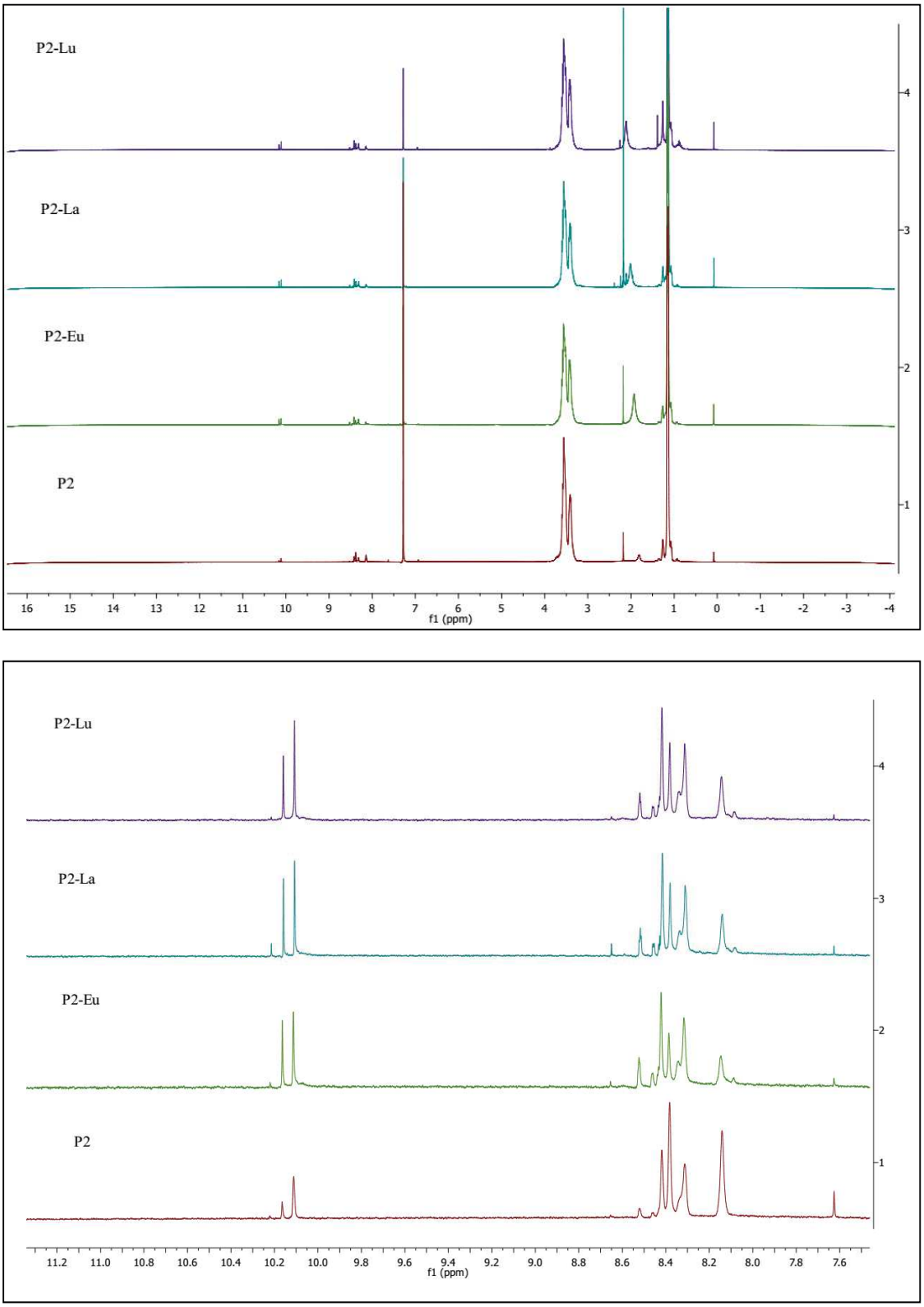

Fig.36: ^{1}HNMR measurements of the membrane (P2) with its metal ions (La^{3+}, Lu^{3+}, Eu^{3+}).

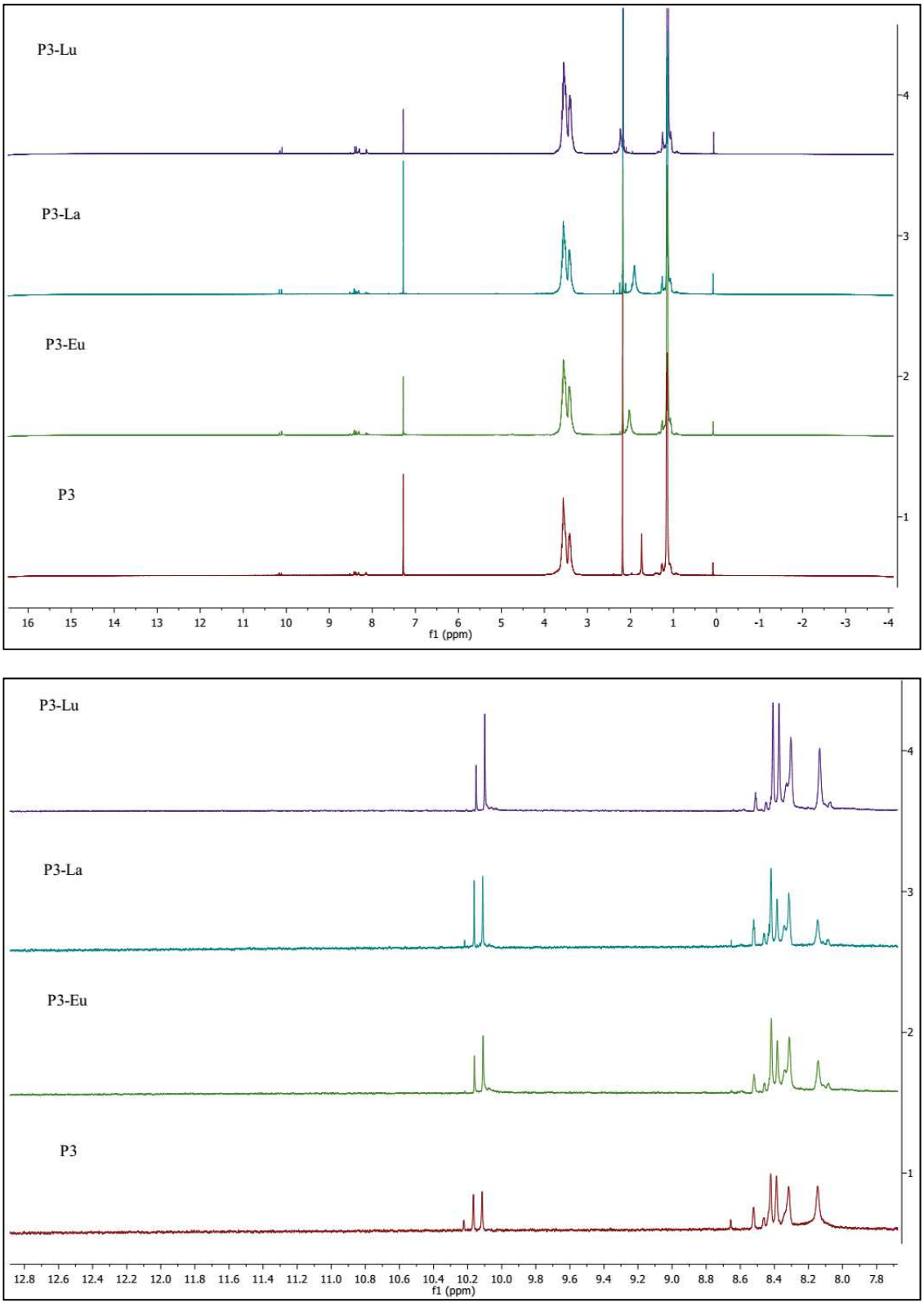

Fig.37: ^{1}HNMR measurements of the membrane (P3) with its metal ions (La^{3+}, Lu^{3+}, Eu^{3+}).

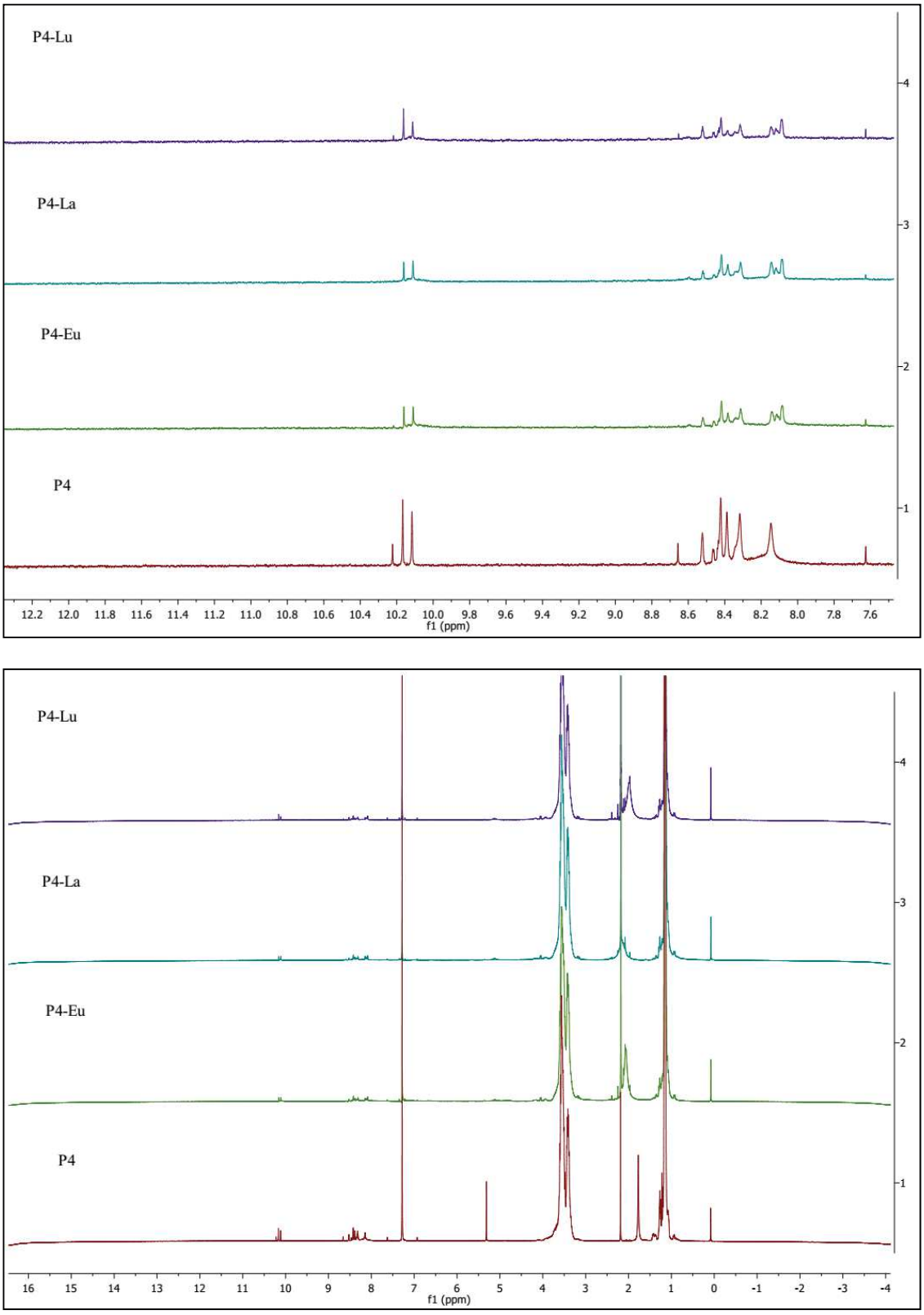

Fig.38: ^{1}HNMR measurements of the membrane (P4) with its metal ions (La^{3+}, Lu^{3+}, Eu^{3+}).

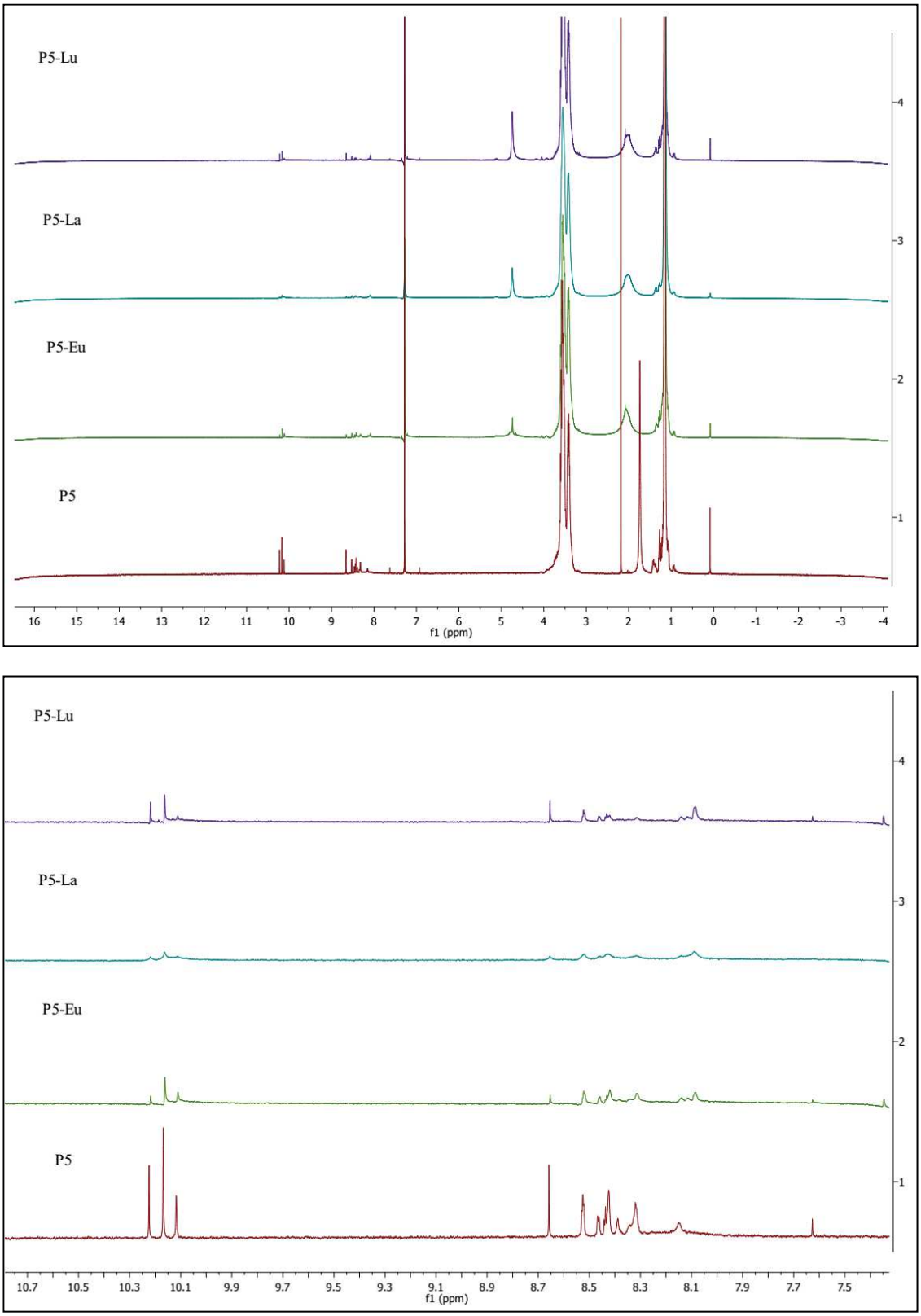

Fig.39: ^{1}HNMR measurements of the membrane (P5) with its metal ions (La^{3+}, Lu^{3+}, Eu^{3+}).

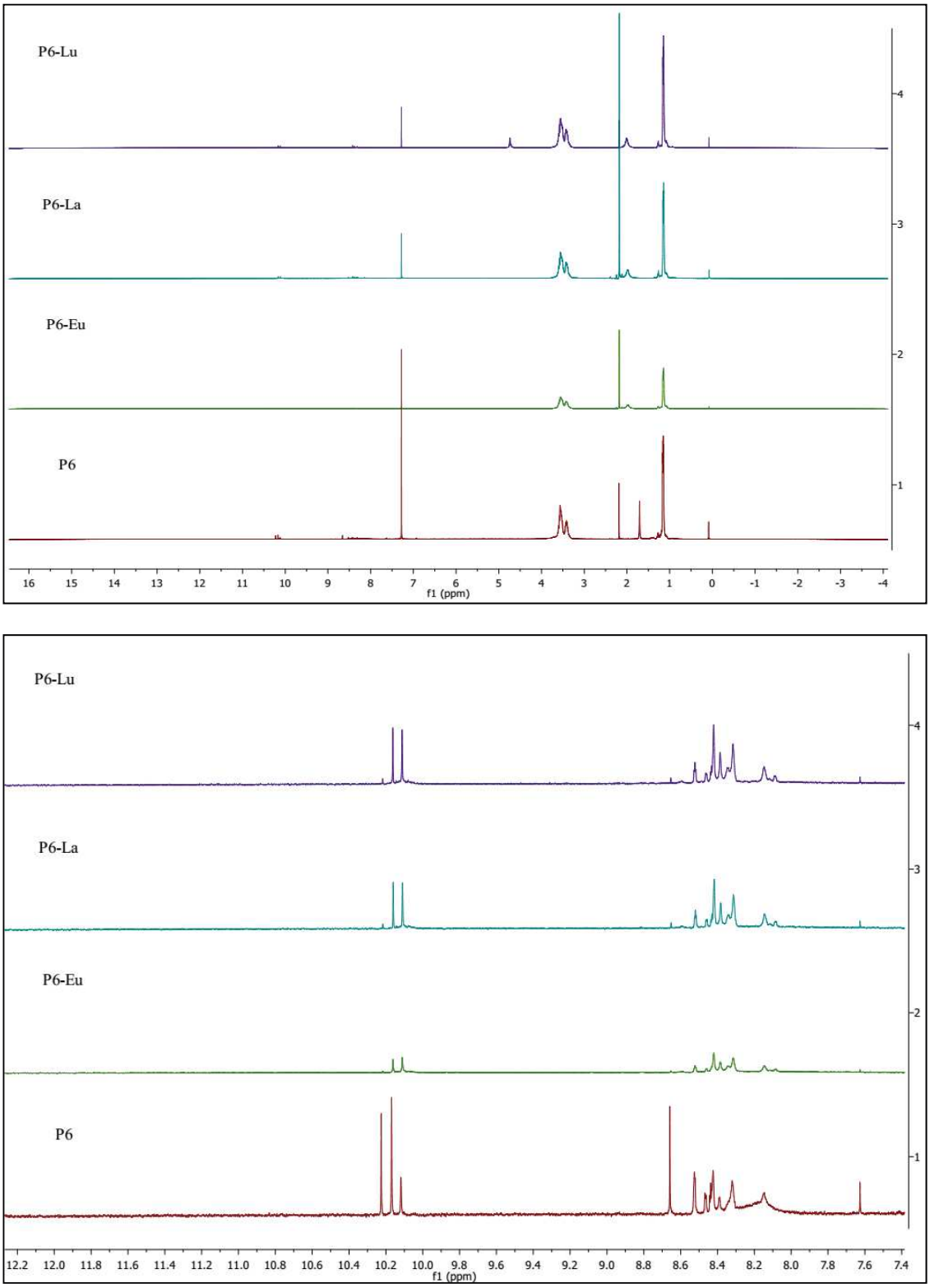

Fig.40: ^{1}HNMR measurements of the membrane (P6) with its metal ions (La^{3+}, Lu^{3+}, Eu^{3+}).

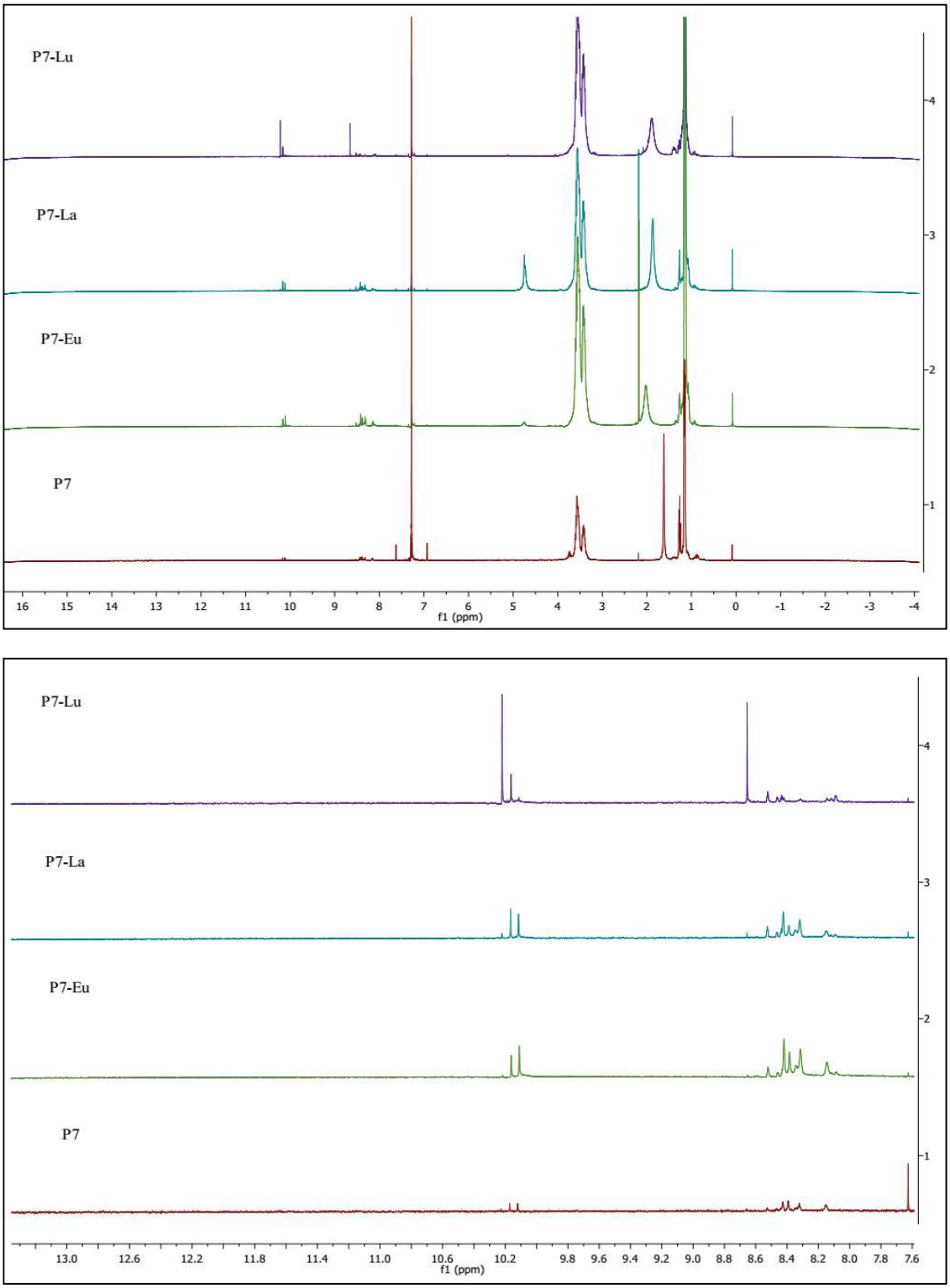

Fig.41: ^{1}HNMR measurements of the membrane (P7) with its metal ions (La^{3+}, Lu^{3+}, Eu^{3+}).

6.3. Appendix: DSC measurements

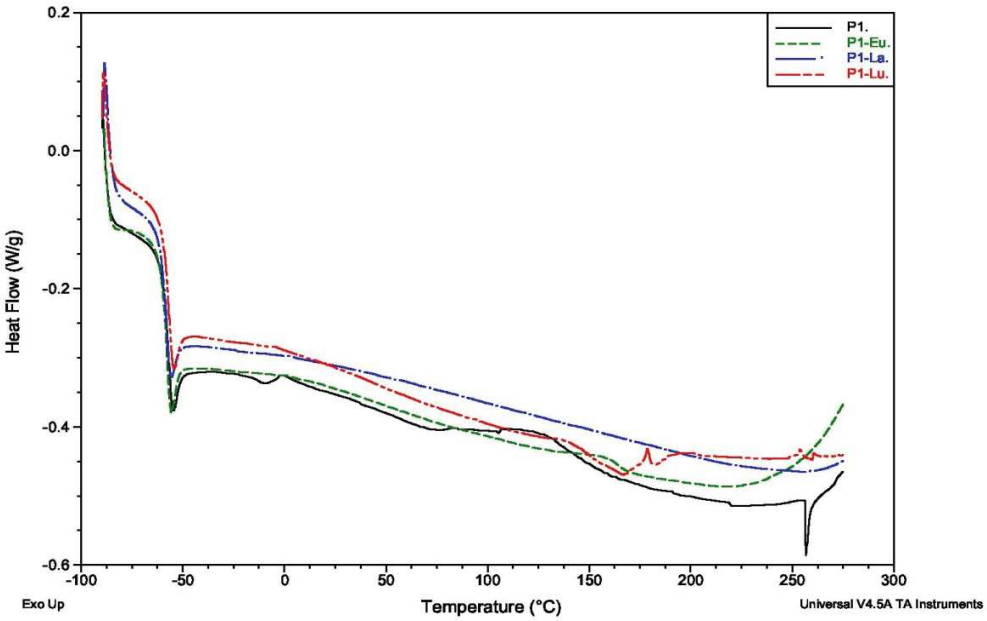

Fig.42: DSC measurements of the membrane (P1) with its metal ions (La^{3+}, Lu^{3+}, Eu^{3+}).

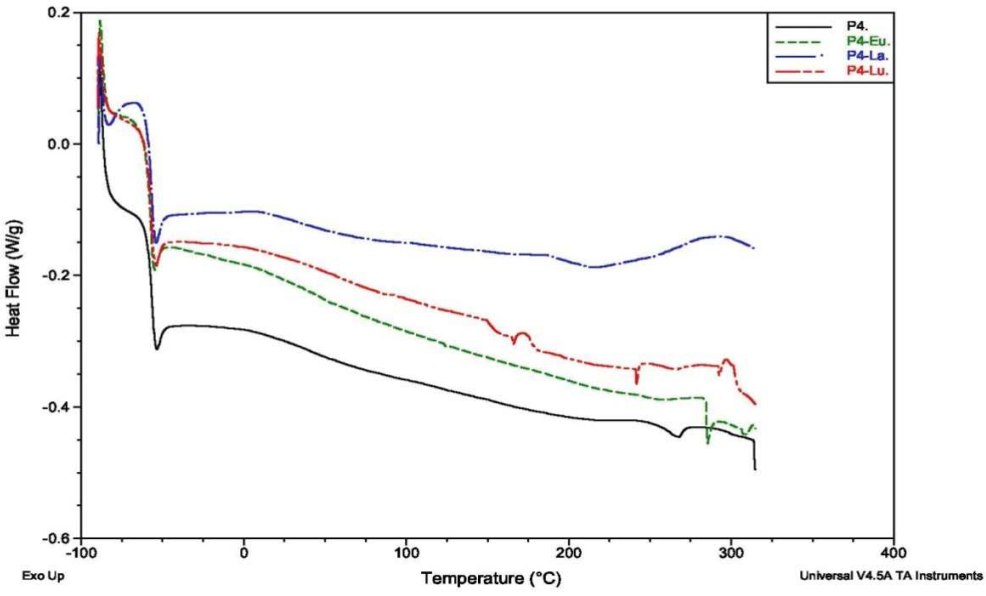

Fig.43: DSC measurements of the membrane (P4) with its metal ions (La^{3+}, Lu^{3+}, Eu^{3+}).

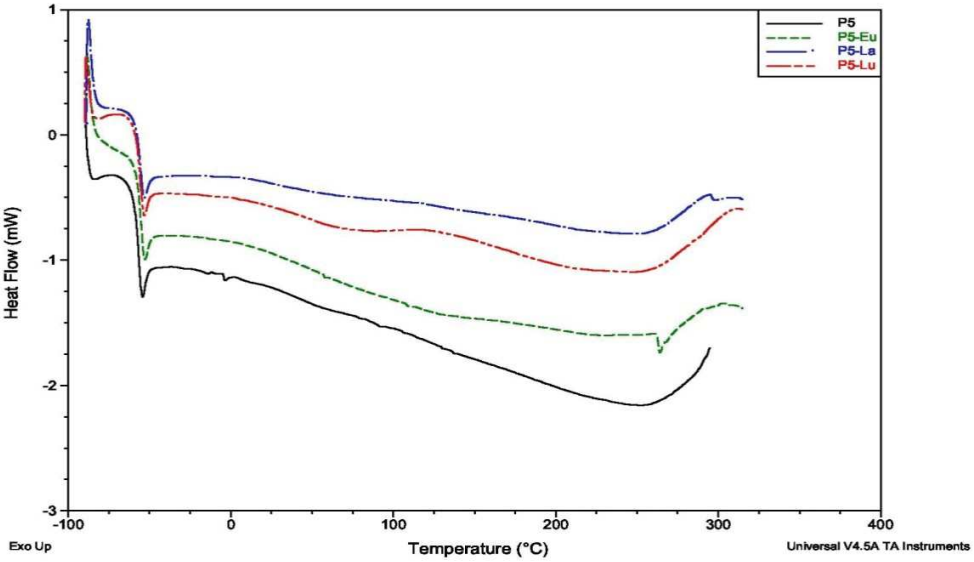

Fig.45: DSC measurements of the membrane (P5) with its metal ions (La^{3+}, Lu^{3+}, Eu^{3+}).

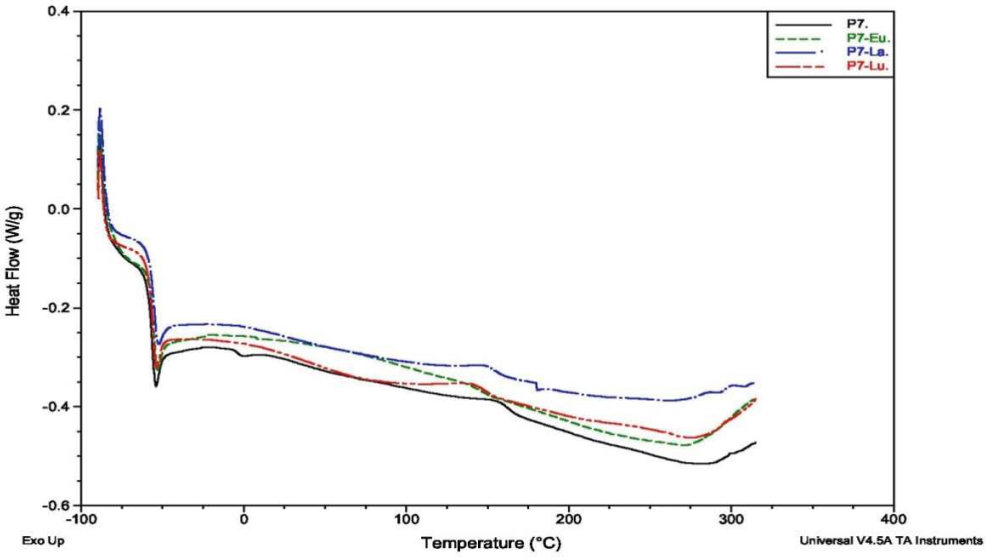

Fig.46: DSC measurements of the membrane (P7) with its metal ions (La^{3+}, Lu^{3+}, Eu^{3+}).

6.4. Appendix: TGA measurements

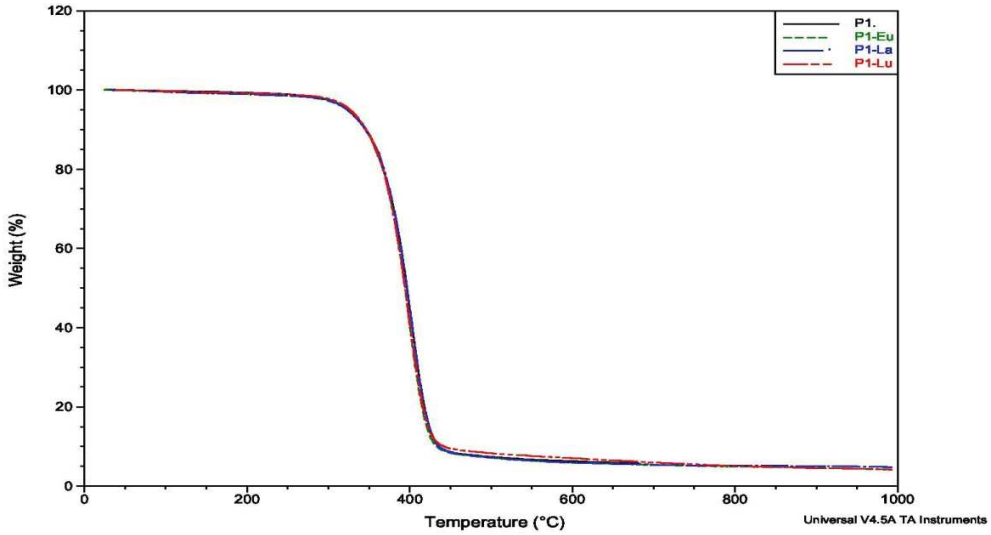

Fig.47: TGA measurements of the membrane (P1) with its metal ions (La^{3+}, Lu^{3+}, Eu^{3+}).

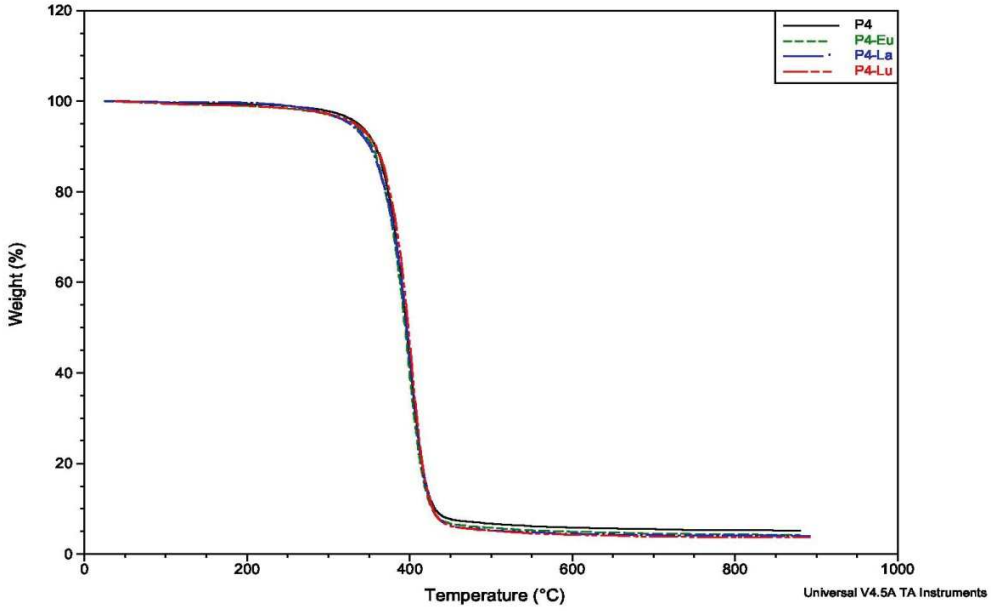

Fig.48: TGA measurements of the membrane (P4) with its metal ions (La^{3+}, Lu^{3+}, Eu^{3+}).

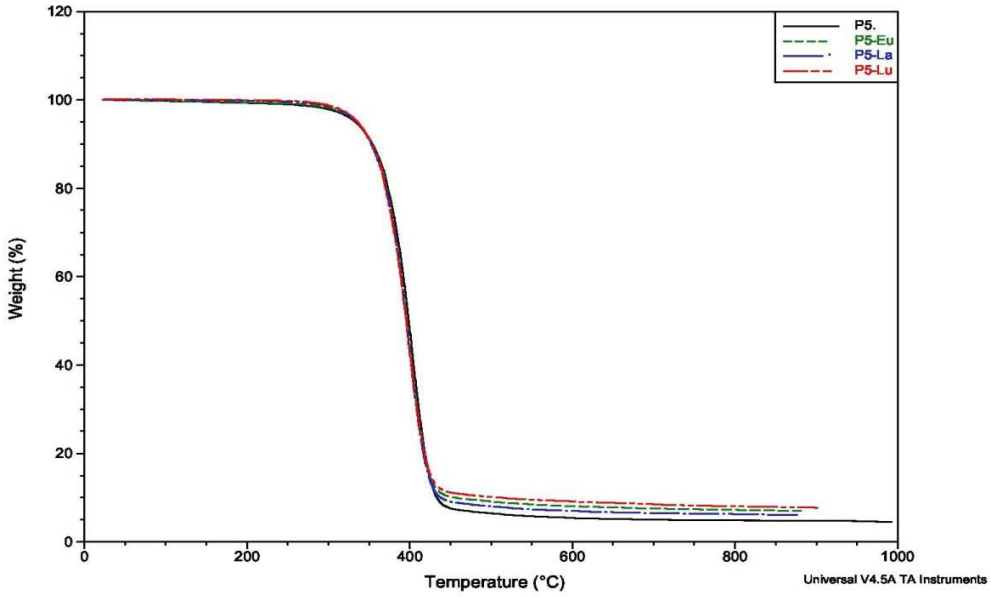

Fig.49: TGA measurements of the membrane (P5) with its metal ions (La^{3+}, Lu^{3+}, Eu^{3+}).

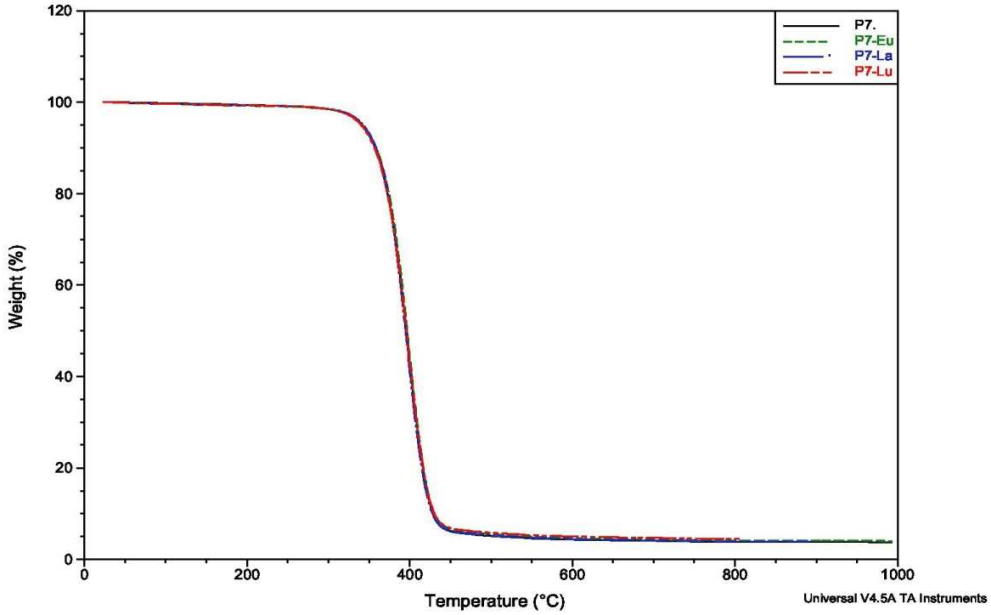

Fig.50: TGA measurements of the membrane (P7) with its metal ions (La^{3+}, Lu^{3+}, Eu^{3+}).

Membranes	TGA (^{0}C)	Tg (°C)
P1	283.26 ^{0}C	-57.99 ^{0}C
P1-La	281.58 ^{0}C	-58.39 ^{0}C
P1-Lu	276.98 ^{0}C	-57.18 ^{0}C
P1-Eu	273.99 ^{0}C	-57.18 ^{0}C
P4	284.42 ^{0}C	-56.78 ^{0}C
P4-La	281.58 ^{0}C	-56.06 ^{0}C
P4-Lu	280.63 ^{0}C	-56.06 ^{0}C
P4-Eu	282.52 ^{0}C	-56.55 ^{0}C
P5	**296.74 ^{0}C**	**-56.56 ^{0}C**
P5-La	**304.32 ^{0}C**	**-55.55 ^{0}C**
P5-Lu	**303.91 ^{0}C**	**-56.56 ^{0}C**
P5-Eu	**303.37 ^{0}C**	**-56.06 ^{0}C**
P7	260.73 ^{0}C	-58.08 ^{0}C
P7-La	285.37 ^{0}C	-57.07 ^{0}C
P7-Lu	285.37 ^{0}C	-56.69 ^{0}C
P7-Eu	268.31 ^{0}C	-57.07 ^{0}C

Table 4: DSC and TGA measurements of the used polymeric membranes (P1, P4, P5, and P7) with their lanthanide metal ions (La^{3+}, Lu^{3+}, Eu^{3+}).

6.5. Appendix: Contact angle measurements

The contact angles meausremnts (The left and right contact angles) for the used polymeric membrane (P5) before and after the transportation of lanthanide metal ions (La, Lu, Eu) have been summarized in Table (2.5).

Membranes	Left contact angle	Right contact angle
P5	57.13	58.19
P5-La	50.94	51.68
P5-Lu	52.54	53.64
P5-Eu	54.72	55.23

Table 5: Summary of the average contact angles measurements on the used dynameric membranes.

Chapter (3)

CO_2 capture using supported ionic liquid membranes immobilized with carbonic anhydrase enzyme.

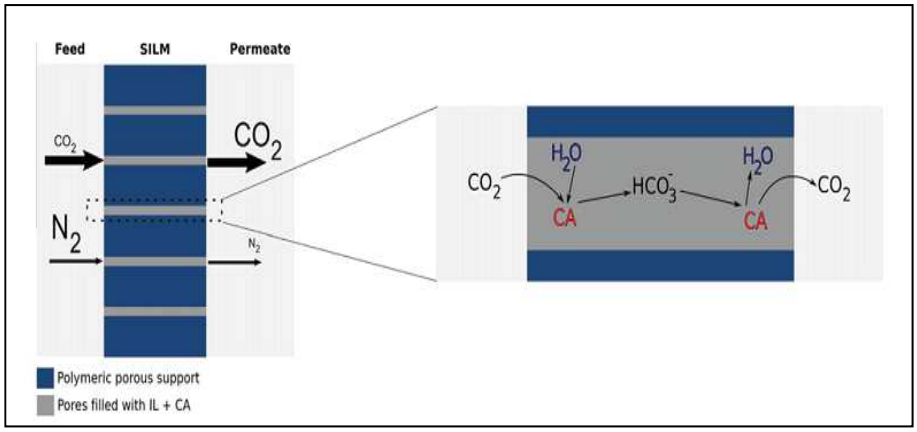

Abstract

The approach proposed in this research work consists on using supported ionic liquid membranes (SILMs) comprising two different carbonic anhydrase enzymes, the thermo resistant SspCA enzyme and the Bovine-CA enzyme, which catalyze the reaction of reversible conversion of CO_2 to bicarbonate, enhancing the driving force for CO_2 transport. Membrane stability, CO_2 and N_2 permeability and CO_2/N_2 ideal selectivity were determined for the membranes developed. The results showed that the supported ionic liquid membranes prepared by immobilizing a selected ionic liquid (1-butyl-3-methylimidazolium bis(trifluoromethanesulfonyl)imide) [C_4MIM][Tf_2N] with and without enzymes in a PVDF hydrophobic polymeric support allowed to obtain stable supported liquid membranes at high temperatures (up to 100ºC), selective towards CO_2 against N_2. Moreover, the selectivity and permeability are affected by different parameters, namely, temperature, water activity and enzyme concentration. The results show that the SILM immobilized with ([C4MIM][Tf2N]+SspCA enzyme) has the highest permeability and selectivity for CO_2 when comparing with other SILMs immobilized with ([C_4MIM][Tf_2N] +BCA enzyme) and [C_4MIM][Tf_2N]. Two different concentration of enzymes (0.1mg enzyme/gm ionic liquid) and (0.25 mg enzyme /gm ionic liquid) immobilized with the ionic liquid were also tested. The results show that, by increasing the enzyme concentration 2.5 times, the permeability and selectivity of CO_2 were duplicated for both enzymes, and the highest permeability and selectivity values have been obtained in case of SILMs immobilized with ([C_4MIM][Tf_2N]+SspCA enzyme). Moreover, it could be concluded that, the SILMs immobilized with ([C_4MIM][Tf_2N]+SspCA enzyme) present higher stability at high temperatures (80ºC and 100ºC) than the other used SILMs. However, the selectivity obtained is still below other reported data available in the literature. In order to improve the selectivity and permeability through the enzyme-solvent system it will be important in further studies to evaluate the behavior of CO_2 task-specific ionic liquids, which combined with the use of higher concentrations of carbonic anhydrase enzymes may lead to efficient and competitive carbon dioxide capture systems.

Keywords: Supported ionic liquid membranes (SILMs), Carbonic anhydrase enzyme; Immobilizing; Permeability; Selectivity; Carbon dioxide capture.

The Aim of the research work: The aim of the present research work is to design high temperature stable supported ionic liquid membranes impregnated with two different kind of carbonic anhydrase enzymes (carbonic anhydrase Isozyme II and (SspCA) enzyme) to be used for capture of CO_2 from flue gas streams. The schematic representation of the proposed concept is illustrated in Fig. 1. As ionic liquids have a negligible vapor pressure, they may be used to develop highly temperature stable supported liquid membranes in contact with gaseous streams, avoiding the problems of evaporation and displacement, experienced when using aqueous solutions. Additionally, ionic liquids with the particular ability to solubilize and concentrate CO_2 (task-specific ionic liquids), will provide the perfect ambient for the reaction that the thermoresistant carbonic anhydrase enzyme catalyzes (as shown in Fig.1). Ionic liquids with affinity for CO_2 assure an enhanced local concentration of CO_2 and the necessary level of water [1,2], which guarantees the adequate enzyme activity and stability. The water present in ionic liquids may be adjusted carefully and its loss is not relevant because it is involved in the solvation of the ionic liquid and the enzyme. It is expected that the presence of the carbonic anhydrase enzyme in the liquid medium will improve the total CO_2 mass transfer due to a combined effect between the increased uptake of CO_2 by the ionic liquid and the extra mechanism of enzymatic conversion of CO_2 to HCO^-_3. To validate this hypothesis, the present work proposes to investigate the following aspects: 1- Design of supported liquid membranes by immobilization of an ionic liquid in a polymeric hydrophobic support; 2- Evaluation of the stability of the SLMs at high temperatures; 3- Determination of CO_2 and N_2 pure gas permeabilities and assessment of the potential of the membranes for the CO_2/N_2 separation; 4- Determination of the effect of water activity present in the selected solvent on the improvement of CO_2 transport and selectivity.

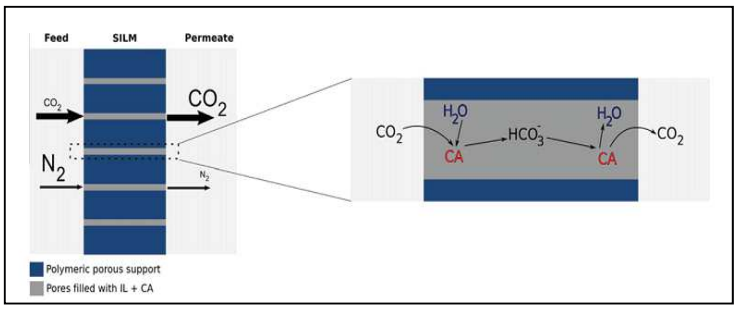

Fig.1: Schematic representation of the proposed concept [1].

1. Introduction

One of the main problems our world is presently facing concerns the capture of anthropic carbon dioxide rejected in the atmosphere by human activities. This gas is considered as one of the main atmospheric components responsible for a green house effect and an increase of the earth atmosphere temperature [3,4], with many unwanted consequences, including the development of infectious diseases [5]. The emission of carbon dioxide (CO_2) from utilization of fossil fuels has received worldwide attention due largely to the rapid growth in worldwide CO_2 emissions predicted to 40.2 Gt by 2030 [6]. Therefore, there is a growing interest in developing technologies for efficient capture and sequestration of large quantities of CO_2. By far, a number of CO_2 capture technologies which have already being practiced on laboratory scale or industrially are processes based on physisorption/chemisorption, membrane separation or molecular sieves, carbamation, amine physical absorption, amine dry scrubbing, mineral carbonation [7].

The traditional technology for CO_2 capture in industry is chemical adsorption by an aqueous solution of amine, which has some advantages such as its maturity, stable operation, good reactivity, and high capacity [8]. However, using aqueous amines like mono ethanolamine (MEA) CO_2 capture consumes almost 30% of the energy that is needed to run a power plant [9], in addition to other drawbacks like insufficient CO_2 capture capacity, high solvent losses caused by evaporation, degradation and poor thermal stability, as well as the equipment corrosion [10, 11]. Therefore, developing the economical and energy efficient CO_2 capture technologies is urgently needed.

Separation of carbon dioxide (CO_2) from emission sources generated by power plants has been attracting much attention due to the enhanced greenhouse effect [12]. Therefore, there is a continuing effort to develop energy efficient separation technologies for the capture of CO_2 from flue gas streams. There are currently three main sources of CO_2 in power plant stations: in post-combustion, pre-combustion, and oxy-fuel combustion processes. The focus of this work will be given to CO_2 capture in post-combustion systems.

The flue gas discharged at atmospheric pressure (1 bar) and high temperature (up to 200°C) is mainly composed by nitrogen (up to 70% by volume) and a low percentage of CO_2 (between 3% and 15% by volume). One of the main challenges in post-combustion capture is the relatively low partial pressure of CO_2, which induces a low driving force in separation processes, with a direct impact on energy and separation process costs [13]. Currently, gas absorption using aqueous amines is the most widely used process in industry for the selective removal of CO_2, being effective even for low CO_2 partial pressures present in the post-combustion systems. However, this process is rather energy intensive, and corrosion and degradation may occur with a direct impact in operation costs [13].

1.1. Carbon dioxide capture

Geological sequestration of carbon dioxide requires two separate steps: the first is the capture of carbon dioxide, and the second is the transport and sequestration of the captured carbon dioxide. The capture, storage and utilization of carbon dioxide (CO_2) have been a hot topic since it can help decrease greenhouse gas emissions and mitigate global climate warming [14,15]. Currently, chemical absorption is widely used for CO_2 capture and sodium/potassium hydroxide, ammonia, and organic amines are common absorbents [16]. However, the further application of chemical absorption to industry is limited for some inherent disadvantages, such as high absorbents loss and energy consumption, low efficiency, equipment corrosion, sensitivity to SO_x and NO_x [17,18]. Several recent researches reported that combination of membrane and chemical absorption can increase gas-liquid interface and improve mass transfer process, resulting in higher CO_2 absorption efficiency [19, 20]. But the corrosion problem, evaporation loss and high energy consumption still remain. The exploration of new capture and storage methods for CO_2 is ongoing worldwide. Of the many candidate techniques being studied principal focus is on absorption, adsorption (chemical and physical) and membrane methods. For low concentration or low pressure CO_2 streams chemical absorption is preferred. The essential choice is between chemistries that yield carbonates or carbamates (produced by means of amines) to realize gas–liquid CO_2 separation [21].

Historically, the preferred operating geometry has been a two compartment device-absorber and stripper. Absorption occurs rapidly and efficiently but desorption requires substantial additional energy, typically in the form of thermal input, applied at the stripper. Both the thermal requirements and the pumping requirements result in substantial energy consumption. In addition, these processes present many operational difficulties due to the bulk fluid gas–liquid contacting design. Among the inherent problems are flooding, foaming, channeling and entrainment [22]. Yet another problem is the corrosive character of many of the chemicals used.

1.2. CO_2 capture processes

The conditions for CO_2 capture, hence also the economics, are determined by the technology used for the production of electricity (or heat) from fossil fuels [23]. Today, a power company planning to build a new power station utilizing fossil fuels, can choose from two technologies, and a third one, which is in the development phase [24]. The characteristics of all the three processes (i.e., postcombustion, precombustion, and oxyfuel combustion) are different, yielding different conditions for CO_2 capture.

1.2.1. Post-combustion Capture

The first option is the postcombustion process,[25] which is widely used at traditional fossil-fuel-fired power stations to produce electricity. Under postcombustion conditions the fuel is burned fully in one step in air, see (Fig.2). The released heat is used to produce high pressure steam, which drives a steam turbine to generate electricity. The flue-gas leaving the boiler contains substantial amounts of particulate matter, which is filtered out in the soot removal step. Subsequently, the sulfur in the flue-gas is scrubbed by limestone slurry to produce gypsum. The cleaned flue-gas, which now contains 10−16% CO_2, would be released into the atmosphere in the absence of a CO_2 capture system. However, as explained in the Introduction, the role of CO_2 in the global warming requires it to be captured and stored safely underground for some time.

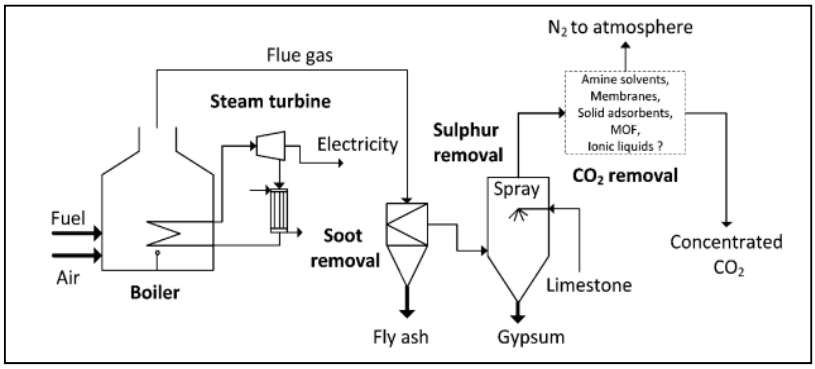

Fig.2: Schematic representation of a simplified postcombustion CO_2 capture system [26,27].

1.2.2. Precombustion Capture

The second option is the precombustion process, [28] which is associated with the integrated gasification combined cycle (IGCC) and is more complex as shown in (Fig.3). In this approach the fuel (coal, oil, etc.) is gasified, rather than burning it completely like in the postcombustion process, in the presence of pure oxygen and Steam to produce syngas. The syngas, which is a mixture of carbon monoxide (CO) and hydrogen (H_2), is purified and fed to the water−gas-shift (WGS) reactor. In this reactor, steam is added to convert the CO, according to the water−gas-shift reaction, to H_2 and CO_2. The gas can be desulphurized either before or after the WGS reactor, but preferentially before since any sulfur may be poisonous to the catalyst used in the WGS reactor [29]. At this stage the gas consists primarily of CO_2 and H_2. Subsequently, the CO_2 is captured and the H_2 is combusted in a gas turbine to produce electricity and heat. The heat produced during the combustion can be recovered by a heat recovery system to generate more electricity. Furthermore, the precombustion process yields a gas mixture with high CO_2 partial pressures, which is favorable for CO_2 separation.

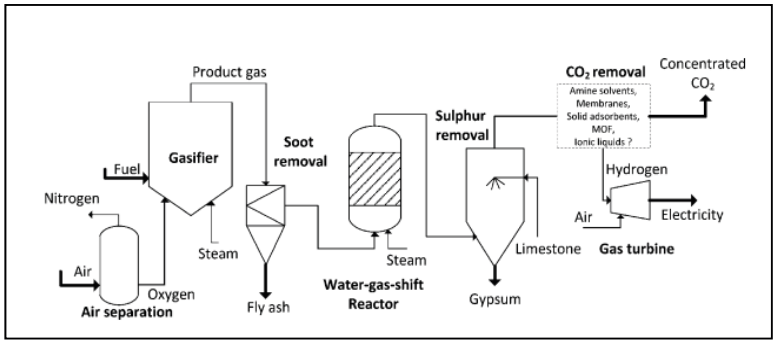

Fig.3: Schematic representation of a simplified precombustion CO_2 capture system [28, 30,31].

1.2.3. Oxyfuel Combustion Capture

The third option is the oxyfuel combustion [32] process, which is a promising concept but still under development. A simplified schematic representation of this process is given in (Fig.4). In this approach concentrated oxygen, instead of air, is used to burn the fuel. The released heat is used to produce high-pressure steam, which turns a steam turbine to generate electricity. The flue-gas, which mainly consists of H_2O and CO_2, is stripped of the soot particles and partly recycled to the boiler to control the temperature. The remaining flue-gas stream is desulphurized and cooled down to condense the water. The result is a concentrated stream of CO_2, which is ready to be stored underground. The fundamental difference between this process and the other two processes is that no CO_2 capture is involved; instead N_2/O_2 is the relevant separation in this process. The concentrated CO_2 stream is a result of excluding nitrogen in the burning step.

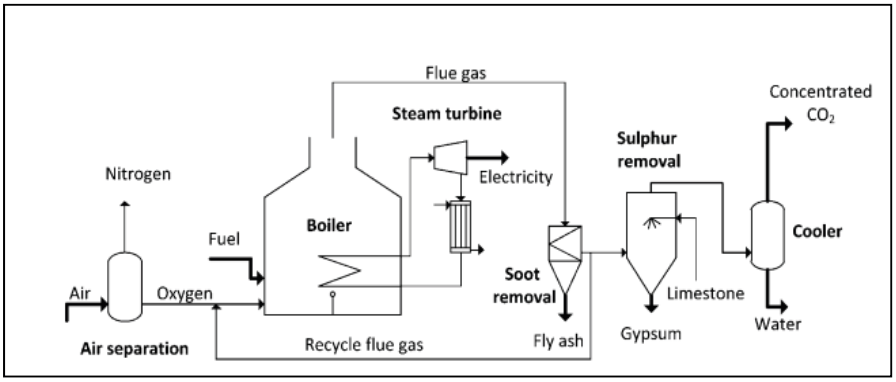

Fig.4: Schematic representation of a simplified oxyfuel-combustion CO_2 capture system [31, 33].

1.3. The Physical chemistry of CO_2 capture in Aqueous Media

The general mechanism of CO_2 capture in aqueous media and its separation from other gases, can be decomposed in the five following steps [34].

(1) Dissolution of the CO_2 gas molecules in water on the CO_2 capture side, at the gas/aqueous medium interface, according to the Henry's equilibrium [35–37].

As a result, neutral aqueous CO_2 (aq) molecules are introduced in the aqueous film in direct contact with the gas.

(2) Reversible conversion by deprotonation of the neutral CO_2 (aq) species, usually termed hydration, to form anionic bicarbonate species HCO_3^-, according to a chemical equilibrium which is pH dependent.

(3) Transport of both the neutral and anionic aqueous CO_2 species, from the CO_2 capture side towards the CO_2 release side, by molecular diffusion inside the aqueous medium and/or by forced fluid circulation.
(4) Reverse conversion of the anionic HCO_3^- species to the neutral CO_2 (aq) ones, according to the same chemical equilibrium as in step 2.
(5) Evaporation of the CO_2 (aq) in the gas to liberate CO_2 gas species, on the CO_2 release side, according to the same Henry's equilibrium as in step 1.

1.4. Ionic Liquids

Ionic liquids (ILs) are organic salts which exist as liquid state over wide temperature ranges [38]. ILs exhibit numerous attractive properties, such as less volatile, high thermal stability, low corrosion, and tenability, making them potential candidates as environment-friendly materials for many industrial chemical processes [39, 40]. Since Lynnette et al [41] reported that CO_2 has a higher solubility in ILs while ILs do not dissolve in CO_2, ILs have received lots of attentions in CO_2 capture and Separation [42]. Anderson et al [43] compared the solubility of various gases in 1-hexyl-3-methylpyridinium bis(trifluoromethylsuflonyl)imide, and found that the primary interaction of the CO_2 turned up with the anion. As CO_2 absorption was generally higher in the ILs containing fluorinated anions [44], ILs with variety of cations and anions have been prepared, expecting excellent CO_2 capture and separation performance [45]. Some simulation studies have reported that ILs could reduce the fixed investment and operating cost comparing with using other commercial chemical absorbents in industrial application [46].

1.4.1. Ionic liquids and their properties

Typical room temperature ionic liquids (RTILs) are composed of an organic cation (most often an alkyl-substituted imidazolium or a pyridinium or a quaternary ammonium ion) and an inorganic anion (see Fig.5). Ionic liquids have low melting points (<100ºC) and remain as liquids within a broad temperature window (<400 °C). The physical, chemical and biological properties of ILs generally depend on the structure of the cation (the symmetry and the length of alkyl substituent, the presence of hydrophobic groups, etc.) as

well as on the degree of anion charge delocalization [47]. Ionic liquids are tailorable solvents in which they can be designed to have specific physicochemical properties through structural changes in the cation and anion. Therefore, ILs properties cover a broad range of values and cannot be generalized. A comprehensive data base on physical properties of ILs such as melting point, density and viscosity has been presented by Zhang and co-workers [48]. The other solvent properties as regards polarity, hydrophobicity and solvent miscibility behavior of ILs have been described in the literature for specific applications [49–51]. Based on the solvation standpoint, ILs are generally considered to be highly polar solvents. A number of different methods have been used to provide information about their polarity, including solvatochromic dyes [52–55], partition [56-58] and fluorescence probe methods [59]. Solvatochromic dyes are compounds with a visible absorption maximum that depends on the polarity of the solvent. In this method, the solvent polarity is determined based on the shift of the charge-transfer absorption band of solvate chromic probe in the presence of the solvent [60]. Empirical polarity scales, developed using solvate chromic dyes, indicate that the polarity of common ILs based on imidazolium cation such as[bmim][BF_4]falls in the range of lower alcohols [52,53,55] and form amide [60]. However, the polarity of ILs generally decreases with an increase in the alkyl chain length appended on the imidazolium ring in the cation for a fixed anionic group[49] .Besides, solvate chromic study shows that ILs possessing non coordinating anion (e.g.,$PF_6^-$and Tf_2N^-) are less polar than the lower alcohols [55]. Recently, Schrodle et al. used the dielectric response of ILs to more accurately and reliably obtain information about polarity [61].The polarity of ILs can affect enzyme stability and selectivity [62-67]. In general, polar solvents increase the solubility of polar substrates and lead to faster and more selective reactions [66,67]. However, this trend is not true for all cases because some reports showed no relationship between reaction rates and ILs polarity [63, 65]. This phenomenon can be explained in terms of viscosity. In fact, the change of the polarity and viscosity of ILs are correlated although the changing rates are different. For example, an IL with shorter alkyl chains on the cation has a lower viscosity and also a higher polarity. The increase of alkyl chain length produces a slight reduction in the polarity of ILs, but a huge increase in their viscosity [68,69]. The reaction rates may be affected by the significant viscosity change.

One of the notable properties of ILs is that they are capable of a wider range of intermolecular interactions [56,70], such as dipolar, hydrogen bonding, dispersive and ionic. Hence, many compounds are significantly soluble in ILs. Interestingly, ILs having coordinating anions (e.g.,Cl^-,NO_3^-,CH_3COO^- and $(MeO)_2PO_2^-$) which are strong hydrogen bond acceptors can dissolve many compounds which are insoluble or sparingly soluble in water and most organic solvents. Examples include cellulose [71, 72] and some compounds having pharmacological activity [73,74]. The ability of ILs to dissolve such compounds generally depends on the hydrogen bonding ability of anions [56,72].

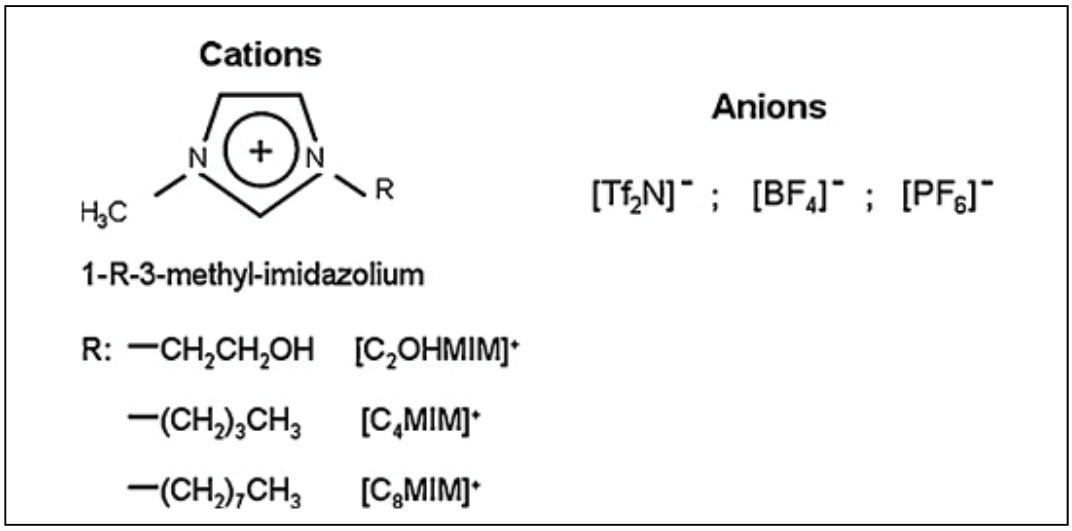

Fig.5:Typical cations and anions present in imidazolium type of RTILs [75].

Based on the solubility of ILs in water, ionic liquids can be divided into two categories: hydrophobic (water immiscible) and hydrophilic (water miscible). This water miscibility generally depends on the anions of ILs. Indeed, water interacts with the anion through the formation of hydrogen bonds [76,77]. However, the miscibility of ionic liquids with water is not well generalized. For example, ILs [bmim][BF_4], [bmim][PF_6] and [bmim][Tf_2N] have almost the same polarity [52] and the coordination strength is also comparable [55] , but first one is water miscible whereas latter two are not. A recent measurement of the H-bond accepting properties of such ILs revealed that [BF_4] was better H-bond acceptors (ß= 0.61) than [PF_6](ß=0.50), which can be considered as a reasonable explanation regarding the difference in water miscibility[78].

Ionic liquids are generally immiscible with many organic solvents such as hexane and ether, whereas some are miscible with polar solvents like lower alcohols, ketones, dichloromethane and tetrahydrofuran [79]. The immiscibility of ILs with either water or organic solvents has made them feasible to be used to form a two-phase system. Generally, ionic liquids are not miscible with supercritical carbon dioxide ($scCO_2$), but they can absorb a large amount of $scCO_2$ [80]. Ionic liquids are well proved as highly stable solvents and are stable above 100°C. In particular, dicationic ILs show much higher thermal stabilities than monocationic ILs [81,82]. For example, ILs Containing bis (2,3-dimethylimidazolium) cation have the excellent thermal stability with only 5% thermal degradation at 440ºC [82]. Consequently, they are very effective as solvents for high temperature reaction systems. The thermal stability of ILs is calculated based on their decomposition temperatures where there is 10% mass loss using thermogravimetric analysis (TGA) [83,84]. The most thermally stable ILs reported were those having the $[Tf_2N]$ anion with various types of cations, including alkylammonium and imidazolium [83]. In contrast, ILs containing a carboxylate anion, particularly formate, may have lower thermal stability due to undergoing a condensation reaction to form amides [84].On the other hand, the instability of anions $BF_4^-$and PF_6^- are well documented [85] . In fact, the hydrolysis of such anions produces the toxic volatiles such as HF, POF_3, which can deactivate the enzymes. The viscosity of ILs is higher compared with that of molecular solvents. Like other solvents, the viscosity of ILs is dependent on the ion-ion interactions, such as van der Waals interactions and hydrogen bonding. Therefore, the value of the viscosity varies significantly with chemical structure, composition, temperature and the presence of solutes of impurities. It has been shown that ionic liquid's viscosity generally increases with an increase in the alkylchain length for a fixed anionic group due to the stronger van der Waals interactions [48,49]. Besides, delocalization of the charge on the anion, such as through fluorination, decreases the viscosity by weakening hydrogen bonding [86]. However, the viscosity of ILs was affected more by the change to the anion than to the cation [87]. In the presence of small amount of water or organic solvents or with the increase of temperature, the viscosity of ILs also decreases markedly [88, 89]. The solvent viscosity could affect the biocatalytic reactions rate in terms of the mass transfer limitation when the reaction is rapid and the IL is relatively viscous.

For example, a higher enzyme activity was observed in [emim][Tf_2N] than in [MTOA][Tf_2N] due to lower viscosity of first one compared to latter one [67]. However, this trend is not true for all biocatalytic reactions performed in ILs [62], particularly when reaction rates are measured in equilibrium instead of kinetics.

RTILs have received increasing interest in applications involving carbon dioxide separations, due to the large solubility of CO2 in selected RTILs [90]. Among the large diversity of RTILs, those based in the imidazolium cation typically present a large solubility for CO2. Additionally, these RTILs based on the imidazolium cation, may exhibit an even higher solubility for CO2by selecting an appropriate RTIL anion, which also plays an important role in the gas solubility due to a weak Lewis acid/base complexation that occurs between $CO_2$and the RTIL anion[91]. Additionally, the solubility of CO_2 in RTILs is also expected to increase with an increase in the alkyl chain length of the RTIL cation [92]. In this way, it is possible to design tailor-made membranes with a defined selectivity for a specific application combining different alkyl chain lengths of the RTIL cation and different anions. Among the diverse gas mixtures, the most attractive seem to be the CO_2/N_2 and CO_2/CH_4 separations, associated respectively with the purification of flue gas streams and natural gas processes [17, 93].

1.4.2. Ionic Liquid membranes

Membrane technologies for CO_2 separation are a promising alternative due to their modularity and ease of operation. Membrane is used here to mean a thin film with selective exclusion/inclusion properties. Performance of such a separation medium is based on differences in reactivity, solubility and diffusivity for various gases in the membrane material. For non reactive materials both permeability and selectivity are typically low [94]. A thin liquid film (liquid membrane (LM)), because of the inherent absence of stable structure, requires a support material for structural integrity. This can be achieved by its deposition into specific pores (immobilized liquid membrane (ILM)), around fibers (supported liquid membrane (SLM)), or between (microporous) surfaces (contained liquid membrane (CLM)). The advantage of these designs is that they operate as contactors avoiding many of the limitations seen in waterfall or bubble mass flow contactors. However, they do have their limitations. SLMs in particular suffer from

gravity-based size limitations due to the formation of catenary curve structures. ILM and SLM, insofar as they are not replenished and if the solvent has a high vapor pressure can fail due to evaporation. Evaporation can be minimized by use of a fluid having a lower vapor pressure than the common solvent-water [95]. They will also fail due to excessive trans membrane pressure differences.

Researchers incorporated ILs into some polymeric or inorganic porous medium to prepare supported ionic liquid membrane (SILM) in recent years. Compared with conventional supported liquid membranes, SILMs are more stable, for there is no evaporation problem occurring [96]. It has been reported that SILMs could increase gas-liquid contact interface, enhance mass transfer rate, and improve selectivity and permeability of liquid membranes [97,98]. More and more works have investigated the performance of SILMs in CO_2 capture and separation. Scovazzo et al [99] prepared SILMs by loading different immobilized ILs on a porous hydrophilic polyether sulfone (PES) support, and investigated their selectivity on CO_2/N_2 separation. Hydrophilic polyvinylidene fluoride (PVDF) membrane was used to immobilize different ILs, such as imidazolium-based ILs and acetate-based ILs, obtaining a good performance of permeability and CO_2 solubility [100 ,101]. And the properties of SILMs are influenced by the type and molecule structure of ILs, for it has been documented that the CO_2 separation capacity was affected by cation type and alkyl-chain length [75, 100, 102, 103].

1.4.3. Supported Ionic Liquid Membrane (SILM)

Supported liquid membranes (SLMs), a porous supports whose pores are filled with a liquid, have been used as a potential carrier for separation of optically active compounds [104–106]. Like other potential applications of ILs, during the recent years, the use of SLMs based on ILs was found to be very effective in selective transport of organic compounds such as alcohols, esters, acids, ketones and amines [107–113]. In ionic liquid supported membranes, mainly hydrophobic ILs are immobilized inside the porous structure of a polymeric or ceramic membrane and act as a separative phase of two

additional phases, named feed phase and receiving phase. In many cases, ionic liquids are confined between two membranes.

Supported ionic liquid membranes (SILM) are another system that can be used for CO_2 capture medium using ionic liquids. In SILM system, just the pores of a membrane are filled with the solvent (e.g. ionic liquid). The more soluble gas is able to permeate across the membrane, while the less soluble gas remains on the feed side. The flux of the gas across the membrane is affected by the thickness of the membrane. A thinner membrane yields a higher flux, but the thinner the layer of solvent, the quicker the solvent evaporates. But, due to non - volatile nature of ionic liquids this problem can be eliminated in case of ionic liquids - SLM systems [114].

In particular, supported Ionic liquid membranes (SILM) in which Ionic liquid is immobilized inside the porous structure of the supporting membrane by capillary forces, have been considered one of the most attractive membrane configurations to be used in gas separation applications [75, 115-117]. However, operating conditions such as high temperature and moderate pressure, as well as lack of differentiated selectivity towards specific gases is still limiting its application. High temperatures may lead to the evaporation of the solvent contained within the membrane pores and moderate pressures may lead to the displacement of the liquid from the membrane pores [116]. The properties of ionic liquids such as viscosity and non-volatility can stop the membrane solvent flowing out from porous membrane, which prolongs the life of the SILM greatly without diminishing the ability and selectivity of separation. The high-thermal stability and non-flammation of IL is suitable for capturing CO_2 from the flue-gases at high temperature, and SILM can enhance the contact area between gas and ionic liquids [118, 119, 123]. There are several works available in the literature where supported ionic liquid membranes were studied for potential applications in gas separations [118–124]. Scovazzo et al. [118] determined the pure gas permeability of N_2, CH_4 and CO_2 and the corresponding ideal selectivities through a porous hydrophilic polyethersulfone support with different RTILs immobilized. After representing the data obtained in a Robeson-plot the authors concluded that these permeabilities/selectivities of SILMs were competitive or even superior to other membrane materials. The facilitated transport of CO_2 and SO_2

through SILMs was studied by Luis et al. [119]. The permeabilities of air, CO_2 and a mixture of SO_2/air were measured using different SILMs, and ideal selectivities were calculated. It was concluded that SILMs can be very selective to CO_2 and SO_2.

Another potential avenue for improvement in CO_2 capture is based on biological systems, with the use of a carbonic anhydrase enzyme [1, 125, 126]. This enzyme catalyzes the reversible reaction of carbon dioxide with water to produce bicarbonate. Carbozyme, Inc. first proposed this approach, where the carbon dioxide presents in the flue gas stream contacts with carbonic anhydrase aqueous solution and produces bicarbonate. The bicarbonate diffuses across the liquid membrane and it is converted back to carbon dioxide upon desorption in the presence of vacuum or a sweep gas in the permeate side. The main problem with this technology is water management, since water evaporates even at relatively low temperatures. Therefore, in order to prevent liquid loss, the feed and sweep gases have to be humidified [127].

Although enzymes in ILs have presented enhanced activity, stability, and selectivity, the practical obstacle of using ILs is that many enzymes do not dissolve readily in most ILs, which has ruled out many potential biotechnological applications. In fact, enzymes that show catalytic activities in ILs normally do not dissolve in ILs. When enzymes become active in ILs, they remain suspended as a powder. Although some ILs can dissolve enzymes through the weak hydrogen bonding interactions, they often induce enzyme conformational changes resulting in inactivation [128,129]. To improve the enzyme solubility as well as activity in ILs various attempts have been made by modifying the form of enzymes in which it is used, including immobilized enzymes, the use of microemulsions, and the use of whole cells. According to that many research groups have modified the enzymes through the immobilization to improve the enzyme solubility as well as activity in ILs. All these strategies provide more robust, more efficient, and more enantioselective biocatalyst suitable for biotransformation with ILs [130]. L. Neves et.al. performed a concept for the capture of CO_2 from using supported liquid membranes with non-volatile ionic liquids (or solvents), comprising an enzyme that enhances the selective transport of CO_2 [126].

2. Materials and methods

2.1. Materials

The supported liquid membranes were prepared using a hydrophobic polymeric porous membrane made of polyvinylidene fluoride (PVDF) from Millipore Corporation, USA, with a pore size of 0.22 μm and thickness of 125 μm. This selection was based on previous results, where the supported liquid membranes prepared with this support material and pore size proved to be more stable when compared with others [131]. The ionic liquid tested in this work was 1-butyl-3-methylimidazolium bis(trifluoromethanesulfonyl)imide, [C4MIM][Tf2N], from Io-Li-Tec (Germany). This ionic liquid was selected due to its relatively low viscosity and a high solubility towards CO_2 [1,75,131]. Moreover, a hydrophobic ionic liquid [132] was selected since it has been reported that the use of hydrophobic ionic liquids is more favorable for enzyme activity and selectivity, when compared with hydrophilic ones [126].

2.2. Viscosity measurements

The viscosity values were obtained by performing rheology tests for the ionic liquids in a RS 75 Rheostress rheometer at the used different temperatures (30, 50, 80, and 100°C). Karl-Fisher system of Methrom AG, Herisu, Switzerland (Model 756KF coulometer) was used to analyze the water content.

2.3. Water content measurements

Determination of the water content of the ionic liquids were conducted using Hydranal-Coulomat CG, as catholyte reagent, for a coulometric KF titrator with a diaphragm, and with Hydranal-Coulomat AG as anolyte for a coulometric KF titrator.

2.4. Carbonic anhydrase enzyme

Two kinds of carbonic anhydrase enzymes have been used in this research work. The first one is (BCA) carbonic anhydrase Isozyme II lyophilized from bovine erythrocytes from Sigma–Aldrich (USA) (reference C3934) without any additional purification.

The second one is (SspCA) enzyme, which is a highly thermostable bacterial α-carbonic anhydrase from Sulfurihydrogenibium yellowstonense YO3AOP1 [133].

2.5. Gases

The gases used in the experiments were nitrogen, N_2, (Industrial Grade (99.99%), Praxair, USA) and carbon dioxide, CO_2, (High-Purity Grade (99.998%), Praxair, USA).

2.6. Preparation of the supported ionic liquid membranes (SILMs)

The procedure to immobilize the solvent inside the pores of the polymeric porous support consisted on placing the support into a desiccator and applying vacuum during 1 h. After this time, and still under vacuum, the solvent is introduced with a syringe in order to fill all the pores of the membrane and the membrane is left inside the desiccator for another hour. Afterward, the membrane surface is cleaned with paper tissue in order to remove the excess of solvent. The membrane thickness was measured using a micrometer Metric (Aldrich), and the membrane weight was measured using an analytical balance (Kern & Sohn GmnH ABJ 220-4M) before and after the immobilization procedure, in order to determine the amount of ionic liquid incorporated inside the membrane pores.

2.7. Pure gas permeability Experiments

Gas permeability experiments were carried out for CO_2 and N_2 using the experimental setup shown in (Fig.6). This rig is composed by two identical compartments (feed and permeate), made of stainless steel separated by the supported liquid membrane (effective area of 9.62 cm^2). Both compartments were pressurized with the pure gas, and after opening the permeate outlet, a pressure difference of about 0.7 bar was imposed. The pressure evolvement in each compartment along time was monitored using two pressure transducers (Druck, PDCR 910 models 99166 and 991675, England). Permeability measurements were performed for the temperatures (30, 50, 80 and 100ºC). The membrane thickness was measured using a Elcometer® 124 Thickness Gauge (United kingdom) and the membrane weight using an analytical balance (Kern & Sohn GmnH ABJ 220-4M) before and after each gas permeation experiment, in order to evaluate the weight loss of these membranes.

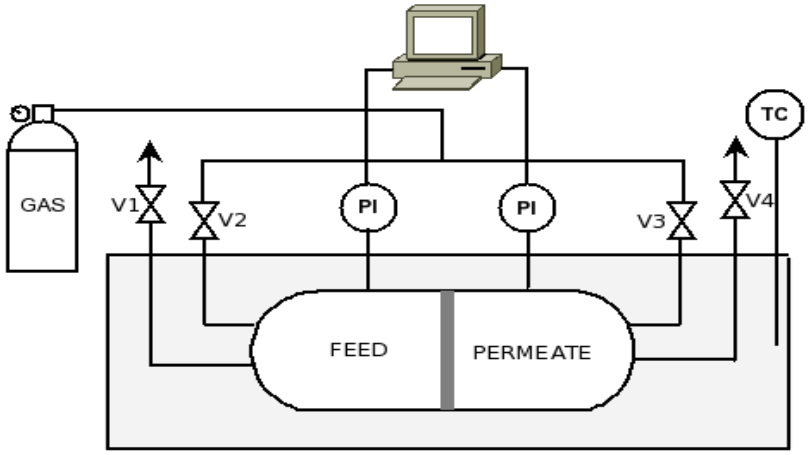

Fig.6: Experimental set-up for measuring the pure gas permeability of the SLMs: V1, V4 are inlet valves; V2, V3 are exhaust valves; PI1, PI2 are the pressure transducers; TC-Temperature controller, the whole setup is placed in a thermostatic water bath.

2.8. Theory

2.8.1. Gas permeability and ideal selectivity of SILM

The permeability of a pure gas through the supported liquid membrane is calculated from the pressure data obtained from both compartments (feed and permeate) shown in (Fig. 6) according to the following Eq. [134].

$$\frac{1}{\beta}\ln\left(\frac{[P_{feed}-P_{perm}]_0}{[P_{feed}-P_{perm}]}\right)=P\frac{t}{l} \qquad (1)$$

Where P_{feed} and P_{perm} correspond, respectively to the pressure in feed and permeate compartment (bar), P is the membrane permeability (m^2s^{-1}), t is the time (s), l is the membrane thickness (m), and β (m^{-1}) is a parameter characteristic of the geometry of the cell, given by:

$$\beta = A\left(\frac{1}{V_{feed}}+\frac{1}{V_{perm}}\right) \qquad (2)$$

where A is the membrane area (m^2), V_{feed} and V_{perm} are the volumes of the feed and permeate compartments (m^3), respectively. The data can be plotted as $\frac{1}{\beta}\ln\left(\frac{\Delta P_0}{\Delta P}\right)$ versus $\frac{t}{l}$, where the slope of this representation corresponds to the gas permeability.

The ideal selectivity ($\alpha_{A/B}$) can be determined by dividing the permeabilities of two different pure gases (A and B), and can also be expressed by the solubility (S) and diffusivity (D) contributions.

$$\alpha_{A/B} = \frac{P_A}{P_B} = \frac{S_A D_A}{S_B D_B} \qquad (3)$$

3. Results and Discussion

3.1. Viscosity measurements

The viscosity at different temperatures (30, 50, 80, and 100ºC) of the used ionic liquids with and without enzymes tested is summarized in Table 1. The additions of enzymes to IL do not provide important variations on viscosities values.

Table 1: The viscosity measurements of the used ionic liquid at different temperatures.

Temperature ºC	Water activity (a_w)	Viscosity (mPas)[a]		
		[C_4MIM][Tf_2N] + SspCA Enzyme	[C_4MIM][Tf_2N] + BCA Enzyme	[C4MIM][Tf_2N]
30	0.843	37 ± 0.52	38 ± 0.24	41 ± 0.25
	0.753	39 ± 0..21	41 ± 0.52	43 ± 0.77
	0.577	42 ± 0.42	43 ± 0.72	45 ± 0.41
	0.226	44 ± 0.88	47 ± 0.57	48 ± 0.66
50	0.843	20 ± 0.99	21 ± 0.17	22 ± 0.52
	0.753	21 ± 0.74	22 ± 0.82	23 ± 0.15
	0.577	24 ± 0.14	25 ± 0.13	25 ± 0.71
	0.226	25 ± 0.41	26 ± 0.84	27 ± 0.59
80	0.843	10 ± 0.92	11 ± 0.12	11 ± 0.31
	0.753	11 ± 0.24	11 ± 0.42	11 ± 0.86
	0.577	11 ± 0.68	12 ± 0.17	12 ± 0.31
	0.226	12 ± 0.07	12 ± 0.56	12 ± 0.93
100	0.843	8 ± 0.09	8 ± 0.24	8 ± 0.48
	0.753	8 ± 0.31	8 ± 0.43	8 ± 0.64
	0.577	8 ± 0.58	8 ± 0.62	8 ± 0.82
	0.226	8 ± 0.67	8 ± 0.86	9 ± 0.68

a) Pre-equilibrated at water activities (0.226, 0.577, 0.753, and 0.843).

3.2. Water content measurements

The water content for the pre-equilibrated ionic liquids were determined at a specific water activity values (a_w= 0.226, 0.577, 0.753, and 0.843), these values were represented in table (2).

Temperature ºC	Water activity (a_w)	Water content (ppm)[b]		
		[C_4MIM][Tf_2N] + SspCA Enzyme	[C_4MIM][Tf_2N] + BCA Enzyme	[C_4MIM][Tf_2N]
30	0.843	831.5	815.2	791.2
	0.753	737.4	721.6	689.2
	0.577	551.7	537.7	521.5
	0.226	221.8	219.8	201.2
50	0.843	649.8	613.7	584.5
	0.753	463.5	421.6	400.9
	0.577	369.1	331.8	305.2
	0.226	181.9	172.3	158.1
80	0.843	425.7	401.5	387.1
	0.753	338.5	315.3	299.1
	0.577	271.9	258.1	234.8
	0.226	161.1	147.5	122.9
100	0.843	339.3	294.3	267.1
	0.753	237.9	218.8	207.5
	0.577	184.8	167.1	117.4
	0.226	139.4	115.2	108.9

Table 2: The water content of the used SILMs at different water activities.

3.3. CO_2 and N_2 permeability and selectivity through SILMs

The CO_2 and N_2 permeability of the supported liquid membranes immobilized with the three different ionic liquids [C_4MIM][Tf_2N], [C_4MIM][Tf_2N] + BCA Enzyme and [C_4MIM][Tf_2N] + SspCA Enzyme were measured. These experiments were carried out at four different temperatures (30, 50, 80, and 100ºC). The membranes were weighed before and after the experiment and a maximum weight loss, between 0.01 and 0.05% was obtained for all membranes tested. These low values indicate that these membranes retained the solvent immobilized, even at high temperatures, and that they may be considered stable at the tested pressure difference of 0.7 bar. As previously mentioned all permeability values were calculated according to Eq. (1), taking into account the pressure data from the feed and permeate compartments, the thickness of the membrane and the

geometry of the cell used. The permeability of both gases (CO_2 and N_2) through the supported liquid membranes obtained at different temperature is represented in Table.3. As it can be observed, the permeability of CO_2 is higher than that of N_2, for the supported ionic liquid membranes. Additionally, it showed in the table (3) that for both gases, the permeability obtained when using SILMs immobilized with the ionic liquid [C_4MIM][Tf_2N] with enzyme or without enzyme as the immobilized phase, the permeability in case of supported ionic liquid membrane with (SspCA) enzyme > supported ionic liquid membrane with (BCA) enzyme > supported ionic liquid membrane without enzyme.

Temperature °C	Water activity (a_w)	Permeability (x 10^{-10} m^2/s)					
		[C_4MIM][Tf_2N] + SspCA Enzyme		[C_4MIM][Tf_2N] + BCA Enzyme		[C_4MIM][Tf_2N]	
		CO_2	N_2	CO_2	N_2	CO_2	N_2
30	0.843	3.93 ± 0.12	0.0926 ± 0.0018	3.70 ± 0.15	0.0915 ± 0.0023	3.40 ± 0.11	0.0899 ± 0.0031
	0.753	3.51 ± 0.23	0.0896 ± 0.0012	3.41 ± 0.18	0.0902 ± 0.0015	3.20 ± 0.21	0.0894 ± 0.0017
	0.577	3.32 ± 0.21	0.0871 ± 0.0021	3.11 ± 0.24	0.086 ± 0.0013	2.80 ± 0.17	0.0854 ± 0.0025
	0.226	3.01 ± 0.11	0.0862 ± 0.0019	2.81 ± 0.12	0.0858 ± 0.0017	2.51 ± 0.17	0.0858 ± 0.0021
50	0.843	4.24 ± 0.16	0.112 ± 0.0031	3.92 ± 0.12	0.110 ± 0.0020	3.75 ± 0.20	0.112 ± 0.0026
	0.753	3.74 ± 0.23	0.111 ± 0.0028	3.75 ± 0.28	0.109 ± 0.0018	3.52 ± 0.18	0.112 ± 0.0014
	0.577	3.52 ± 0.27	0.110 ± 0.0015	3.56 ± 0.20	0.110± 0.0021	3.31 ± 0.23	0.11 ± 0.0029
	0.226	3.10 ± 0.19	0.109 ± 0.0023	2.97 ± 0.13	0.103± 0.0028	2.82 ± 0.21	0.105 ± 0.0027
80	0.843	4.46 ± 0.12	0.137 ± 0.0034	4.02 ± 0.16	0.129± 0.0041	4.12 ± 0.19	0.131 ± 0.0038
	0.753	3.91 ± 0.25	0.121 ± 0.0029	3.54 ± 0.22	0.127± 0.0021	3.61 ± 0.31	0.129 ± 0.0025
	0.577	3.81 ± 0.32	0.125 ± 0.0026	3.36 ± 0.26	0.125± 0.0033	3.51 ± 0.23	0.127 ± 0.0024
	0.226	3.20 ± 0.25	0.129 ± 0.0031	2.78 ± 0.28	0.128± 0.0028	2.95 ± 0.29	0.131 ± 0.0035
100	0.843	4.68 ± 0.22	0.161 ± 0.0032	4.23 ± 0.28	0.154± 0.0035	4.31 ± 0.29	0.157 ± 0.0022
	0.753	4.13 ± 0.18	0.143 ± 0.0030	3.72 ± 0.21	0.153± 0.0027	3.92 ± 0.15	0.156 ± 0.0034
	0.577	3.92 ± 0.23	0.142 ± 0.0020	3.42 ± 0.19	0.148± 0.0018	3.61 ± 0.16	0.15 ± 0.0024
	0.226	3.40 ± 0.12	0.145 ± 0.0016	2.97 ± 0.18	0.149± 0.0018	3.11 ± 0.14	0.151 ± 0.0021

Table 3: The permeability of CO_2 and N_2 through the SILMs.

3.3.1. Effect of water activity on the permeability and selectivity

Fig.7 represents the effect of water activity on the permeability obtained at 30ºC when using the immobilized supported liquid membranes. By analysis the Figure, it can be observed that the presence of carbonic anhydrase enzyme increases the permeability of CO_2 through the supported ionic liquid membranes immobilized with $[C_4MIM][Tf_2N]$, when comparing with the supported ionic liquid membrane without enzyme as mentioned before. Additionally, the permeability is increasing with the increase of water activity; this might be related to the increasing of the diffusion coefficient with an increase in water activity, since with the higher water content the ionic liquid viscosity decreases (Table 1). This increase is more pronounced for the membrane immobilized with the pure ionic liquid, for which the diffusion coefficient reaches a higher value for the highest water activity used (a_w= 0.843).

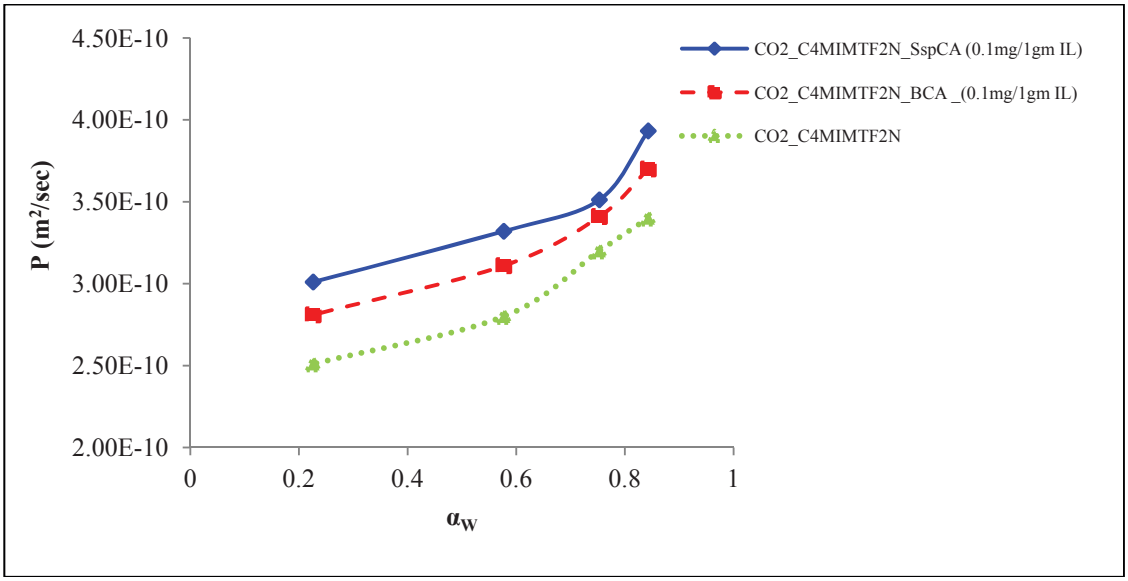

Fig.7. Gas Permeability (P) in supported liquid membranes with the pure IL, IL+BCA and IL+SspCA as a function of water activity (a_w), at T=30ºC.

In the case of the membrane immobilized with the pure IL, permeability is shown to increase with an increase in water activity, attaining values that are considerably higher than those reported for lower water activities. As previously observed in Fig.7, The increment in water activities leads to increment in permeability, this might related to the increment in diffusion coefficient, and then decrease in viscosity up to values of water

activity (a_w = 0.843, resulting in a higher CO_2 permeability. In what concerns the effect of the enzyme, it can be observed that an improvement in permeability and selectivity depends from the water activity. For the lowest water activity value studied, the enzyme lead to the less improvement. As water activity increases, both permeability and selectivity are positively impacted by the enzymatic reaction contribution. For the higher water activity values, Fig.8 shows that the selectivity values are higher than those of the lowest water activity. This result suggests that, for CO_2 capture, the enzymatic reaction may be used for enhancement of the performance of SILMs impregnated with ionic liquids with a controlled water activity.

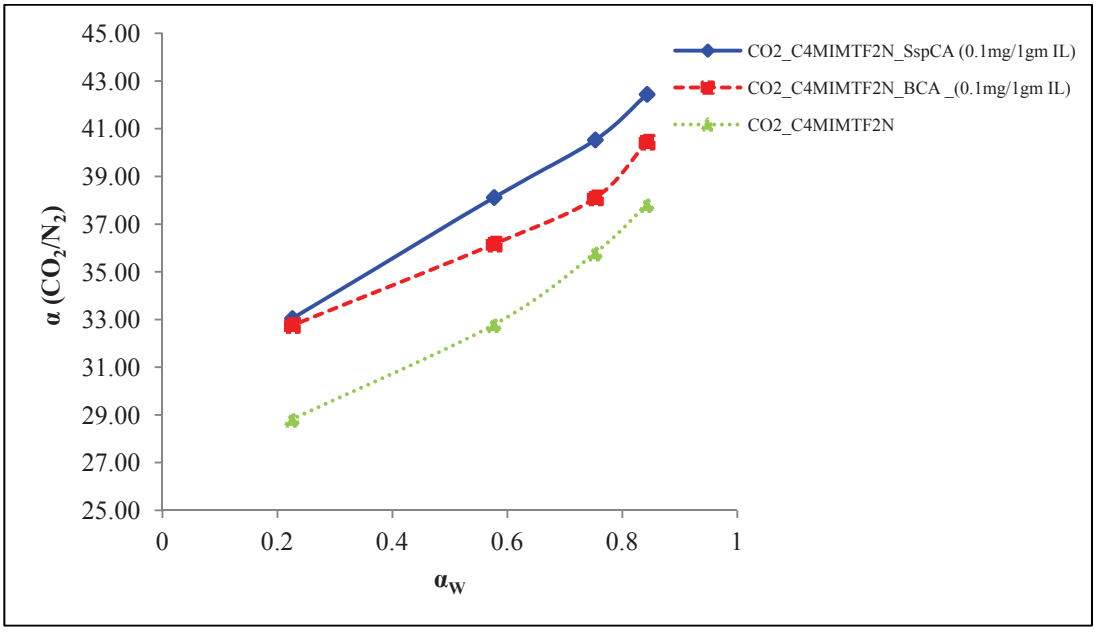

Fig.8: CO_2/N_2 ideal selectivity (α) in supported liquid membranes with the pure [C_4MIM][Tf2N], [C_4MIM][Tf_2N] + BCA Enzyme , and [C_4MIM][Tf_2N] + SspCA Enzyme as a function of water activity (a_w), at T=30ºC.

3.3.2. Effect of temperature on the permeability

Fig.9 and Fig.10 show the temperature effect on the gas permeability in supported liquid membranes impregnated with [C_4MIM][Tf_2N], [C_4MIM][Tf_2N] + BCA Enzyme and [C_4MIM][Tf_2N] + SspCA Enzyme at the highest water activity (a_w = 0.843). It is clearly observed that for both gases (CO_2 and N_2) permeability increases with an increase in temperature, which may be related with a decrease of the ionic liquid viscosity with temperature. This might give an indication that the permeability increase obeys to an

Arrhenius type of equation, $P = P_0\, x \exp\ (-\frac{E_a}{RT})$), where P is the permeability (m^2/s^{-1}), P_0 is the permeability independent constant, Ea is the energy activation (J mol^{-1}), R is the ideal gas constant (J mol^{-1} K^{-1}), and T is the temperature (K).

In (Fig.9), the Arrhenius equations (P_1, P_2, P_3) represent the permeability of CO_2 through the supported liquid membranes immobilized with [C4MIM][Tf2N]), [C_4MIM][Tf_2N] + BCA Enzyme, and [C_4MIM][Tf_2N] + SspCA Enzyme respectively, from these equations the activation energy at different temperature for both SILMs can be calculated, Also in (Fig.10), the Arrhenius equations (P_4, P_5, P_6) represent the permeability of N_2 through the supported Ionic liquid membranes immobilized with [C_4MIM][Tf_2N]), [C_4MIM][Tf_2N] + BCA Enzyme, and [C_4MIM][Tf_2N] + SspCA Enzyme respectively, and the calculated of the activation energy the same like in case of CO_2 permeability.

Moreover, (Fig.9) and (Fig.10) show that the values of activation energies in case of membranes immobilized with ([C_4MIM][Tf_2N] + BCA Enzyme) are the lowest values comparing with others, this might related to the slightly decrease in the permeability at very high temperature (80°C and 100°C) comparing with SILM immobilized with [C_4MIM][Tf_2N] + SspCA Enzyme or [C_4MIM][Tf_2N], this might related to the decreasing in the Enzyme activity of BCA Enzyme immobilized with Ionic liquids on SILM, as shown in the table (3). Additionally, the CO_2 transport through the selected supported Ionic liquid membranes with [C_4MIM][Tf_2N] + SspCA Enzyme, is the highest values comparing with others. It's clear that the permeability of CO_2 through the supported Ionic liquid membranes is higher than in case of N_2. Even though the supported Ionic liquid membranes tested in this work are stable at high temperatures (up to 100°C), for a pressure difference of 0.7 bar, and that they are selective towards CO_2 when compared with N_2, when compared with other membrane materials in the literature their selectivity is lower. In case of supported ionic liquid membrane immobilized with [C_4MIM][Tf_2N] + BCA Enzyme, the permeability for both gases that measured at (30°C and 50ºC) is higher than SILM immobilized with [C_4MIM][Tf_2N],but at very high temperatures (80ºC and 100ºC) the opposite happened and the permeability is lower, this might related to the decreasing in the Enzyme activity (Bovine CA enzyme) that

immobilized with the [C_4MIM][Tf_2N] ionic liquid at high temperature, which might cause denaturation / deactivation of the Enzyme, which decreased the transport of the CO_2 gas through the membranes.

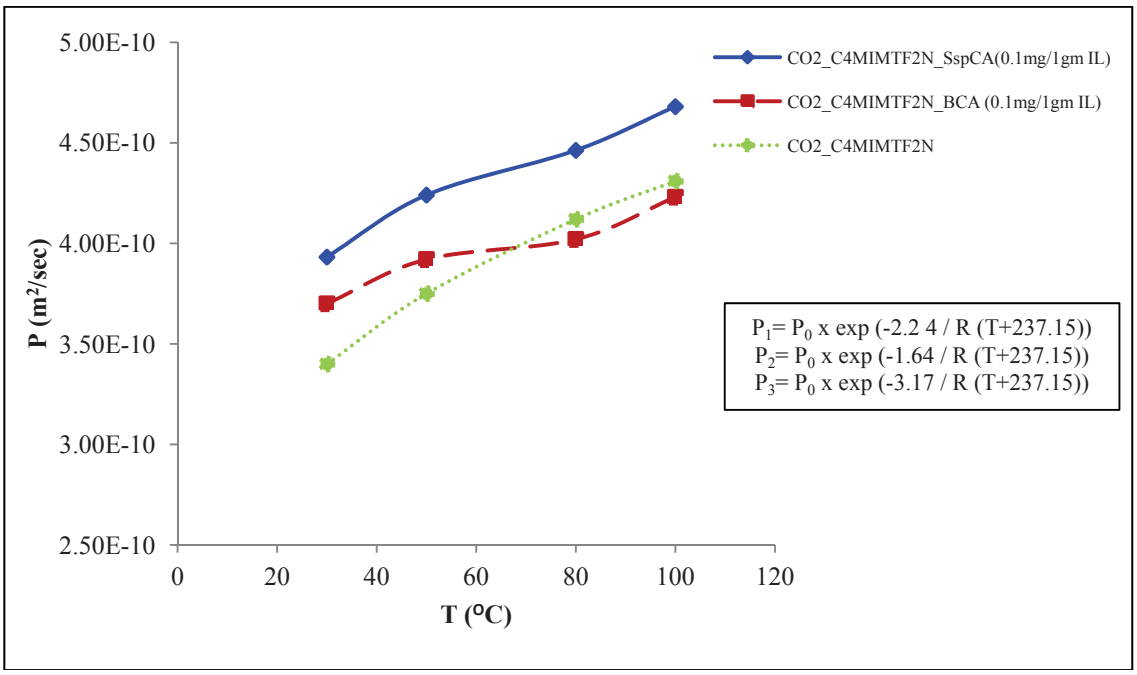

Fig.9: The effect of temperature on CO_2 permeability in a supported liquid membranes with [C_4MIM][Tf2N], [C_4MIM][Tf_2N] + BCA Enzyme and [C_4MIM][Tf_2N] + SspCA Enzyme at water activity (a_w = 0.843).

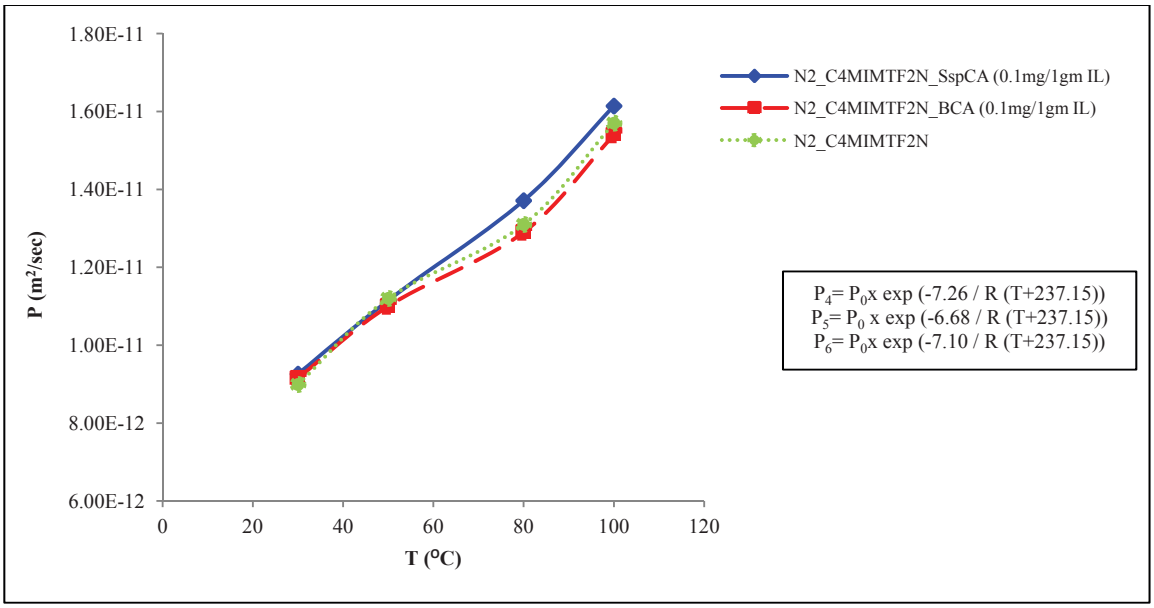

Fig.10: The effect of temperature on N_2 permeability in a supported liquid membranes with [C_4MIM][Tf_2N], [C_4MIM][Tf_2N] + BCA Enzyme and [C_4MIM][Tf_2N] + SspCA Enzyme at water activity (a_w = 0.843).

3.3.3. The effect of temperature on the Selectivity

Table (4) shows the CO_2/N_2 ideal selectivities obtained for the membranes tested. The ideal selectivity was calculated taking into account the ratio of the permeabilities measured for pure gases (Eq. (3)). It was observed that the selectivity of SLMs towards CO_2 was higher than that of N_2. Additionally at 30ºC, the ideal selectivity is much higher for the support impregnated with $[C_4MIM][Tf_2N]$ + SspCA Enzyme and $[C_4MIM][Tf_2N]$ + BCA Enzyme when compared with $[C_4MIM][Tf_2N]$. With increasing temperature, the selectivity of the SILM impregnated with and without enzyme decreases sharply at very high temperatures.

The table (4) shows that in case of membranes used at temperatures (30ºC and 50ºC), the selectivities are increasing as the following: Supported ionic liquid membrane immobilized with $[C_4MIM][Tf_2N]$ + SspCA Enzyme > $[C_4MIM][Tf_2N]$ + BCA Enzyme > $[C_4MIM][Tf_2N]$, this might related to the presence of the enzyme with the ionic liquid which increase the permeability of CO_2 than N_2 gas. In mean while the selectivity at very high temperatures (80ºC and 100ºC), the selectivity of SILM immobilized with $[C_4MIM][Tf_2N]$ + BCA Enzyme is decreased and becomes slightly lower than (closer to) the SILM immobilized with $[C_4MIM][Tf_2N]$, this might related to the slightly decrease of CO_2 permeability through SILM immobilized with $[C_4MIM][Tf_2N]$ + BCA Enzyme, due to the decrease in the activity of BCA Enzyme at very high temperature, comparing with SILM immobilized with $[C_4MIM][Tf_2N]$ as shown in the table (3).

Additionally, the table (4) shows that the selectivities are increasing with increasing the water activity. The selectivity is increasing due to the increment of the CO_2 and N_2 permeability; this might be related to the increasing in the diffusion coefficient increases with an increase in water activity, since with the higher water content the ionic liquid viscosity decreases as shown in the table (1).

Temperature °C	Water activity (a_w)	Selectivity α(CO_2/N_2)		
		[C_4MIM][Tf_2N] + SspCA Enzyme	[C_4MIM][Tf_2N] + BCA Enzyme	[C_4MIM][Tf_2N]
30	0.843	42.44 ± 0.21	40.44 ± 0.16	37.82 ± 0.19
	0.753	39.17 ± 0.32	37.80 ± 0.24	35.79 ± 0.15
	0.577	38.12 ± 0.18	36.16 ± 0.22	32.79 ± 0.13
	0.226	34.92 ± 0.31	32.75 ± 0.12	29.25 ± 0.20
50	0.843	37.86 ± 0.17	35.64 ± 0.11	33.48 ± 0.09
	0.753	33.69 ± 0.19	34.40 ± 0.26	31.43 ± 0.13
	0.577	32.01 ± 0.31	32.36 ± 0.24	30.09 ± 0.22
	0.226	28.18 ± 0.28	28.83 ± 0.37	26.86 ± 0.24
80	0.843	32.55 ± 0.32	31.16 ± 0.25	31.45 ± 0.18
	0.753	32.31 ± 0.27	27.87 ± 0.37	27.91 ± 0.30
	0.577	30.48 ± 0.41	26.88 ± 0.31	27.56 ± 0.27
	0.226	24.81 ± 0.21	21.75 ± 0.21	22.69 ± 0.15
100	0.843	29.07 ± 0.31	27.48 ± 0.23	27.45 ± 0.15
	0.753	28.85 ± 0.26	24.64 ± 0.13	25.13 ± 0.34
	0.577	27.61 ± 0.08	23.11 ± 0.18	24.07 ± 0.16
	0.226	23.45 ± 0.12	19.95 ± 0.07	20.60 ± 0.14

Table (4): CO2/N2 ideal selectivity for the SLMs tested.

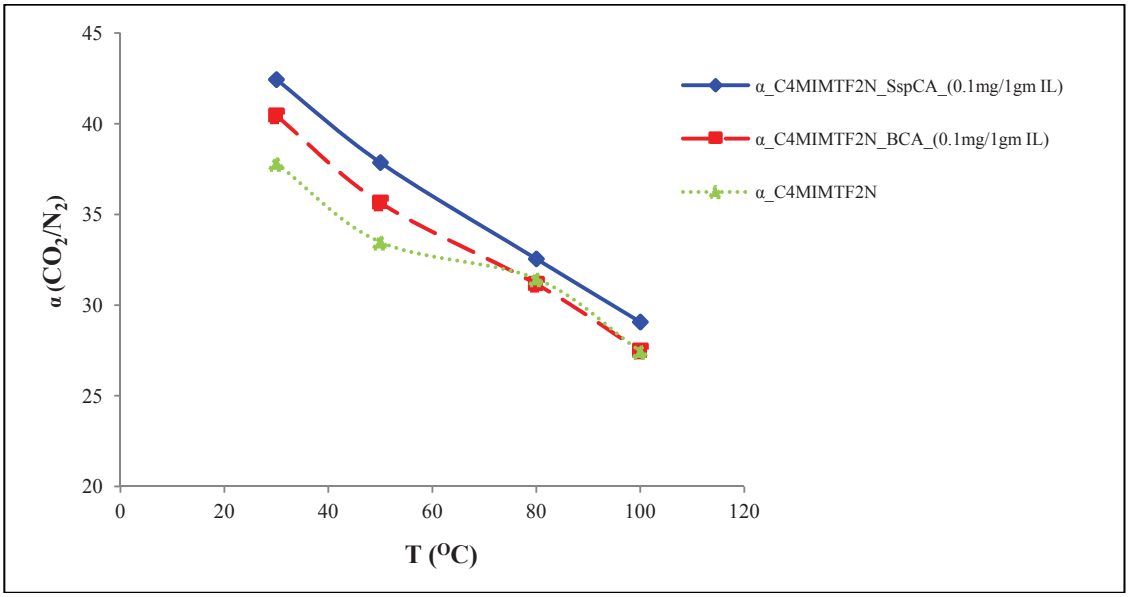

Fig.11: The effect of temperature on the selectivity (CO_2/N_2) in a supported liquid membranes with [C_4MIM][Tf_2N], [C_4MIM][Tf_2N] + BCA Enzyme and [C_4MIM][Tf_2N] + SspCA Enzyme.

Fig.11 shows that the increment on temperature affects on the selectivities of the transported gas (CO_2, N_2) through the supported liquid membranes. By increasing the temperature the selectivity is decreasing, this might be related to the increment of the permeability with an increase in temperature, which may be related with a decrease of the ionic liquid viscosity with temperature as shown in table (1), also the activity of the enzyme may be influenced by the increasing of the temperature. From the above discussion, we can conclude that the ideal selectivities obtained with using SILM

impregnated with [C_4MIM][Tf_2N] + SspCA Enzyme is higher than SILM impregnated with [C_4MIM][Tf_2N] + BCA Enzyme or [C_4MIM][Tf_2N], even at very high temperatures and different water contents. This might related to the high sensitivity of SspCA Enzyme towards CO_2 gas and its stability and activity even at very high temperatures.

3.4. Stability of the supported ionic liquid membranes (SILMs)

To study the stability of supported ionic liquid membranes, the used SILMs impregnated with [C4MIM][Tf2N] + SspCA, [C4MIM][Tf2N] + BCA Enzyme, and [C4MIM][Tf2N] have been tested for one week at the same conditions (temperature, water activity, and pressure). The stability experiments were performed at the highest (100ºC) and lowest (30ºC) temperatures, both the permeability and selectivity of the used SILM have been tested. Table (5) represents the permeability of CO_2 and N_2 gases through the used supported ionic liquid membranes with time at (30ºC). The table shows that there is little decrease in the permeability of CO_2 with time; this might related to the little decrease in the enzyme activities with time, also the lost of the ionic liquid immobilized with the supported ionic liquid membranes. Moreover, the figure (12) shows that the permeability through SILMs impregnated with [C_4MIM][Tf_2N] + SspCA is higher comparing with other SILMs membranes even with long time measurements (one week) at water activity (a_w = 0.843), this might related to the stability of thermophilic (SspCA) enzyme immobilized with the ionic liquid inside the porous of the membranes.

Permeability (x 10^{-10} m^2/s)						
Time (Day)	[C_4MIM][Tf_2N] + SspCA Enzyme		[C_4MIM][Tf_2N] + BCA Enzyme		[C_4MIM][Tf_2N]	
	CO_2	N_2	CO_2	N_2	CO_2	N_2
1	3.93 ± 0.12	0.0926 ± 0.0018	3.70 ± 0.21	0.915 ± 0.0023	3.40 ± 0.11	0.0899 ± 0.0031
2	3.91 ± 0.09	0.115 ± 0.0021	3.65 ± 0.15	0.124 ± 0.0016	3.38 ± 0.26	0.125 ± 0.0015
3	3.85 ± 0.18	0.123 ± 0.0028	3.61 ± 0.13	0.132 ± 0.0011	3.36 ± 0.17	0.133 ± 0.0018
4	3.79 ± 0.07	0.129 ± 0.0031	3.57 ± 0.17	0.141 ± 0.0019	3.35 ± 0.13	0.149 ± 0.0034
5	3.71 ± 0.11	0.135 ± 0.0022	3.51 ± 0.19	0.151 ± 0.0012	3.31 ± 0.21	0.155 ± 0.0025
6	3.68 ± 0.14	0.141 ± 0.0012	3.47 ± 0.05	0.158 ± 0.0009	3.28 ± 0.26	0.162 ± 0.0011
7	3.63 ± 0.22	0.149 ± 0.0012	3.43 ± 0.28	0.162 ± 0.0017	3.26 ± 0.24	0.172 ± 0.0022
8	3.62 ± 0.18	0.151 ± 0.0017	3.39 ± 0.15	0.169 ± 0.0021	3.19 ± 0.11	0.178 ± 0.0032

Table 5: CO_2 and N_2 Permeabilities in supported liquid membranes with the pure [C_4MIM][Tf_2N], [C_4MIM][Tf_2N] + BCA Enzyme and [C_4MIM][Tf_2N] + SspCA Enzyme as a function of time at same water activity (a_w = 0.843) and Temperature (T=30ºC).

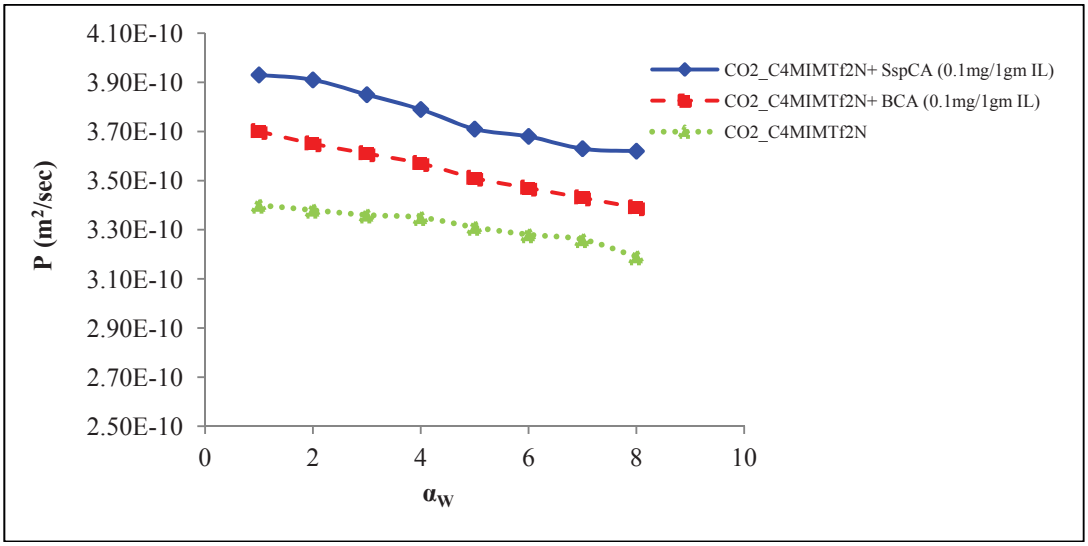

Fig. 12: CO_2 Permeability (P_{CO2}) in supported liquid membranes with the pure [C_4MIM][Tf_2N], [C_4MIM][Tf_2N] + BCA Enzyme and [C_4MIM][Tf_2N] + SspCA Enzyme as a function of time (Day) at water activity (a_w = 0.843), Temperature (T=30ºC).

Fig.13 represents the selectivity of the used SILMs for one week at the same water activity and temperature (30ºC), the figure shows that the selectivities were deceasing with the time, and the selectivities for the SILM impregnated with [C_4MIM][Tf_2N] + SspCA > [C_4MIM][Tf_2N] + BCA Enzyme, > [C_4MIM][Tf_2N] membranes even with the decreasing in the permeability of CO_2 with time, this might related to the enzyme immobilized with ionic liquid is still stable with the same SILMs used, even after measuring the permeability for one week for both gases (CO_2 and N_2).

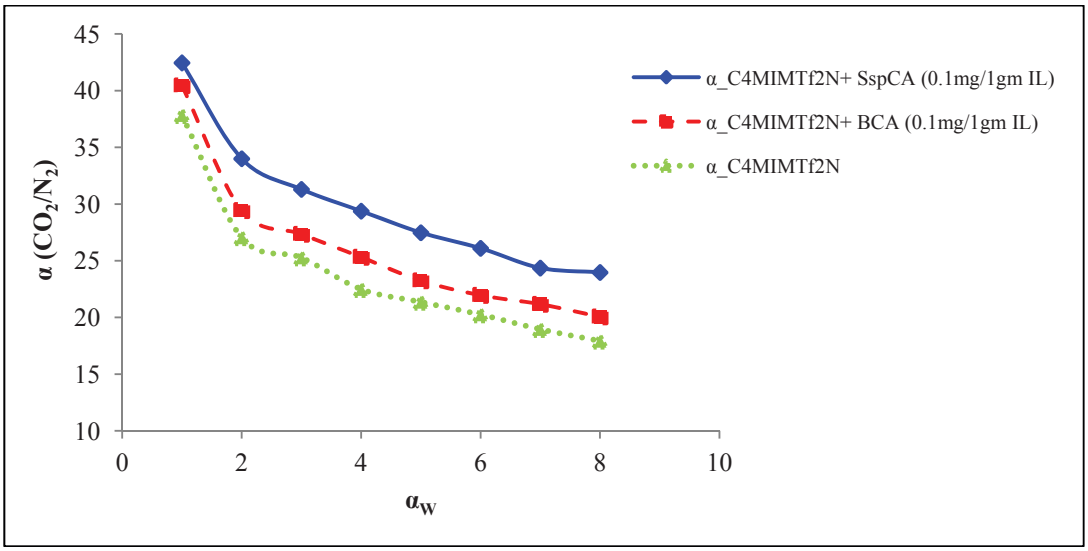

Fig.13. CO_2/N_2 ideal selectivity (α) in supported liquid membranes with the pure [C_4MIM][Tf_2N], [C_4MIM][Tf_2N] + BCA Enzyme and [C_4MIM][Tf_2N] + SspCA Enzyme as a function of time (Day) at water activity (a_w = 0.843), Temperature (T=30ºC).

Table (6) represents the permeability of CO_2 and N_2 gases through the used supported ionic liquid membranes with time at (100^{O}C). The table shows that there is little decrease in the permeability of CO_2 with time; this might related to the little decrease in the enzyme activities with time, also the lost of the ionic liquid immobilized with the supported ionic liquid membranes. Moreover, (Fig.14) shows that the permeability through SILM impregnated with [C_4MIM][Tf_2N] + SspCA > [C_4MIM][Tf_2N] > [C_4MIM][Tf_2N]+BCA Enzyme, even with the decreasing in the permeability of CO_2 with time. This decrease in the permeability of SILM impregnated with [C4MIM][Tf2N] + BCA comparing with others might related to the huge decrease in the activity of BCA enzyme immobilized with ionic liquid at very high temperature. In additional to, (Fig.15) represents the selectivity between both gases (CO_2 and N_2) at very high temperature, shows that the ideal selectivity in case of SILM impregnated with [C_4MIM][Tf_2N]+BCA Enzyme is the lowest one comparing with others at very high temperature (100^{O}C), that used to check the stability of enzymes.

Permeability (x 10^{-10} m^2/s)						
Time (Day)	[C4MIM][Tf2N] + SspCA Enzyme		[C4MIM][Tf2N] + BCA Enzyme		[C4MIM][Tf2N]	
	CO_2	N_2	CO_2	N_2	CO_2	N_2
1	4.68 ± 0.15	0.161 ± 0.0022	4.23 ± 0.21	0.154 ± 0.0019	4.31 ± 0.14	0.157 ± 0.0023
2	4.59 ± 0.21	0.169 ± 0.0011	4.10 ± 0.16	0.168 ± 0.0015	4.27 ± 0.27	0.165 ± 0.0017
3	4.49 ± 0.19	0.172 ± 0.0013	3.84 ± 0.23	0.175 ± 0.0026	4.21 ± 0.12	0.171 ± 0.0032
4	4.31 ± 0.17	0.178 ± 0.0024	3.73 ± 0.14	0.180 ± 0.0032	4.15 ± 0.22	0.179 ± 0.0012
5	4.26 ± 0.31	0.182 ± 0.0016	3.61 ± 0.20	0.186 ± 0.0035	4.01 ± 0.15	0.183 ± 0.0028
6	4.19 ± 0.24	0.189 ± 0.0038	3.44 ± 0.18	0.191 ± 0.0052	3.95 ± 0.10	0.195 ± 0.0041
7	3.97 ± 0.16	0.193 ± 0.0023	3.35 ± 0.26	0.199 ± 0.0018	3.89 ± 0.32	0.205 ± 0.0034
8	3.91 ± 0.35	0.195 ± 0.0022	3.21 ± 0.18	0.211 ± 0.0031	3.81 ± 0.23	0.218 ± 0.0029

Table 6: CO_2 and N_2 Permeability in supported liquid membranes with the pure [C_4MIM][Tf_2N], [C_4MIM][Tf_2N] + BCA Enzyme, and [C_4MIM][Tf_2N] + SspCA Enzyme as a function of time at temperature (T=100ºC).

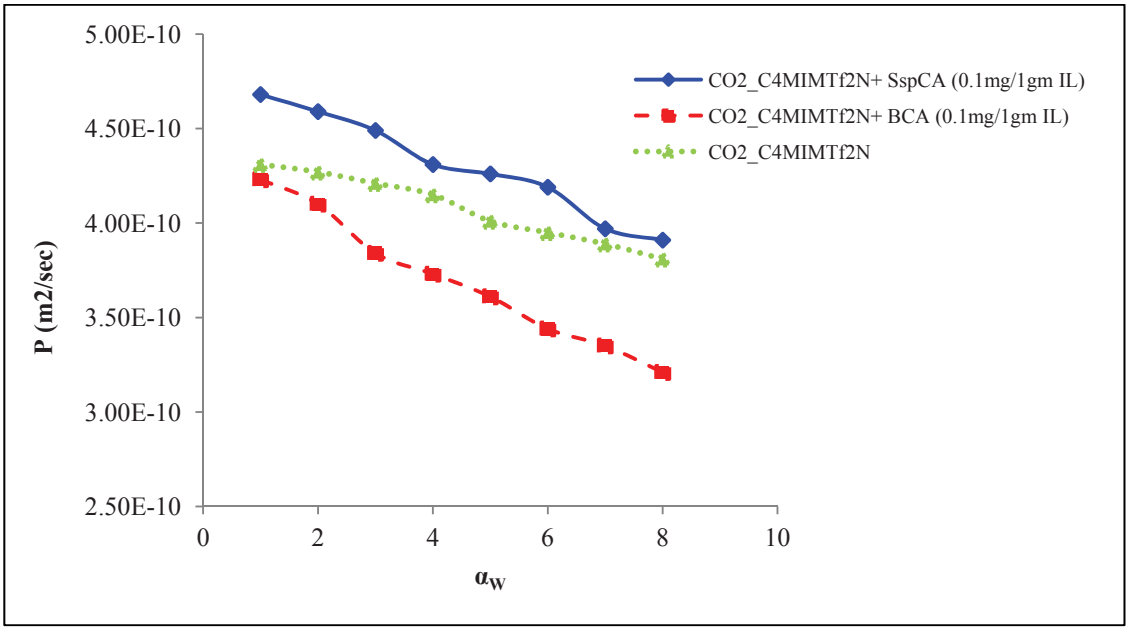

Fig.14: CO_2 Permeability (PCO_2) in supported liquid membranes with the pure $[C_4MIM][Tf_2N]$, $[C_4MIM][Tf_2N]$ + BCA Enzyme, and $[C_4MIM][Tf_2N]$ + SspCA Enzyme as a function of time, temperature (T=100°C).

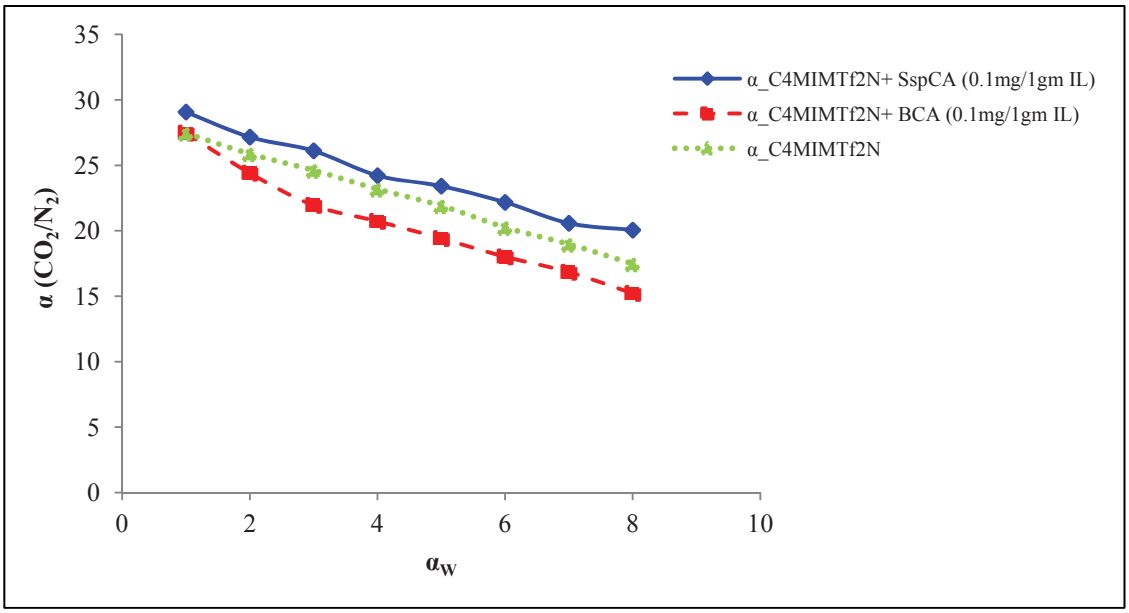

Fig.15: CO_2/N_2 ideal selectivity (α) in supported liquid membranes with the pure $[C_4MIM][Tf_2N]$, $[C_4MIM][Tf_2N]$ + BCA Enzyme, and $[C_4MIM][Tf_2N]$ + SspCA Enzyme as a function of time at temperature (T=100ºC).

3.5. The effect of Enzyme concentration

The effect of increasing the enzyme concentration that immobilized with the ionic liquids on the supported ionic liquid membranes has been tested at different temperatures (30, 50, 80, and 100ºC). The concentrations of enzymes (BCA and SspCA) have been increased (2.5 times) than the initial one (0.1mg enzyme/gm of IL).

Fig.16 represents the permeability of gases (CO_2) gas through the SILMs at low and high (BCA and SspCA) Enzymes concentrations as a function of temperature. The figure shows that by increasing the enzymes concentration, the permeability of CO_2 gas through the SILMs increased than the initial concentration, This might related to the increment in the enzymes concentration helped to increase the bio-conversion enzymatic reaction of CO_2 to HCO_3^-, then the activity of the enzymes for CO_2 capture, this leads to enhance the performance of SILMs impregnated with ionic liquids and high enzyme concentration (0.25mg/1gm IL) comparing with the initial ones (0.1mg/1gm IL) at different temperatures. Moreover, Figure 12 shows that the permeability through the SILMs are observed as the following [C_4MIM][Tf_2N] + SspCA [0.25mg/1gm IL]> [C_4MIM][Tf_2N] + BCA [0.25mg/1gm IL] > [C_4MIM][Tf_2N] + SspCA [0.1mg/1gm IL]> [C_4MIM][Tf_2N] + BCA [0.1mg/1gm IL]. This gives indication that with increasing the enzymes concentration, the permeability through SILMs increased too. Moreover, (Fig.16) shows that the permeability of CO_2 gas through SILMs increased, when the temperature increased. This might be related to the decreasing in the viscosity of the ionic liquids at high temperatures as shown in the tables (1) and (7).

Temperature ºC	Viscosity (mPas)[a]		
	[C_4MIM][Tf_2N] +SspCA Enzyme [0.25 mg/1gm IL]	[C_4MIM][Tf_2N] + BCA Enzyme [0.25 mg/1gm IL]	[C_4MIM][Tf_2N]
30	34 ± 0.18	35 ± 0.16	41 ± 0.25
50	19 ± 0.12	20 ± 0.25	22 ± 0.52
80	9 ± 0.03	10 ± 0.14	11 ± 0.31
100	7 ± 0.39	8 ± 0.11	8 ± 0.48

Table 7: The viscosity measurements of the used ionic liquid immobilized with high concentration of enzymes (0.25 mg/1gm IL) at different temperatures.

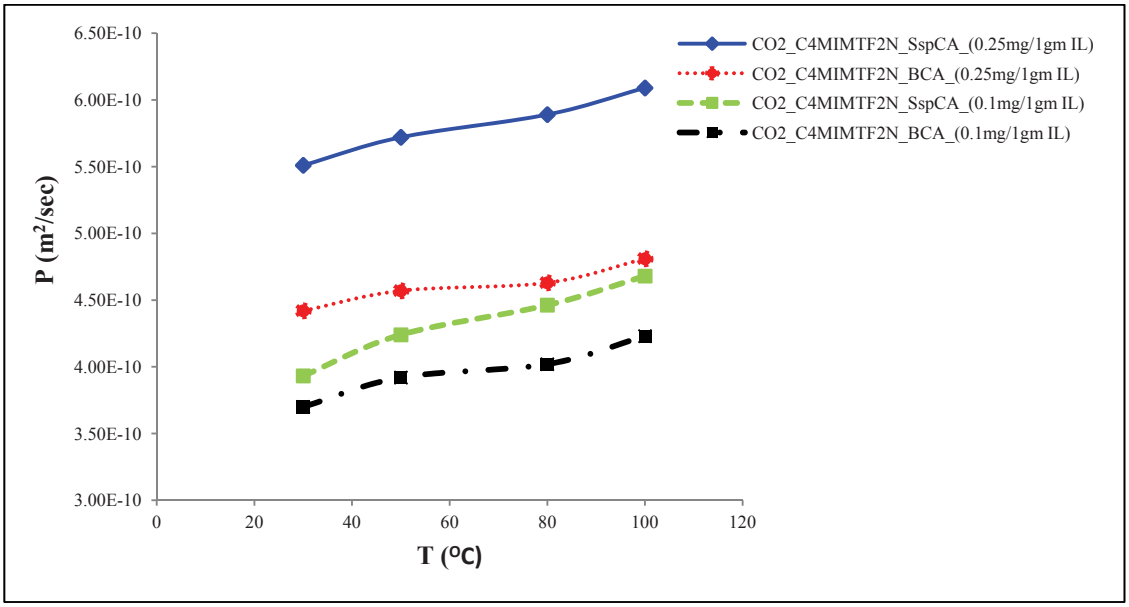

Fig.16: Comparing the permeability of (CO_2) through supported liquid membranes immobilized with high and low concentration of enzymes.

Fig.17 represents the permeability of (N_2) gas through the SILMs at low and high (BCA and SspCA) Enzyme concentrations. The figure shows that there is no much difference in the permeability of N_2 gas when increasing the enzymes concentration than the initial concentration. Moreover, the permeability of N_2 gas through SILM still much lower than the permeability of CO_2 gas through the SILMs with low and high enzyme concentration. This might be related to the presence of enzymes, which helped to accelerate the permeability of CO_2 gas through the SILMs comparing with N_2 gas. In additional to the polarity properties and small size of CO_2 comparing with N_2 gas.

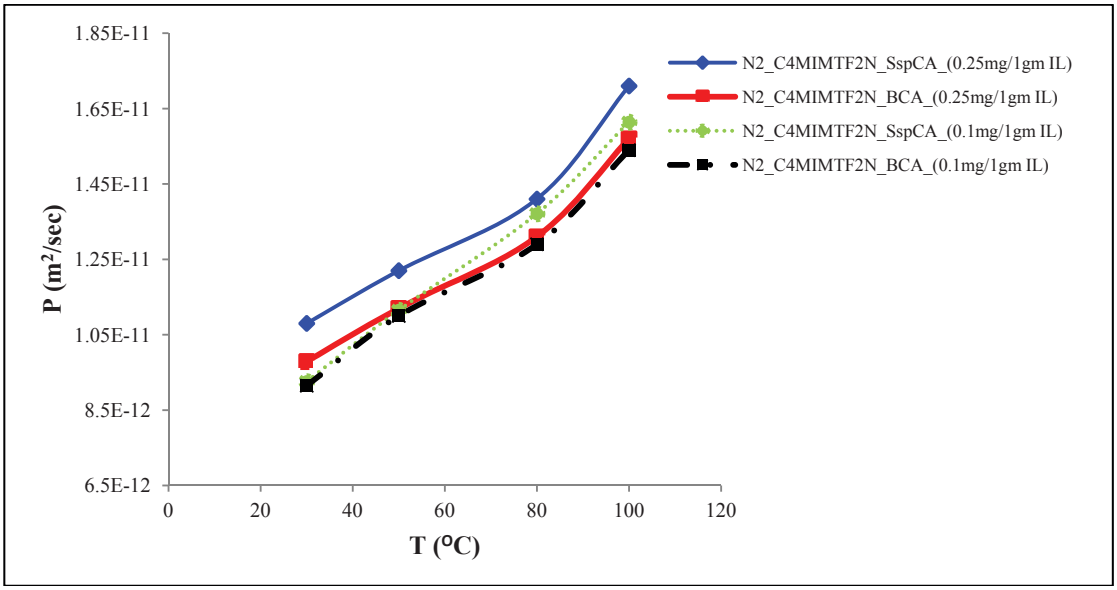

Fig.17: Comparing the permeability of (N_2) through supported liquid membranes immobilized with high and low concentration of enzymes.

In additional to (Fig.18) represents the comparing between ideal selectivity (CO_2/N_2) at low and high concentration of enzymes. The figure shows that the ideal selectivity in case of SILM impregnated with [C_4MIM][Tf_2N]+SspCA (0.25mg/1gm IL) Enzyme is the highest one comparing with other SILMs impregnated with enzymes. This is due to the increment in the enzymes concentration, increase the permeability of CO_2 over N_2 through the SILMs as mentioned before. Moreover, the figure showed the change in selectivity with temperature. In additional to the figure shows that the selectivity of the SILM immobilized with [C_4MIM][Tf_2N] + SspCA [0.25mg/1gm IL] > [C_4MIM][Tf_2N] + BCA [0.25mg/1gm IL] > [C_4MIM][Tf_2N] + SspCA [0.1mg/1gm IL]> [C_4MIM][Tf_2N] + BCA [0.1mg/1gm IL] at the same temperature. Moreover, the selectivity of the membranes is decreasing with the increasing in the temperatures; this might be related to the decreasing of the viscosity by increasing temperatures as shown in Table (1) and (7), which leads to the increasing in the permeabilities, then decreasing in the selectivities (See Fig.18).

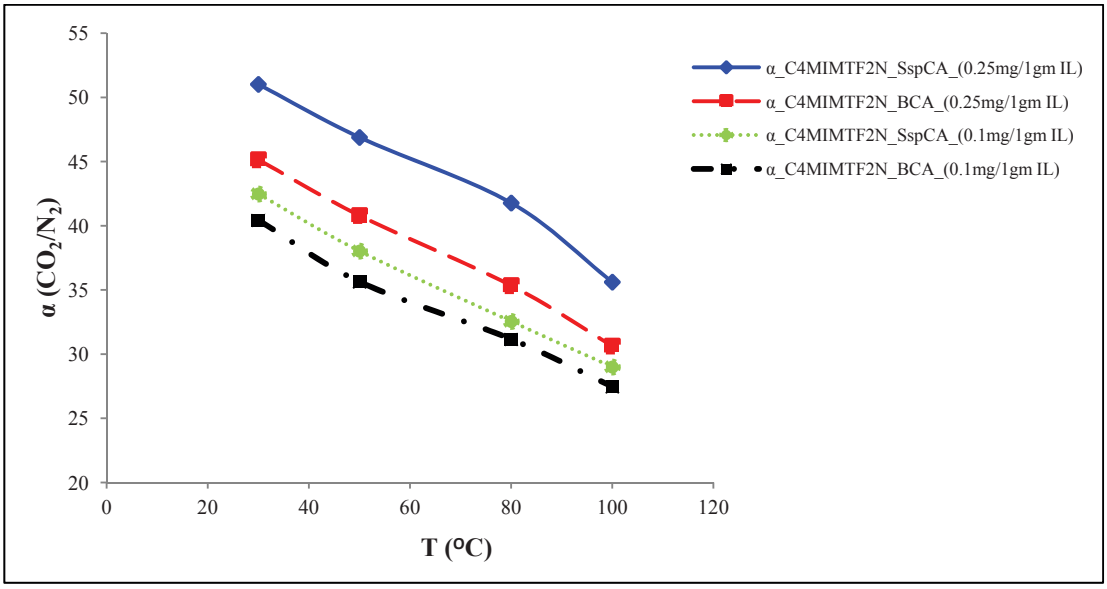

Fig.18: Comparing the effect of temperature on the ideal selectivity (CO_2/N_2) of the supported liquid membranes immobilized with high and low concentration of enzymes.

3.6. Robeson Upper bound correlation

In order to compare the ideal selectivities obtained in this work with data available in the literature, the CO_2/N_2 ideal selectivity as a function of the CO_2 permeability at 30°C is represented in (Fig.19). These upper bound correlations were obtained by Robeson et al. [135, 136] from literature data. The line represented corresponds to the Robeson's upper bound for a specific temperature used (30°C), while data points correspond to experimental values obtained in this work. Therefore, data points above this line may be considered as an improvement over the results published so far.

From the figure, it is observed that the results obtained in this work are generally closer to those available in the literature. The results obtained in this research work are represented in black while the results available in literature are represented in colored. The figure showed that in case of SILMs immobilized with pure $[C_4MIM][Tf_2N]$ ionic liquid are below the upper bound line, while the results obtained from using SILMs immobilized with pure ionic liquid and low enzyme concentration (0.1mg/1gIL) are little higher and closer to the upper bound line. Moreover, the figure shows that the best results obtained when using the SILMs immobilized with pure ionic liquid and higher enzyme concentration (0.25mg/1gIL) at (30ºC), as the results access the upper bound line,

this mean the obtained results by using these SILMs may be considered as an improvement over the results published so far.

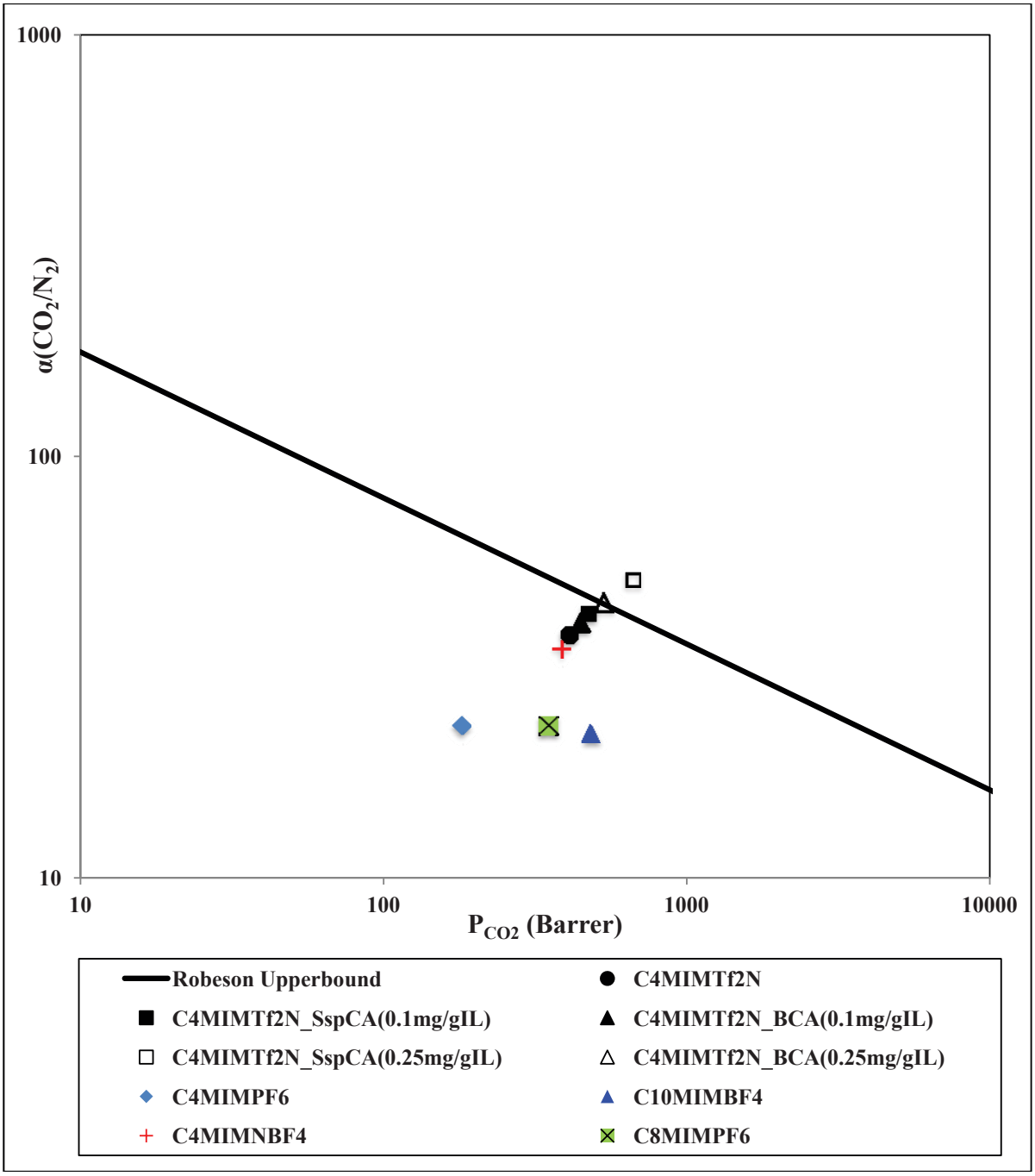

Fig.19: (CO_2/N_2) ideal selectivity (a) as a function of CO_2 permeability (P_{CO2}). (1 Barrer = 10^{-10} cm (STP) cm cm^{-2} s^{-1} cm Hg^{-1}).

4. Conclusion

The approach proposed in this research work consists on using supported ionic liquid membranes (SILMs) comprising two different carbonic anhydrase enzymes, the thermo resistant SspCA enzyme and the Bovine-CA enzyme, which catalyze the reaction of conversion of CO_2 to bicarbonate, enhancing the driving force for CO_2 transport. Membrane stability, CO_2 and N_2 permeability and CO_2/N_2 ideal selectivity were determined for the membranes developed. The results showed that the supported ionic liquid membranes prepared by immobilizing a selected ionic liquid $[C_4MIM][Tf_2N]$ with and without enzyme in a PVDF hydrophobic polymeric support allowed to obtain stable supported liquid membranes at high temperatures (up to 100ºC), selective towards CO_2 against N_2. Moreover, the selectivity and permeability are affected by different parameters, namely, temperature, water activity and enzyme concentration.

The results showed that, the selectivity and permeability through the supported ionic liquid membranes with and without enzymes are affected by different important factors like temperature, water activity and the presence of enzyme. Temperature has a great effect on the selectivity and permeability, when the temperature is increasing the selectivity is decreasing, this might be related to the increment of the permeability with an increase in temperature, which may be related with a decrease of the ionic liquid viscosity with temperature, also the activity of the enzyme may be influenced by the increasing of the temperature. Also the selectivity and permeability are increasing with increasing the water activity; this might be related to the increasing in the diffusion coefficient increases with an increase in water activity, since with the higher water content the ionic liquid viscosity decreases. This increase is more pronounced for the ionic liquid, for which the diffusion coefficient reaches a higher value for the highest water activity used (a_w= 0.843).

The main important factor was the presence of enzyme, as the presence of carbonic anhydrase enzyme increased the permeability and selectivity of CO_2 through the supported ionic liquid membranes immobilized with $[C_4MIM][Tf_2N]$, when compared with the supported ionic liquid membrane without enzyme. The permeability was

increased as the following: Supported ionic liquid membrane with (SspCA) enzyme > Supported ionic liquid membrane with (BCA) enzyme > Supported ionic liquid membrane without enzyme.

The results showed that the SILM immobilized with ([C_4MIM][Tf_2N]+SspCA enzyme) at (30ºC) has the highest permeability (3.93 x 10^{-10} m^2/sec) and idea selectivity (CO_2/N_2) (42.44) for CO_2 when compared with other SILMs immobilized with ([C_4MIM][Tf_2N] +BCA enzyme) (3.70 x 10^{-10} m^2/sec) and [C_4MIM][Tf_2N] (3.40 x 10^{-10} m^2/sec). Moreover, Two different concentration of enzymes (0.1mg enzyme/g ionic liquid) and (0.25 mg enzyme /g ionic liquid) immobilized with the ionic liquid were also tested.

The results showed that by increasing the enzyme concentration (2.5 times), the permeability and selectivity of CO_2 were duplicated for both enzymes. The permeability (5.51 x 10^{-10} m^2/sec) and selectivity (51.02) values obtained at 30ºC in case of SILMs immobilized with ([C_4MIM][Tf_2N]+SspCA enzyme (0.25mg/g IL)) is higher than the values in case of SILM immobilized with ([C_4MIM][Tf_2N]+BCA enzyme (0.25mg/g IL)). In additional too, at higher temperature (100°C), the highest permeability (6.09 x 10^{-10} m^2/sec) and selectivity (35.61) values were obtained in case of SILMs immobilized with ([C_4MIM][Tf_2N]+SspCA enzyme (0.25mg/g IL)). Moreover, it could be concluded that, the SILMs immobilized with ([C_4MIM][Tf_2N]+SspCA enzyme) present higher stability at high temperatures (80ºC and 100ºC) than the other used SILMs immobilized with([C_4MIM][Tf_2N]+BCA enzyme) or ([C_4MIM][Tf_2N]).

In order to compare the ideal selectivities obtained in this work with data available in the literature, the CO_2/N_2 ideal selectivity as a function of the CO_2 permeability at 30ºC is represented in upper bound correlations plot. The results showed that, the data obtained in this work are generally closer to those available in the literature. In case of SILMs immobilized with pure [C_4MIM][Tf_2N] ionic liquid are below the upper bound line, while the results obtained from using SILMs immobilized with pure ionic liquid and low enzyme concentration (0.1mg/1gIL) are little higher and closer to the upper bound line. Moreover, the figure shows that the best results obtained when using the SILMs

immobilized with pure ionic liquid and higher enzyme concentration (0.2mg/1gIL), as the results access the upper bound line, this mean the obtained results by using these SILMs may be considered as an improvement over the results published so far. However, In order to improve the selectivity and permeability through the enzyme-solvent system it will be important in further studies to evaluate the behavior of CO_2 task-specific ionic liquids, which combined with the use of higher concentrations of carbonic anhydrase enzymes may lead to efficient and competitive carbon capture systems.

5. Reference

[1] L.A. Neves, C. Afonso, I. M. Coelhoso, J. G. Crespo, "Integrated CO_2 capture and enzymatic bioconversion in supported ionic liquid membranes", Sep. Purif. Technol., 97 (2012) 34–41.

[2] R. Fortunato, M. González-Muñoz, M. Kubasiewicz, S. Luque, J. Alvarez, C.A.M. Afonso, I.M. Coelhoso, J. Crespo, "Liquid membranes using ionic liquids: influence of water on solute transport", J. Membr. Sci., 249 (2005) 153–162.

[3] C.D. Keeling, T.P. Whorf, M. Wahlen, J. VanDerPlicht, "Interannual extremes in the rate of rise of atmospheric carbon dioxide since 1980", Nature, 6533 (1995) 666–670.

[4] M. R. Raupach, G. Marland, P. Ciais, C. Le Quere, J. G. Canadell, G. Klepper, C. B. Field, "Global and regional drivers of accelerating CO_2 emissions", PNAS, 24 (2007) 10288–10293.

[5] A.J. Mc Michael, R. E. Woodruff , S. Hales, "Climate change and human health: present and future risks", The Lancet, 9513 (2006) 859–869.

[6] CO_2 Emissions From Fuel Combustion Highlights, International Energy Agency, Paris (2010), http:/www.iea.org.

[7] M. Hasib-ur-Rahman, M. Siaj, F. Larachi, "Ionic liquids for CO_2 capture-Development and progress", Chem. Eng. Process., 49 (2010) 313-322.

[8] B.A. Oyenekan, G.T. Rochelle, "Energy performance of stripper configurations for CO_2 capture by aqueous amines", Ind. Eng. Chem. Res., 45 (2006) 2457-2466.

[9] K.S. Fisher, G.T. Rochelle, S. Ziaii, C. Schubert, "Advanced amine solvent formulations and process integration for near-term CO_2 capture success", Trimeric Corporation., Pennsylvania (2007).

[10] O.F. Dawodu, A. Meisen, "Degradation alkanolamine blends by carbon dioxide", Can. J. Chem. Eng., 74(6), (1996) 960-966.

[11] S. Ahn, H. J. Song, J. W. Park, J.H. Lee, I.Y. Lee, K.R. Jang, "Characterization of metal corrosion by aqueous amino acid salts for the capture of CO_2", Kor. J. Chem. Eng., 27(5), (2010) 1576-1580.

[12] D. M. D Alessandro, B. Smit, J.R. Long, "Carbon dioxide capture: prospects for new materials", Angew. Chem. Int. Ed., 49 (2010) 6058–6082.

[13] T.C. Merkel, H. Lin, X. Wei, R. Backer, "Power plant post-combustion carbon dioxide capture: an opportunity for membranes" , J. Membr. Sci., 359 (2010) 126–139.

[14] C.W Jones, "CO_2 Capture from dilute gases as a component of modern global carbon management", Annu Rev Chem Biomol., 2 (2011) 31-52.

[15] P. J. Carvalho, V. H. Alvarez, J.J.B. Machado, J. Pauly, J.K. Daridon, I.M. Marrucho , M. Aznar, J. A. P. Coutinho, "High pressure phase behavior of carbon dioxide in 1-alkyl-3-methylimidazoliumbis(trifluoromethylsulfonyl)imide ionic liquids", J. Supercrit Fluids., 48, (2009) 99-107.

[16] D. M. D'Alessandro, B. Smit, J. R. Long, "Carbon dioxide capture: prospects for new materials", Angew. Chem. Int. Ed., 49 (2010) 6058-6082.

[17] J.E. Bara, T.K. Carlisle, C.J. Gabriel, D. Camper, A. Finotello, D.L. Gin, and R.D. Noble, "Guide to CO_2 separations in imidazolium-based room-temperature ionic liquids", Ind. Eng. Chem. Res., 48 (2009) 2739-2751.

[18] k. Han, C.K. Ahn, M.S. Lee, C.H. Rhee, J.K. Kim, H.D. Chun, "Current status and challenges of the ammonia-based CO_2 capture technologies toward commercialization", Int. J. Green Gas Con.,14 (2013) 270-281.

[19] J.G. Lu, A.C. Hua , Z.W. Xu , J.T. Li, S.Y. Liu, Z.L. Wang, Y.L. Zhao, C. Pan, "CO_2 capture by membrane absorption coupling process: experiments and coupling process evaluation", J. Membr. Sci., 431, (2013) 9-18.

[20] J. Wang J, M. Li, W.H. Yan,"The engineering application of CO_2 capture by chemical absorption in China", Adv Mater Res., 512-515 (2012) 2457-2462.

[21] G. Astarita, A. Savage, A. Bisio, "Gas Treating with Chemical Solvents", John Wiley and Sons., New York, 1984.

[22] A. Gabelman, S.T. Huang, "Hollow fiber membrane contactors", J. Membr. Sci., 159 (1996) 61–106.

[23] P.H.M. Feron, C.A. Hendriks, "CO_2 capture process principles and costs", Oil Gas Sci. Technol., 60 (2005) 451−459.

[24] D. Biello, "Can captured carbon save coal?", Sci. Am. Earth., 3 (2009) 52−59.

[25] D.W. Bailey, P.H.M. Feron, "Post-combustion decarbonisation processes", Oil Gas Sci. Technol., 60 (2005) 461−474.

[26] D. W. Bailey, P. H. M. Feron, "Post-combustion decarbonisation processes", Oil Gas Sci. Technol., 60 (2005) 461−474.

[27] K.R. Seddon, "Ionic Liquids for Clean Technology", J. Chem. Technol. Biotechnol., 68 (1997) 351–356.

[28] L.I. Eide, D.W. Bailey, “Precombustion decarbonisation processes”, Oil Gas Sci. Technol., 60 (2005) 475−484.

[29] J. A. Moulijn, M. Makkee, A. E. van Diepen, “Chemical Process Technology”, Wiley., New York, 2013.

[30] D. Jansena, A. Ramirez, “Performance requirements for CO_2 capture technologies; How realistic are capture cost targets?”, Energy Procedia 63 (2014) 45 – 52

[31] M. Ramdin, T. W. de Loos, T. J.H. Vlugt, “State-of-the-Art of CO_2 Capture with Ionic Liquids” , Ind. Eng. Chem. Res., 51 (2012) 8149−8177.

[32] M. Anheden, J. Yan, G. De Smedt, “Denitrogenation (or oxyfuel concepts)”, Oil Gas Sci. Technol., 60 (2005) 485−495.

[33]M. Anheden, J. Yan, G. De Smedt, “ Denitrogenation (or oxyfuel concepts).”, Oil Gas Sci. Technol.,60 (2005) 485−495.

[34] J. Ge, R. M. Cowan, C. Tu, M. L. McGregor, M. C.Trachtenberg, “Enzyme-based CO_2 capture for advanced life support,” Life Support Biosph Sci., 8 (2002)181–189,

[35] L. W. Diamond, N. N. Akinfiev, “Solubility of CO_2 in water from -1.5 to 100°C and from 0.1 to 100 MPa: evaluation of literature data and thermodynamic modelling”, Fluid Phase Equilib., 208 (2003) 265–290.

[36] J. J. Carroll, J. D. Slupsky, A. E. Mather, “The solubility of carbon dioxide in water at low pressure,” J. Phys. Chem. Ref. Data., (20) (1991) 1201–1209.

[37] R. Crovetto, “Evaluation of solubility data of the system CO_2-H_2O from 273K to the critical point of water,” J. Phys. Chem. Ref. Data., 20 (1991) 575–589.

[38] R.D. Rogers, K.R. Seddon, “Ionic liquids- solvents of the future?”, Science., 302 (2003) 792-793.

[39] N.V. Plechkova, K.R. Seddon, “Application of ionic liquid in the chemical industry” Chem. Soc. Rev., 37 (2008) 123-150.

[40] M. N. Roy, I. Banik, D. Ekka, “Physics and chemistry of an ionic liquid in some industrially important solvent media probed by physicochemical techniques”, J. Chem Thermodyn., 57, (2013) 230-237.

[41] L. A. Blanchard, D. Hancu, E. J. Beckman, J. F. Brennecke, “Green processing using ionic liquids and CO_2.”, Nature., 399 (1999) 28-29.

[42] J. E. Bara, D. E. Camper, D. L. Gin, R. D. Noble, "Room-temperature ionic liquid and composite materials: platform technologies for CO_2 capture.", Acc. Chem. Res., 43 (2010) 152-159.

[43] J. K. Anderson, J. K. Dixon, J. F. Brennecke, "Solubility of CO_2, CH_4, C_2H_6, C_2H_4, O_2, and N_2 in 1-hexyl-3-methylpyridinium bis(trifluoromethylsulfonyl)imide: comparison to other ionic liquids.", Acc. Chem. Res., 40 (2007) 1208-1216.

[44] J. M. Pringle, J. Golding, K. Baranyai, "The effect of anion fluorination in ionic liquids- physical properties of a range of bis(methanesulfonyl)amide salts.", New. J Chem., 27 (2003) 1504-1510.

[45] P.C. Hillesheim, S. M. Mahurin, P. F. Fulvio, J. S. Yeary, Y. S. Oyola, D. E. Jiang , S. Dai, "Synthesis and characterization of thiazolium-based room temperature ionic liquids for gas separations.", Ind. Eng. Chem. Res., 51 (2012) 11530-11537.

[46] B. M. Shiflett, D.W. Drew, R. A. Cantini RA, A. Yokozeki, " Carbon dioxide capture using ionic liquid 1-butyl-3-methylimidazolium acetate.", Energ. Fuel., 24 (2010) 5781-5789.

[47] S. Zhang, N. Sun, X. He, X. Lu, X. Zhang, "Physical Properties of Ionic Liquids: Database and Evaluation", J. Phys. Chem. Ref. Data., 35 (2006) 1475–1517.

[48] P. Bonhôte, A. P. Dias, N. Papageorgiou, K. Kalyanasundaram, M. Grätzel, " Hydrophobic, Highly Conductive Ambient-Temperature Molten Salts", Inorg. Chem., 35 (1996) 1168–1178.

[49] J.G. Huddleston, A.E. Visser, W.M. Reichert, H.D. Willauer, G.A. Broker, R.D. Rogers," Characterization and comparison of hydrophilic and hydrophobic room temperature ionic liquids incorporating the imidazolium cation", Green Chem., 3 (2001) 156–164.

[50] H. Tokuda, K. Ishii, M.A.B.H. Susan, S. Tsuzuki, K. Hayamizu, M. Watanabe, "Physicochemical properties and structures of room-temperature ionic liquids. 3. Variation of cationic structures", J.Phys. Chem. B., 110 (2006) 2833–2839.

[51] P. Galletii, F. Moretti, C. Samori, E. Tagliavini, "Enzymatic acylation of levoglucosan in acetonitrile and ionic liquids", Green Chem., 9 (2007) 987–991.

[52] C. Reichardt, "Polarity of ionic liquids determined empirically by means of solvatochromic pyridinium N-phenolate betaine dyes". Green Chem., 7 (2005) 339–351.

[53] A.J. Carmichael, K.R. Seddon, "Polarity study of some 1-alkyl-3-methylimidazolium ambient-temperature ionic liquids with the solvatochromic dye, Nile Red"J. Phys. Org. Chem., 13 (2000) 591–595.

[54] K.R. Fletcher, I.A. Storey, A.E. Hendricks, S. Pandey, "Behavior of the solvatochromic probes Reichardt's dye, pyrene, dansylamide, Nile Red and 1-pyrenecarbaldehyde within the room-temperature ionic liquid bmimPF_6", Green Chem., 3 (2001) 210–215.

[55] M.J. Muldoon, C.M. Gordon, I.R. Dunkin, "Investigations of solvent–solute interactions in room temperature ionic liquids using solvatochromic dyes", J. Chem. Soc. Perkin Trans., 2 (2001) 433–416.

[56] J.L. Anderson, J. Ding, T. Welton, D.W. Armstrong, "Characterizing Ionic Liquids On the Basis of Multiple Solvation Interactions", J. Am. Chem. Soc., 124 (2002)14247–14254.

[57] M.H. Abaham, A.M. Zissimos, J.G. Huddleston, H.D. Willauer, R.D. Rogers, W.E. Acree, "Some Novel Liquid Partitioning Systems: Water−Ionic Liquids and Aqueous Biphasic Systems", Ind. Eng. Chem. Res., 42 (2003) 413–418.

[58] L. Ropel, L.S. Belveze, S.N.V.K. Aki, M.A. Stadtherr, J.F. Brennecke, "Octanol–water partition coefficients of imidazolium-based ionic liquids" Green Chem.,7 (2005) 83–90.

[59] S.N.V.K. Aki, J.F. Brennecke, M.A. Stadtherr, "How polar are room-temperature ionic liquids?" Chem. Commun., (2001) 413–414.

[60] C. Reichardt, "Solvatochromic Dyes as Solvent Polarity Indicators", Chem. Rev., 94 (1994) 2319–2358.

[61] S. Schrodle, G. Annat, D.R. MacFarlane, M. Forsyth, R. Buchner, G. Hefter, "Broadband dielectric response of the ionic liquid N-methyl-N-ethylpyrrolidinium dicyanamide", Chem.Commun., (2006) 1748–1750.

[62] A. Basso, S. Cantone, P. Linda, C. Ebert, "Stability and activity of immobilised penicillin G amidase in ionic liquidsat controlled aw" Green Chem., 7 (2005) 671–676.

[63] S.H. Schofer, N. Kaftzik, P. Wasserscheid, U. Kragl, "Enzyme catalysis in ionic liquids: lipase catalysed kinetic resolution of 1-phenylethanol with improved enantioselectivity", Chem. Commun., (2001) 425–426.

[64] S. Park, R.J. Kazlauskas, "Improved Preparation and Use of Room-Temperature Ionic Liquids in Lipase-Catalyzed Enantio- and Regioselective Acylations", J. Org. Chem., 66 (2001) 8395–8401.

[65] J.L. Kaar, A.M. Jesionowski, J.A. Berberich, R. Moulton, A.J. Russell, "Impact of Ionic Liquid Physical Properties on Lipase Activity and Stability", J. Am. Chem. Soc., 125 (2003) 4125–4131.

[66] P. Lozano, T. De Diego, D. Carrie, M. Vaultier, J.L. Iborra, "Over-stabilization of Candida antarctica lipase B by ionic liquids in ester synthesis", Biotechnol. Lett., 23 (2001) 1529–1533.

[67] P. Lozano, T. De Diego, J.P. Guegan, M. Vaultier, J.L. Iborra, "Stabilization of α-chymotrypsin by ionic liquids in transesterification reactions", Biotechnol. Bioeng.,75 (2001) 563–569.

[68] J.P. Mann, A. McLuskey, R. Atkin, "Activity and thermal stability of lysozyme in alkylammonium formateionic liquids—influence of cation modification", Green Chem., 11 (2009) 785–792.

[69] T. Kanatani, K. Matsumoto, R. Hagiwara, "Syntheses and Physicochemical Properties of New Ionic Liquids Based on the Hexafluorouranate Anion", Chem. Lett., 38 (2009) 714–715.

[70] T.L. Greaves, C.J. Drummond, "Physicochemical Properties of Ionic Liquids Containing N-alkylamine-Silver(I) Complex Cations or Protic N-alkylaminium Cations", Chem. Rev., 108 (2008) 206–237.

[71] R.P. Swatloski, S.K. Spear, J.D. Holbrey, R.D. Rogers, "Dissolution of Cellose with Ionic Liquids", J. Am. Chem. Soc., 124 (2002) 4974–4975.

[72] Y. Fukaya, K. Hayashi, M. Wada, H. Ohno, "Cellulose dissolution with polar ionic liquids under mild conditions: required factors for anions", Green Chem., 10 (2008) 44–46.

[73] D.M. Anderson, Patent WO000057-A1 (2003).

[74] P.T. Spicer, W.B. Small, M.L. Lynch, Patent WO066014-A2 (2002).

[75] L.A. Neves, J. G. Crespo, I. M. Coelhoso, "Gas permeation studies in supported ionic liquid membranes", Journal of Membrane Science., 357 (2010) 160–170.

[76] L. Cammarata, S.G. Kazarian, P.A. Salter, T. Welton, "Molecular states of water in room temperature ionic liquids", Phys. Chem.,3 (2001) 5192–5200.

[77] T. Koddermann, C. Wertz, A. Heintz, R. Ludwing, "The Association of Water in Ionic Liquids: A Reliable Measure of Polarity", Angew. Chem. Int. Ed., 45 (2006) 3697–3702.

[78] A. Oehlke, K. Hofmann, S. Spange, "New aspects on polarity of 1-alkyl-3-methylimidazolium salts as measured by solvatochromic probes", New. J. Chem., 30 (2006) 533–536.

[79] S. Park, R.J. Kazlauskas, "Biocatalysis in ionic liquids – advantages beyond green technology", Curr. Opin. Biotechnol., 14 (2003) 432–437.

[80] L.A. Blanchard, Z. Gu, J.F. Brennecke, "High-Pressure Phase Behavior of Ionic Liquid/CO2 Systems", J. Phys. Chem. B., 105 (2001) 2437–2444.

[81] J.L. Anderson, R. Ding, A. Ellern, D.W. Armstrong, "Structure and Properties of High Stability Geminal Dicationic Ionic Liquids", J. Am. Chem. Soc., 127 (2005) 593–604.

[82] T. Payagala, J. Huang, Z.S. Breitbach, P.S. Sharma, D.W. Armstrong, "Unsymmetrical Dicationic Ionic Liquids: Manipulation of Physicochemical Properties Using Specific Structural Architectures", Chem. Mater., 19 (2007) 5848–5850.

[83] M.A.B.H. Susan, A. Noda, S. Mitsushima, M. Watanabe, "Brønsted acid–base ionic liquids and their use as new materials for anhydrous proton conductors", Chem. Commun., (2003) 938–939.

[84] Z.Y. Du, Z.P. Li, S. Guo, J. Zhang, L.Y. Zhu, Y.Q. Deng, “Investigation of Physicochemical Properties of Lactam-Based Brønsted Acidic Ionic Liquids”, J. Phys. Chem. B., 109 (2005)19542–19546.

[85] T.L. Greaves, A. Weerawardena, C. Fong, I. Krodkiewska, C.J. Drummond, Protic Ionic Liquids: Solvents with Tunable Phase Behavior and Physicochemical Properties”, J. Phys. Chem. B., 110 (2006) 22479–22487.

[86] R.P. Swatloski, J.D. Holbrey, R.D. Rogers, “Ionic liquids are not always green: hydrolysis of 1-butyl-3-methylimidazolium hexafluorophosphate”, Green Chem., 5 (2003) 361–363.

[87] A. Bagno, C. Butts, C. Chiappe, F. D’amico, J.C.D. Lord, D. Pieraccini, F. Rastrelli, “The effect of the anion on the physical properties of trihalide-based N,N-dialkylimidazolium ionic liquids” , Org. Biomol. Chem., 3 (2005) 1624–1630.

[88] Z.B. Zhou, H. Matsumoto, K. Tatsumi, “Low-Melting, Low-Viscous, Hydrophobic Ionic Liquids: Aliphatic Quaternary Ammonium Salts with Perfluoroalkyltrifluoroborates”, Chem. Eur. J., 11 (2005) 752–766.

[89] M.S. Kelkar, E.J. Maginn, “Effect of Temperature and Water Content on the Shear Viscosity of the Ionic Liquid 1-Ethyl-3-methylimidazolium Bis(trifluoromethanesulfonyl) imide As Studied by Atomistic Simulations”, J. Phys. Chem. B., 111 (2007) 4867–4876.

[90] R.E. Baltus, R.M. Counce, B.H. Culbertson, H. Luo, D.W. DePaoli, S. Dai, C. Duckworth, "Examination of the potential of ionic liquids for gas separations", Sep. Sci. Technol., 40 (2005) 525–541.

[91] C. Cadena, J.L. Anthony, J.K. Shah, T.I. Morrow, J.F. Brennecke, E.J. Maginn, "Why is CO_2so soluble in imidazolium-based ionic liquids?", J. Am. Chem. Soc., 126 (2004) 5300–5308.

[92] P.J. Carvalho, V.H. Álvarez, J.J.B. Machado, J. Pauly, J. Daridon, I.M. Marrucho, M. Aznar, J.A.P. Coutinho, "High pressure phase behavior of carbon dioxide in 1-alkyl-3-methylimidazolium bis(trifluoromethylsulfonyl)imide ionic liquids", J. Supercrit. Fluids., 48 (2009) 99–107.

[93] P. T. Nguyen, B. A. Voss, E. F. Wiesenauer, D. L. Gin, R. D. Noble, “Physically Gelled Room-Temperature Ionic Liquid-Based Composite Membranes for CO_2/N_2 Separation: Effect of Composition and Thickness on Membrane Properties and Performance”, Ind. Eng. Chem. Res., 52 (2013) 8812−8821.

[94] D. Yang, S. Majumdar, S. Kovenklioglu, K.K. Sirkar, "Hollow fiber contained liquid membrane pervaporation system for the removal of toxic volatile organics from wastewater", J. Membr. Sci., 103 (1995) 195–210.

[95] A.S. Kovvali, K.K. Sirkar, "Stable liquid membranes recent developments and future directions", Ann. N. Y. Acad. Sci., 984 (2003) 279–288.

[96] FJ. Hernández-Fernandez, AP. De los Ríos, F. Tomás-Alonso, J. M. Palacios, G. Víllora, "Preparation of supported ionic liquid membranes: influence of the ionic liquid immobilization method on their operational stability", J. Membr. Sci., 341,172-177(2009).

[97] SH. Barghi, M. Adibi and D. Rashtchian, "An experimental study on permeability, diffusivity, and This article is protected by copyright. All rights reserved selectivity of CO_2 and CH_4 through [bmim][PF_6] ionic liquid supported on an alumina membrane: investigation of temperature fluctuations effects", J. Membr. Sci., 362, 346-352(2010).

[98] DH. Kim, IH. Beak, SU. Hong and HK. Lee, "Study on immobilized liquid membrane using ionic liquid and PVDF hollow fiber as a support for CO_2/N_2 separation", J. Membr. Sci., 372, 346-354(2011).

[99] P. Scovazzo, J. Kieft, DA. Finan, C. Koval, D. Dubois and R. Noble, "Gas separations using non-hexafluorophosphate [PF_6^-] anion supported ionic liquid membranes", J. Membr. Sci., 238, 57-63(2004).

[100] P. Cserjési, N. Nemestóthy and K. Bélafi-Bakó, "Gas separation properties of supported liquid membranes prepared with unconventional ionic liquids", J. Membr. Sci., 349, 6-11(2010).

[101] E. Santos, J. Albo, A. Irabien, "Acetate based Supported Ionic Liquid Membranes (SILMs) for CO2 separation: influence of the temperature", J. Membr. Sci., 452, 277-283(2014).

[102] L.C. Tomé, D. Mecerreyes, C.S. Freire, L.P.N. Rebelo and I.M. Marrucho, "Pyrrolidinium-based polymeric ionic liquid materials: new perspectives for CO_2 separation membranes", J. Membr. Sci., 428, 260-266(2013).

[103] R. Couto, L. Neves, P. Simões, I. Coelhoso, "Supported Ionic Liquid Membranes and Ion-Jelly Membranes with [BMIM][DCA]: Comparison of Its Performance for CO_2 Separation", Membranes, 5 (2015) 13-21.

[104] J.A. Jonsson, L. Mathiasson, “Membrane-based techniques for sample enrichment”, J. Chromatogr. A., 902 (2000) 205–225.

[105] E. Miyako, T. Maruyama, N. Kamiya, M. Goto, “Highly Enantioselective Separation Using a Supported Liquid Membrane Encapsulating Surfactant−Enzyme Complex.”, J. Am. Chem. Soc., 126 (2004) 8622–8623.

[106] J.A. Jonsson, L. Mathiasson, “Liquid membrane extraction in analytical sample preparation: I. Principles.”, Trends Anal. Chem., 18 (1999) 318–325.

[107] L.C. Branco, J.G. Crespo, C.A.M. Afonso, "Highly Selective Transport of Organic Compounds by Using Supported Liquid Membranes Based on Ionic Liquids”, Angew. Chem. Int. Ed., 41 (2002) 2771–2773.

[108] L.C. Branco, J.G. Crespo, C.A.M. Afonso, "Studies on the Selective Transport of Organic Compounds by Using Ionic Liquids as Novel Supported Liquid Membranes”, Chem. Eur. J., 8 (2002) 3865–3871.

[109] E. Miyako, T. Maruyama, N. Kamiya, M. Goto, “Enzyme-facilitated enantioselective transport of (S)-ibuprofen through a supported liquid membrane based on ionic liquids”, Chem. Commun., (2003) 2926–2927.

[110] E. Miyako, T. Maruyama, N. Kamiya, M. Goto, “Use of ionic liquids in a lipase-facilitated supported liquid membrane”, Biotechnol. Lett., 25 (2003) 805–808.

[111] E. Miyako, T. Maruyama, N. Kamiya, M. Goto, “Transport of organic acids through a supported liquid membrane driven by lipase-catalyzed reactions”, J. Biosci. Bioeng., 96 (2003) 370–374.

[112] F.J. Hernandez-Fernandez, A.P. delos Rıos, F.T. Alonso, G. Vıllora, “Kinetic resolution of 1-phenylethanol integrated with separation of substrates and products by a supported ionic liquid membrane”, J. Chem. Technol. Biotechnol., 84 (2009) 337–342.

[113] A.P. delos Rıos, F.J. Hernandez-Fernandez, F.T. Alonso, D.R.M. Gomez, G. Vıllora, “On the importance of the nature of the ionic liquids in the selective simultaneous separation of the substrates and products of a transesterification reaction through supported ionic liquid membranes”, J. Membr. Sci., 307 (2008) 233–238.

[114] M. Mulder, "Basic Principles of Membrane Technology", 2nd edition. Kulwer Academic Publishers., The Netherlands(2003).

[115] I.M. Coelhoso, T.F. Moura, J. Crespo, M.J.T. Carrondo, "Transport mechanisms in liquid membranes with ion exchange carriers", J. Membr. Sci., 108 (1995) 231–244.

[116] F.F. Krull, C. Fritzmann, T. Melin, "Liquid membranes for gas/vapor separations", J. Membr. Sci., 325 (2008) 509–519.

[117] L.J. Lozano, C. Godínez, A. P. de los Ríos, F.J. Hernández-Fernández, S. Sánchez-Segado, F.J. Alguacil, " Recent advances in supported ionic liquid membrane technology", J. Membr. Sci. 376 (2011) 376, 1–14.

[118] P. Scovazzo, J. Kieft, D.A. Finan, C. Koval, D. DuBois, R. Noble, "Gas separations using non-hexafluorophosphate [PF6]−anion supported ionic liquid membranes", J. Membr. Sci., 238 (2004) 57–63.

[119] P. Luis, L.A. Neves, C.A.M. Afonso, I.M. Coelhoso, J.G. Crespo, A. Garea, A. Irabien, "Facilitated transport of $CO_2$and SO_2through supported ionic liquid membranes (SILMs)", Desalination., 245 (2009) 485–493.

[120] J. Ilconich, C. Myers, H. Pennline, D. Luebke, "Experimental investigation of the permeability and selectivity of supported ionic liquid membranes for CO_2/He separation at temperatures up to 125◦C", J. Membr. Sci., 298 (2007) 41–47.

[121] P. Scovazzo, D. Havard, M. McShea, S. Mixon, D. Morgan, "Long-term, continuous mixed-gas dry fed CO_2/CH_4 and CO_2/N_2 separation performance and selectivities for room temperature ionic liquid membranes", J. Membr. Sci., 327 (2009) 41–48.

[122] S. Hanioka, T. Maruyama, T. Sotani, M. Teramoto, H. Matsuyama, K. Nakashima, M. Hanaki, F. Kubota, M. Goto, "CO_2separation facilitated by task-specific ionic liquids using a supported liquid membrane", J. Membr. Sci., 314 (2008) 1–4.

[123] P. Cserjési, N. Nemestóthy, K. Bélafi-Bakó, "Gas separation properties of supported liquid membranes prepared with unconventional ionic liquids", J. Membr. Sci., 349 (2010) 6–11.

[124] P. Cserjési, N. Nemestóthy, A. Vass, Z. Csanádi, K. Bélafi-Bakó, "Study on gas separation by supported liquid membranes applying novel ionic liquids", Desalination., 245 (2009) 743–747.

[125] <http://www.carbozyme.us>.

[126] H. Zhao, "Effect of ions and other compatible solutes on enzyme activity, and its implication for biocatalysis using ionic liquids", J. Mol. Catal. B: Enzym, 37 (2005) 16-25.

[127] S. K. Kawatra, T.C.Eisele, J.J. Simmons, "Capture and sequestration of carbon dioxide in flue gases", US 2011/0182779 A1, 2011.

[128] R.M. Lau, M.J. Sorgedrager, G. Carrea, F. van Rantwijk, F. Secundo, R.A. Sheldon, “Dissolution of Candida antarctica lipase B in ionic liquids: effects on structure and activity”, Green Chem., 6 (2004) 483–487.

[129] R.A. Sheldon, L.R. Madeira, M.J. Sorgedrager, F. van Rantwijk, K.R. Seddon, “Biocatalysis in ionic liquids”, Green Chem., 4 (2002) 147–151.

[130] M. Moniruzzamana, K. Nakashima, N. Kamiya, M. Goto, "Recent advances of enzymatic reactions in ionic liquids", Biochem. Eng. J., 48 (2010) 295–314.

[131] P. Luis, L.A. Neves, C.A.M. Afonso, I.M. Coelhoso, J.G. Crespo, A. Garea, A. Irabien, "Facilitated transport of CO_2 and SO_2 through supported ionic liquid membranes (SILMs)", Desalination., 245 (2009) 485–493.

[132] M.G. Freire et.al., "Mutual Solubilities of Water and the [Cnmim][Tf2N] Hydrophobic Ionic Liquids", J. Phys. Chem. B2008,112, 1604-1610.

[133] C. Capasso, V. De Luca, V. Carginale, R. Cannio, M. Rossi, "Biochemical properties of a novel and highly thermostable bacterial α-carbonic anhydrase from Sulfurihydrogenibium yellowstonense YO3AOP1", J. Enzyme Inhib. Med. Chem., 27(2012) 892-897.

[134] E.L. Cussler," Diffusion: Mass Transfer in Fluid Systems", third ed., Press Syndicate of the University of Cambridge, Cambridge, 2009.

[135] L.M. Robeson, "The upper bound revisited", J. Membr. Sci., 320 (2008) 390–400.

[136] B.W. Rowe, L.M. Robeson, B.D. Freeman, D.R. Paul, J. Membr. Sci.,360 (2010) 58–69.

6. Appendix

6.1. Appendix: Estimation of "β"

To find the geometric parameter "β", a PDMS membrane was used due to its well – known Permeability, as the reported permeabilities values of standard PDMS available, [$P_{N2/PDMS}$= 2.075 x 10^{-10} m^2/s & $P_{CO2/PDMS}$= 2.24 x 10^{-9} m^2/s]. The test gases used was carbon dioxide, and the feed and permeate pressure data obtained over time are represented in (Fig.20), below:

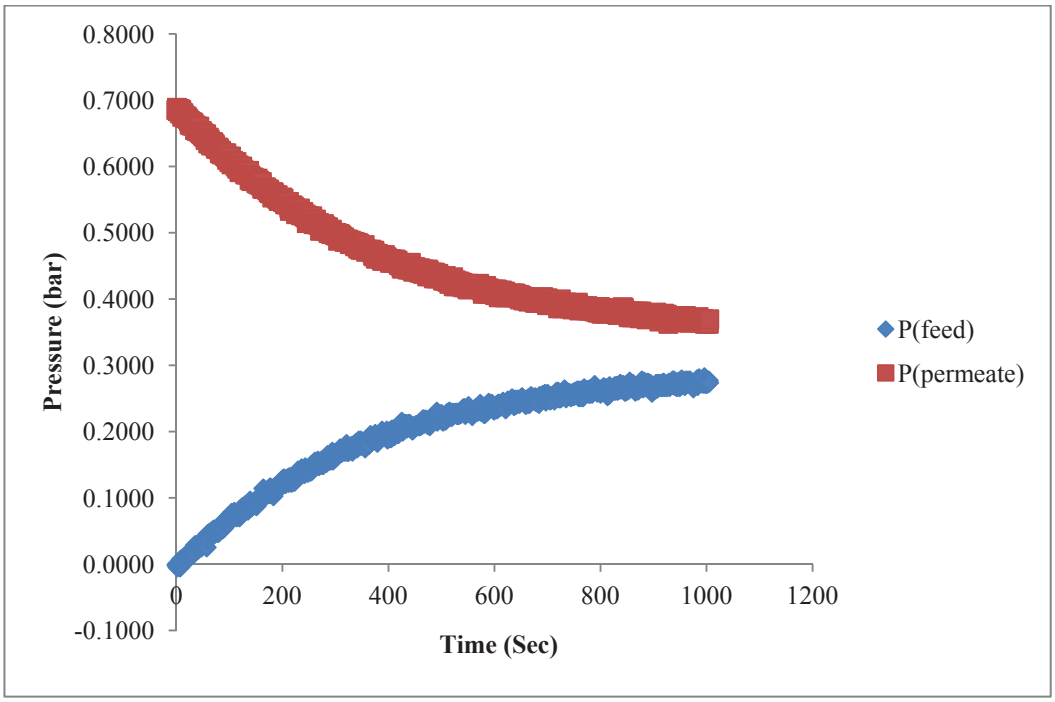

Fig.20: Feed and Permeate Pressure Profiles in the permeation cell.

By modifying the following equation:

$$\frac{1}{\beta}\ln\left(\frac{[P_{feed}-P_{perm}]_0}{[P_{feed}-P_{perm}]}\right)=P\frac{t}{l}$$

we can linearize it to the form shown below equation (1) and using CO_2 permeability value for the PDMS membrane referred to in bibliography the curve of $\frac{1}{P}\ln\left(\frac{\Delta P_0}{\Delta P}\right)$ versus $\frac{t}{l}$ were traced, the slope of which gives the value of (β= 88.78) as shown in (Fig.21).

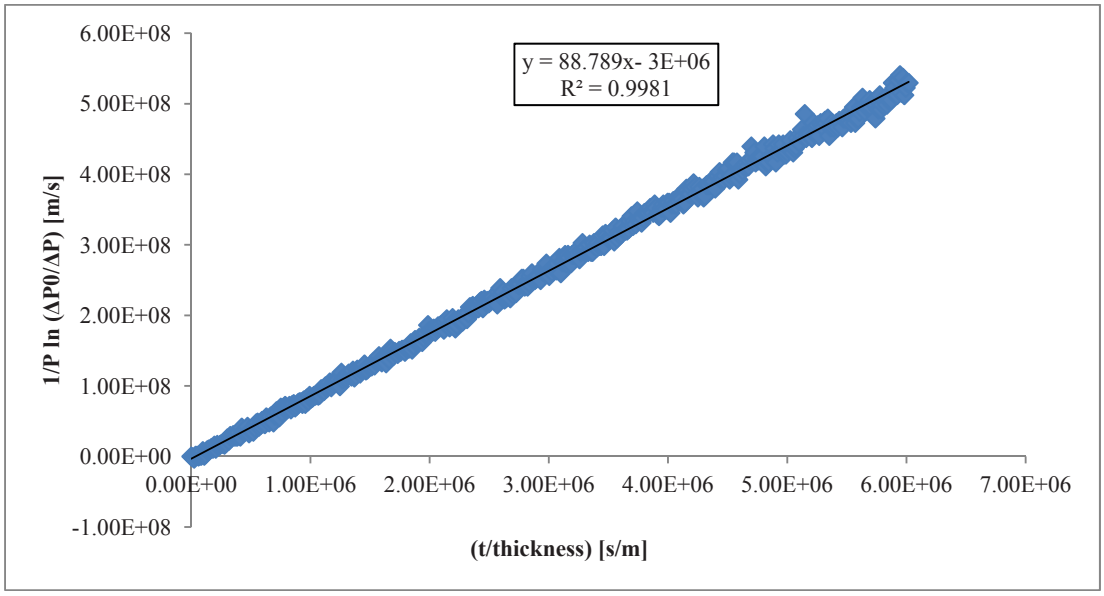

Fig.21: Graphical representation of Equation (1) where the slope gives the value of (β).

6.2. Appendix: Estimation of Gas Permeability and Pressure Profiles

The feed and permeate pressure data obtained over time from the software Lab View for SILM membranes are represented in (Fig.21). The graphical representation for the permeability of N_2 and other with CO_2 through SILM membranes at the same temperature is represented in (Fig.22) and (Fig.23), the same procedure was followed for all the membranes and gases tested in this research work at different temperatures.

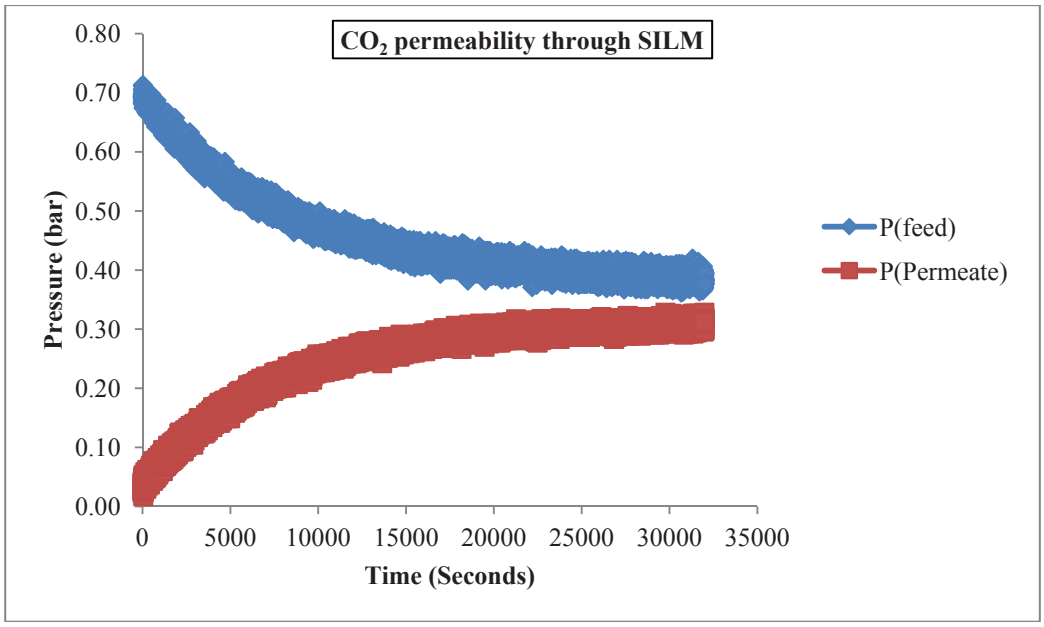

Fig. 22: The graphical representation for CO_2 permeability through one SILM tested.

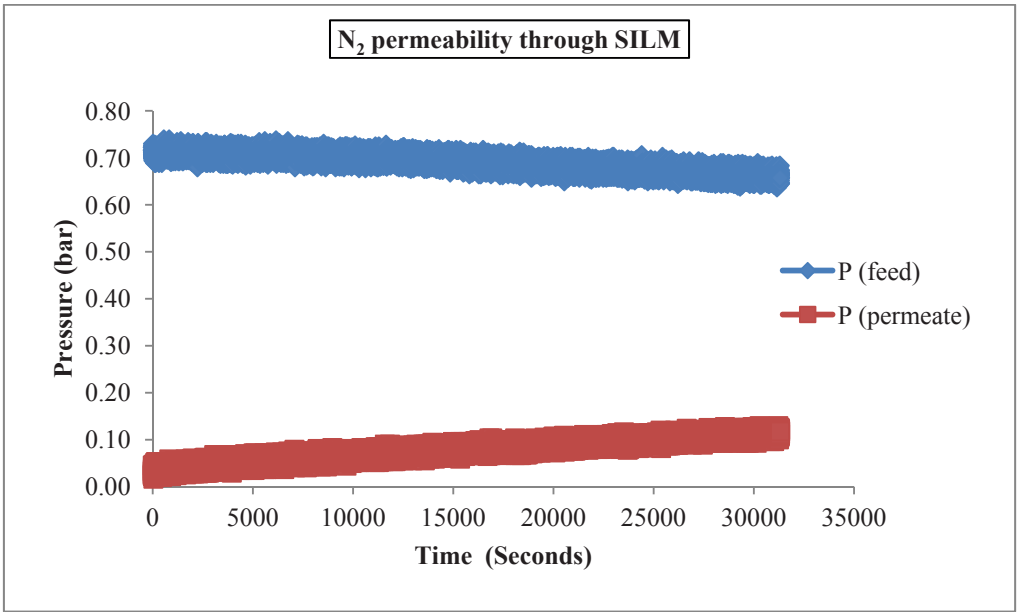

Fig. 23: The graphical representation for N_2 permeability through one SILM tested.

Chapter (4)

Synthesis and characterization of polymeric membranes for gas separation.

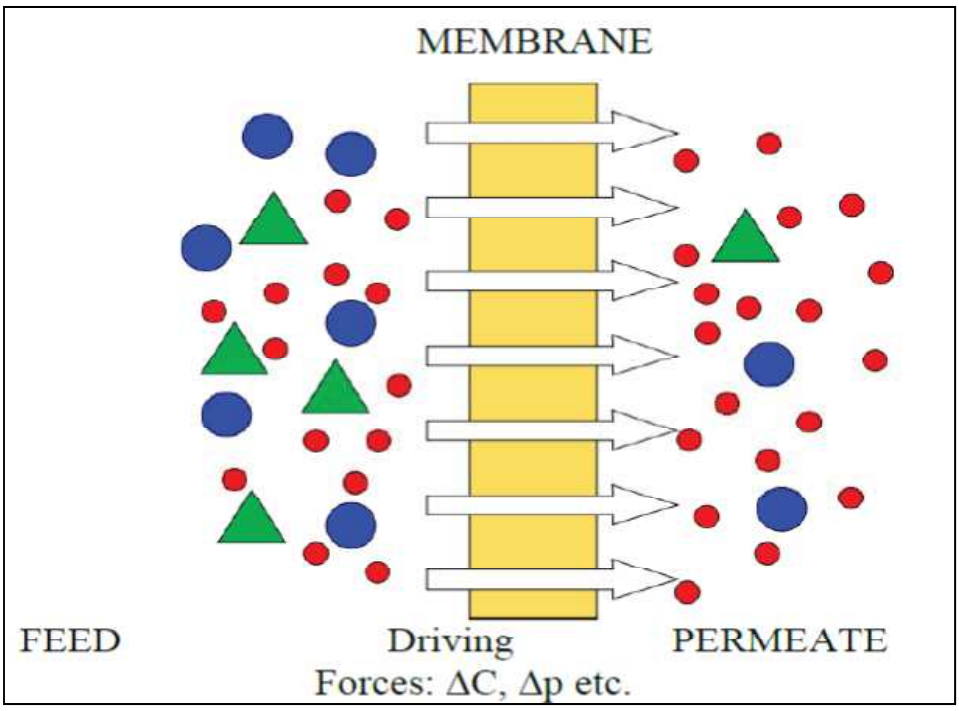

Abstract

In membrane industry, recent developments have shown the combination or replacement of classical glassy polymers with crystalline Metallic Organic Frameworks (MOFs), Zeolite Imidazolate Frameworks (ZIFs) or zeolites provides molecularly controlled permeability and selectivity of membranes. However, the main challenges are to get mechanically stable and homogeneous layers of the membranes. By taking advantage of high permeability observed with the rubbery polymers and to their flexible casting properties, Rubbery Organic Frameworks (ROFs) could be used as alternative as gas separation membrane systems. Therefore, nanometric macro-monomers and core connectors have been used to conceive dense (ROFs) for the preparation of polymeric membranes for selective gas transport. With the above concept, in this project, new polymeric membranes based on supramolecular polymeric structures using covalent bonds, were designed selectively for CO_2 separation from light gases like N_2, and CH_4. Then the resulting polymer membranes were characterized spectrometry by (FTIR,^{1}HNMR), their thermal stability were characterized by (TGA and DSC), and the morphological structure was characterized by (SEM and contact angle). The gas permeability measurements for the tested polymeric membranes showed that the permeability of CO_2 is higher than other tested gases (N_2 and CH_4) for the polymeric membranes. Additionally, it is observed that the CO_2 permeability and ideal selectivities of the synthesized polymeric membranes depend of the hydrophobic and rubbery behavior of the membranes, which effect on the morphological structure and the permeability of the tested gases through it. Generally, the synthesized polymeric membranes in this research work are stable at the (30ºC) for a pressure difference of (0.7 bar), and they are selective towards CO_2 when compared with (N_2) and (CH_4) gases. Finally, thanks to the possibility to combine the structural and functional features of different monomers, the heteropolymeric membrane materials can exhibit very different properties from their original homopolymeric components. In the above-developed examples, this strategy revealed itself to be a versatile way for the synthesis of new membranes presenting different permeabilities and preserving their selectivity towards gas separation application.

Keywords:
Rubbery Organic Frameworks (ROFs); Polymeric membranes; Morphological structure; Thermal stability; Gas separation application; Permeability; Ideal selectivity.

Aim of the research work

The main goals for the approach proposed in this research work consist on the synthesis and characterization of dense polymeric membranes for gas separation application. Firstly the different polymeric membranes were synthesized by condensation polymerization between one of main subtracts [(2,2`ethylene dioxide) bis(ethylamine)) / DEG] or (4,7,10-trioxa-1,13-tridecanediamine) / TEG] with [Benzene-1,3,5 tricarbaldehyde / TCA] as core contactor for polymerization with amine compounds. The resulting polymeric membranes were characterized spectrometry by (FTIR, ^{1}HNMR) for chemical structure analysis, their thermal stability were characterized by (TGA and DSC), and the morphological structure was characterized by (SEM and contact angle). Then the synthesized polymeric membranes were tested for gas separation application with the following gases (CO_2, N_2, and CH_4) to determine the permeability and idea selectivities for these gases. In summary, the main goals for this research project consist of 3 main parts:

- ❑ Synthesis some polymeric membranes, then identify the blending behavior of the polymers glassy and rubbery polymers.
- ❑ Characterize the developed membrane in order to find its physico-chemical and thermal properties.
- ❑ To evaluate the performance of the developed membrane in terms of selectivity and permeability for the gas separation .
- ☐ Comparing the obtained data with the data available in the literature.

1. Introduction

Anthropogenic climate change is rapidly becoming one of the major issues in environmental science. Global temperatures are projected to rise between 1.4 and 5.8°C by 2100 in the absence of climate change policies [1]. This increase in global temperatures is likely to cause a number of negative effects; including rising sea levels, changes in ecosystems, loss of biodiversity and reduction in crop yields [2]. These effects can be partially alleviated by reductions in emissions of greenhouse gases. Reduction of greenhouse gas emissions can occur in a number of ways; such as improvements in energy efficiency, increased use of non-fossil fuel power sources, improved soil management and the geological sequestration of carbon dioxide from significant greenhouse gas producing point sources [3]. Membranes have been investigated for over 150 years [4,5], and since 1980 gas separation membranes have been used commercially[6]. Gas separation membranes are used in a number of industrial processes; such as the production of oxygen enriched air, separation of CO_2 and H_2O from natural gas, purification of H_2, and recovery of vapours from vent gases. A number of reviews examining gas separation membranes have been published [6–13]. Different strategies towards the construction of more efficient membranes have suggested by Koros and Mahajan [14].

1.1. Membranes for gas separation

Membrane based processes are useful in many industrial gas separations [15]. Gas separations currently comprise a membrane market of over four hundred million dollars per year, which constitutes 24 % of the total membrane market [15]. Membranes result in preferential separation of one or more components from a feed mixture based on size, shape and physiochemical properties of the components in the feed mixture. Inorganic, polymeric as well as composite membranes have been used and studied for gas separation over the last few decades [16, 17]. Inorganic membranes e.g. alumina, zeolite, carbon etc. generally have exceptional separation efficiency compared to polymer membranes as well as higher chemical and thermal stability, but their brittleness (poor mechanical properties), difficult processing and high cost make them less attractive [18, 19]. The majority of gas separation membranes used in the recent years in industry are

polymeric membranes, because of their inherent advantages such as low cost, easy processing and reasonable gas separation properties [20]. Some of the principal applications of gas separations using membrane technology are natural gas treatment (removal of CO_2), hydrogen recovery, oxygen enrichment from air (medical devices) and nitrogen enrichment from air (used as protecting atmosphere for oxygen sensitive compounds) [21-23]. Natural gas is one of the cleanest and efficient burning fuels. The worldwide demand of natural gas is increasing constantly with the global increase in population. The global consumption of natural gas is expected to increase to 182 trillion cubic feet by 2030 [24]. Although methane is the main component of natural gas, it also contains considerable concentrations of various impurities including water, carbon dioxide, hydrogen sulphide and other hydrocarbons. The focus of natural gas treatment is typically on acid gas removal [25]. For fuel applications, natural gas sweetening is essential to (1) increase the calorific value, (2) reduce pipeline corrosion within the gas distribution network and (3) prevent atmospheric pollution [25-27]. Air separation to generate nitrogen-enriched streams from air is another main application of membrane gas separation and is predicted to cover 49 % of the gas separation membrane market by 2020 [28]. Nitrogen and oxygen are the third and fifth largest bulk chemicals produced worldwide [29]. Nitrogen-enriched streams (purity 98-99%) are used as inert blanketing for fuel storage tanks and pipelines to minimize fire hazards and to reduce oxidation during various heating operations. Oxygen-enriched air (30-40% O_2) is relatively a less explored application of membranes. Oxygen-enriched streams are most commonly used in power plants to increase the efficiency of combustion processes [29]. Hydrogen recovery was among the first large scale commercial applications of gas separation membranes [30]. The main sources of hydrogen gas are steam reforming of natural gas, petroleum hydrocarbon purge streams, or electrolysis of water. Major use of recovered hydrogen is in the petroleum and chemical industries. The largest application of H_2 is for the processing ("upgrading") of fossil fuels, and in the production of ammonia and methanol, hydrogenation of oils and fats and also as coolant in power station generators [16, 18].

1.2. Initial concept of membrane separation

Membrane can be defined as: It is a semi-permeable active or passive barrier which, under a certain driving force, permits preferential passage of one or more selected species or components (molecules, particles or polymers) in a gaseous and/or liquid mixture solution [31,32].

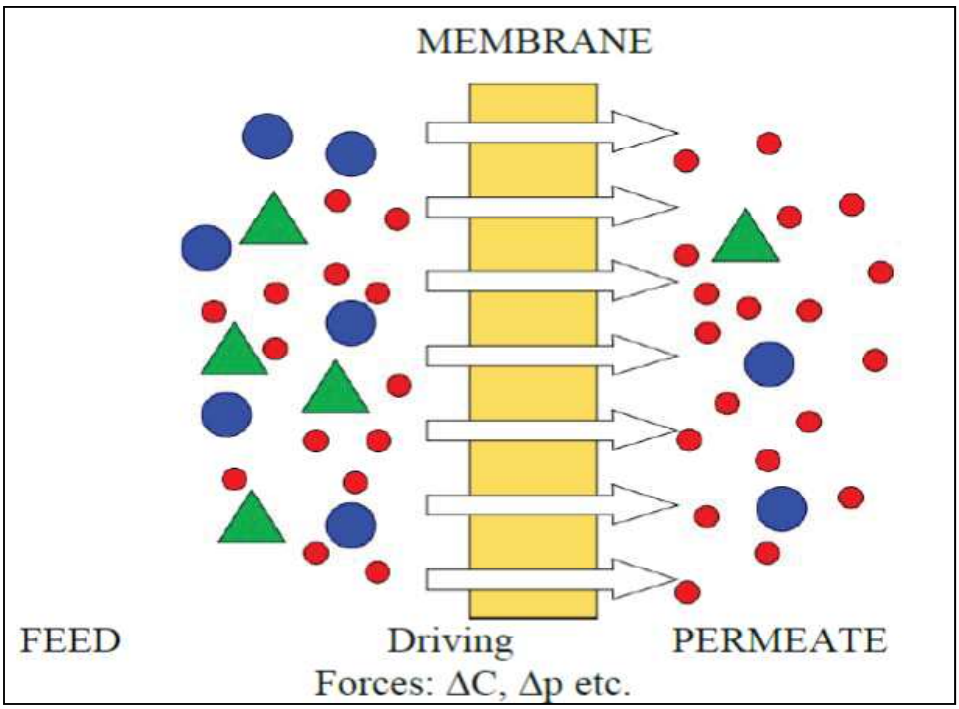

Fig.1: Schematic diagram of gas separation process by a membrane [33].

The primary species rebound back by the membrane is called retentate or solute, while those species passing through the membrane is called permeate or solvent, which shown in (Fig.1). There are three different important mechanisms by which membrane can perform separations:

- By having pores which are of such a size that certain species can pass through and others cannot, this mechanism is called size exclusion.
- By selective retardation by the pores when its diameters are close to molecular sizes, this mechanism is called pore flow.
- By dissolution into the membrane, movement by molecular diffusion across the membrane, and re-emergence from the other side, called solution diffusion.

The driving force also exists in the form of pressure, concentration, or voltage difference across the membrane. The driving force depending on the physical sizes of the separated species, so that the membrane processes are classified as:

- Microfiltration (MF) Membrane.
- Ultrafiltration (UF) Membrane.
- Nanofiltration (NF) Membrane.
- Reverse Osmosis (RO) Membrane.

1.3. Materials for gas separation membrane

The size of materials retained for each process, the driving force behind separation and the type of membrane. The selection of material membrane is the most important factor for Gas Separation. Chemical interaction between a membrane material and a gas penetrant determined the separation efficiency of a membrane separation process [9]. The choice of material is based on the application and cost-effectiveness. The most important requirements of effective separation material are: [34,35]

1. Engineering feasibility.
2. Good chemical resistance.
3. High separation efficiency with reasonable high flux.
4. Good mechanical stability.
5. High thermal stability.
6. Low cost.

1.4. Issues and challenges in membrane applications for gas separation

The following issues and challenges occur in membranes application for gas separation:

1. High Cost
2. Lack of selectivity
3. Lack of mechanical resistance
4. Sensitivity to chemical attack
5. Membrane cleaning
6. Module Design

1.5. Membrane separation mechanism

In gas separation processes there are two streams; Upstreams and Downstreames. Pressure gradient between in these two streams which occur the separation processes. Permeation is a rate-controlled process and separation degree is determined by the selectivity of membrane at the conditions of separation, including temperature, pressure, flow rate, and area of membrane [36]. The membrane separate gases only, some component passes more rapidly than the other, it also depends upon the pore size. There are three fundamental transport membrane separation mechanisms, which shown in (Fig.2).

1. Knudsen diffusion
2. Molecular sieving
3. Solution-diffusion.

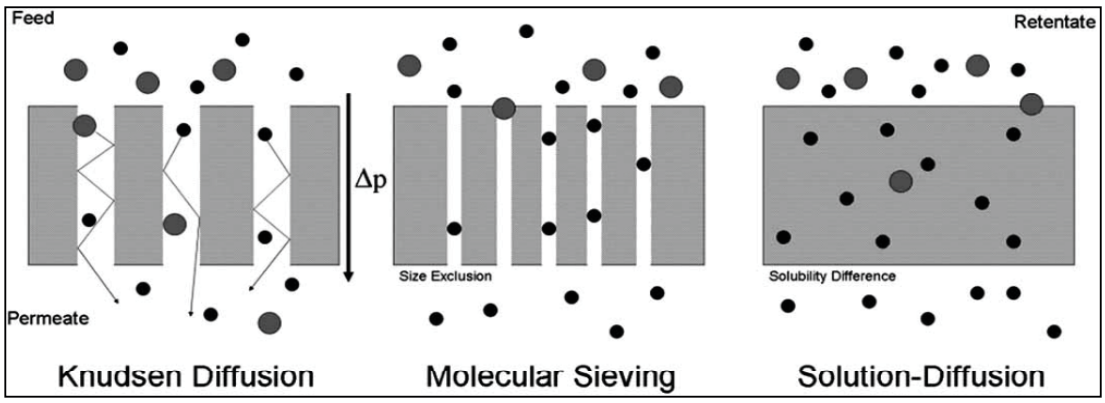

Fig 2: Schematic representation of three of the different possible mechanisms for membrane gas separation, Knudsen diffusion, molecular sieving and solution-diffusion [37].

1.6. Polymeric membranes

Polymeric membranes perform their process by different mechanisms which are based upon the properties of membrane [38]. It can be classified into two types: porous and non porous [39]. A porous membrane is a rigid, highly voided structure with randomly distributed interconnected pores like a conventional filter. Separation is dependent on molecular size of polymer and pore size distribution. These membranes exhibit high fluxes but they are inherently low selective. Non porous membrane also called as dense

membrane consists of a dense film. Permeate molecules are first absorbed and then diffused through polymer matrix under the driving force of pressure or concentration gradient. Dense membranes are highly selective but transport of gas through the polymer medium is very low. Permeate of similar sizes can be separated by dense membranes if they have significantly different solubility in polymer. Polymeric membranes can be classified on the basis on polymer material.

I. Glassy polymer: At low temperatures molecular motion in an amorphous region is restricted to molecular vibrations, but the chains cannot move or rotate in space. This form is the glassy state of the amorphous region. The glassy state can be considered as a super cooled liquid where the molecular motions have been frozen in. The glassy state is brittle, hard and rigid like a crystalline solid, but it retains the molecular disorder of a liquid. [33] At a low temperature the amorphous regions of a polymer in the glassy state, the molecules are frozen on place. They may be able to fluctuate slightly, but they do not have any segmental motion in which portions of the molecule wiggles around. Whenever the amorphous regions of a polymer are in the glassy state, it generally will be brittle, hard and rigid.

II. Rubbery polymer: When the material is heated the polymer will reach a temperature at which segments of the entangled chains can move. The amorphous region becomes rubbery at this temperature, which is called the glass transition temperature. When an amorphous polymer in rubbery state, it is soft and flexible[33]. If the polymer is heated it eventually will reach its glass transition temperature. The molecules can start to wiggle around at this temperature. The polymer now is in its rubbery state. The rubbery state tends to softness and flexibility to a polymer. Semi-crystalline solids have both crystalline and amorphous regions. Accordingly the temperature, in the amorphous regions can be either in the rubbery or glassy state. Temperature at which the transition in the amorphous regions between the glassy and rubbery state occurs is called the glass transition temperature. The amorphous portion of semi-crystalline solid contains the glass transition property. During the glass transition the crystalline portion remains crystalline.
There is a general tradeoff between permeability and selectivity for polymeric membranes with rubbery polymeric membranes with high permeability and low

selectivity and vice versa for glassy polymeric membranes. Despite their mechanical strength, reproducibility and economical processing capacity, dense membranes are still not much attractive because they suffer from upper bound tradeoff between permeability and selectivity. Robeson in 1991 proposed this upper bound trade off and is shown in below figure graph between Permeability and Selectivity.

1.7. Comparison of polymeric, inorganic and mixed matrix membranes

A comparison of polymeric, organic and mixed matrix membrane is given in table in terms of cost, chemical and thermal stability, and mechanical strength, compatibility to solvent, swelling, separation performance and handling. It is clear from the table that polymeric membranes are economical to fabricate and have good mechanical strength. Their separation performance and stability is moderate and these are robust in handling. Their main disadvantage lies in swelling and compatibility to solvent. However still for industrial applications polymeric membranes are preferred.

Properties	Polymeric membranes	Inorganic membranes	Mixed matrix membranes (MMMs).
Cost	Economical to fabricate	High fabrication cost	Moderate
Chemical & Thermal stability	Moderate	High	High
Mechanical strength	Good	Poor	Excellent
Compatibility to solvent	Limited	Wide range	Limited
Swelling	Frequently occurs	Free of swelling	Free of swelling
Separation performance	Moderate	Moderate	Exceed Robeson upper boundary
Handling	Robust	Brittle	Robust

Table 1: COMPARISON OF VARIOUS MEMBRANES [40]

Different techniques are being used to improve the performance of polymeric membranes to withstand required duties. Blending is a cost and time effective method to develop materials with desired properties. However, blending of glassy and rubbery polymers has not been studied.

1.8. Gas transport theory

The utility of membranes in gas separation processes depends on the permeability through the membrane and the selectivity towards the different components in the mixtures [22, 23]. The permeability for component A, P_A, is the intrinsic ability of a membrane material to control the rate at which gas molecules are allowed to permeate through the membrane. It equals the penetrant diffusive flux (J_A) through the membrane normalized by the change in partial pressure across the membrane, Δp_A (cmHg), multiplied by the thickness of the membrane (l cm):

$$P_A = \frac{J_A . l}{\Delta P_A} \qquad \text{Eq. (1)}$$

Permeability is given in units of Barrer, defined as:

$$1\ \text{Barrer} = 1.10^{-10}\ \frac{\text{cm}^3\ (\text{STP}).\text{cm}}{\text{cm}^2.\text{s.cm.Hg}} \qquad \text{Eq. (2)}$$

Generally gas molecules are transported through a polymeric membrane by the solution-diffusion mechanism [17]. Through Fick's first law, eq. 1.1 can be rearranged so that permeability is expressed as a product of the solubility coefficient (S) (cm^3 (STP)/cm^3·cmHg) and the diffusivity coefficient, D (cm^2/s) of penetrate A [22]:

$$P_A = D_A . S_A \qquad \text{Eq. (3)}$$

The solubility coefficient through a membrane can be expressed as [18]:

$$S_A = \frac{C_A}{P_A} \qquad \text{Eq. (4)}$$

where (S_A) is the solubility coefficient of component 'A' in the membrane, (C_A) is the upstream concentration of component 'A' sorbed into the membrane, and P_A is the corresponding partial pressure [22]. For glassy polymers, the sorption of molecules is usually described by the dual mode sorption model, which consist of two types of sorption sites e.g. a Henry's site (solution) and a Langmuir site (hole filling) [19]. Diffusion of a penetrate through a polymeric membrane can be described by a series of diffusional jumps through temporary cavities created by the constantly vibrating polymer chains. Thus, the diffusion coefficient of component 'A', D_A, is a function of the frequency of the diffusive "jumps" made by gas molecules in the polymer matrix 'f_A', and the jump length (λ_A). The diffusion coefficient for a given gas penetrant 'A' can be given as [20]:

$$D_A = \frac{f_A \cdot \lambda_A^2}{6} \qquad \text{Eq. (5)}$$

The selectivity of a membrane for a gas pair A and B is the ratio of the permeability of component 'A' over the permeability of component 'B'.

$$\alpha_{A/B} = \frac{P_A}{P_B} \qquad \text{Eq. (6)}$$

The above equation is used when the individual permeabilities of the two pure components in a gas pair are known, which are typically estimated from pure gas experiments. Above equation can be extended when combined with Eq.3.

$$\alpha_{A/B} = \frac{P_A}{P_B} = \frac{D_A}{D_B} \cdot \frac{S_A}{S_B} \qquad \text{Eq. (8)}$$

Where (S_A/S_B) is the solubility selectivity and (D_A/D_B) is the diffusion selectivity. For a mixed gas feed, the composition of the feed needs to be take into account and the separation factor can be calculated as,

$$\alpha_{A/B} = \frac{y_A/y_B}{x_A/x_B} \qquad \text{Eq. (9)}$$

where (y_A) and (y_B)are the mole fractions of the components (A and B) produced in the permeate, while (x_A) and (x_B) are their corresponding mole fractions in the feed [21]. In the solution-diffusion model, the gas molecules absorb on the feed side of the membrane and then diffuse through the membrane through the free volume between the polymer chains, driven towards the downstream side by, for example a concentration or pressure gradient and desorb at the permeate side. The thermodynamic parameter solubility is dependent on the condensability of the penetrant gas, which is directly influenced by the critical temperature of the gas (defined as the temperature at or above which the gas molecules cannot be liquefied whatever the pressure). Generally, gas molecules with a higher critical temperature (T_c) possess higher polymer solubility than the ones with a lower (T_c) [1]. Solubility is also influenced by the size and chemical affinity of the penetrant with the polymer. As the size of the penetrant increases, the solubility usually increases. Similarly, polar gases have higher solubility in polymers [22]. In contrast, the diffusivity of a gas in a polymer is a kinetic parameter and depends on the penetrant size and shape [18]. Smaller molecules diffuse faster through a polymeric membrane. The shape of the molecule is also important as linear molecules can diffuse faster than spherical molecules because of their

ability to diffuse along their smallest dimension [18]. However, both high solubility and diffusion are important to have higher permeabilities.

Gas	Molecular mass (g/mol)	Critical temperature (K)	Kinetic diameter (nm)
CO_2	44	304	0.33
N_2	28	126	0.36
CH_4	16	190	0.38

Table 2: General properties of gases CO_2, N_2 and CH_4 [23].

As shown in Table (1) CO_2 has a smaller kinetic diameter and much higher critical temperature compared to N_2 and CH_4. The smaller kinetic diameter and high critical temperature (higher condensability) of CO_2 aids in higher diffusion and solubility coefficients and hence the higher permeability compared to N_2 and CH_4.

1.9. Limitations of polymeric membranes

Many different polymers have been investigated as gas separation materials such as polycarbonate (PC) [41], cellulose acetate (CA) [42], polysulfone (PSF) [43] and Polyimides (PI) [45] etc. CA, PSF and PI have been widely used for industrial scale applications [44]. Several companies are currently producing gas separation membranes on commercial scale (e.g. Membrane Technology Research, Air Products, UOP, Air Liquide, Paxair and GKSS Licensees etc.) [46]. Despite their advantages (low cost, good mechanical stability and easy processing) [47], polymeric membranes often limited by either low permeability or low selectivity. In polymeric membrane systems, a trade-off relationship exists between the permeability and selectivity of the membrane. This trade-off relationship was best presented graphically by Robeson in 1991, summarizing all pure gas separation data from literature for a specific gas pair at 1 bar pressure and 35^{o}C. This so-called Robeson plot is considered as a benchmark in gas separation membrane development [48] (Fig.3). This trade-off established an upper bound when permeability and selectivity for most industrially relevant gas pairs are plotted on a log-log scale. The permeability and selectivity plot of 1991 was redrawn in 2008 [49] (Fig. 3). It shows that most of the glassy and rubbery membrane materials are below the previous and currently available trade-off lines. Nevertheless, over the last

decades notable improvements in CO_2/CH_4 selective membranes have taken place especially in mixed gas separation performance and at more extreme conditions such as higher temperatures or pressures. The polymers of intrinsic microporosity (PIM-1 and PIM-7) showed good $CO2/CH_4$ separation capabilities [49]. A series of rigid (thermally rearranged) polymer variants has recently been published which exhibit even improved separation characteristics (above the trade-off line of 2008) but involve complicated synthesis [50]. It is recognized that polymeric membranes have the potential to replace the conventional gas separation processes e.g. Pressure swing adsorption (PSA), cryogenic distillation and absorption [51]. In order for polymeric membranes to be economically viable in industry, these materials need to surpass the gas transport properties of the state of the art polymeric materials [49].

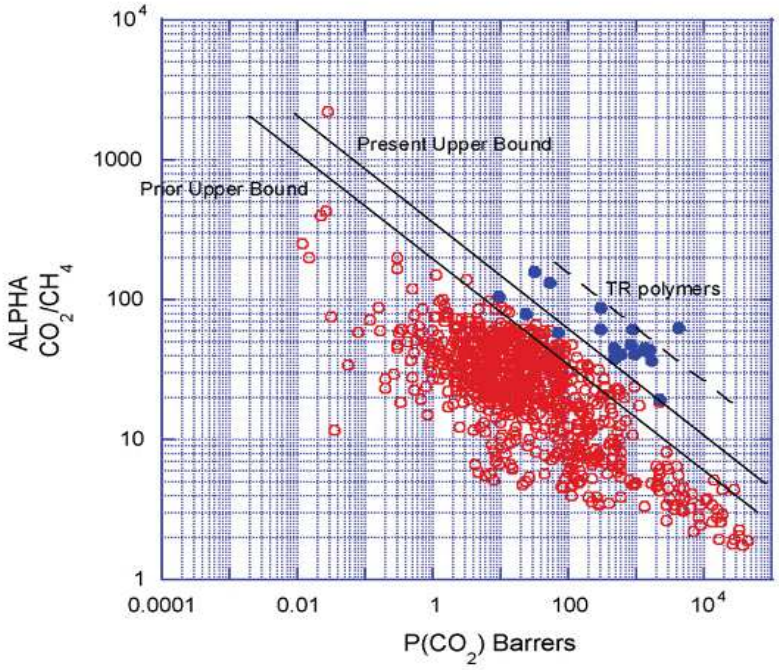

Fig.3: Permeability and selectivity trade-off with the 1991 and 2008 Robeson upper bounds [49, 50].

Another issue, plasticization, is of particular concern for glassy polymer membranes for separation of gaseous mixtures (CO_2/CH_4, CO_2/N_2, propane/propene etc.). Plasticization has not been accounted for on the Robeson plot as it only shows the pure gas separation results at 1 bar pressure. Plasticization is defined as an increase in the segmental motion of polymer chains, due to the presence of one or more sorbates, such that the

permeability of all components increases and the selectivity decreases [52]. The highly sorbing gas in the polymer matrix disrupts chain packing and enhances the segmental mobility of the polymer chains. Since the permeability of slower components (CH_4, N_2) increases more than that of the faster component (CO_2), plasticization causes a decrease in membrane selectivity [52]. This loss in selectivity is mainly caused by the reduction in diffusivity selectivity due to excessive segmental motion. In other words, the membrane loses its ability to discriminate between the subtle size and shape differences. Fig.4 is a schematic of CO_2 permeability versus pressure in a CO_2 gas separation.

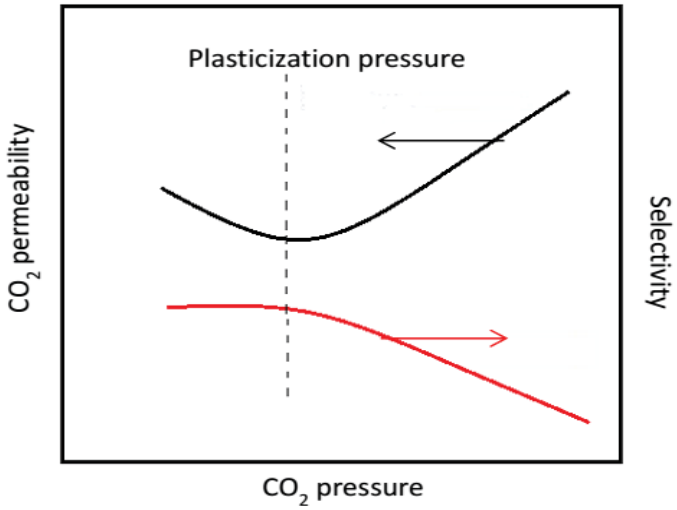

Fig.4: Schematic of CO_2-induced plasticization behavior in polymer membranes.

As CO_2 pressure increases, the onset of plasticization occurs, the pressure at which the Permeability versus CO_2 pressure curve shows a minimum is known as the plasticization Pressure (dashed line). Below the plasticization pressure the permeability decreases due to saturation of the Langmuir sites. Above the plasticization pressure polymer chain mobility increases due to swelling by the dissolved CO_2, which results in upward inflection of CO_2 permeability with a corresponding loss of membrane selectivity. For a CO_2/CH_4 binary mixture for instance, increased feed pressures and CO_2 concentrations (10-45 mol %) lowered the CO_2/CH_4 selectivity for CA membranes by a factor of 1.5-1.2 between 10 and 50 bar [53]. In a similar study, the ideal selectivity of CO_2 over CH_4 was 3-5 times higher than the selectivity of the mixed gases for CA membranes at feed CO_2

concentrations higher than 50% and pressure up to 54 bar [54]. This is attributed to swelling or/and plasticization effects of CO_2, since CO_2 is much more soluble in CA than CH_4. However, it was proven that CA membranes can still be used to remove both CO_2 and H_2S and reach the US pipeline specification for sour gases, if the feed gas contains CO_2 less than 15 % CO_2 and 250 ppm H_2S, and no water vapor [55]. A detailed overview of plasticization phenomena in gas separation membranes is given by Ismail and Lorna [56].

There are several methods which have generally been utilized to suppress CO_2 plasticization. A short overview of these approaches is presented below. Chemical, thermal and radiation cross-linking are among the most comprehensive approaches being used to improve the gas separation properties of membranes for applications in rigorous environments. Chemical cross-linking modification imparts anti-plasticization properties to the material, enhances chemical stability and reduces ageing [57]. Diamine cross-linking has proven to be one of the most simple and effective methods of cross-linking for polyimide membranes. p-Xylenediamine cross-linked 6FDA-(2,6-diamino toluene) (DAT) PI-membranes resulted in reduced CO_2 plasticization and increased CO_2/CH_4 selectivity [58]. 1, 3-Propanediol (PDL) cross-linked PI-membranes showed a greatly suppressed CO_2 plasticization as well [59].

Another approach for cross-linking membranes is the formation of hyper-branched polyimides by reaction of triamines with dianhydrides [60]. Bos et al. [52] thermally cross-linked the polyimide films to stabilize against plasticization. At high temperature, polymer matrix cross-linked and resulted in a reduced segmental mobility of polymer chains, thereby suppresses plasticization. Kita et al. [61] studied the cross-linking of polyimides containing benzophenone using UV radiation. It was observed that duration of irradiation has a direct influence on the performance of membranes. The selectivity of gas pair showed improvement at the cost of reduced permeability, presumably due to densification of the membrane structure.

Polymer blending is another possibility to modify polymer properties. Kapantaidakis et al. prepare membranes with Matrimid®/PSF and observed a delay in plasticization pressure with increasing PSF fraction [62]. In another study, Bos and co-workers blended Matrimid with polysulfone and the co-polyimide P84 to improve membrane plasticization resistance [63-64]. The resulting membranes showed excellent resistance against plasticization at the cost of drop in permeability. Despite of excellent plasticization resistance of these above mentioned treated (chemically, thermally and UV cross-linked or blended) membranes their resulting transport properties lie significantly below the state of the art performance for polymers [49].

2. Materials and methods

2.1. Materials

In our experiments, Benzene-1,3,5–tricarbaldehyde (TCA) (98%, Manchester Organics Ltd) , [(2,2`ethylene dioxide) bis(ethylamine)) / DEG] and (4,7,10-trioxa-1,13-tridecanediamine) / TEG] were used to make the polymeric membranes. TCA was used as the core connectors of the membrane structures. [(2,2(ethylene dioxide) bis(ethylamine))] and (4,7,10-trioxa-1,13-tridecanediamine)] were used as monomers and purchased from Sigma, Aldrich. All the products were used original as purchased without modifications. For all the solutions, Acetonitrile and N-Methyl-2-pyrrolidone (NMP) were used as a solvent and purchased from Sigma, Aldrich.

2.2. The synthesis of the polymeric materials

The polymeric materials have been prepared by using condensation polymerization between one of main subtracts [DEG] or [TEG] with [Benzen-1,3,5-tricarbaldehyde / TCA]. TCA was used as the core connector of the prepared polymeric membrane. The cross-linking degree will be varied by changing the molar fraction of [DEG] or [TEG], while the molar fraction of [TCA] reactant is held constant. The structures and stability of the synthesized polymer membranes are confirmed by (^{1}HNMR) analysis BRUKER NMR AVANCE 300MHz spectrophotometer.

The procedures for synthesizing the polymeric membranes are summarized as the following:

1. Weigh the suitable amount of reactant substances according to the above table.
2. Dissolve the reactant substances in 50 ml of Acetonitrile or N-Methyl-2-pyrrolidone (NMP) solvent.
3. Place the dissolved reactants in 100 ml rounded flask and then reflux it at 70ºC with stirring the reaction mixture around 450 rpm.
4. Keep the reactions running until it is completed, this is recognized by ^{1}HNMR instrumental analysis.

5. Use the rotary evaporator at 40ºC and 200 rpm to decrease the amount of used solvent.
6. Casting the resulting polymeric materials by putting it in a Teflon plate, then place it inside the oven at 60ºC and 120ºC overnight, sometime it need more time (2 days).
7. Removing the synthesized membranes carefully from the Teflon plates to obtain solid dense polymeric membranes.

2.3. The chemical structures of the polymeric materials

(Fig.5) and (Fig.6) represent the chemical structure of the prepared polymeric membranes that have been used for the gas separation.

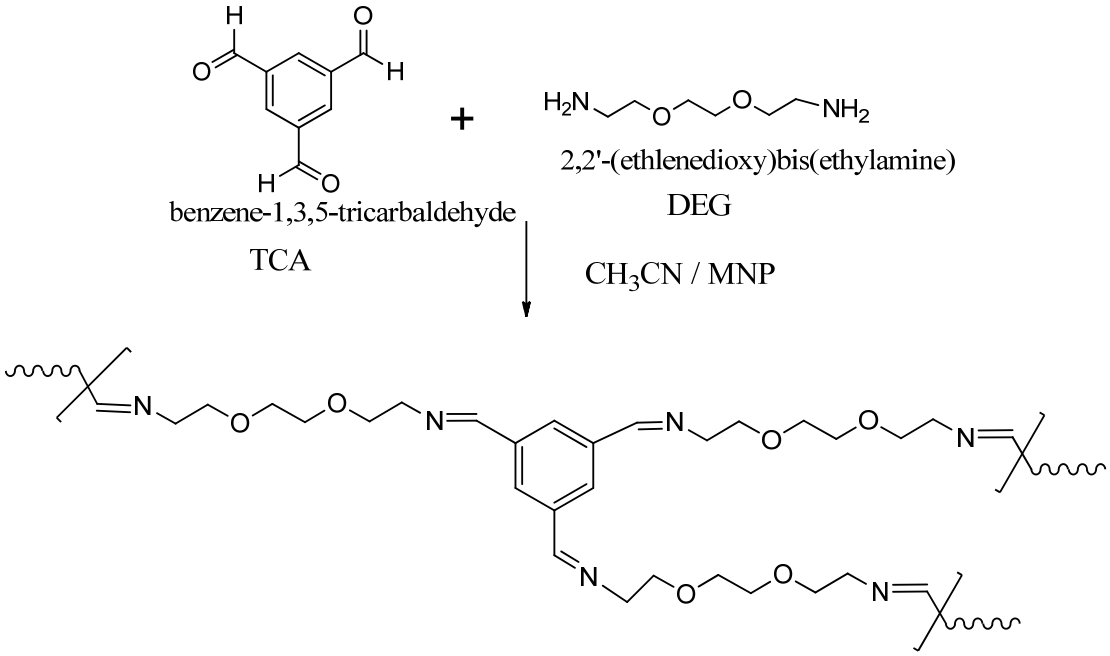

Fig.5: The chemical structure of the (M1-DEG-in Acetonitrile solvent) and (M2-DEG-(in NMP solvent).

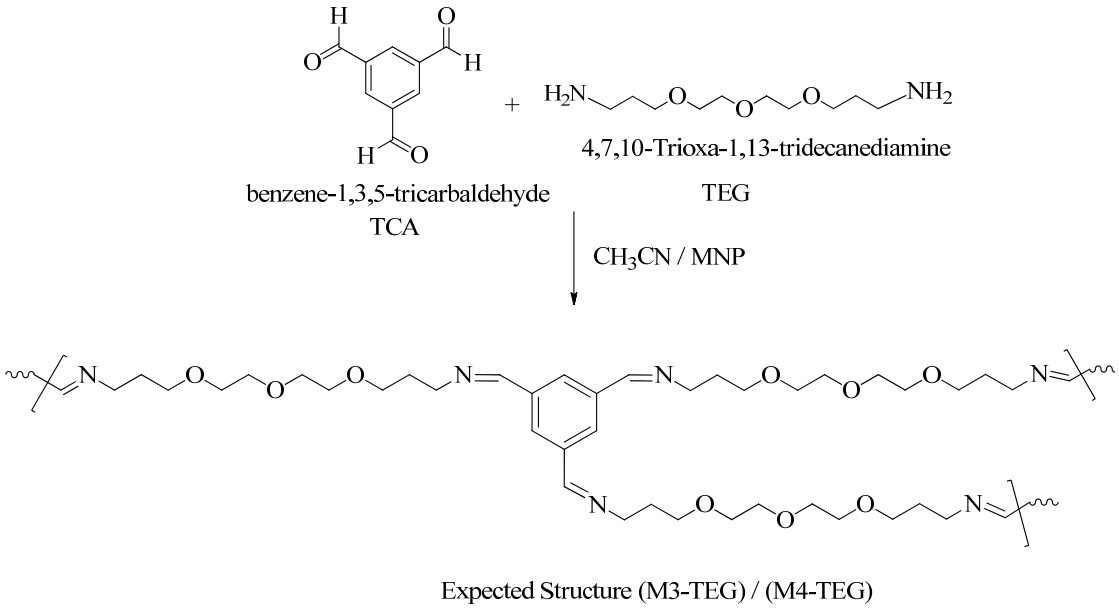

Fig.6: The chemical structure of the (M3-DEG-in Acetonitrile solvent) and (M4-DEG-(in NMP solvent).

2.4. Characterization of the polymeric membranes

The used polymeric membranes for gas separation have been synthesized by reflux method, then it casted in a Teflon plate inside the oven at 60ºC overnight. After the membranes were dried at room temperature, the membrane materials were characterized by the following techniques: (^{1}HNMR) analysis (BRUKER NMR AVANCE 300MHz spectrophotometer) and FTIR Spectrometer (model Nicolet 710), these techniques used to give information about the chemical structure of the polymeric membranes. Thermogravimetric analysis (Hi-Res TGA 2950,TA Instruments) and Differential Scanning Calorimetry (DSC 2920Modulated DSC, TA Instruments), were used to give information about the thermal-stability. The contact angle analysis was used to give information about the hydrophobicity of membranes. In additional too the scanning electron microscopy (SEM) (a Hitachi S4800 Field effect microscope detector) allowed the thickness and the quality of the active deposited layer to be determined. The principles of the used characterization techniques are mentioned before in (chapter (2), section (2.4)).

2.5. Gases tested

The gases used in the experiments were nitrogen (industrial grade (99.99%), Praxair, USA), methane (industrial grade (99.5%), Praxair, USA) and carbon dioxide (high-purity grade (99.998%), Praxair, USA).

2.5.1. Pure gas permeability experiments

Gas permeability experiments were carried out for CO_2, N_2, and CH_4 using the experimental setup shown in (Fig.7). This setup is composed by two identical compartments (feed and permeate), made of stainless steel separated by the polymeric membranes (effective area of 9.62 cm^2). Both compartments were pressurized with the pure gas, and after opening the permeate outlet, a pressure difference of about 0.7 bar was imposed. The pressure evolvement in each compartment along time was monitored using two pressure transducers (Druck, PDCR 910 models 99166 and 991675, England). Permeability measurements were performed at 30ºC the. The membrane thickness was measured using a Elcometer® 124 Thickness Gauge (United kingdom) and the membrane weight using an analytical balance (Kern & Sohn GmnH ABJ 220-4M) before and after each gas permeation experiment, in order to evaluate the weight loss of these membranes.

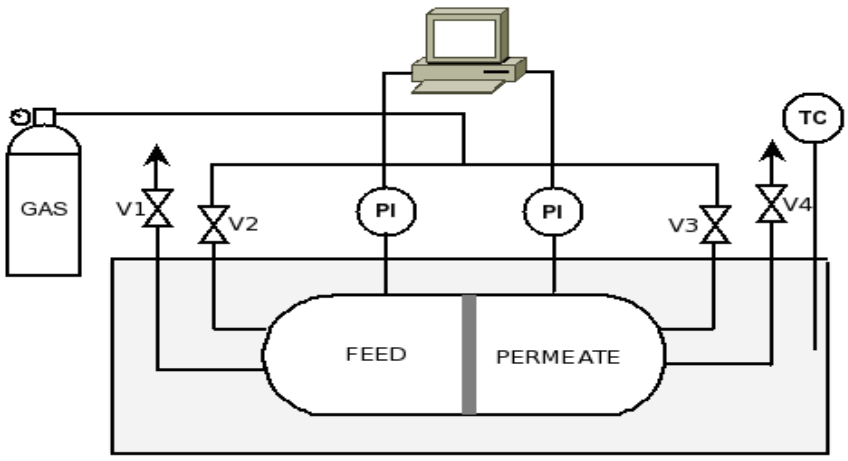

Fig. 7: Experimental set-up for measuring the pure gas permeability of the polymeric membranes: V1, V4 are inlet valves; V2, V3 are exhaust valves; PI1, PI2 are the pressure transducers; TC-Temperature controller, the whole setup is placed in a thermostatic water bath [65-66].

2.5.2. Theory

Gas permeability and ideal selectivity of the polymeric membranes

The permeability of a pure gas through the supported liquid membrane is calculated from the pressure data obtained from both compartments (feed and permeate) shown in (Fig.7) according to the following Eq. (10) [67].

$$\frac{1}{\beta}\ln\left(\frac{[P_{feed}-P_{perm}]_0}{[P_{feed}-P_{perm}]}\right)=P\frac{t}{l} \qquad (10)$$

Where P_{feed} and P_{perm} correspond respectively to the pressure in feed and permeate compartment (bar), P is the membrane permeability (m^2/s), t is the time (s), l is the membrane thickness (m), and β (m^{-1}) is a parameter characteristic of the geometry of the cell, given by:

$$\beta = A\left(\frac{1}{V_{feed}}+\frac{1}{V_{perm}}\right) \qquad (11)$$

Where A is the membrane area (m^2), V_{feed} and V_{perm} are the volumes of the feed and permeate compartments (m^3), respectively. The data can be plotted as $\frac{1}{\beta}\ln\left(\frac{\Delta P_0}{\Delta P}\right)$ versus $\frac{t}{l}$, where the slope of this representation corresponds to the gas permeability.

The ideal selectivity ($\alpha_{A/B}$) can be determined by dividing the permeabilities of two different pure gases (A and B), and can also be expressed by the solubility (S) and diffusivity (D) contributions

$$\alpha_{A/B} = \frac{P_A}{P_B} = \frac{S_A D_A}{S_B D_B} \qquad (12)$$

3. Results and discussion

3.1. Characterization of the polymeric membranes

The polymeric membranes that used for gas separation have been characterized before testing the gas permeability and the obtained results from the characterization techniques are summarized below as the following:

3.1.1. Scanning electron microscopy (SEM) measurements

Fig.8 and Fig.9 represent the Scanning electron microscopy (SEM) measurements for the used polymeric membranes, the cross section view and top view, allowed the thickness of the membranes, and the quality of the active deposited layer to be determined. The figures show that all membranes were found dense and nonporous and two layers were found one was smooth and other is wavy.

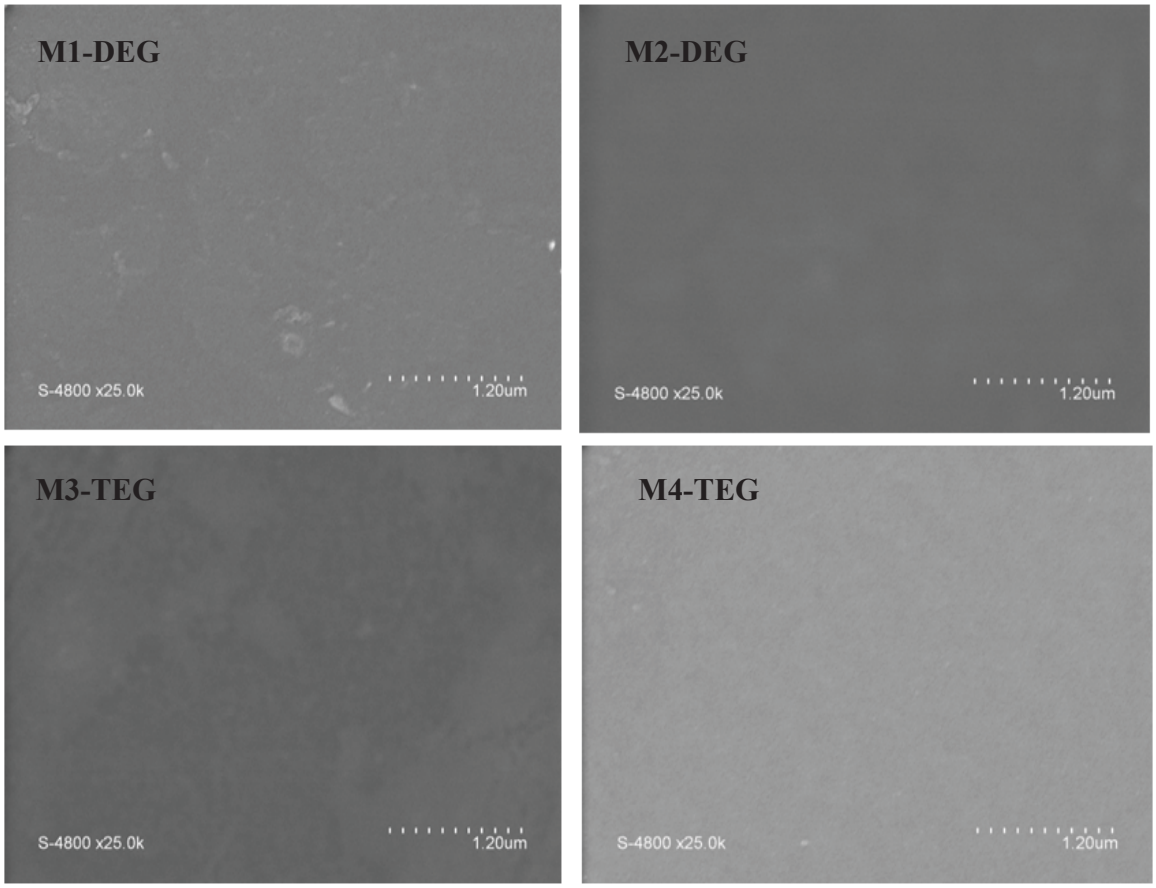

Fig.8: SEM images of the polymeric membranes (surface view).

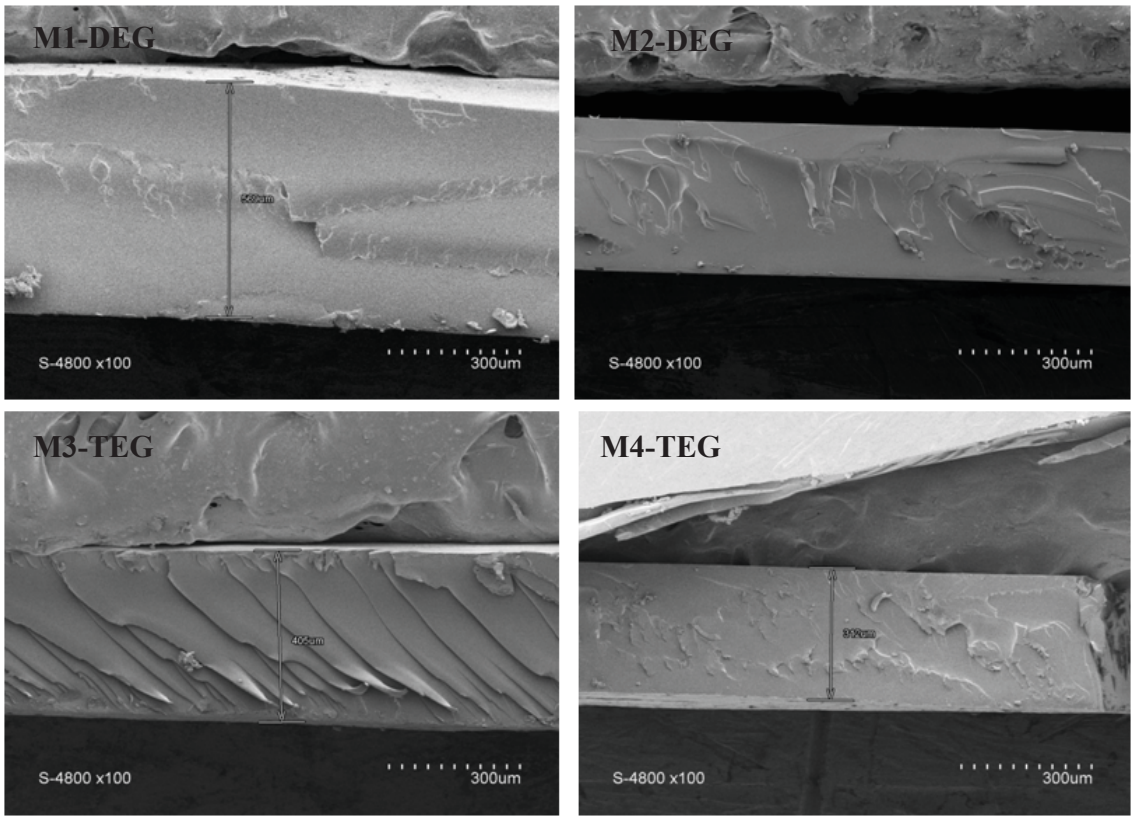

Fig.9: SEM images of the polymeric membranes (cross section view).

3.1.2. FTIR spectroscopy measurements

This is a technique that provides structural information based on the nature of existing bonds in the structure of organic compounds or inorganic materials. It is based on absorption of infrared radiation leads to linear and angular vibration molecular bonds. The modes of vibration associated with certain functional groups give rise to absorption bands which extend in specific regions; also the exact position of the absorption frequency reveals additional information about the group's environment. The composition of the obtained polymeric membranes was determined qualitatively by FTIR Spectroscopy on the basis of the following characteristic bands illustrated in the table (3). Moreover, (Fig.17) and (Fig.18) represent the FTIR spectra of the used polymeric membranes for gas separation; the figures gave good information about the structure of these prepared polymeric membranes. See the Appendix (6.1) for the FTIR spectra for the used polymeric membranes (Fig.17) and (Fig.18).

Table (3): FTIR Spectroscopy of the prepared polymer membranes.

M1-DEG	M2-DEG	M3-TEG	M4-TEG	Band peak
3422.8 cm^{-1}	3410.3 cm^{-1}	3427.5 cm^{-1}	3454.9 cm^{-1}	N-H band (medium, stretching, amine)
2863.2 cm^{-1}	2872.7 cm^{-1}	2857.7 cm^{-1}	2857.7 cm^{-1}	C-H band (medium, stretching, aldehyde)
2323.6 cm^{-1}	2327.6 cm^{-1}	2326.3 cm^{-1}	2320.8 cm^{-1}	C-H band (weak, bending, aromatic)
1666.2 cm^{-1}	1672.5 cm^{-1}	1644.2 cm^{-1}	1636.0 cm^{-1}	C=N band (medium, stretching, Imine)
1466.2 cm^{-1}	1462.5 cm^{-1}	1438.8 cm^{-1}	1455.2 cm^{-1}	C-H band (medium, bend, aromatic)
1356.6 cm^{-1}	1347.5 cm^{-1}	1332.0 cm^{-1}	1351.1 cm^{-1}	C-N (medium, stretching, amine)
1097.0 cm^{-1}	1095.0 cm^{-1}	1112.8 cm^{-1}	1099.1 cm^{-1}	C-O band (strong, stretching, ether)
926.6 cm^{-1}	909.9 cm^{-1}	970.4 cm^{-1}	973.1 cm^{-1}	C=C band (strong, bending, alkene)

3.1.3. ^{1}HNMR spectroscopy measurements

The composition of the polymeric membranes that used for gas separation was determined by ^{1}HNMR spectroscopy on the basis of the characteristic bands that appeared in the spectra of polymeric materials are illustrated in (Fig.10). The spectra were recorded on a Bruker instrument operated at 300 MHz. All samples were dissolved in $CDCl_3$ and analyzed at room temperature. The chemical shifts were recorded in ppm as shown in (Fig.10). See the Appendix (6.2) for the ^{1}HNMR spectra for the used membranes.

The assignments of the signals in the NMR spectra (Fig.10) are the following:

- The peaks at 9.75 ppm are attributed to unreacted bis-aldehyde and monoaldehyde groups in agreement with the mono-imine and di-imine peaks, respectively, observed at 8.5-8.7 ppm.
- On the addition of DEG and TEG we observe two kind of imine C<u>H</u>=N protons at 8.5 ppm attributed to PEG-N=C<u>H</u> protons and at 8.1 ppm attributed to PEG-N=CH protons
- The peaks between 8.5-7.75 ppm correspond thus to the aromatic protons of BTC with variable imino-subtitution degrees.
- The aliphatic region of spectra we may identify the methylene protons of PEGs.

- Once the PEG is added the spectra become broad probably due to specific encapsulation of aromatic residues within a highly charged shell of PEG.

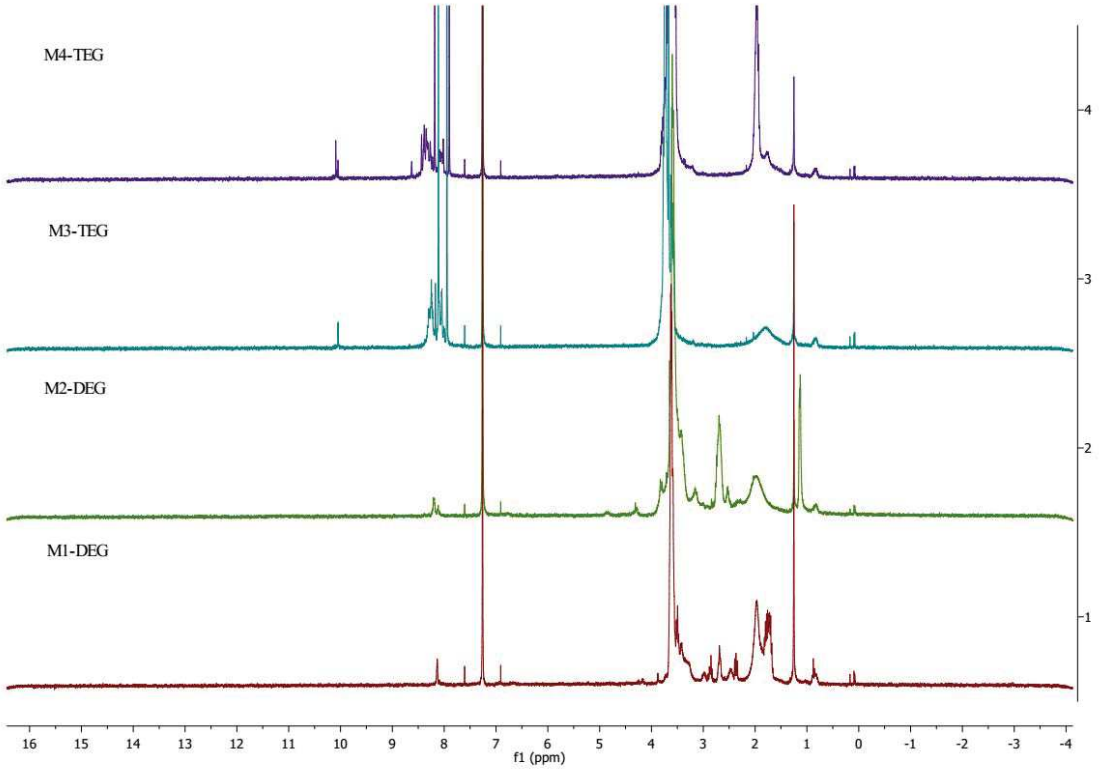

Fig.10: The ^{1}HNMR spectra for the used polymeric membranes for gas separation.

3.1.4. TGA measurements

The TGA measurements were performed to the used membranes [(M1-DEG), (M2-DEG), (M3-TEG), and (M4-TEG)] for gas separation. The obtained (TGA) values for membranes are represented in (Fig.11). As shown in the figures, the higher thermal stability observed in case of polymeric membranes that contain (TEG) substrate than others that contain (DEG) substrate, this might indicate that the presence of (TEG) substrate inside the polymeric structure increase the cross linking and glassy properties of the polymeric materials when compared with other membranes that contain (DEG) substrate inside the polymeric structures. See the Appendix (6.3) for the TGA spectra for the used membranes.

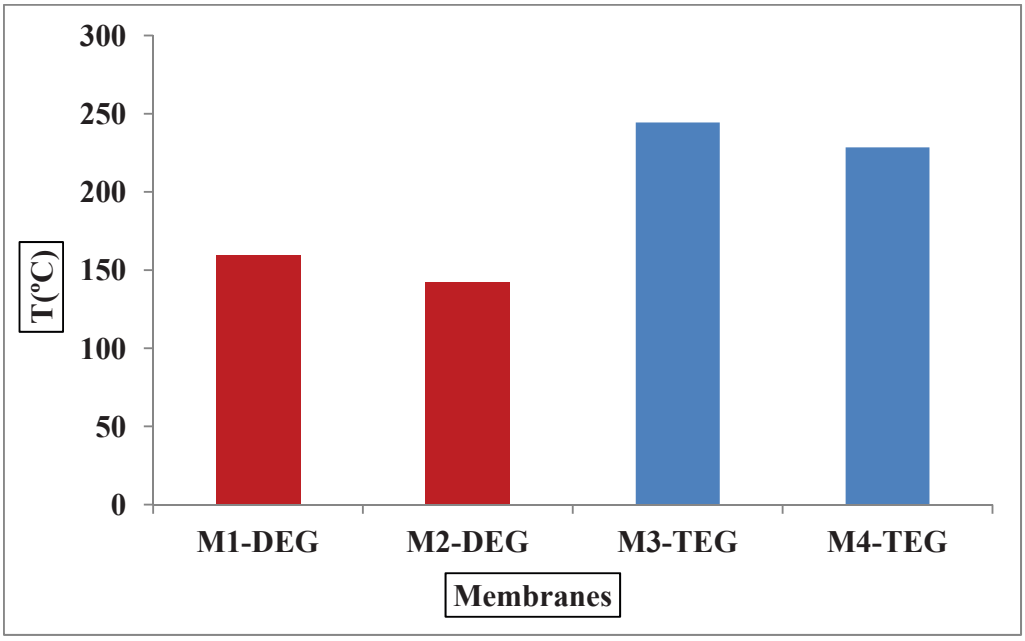

Fig.11: TGA measurements of the used polymeric membranes for gas separation.

3.1.5. DSC measurements

The DSC measurements were performed to the used membranes [(M1-DEG), (M2-DEG), (M3-TEG), and (M4-TEG)] for gas separation. The obtained (DSC) values for membranes are represented in (Fig.12). As shown in the figures, the higher glass transition temperatures (Tg) values were observed in case of polymeric membranes [(M3-TEG) and (M4-TEG)] that contain (TEG) substrate than others that contain (DEG) substrate, this might indicate that the using of long chain (TEG) substrate instead of (DEG) substrate within the chemical composition of the polymeric membranes increase the cross linking and thermal stability properties of the polymeric materials when compared with other membranes that contain (DEG) substrate inside the polymeric structures. See the Appendix (6.4) for the DSC spectra for the used membranes.

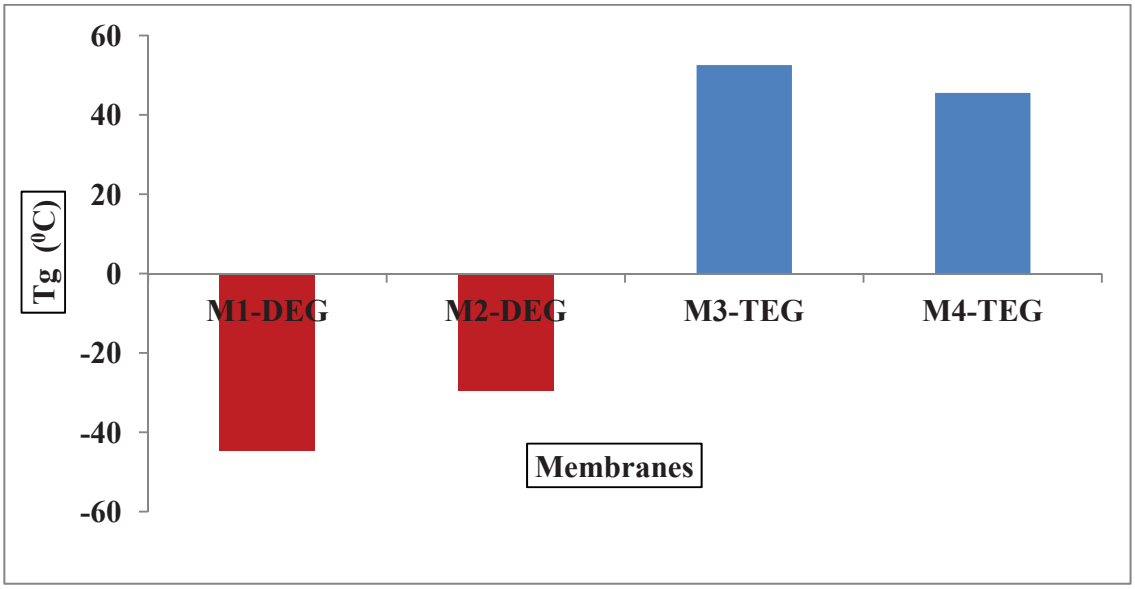

Fig.12: DSC Values of the used polymeric membranes for gas separation.

3.1.6. Contact angel measurements

Surface properties of a membrane give information about its hydrophobicity. The contact angle increases with increasing surface hydrophobicity. This can help better understand the kinetic interaction of the gases with the membrane surface. The measurements on the contact angle of the polymeric membranes were carried out on all the used polymeric membranes in order to explain the effect of hydrophobic character of the used membranes for the permeability and selectivity of the used gases through the membranes. The contact angle was measured using the software called Imagej method. In this method, the contact angle of the used membranes was measured using a drop of water on the membrane, then using the pictures taken by the camera, the contact angle was measured before the transportation of the gases, then the contact angle was used for comparison between the used membranes for gas permeability through the membranes. Fig.13 and Fig.14 are represented the contact angle measurements for the used polymeric membrane before the transportation of gases through the membranes. It is clear from the figure that the used membranes materials have partially hydrophobic and symmetrical characters as the left and right contact angle are almost equal. In additional to the hydrophobic character of the used membranes that contain (TEG) substrate is higher than the polymeric membranes that contain (DEG) substrate, this might indicate that the presence of (TEG) substrate

inside the polymeric structure increases the cross linking and hydrophobic properties of the polymeric materials. See the Appendix (6.5) for the contact angles measurements for the used membranes.

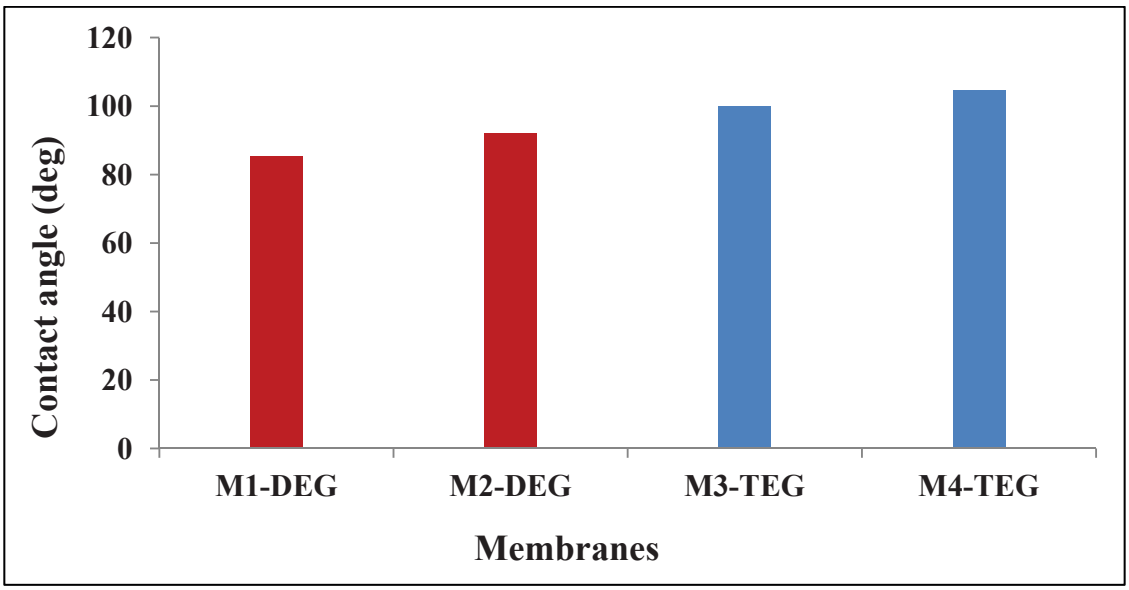

Fig.13: Contact angles measurements for the used polymeric membranes for gas separation.

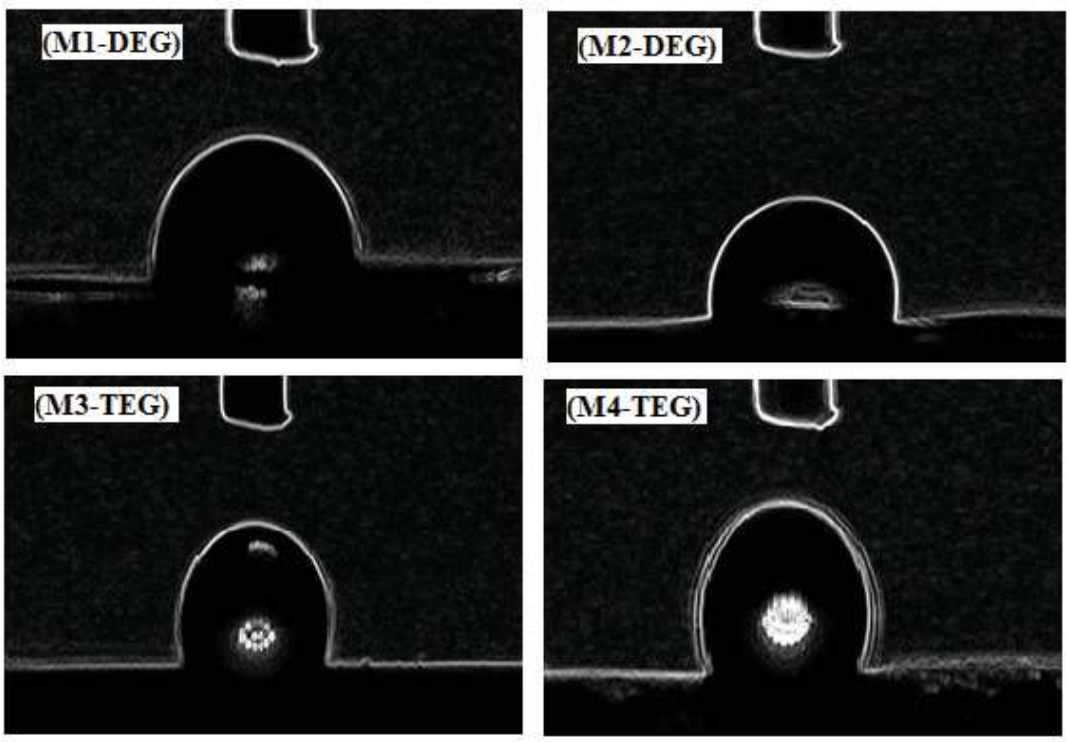

Fig.14: Contact angle for the used polymeric membranes for gas separation.

3.2. Gas permeability and selectivity through the polymeric membranes

3.2.1. The permeability of (CO_2, N_2 and CH_4) gases

The permeability of (CO_2, N_2 and CH_4) gases through the used polymeric membranes was measured; the experiments were carried out at (30ºC). The membranes were weighed before and after the experiment to check the loss in membranes weight. There is no weight loss obtained for all membranes tested. This gave indicate that these membranes retained stable at the tested temperature (30ºC) and tested pressure difference of 0.7 bar. As previously mentioned all permeability values were calculated according to Eq. (10), taking into account the pressure data from the feed and permeate compartments, the thickness of the membrane and the geometry of the cell used.

The permeability of the selected gases (CO_2, N_2, and CH_4) through the used polymeric membranes obtained is represented in table (4). As it can be observed, the permeability of CO_2 is higher than other used gases (N_2 and CH_4) for the polymeric membranes. Additionally, it can be observed that, the CO_2 permeability through polymeric membranes that contain (DEG) substrate material for synthesizing the membranes are higher than other membranes that have (TEG) substrate material. This might be related to the hydrophobic and rubbery behaviors of the (TCA-DEG) membranes comparing with (TCA-TEG) membranes, which effect on the morphological structure, then the permeability of the gases through the polymeric membranes. Moreover, the table showed that, the permeability of CO_2 through the used membranes arranged as the following: M2-DEG (in NMP solvent) > M1-DEG (in Acetonitrile solvent) > M4-TEG (in NMP solvent) > M3-TEG (in Acetonitrile solvent). The same behavior has been occurred in case of permeability of other gases (N_2 and CH_4) through the used polymeric membranes, but there is no much difference between (N_2 and CH_4) gases permeabilities through the used polymeric membranes. In case of comparing the permeabilities of used gases (CO_2) and (N_2, and CH_4) through the same polymeric membranes, it is clear that the permeability of CO_2 gas > N_2 gas > CH_4 gas. This might related to the polarity behaviour of CO_2 gas comparing with other non-polar gases (N_2, CH_4), this might help to accelerate the diffusion and permeability of CO_2 through the used polymeric membranes.

Moreover, the kinetic diffusion diameter of gases effect on the permeability through the dense membranes, as the kinetic diffusion diameter (Å) of used gases are the following (CO_2 = 3.325) < (N_2 = 3.568) < (CH_4 = 3.817), this might give an indication about the permeabilities of gases through the used polymeric membranes are arranged as the following (CO_2 gas) > (N_2 gas) > (CH_4 gas).

Table (4): The permeability of (CO_2, N_2, and CH_4) through the tested membranes.

Membranes	Permeability (m^2/sec) x10^{-11}			Permeability (Barrer)		
	P_{CO2}	P_{N2}	P_{CH4}	P_{CO2}	P_{N2}	P_{CH4}
M1-DEG	6.12	0.295	0.221	73.73	3.55	2.66
M2-DEG	6.62	0.245	0.211	79.76	2.95	2.54
M3-TEG	2.95	0.231	0.191	35.54	2.78	2.30
M4-TEG	3.72	0.262	0.218	44.82	3.16	2.63

3.2.2. Ideal selectivities for gases

Table (5) showed the ideal selectivities obtained for the membranes tested at 30 ^{0}C. The ideal selectivity was calculated taking into account the ratio of the permeabilities measured for pure gases (Eq. (10)). It was observed that the selectivity of polymeric membranes towards CO_2 was higher than other tested gases (N_2 and CH_4). Additionally, the ideal selectivity is much higher for polymeric membranes contain (DEG) substrate when compared with other polymeric membranes that contain (TEG) substrate. Moreover, table (5) shows that the selectivities for the used polymeric membranes are increasing as the following: M2-DEG (in NMP solvent) > M1-DEG (in Acetonitrile solvent) > M4-DEG (in NMP solvent) > M3-TEG (in Acetonitrile solvent). This might relate to the increasing in the permeability of (CO_2) gas through the polymeric membranes comparing with other gases (N_2) and (CH_4). In additional to the increasing in the rubbery and hydrophilic behaviour of the polymeric membranes that contain (DEG) substrate when compared with other polymeric membranes contains (TEG) substrate.

The (TGA) and (DSC) analysis gave indication about the rubbery properties of the used polymeric membranes, see sections (3.1.4) and (3.1.5). Moreover the contact angle measurements gave information about the hydrophobic/ hydrophilic behavior of the used polymeric membranes, see section (3.1.6).

Table (5): (CO_2/N_2) and (CO_2/CH_4) ideal selectivities of the tested membranes.

Membranes	Ideal selectivity α (CO_2/N_2)	Ideal selectivity α (CO_2/CH_4)
M1-DEG	20.75	27.69
M2-DEG	27.02	31.37
M3-TEG	12.77	15.45
M4-TEG	14.20	17.06

3.2.3. The Robeson Upper bound correlation

In order to compare the ideal selectivities obtained in this work with data available in the literature, the (CO_2/N_2) and (CO_2/CH_4) selectivities as a function of the CO_2 permeability at 30ºC is represented in (Fig.15) and (Fig.16). These upper bound correlations were obtained by Robeson et al. [49, 68] from literature data. Each one of the lines represented corresponds to the Robeson's upper bound for the specific temperature (30ºC) while data points correspond to experimental values obtained in this work. Therefore, data points above this line may be considered as an improvement over the results published so far. It is observed that the results obtained in this work are generally below the upper bound lines at 30ºC. Moreover, the results obtained by using the polymeric membranes that contain [DEG] substrate are closer from the lines and higher than the values obtained in case of using the polymeric membranes, that contain [TEG] substrate . In additional too, the used membranes tested in this work are stable at the (30ºC) for a pressure difference of (0.7 bar), and they are selective towards CO_2 when compared with (N_2) and (CH_4) gases, also when compared with other membrane materials in the literature their selectivity is lower.

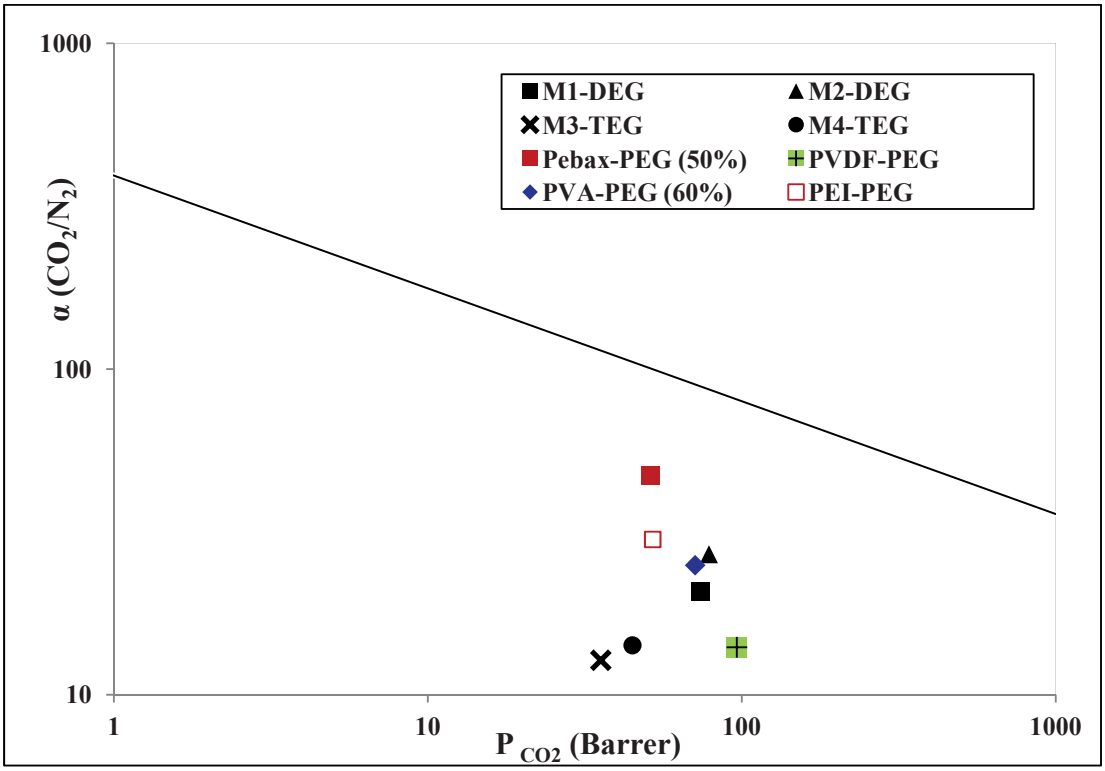

Fig.15: Robeson plot for (CO_2/N_2) with results from the current work.

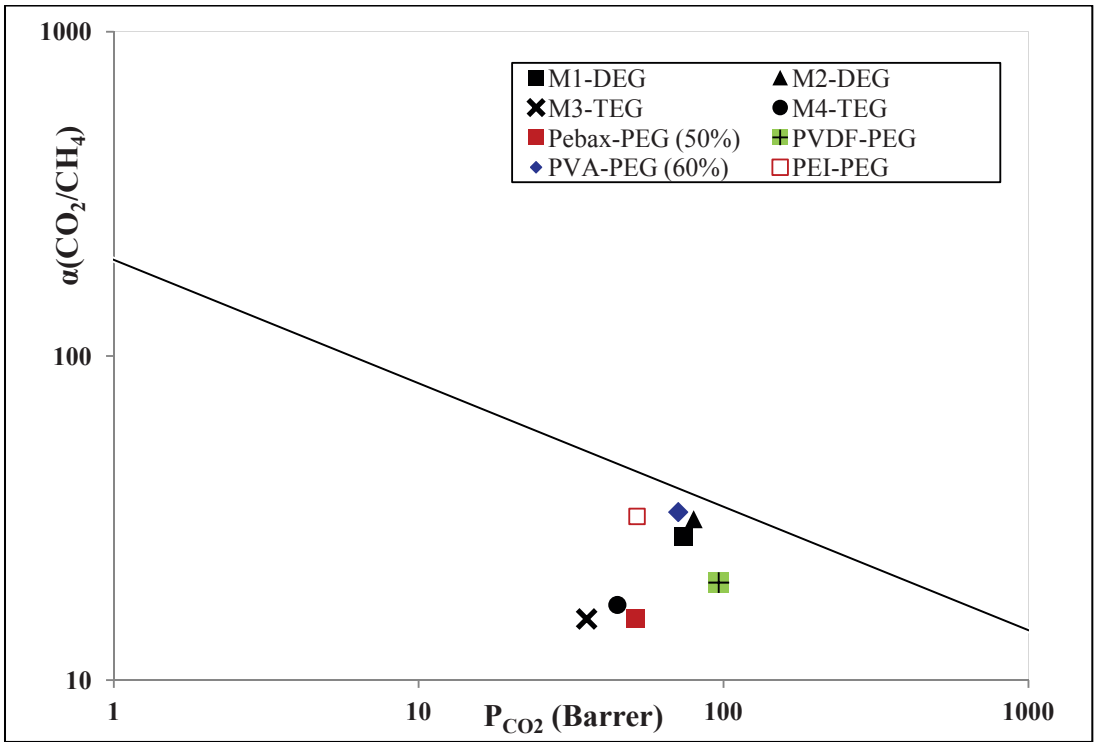

Fig.16: Robeson plot for (CO_2/ CH_4) with results from the current work.

4. Conclusion

The approach proposed in this research work consists on the synthesis and characterization of dense polymeric membranes for gas separation application. Firstly the different polymeric membranes were synthesized by condensation polymerization between one of main subtracts [(2,2`ethylene dioxide) bis(ethylamine)) / DEG] and (4,7,10-trioxa-1,13-tridecanediamine) / TEG] with [Benzene-1,3,5-tricarbaldehyde / TCA]. The resulting polymer membranes were characterized spectrometry by (FTIR,^{1}HNMR), their thermal stability were characterized by (TGA and DSC), and the morphological structure was characterized by (SEM and contact angle). The gas permeability measurements for the tested polymeric membranes showed that the permeability of CO_2 is higher than other used gases (N_2 and CH_4) for the polymeric membranes. This might related to the polarity behaviour of CO_2 gas comparing with other non-polar gases (N_2, CH_4), this might help to accelerate the diffusion and permeability of CO_2 through the used polymeric membranes. Moreover, the kinetic diffusion diameter of gases effect on the permeability through the dense membranes, as the kinetic diffusion diameter (Å) of used gases are the following (CO_2 = 3.325) < (N_2 = 3.568) < (CH4 = 3.817), this might give an indication about the permeabilities of gases through the used polymeric membranes are arranged as the following (CO_2 gas) > (N_2 gas) > (CH_4 gas).

Additionally, it is observed that the CO_2 permeability and the ideal selectivity through the tested polymeric membranes that contain (DEG) substrate material within the membrane polymeric structures are higher than other polymeric membranes that have (TEG) substrate material. This might relate to the increment in the hydrophilic and rubbery behaviors of the (TCA-DEG) membranes comparing with (TCA-TEG) membranes, which effect on the morphological structure and the permeability of the gases through the polymeric membranes. Moreover, the permeability and ideal selectivity of CO_2 through the used polymeric membranes are arranged as the following [M2-DEG (in NMP solvent) > M1-DEG (in Acetonitrile solvent) > M4-TEG (in NMP solvent) > M3-TEG (in Acetonitrile solvent)] as shown in tables (4 and 5).

Generally, the tested polymeric membranes in this research work are stable at the (30ºC) for a pressure difference of (0.7 bar), and they are selective towards CO_2 when compared with (N_2) and (CH_4) gases, also when compared with other polymeric membrane materials in the literature their selectivity is lower than the common used polymeric membranes for CO_2 permeability. Finally, thanks to the possibility to combine the structural and functional features of different monomers, the heteropolymeric membrane materials can exhibit very different properties from their original homopolymeric components. In the above-developed examples, this strategy revealed itself to be a versatile way for the synthesis of new membranes presenting different permeabilities and preserving their selectivity towards gas separation application.

5. References

[1] J.T. Houghton, "Climate Change 2001: The Scientific Basis", Cambridge University Press, Cambridge, 2001.
[2] J.J. Mc Carthy, O.F. Canziani, N.A. Leary, D.J. Dokken, K.S. White, "Climate Change 2001: Impacts, Adaptation, and Vulnerability", Cambridge University Press, Cambridge, 2001.
[3] S. Pacala, R. Socolow, "Stabilization wedges: solving the climate problem for the next 50 years with current technologies", Science, 305 (2004) 968-972.
[4] T. Graham, "On the law of the diffusion of gases", J. Membr. Sci., 100 (1995)17.
[5] T. Graham, "Notice of the singular inflation of a bladder", J. Membr. Sci., 100 (1995)9.
[6] R.W. Baker, "Future directions of membrane gas separation technology", Ind. Eng. Chem. Res., 41 (2002) 1393.
[7] W.J. Koros, "Gas separation membranes: needs for combined materials science and processing approaches", Macromol. Symp., 188 (2002) 13.
[8] G. Maier, "Gas separation with polymer membranes", Angew. Chem. Int. Ed., 37 (1998) 2960.
[9] S. A. Stern, "Polymers for gas separations: the next decade", J. Membr. Sci., 94 (1994) 1.
[10] D.R. Paul, Y.P. Yampol'skii, "Polymeric Gas Separation Membranes", CRC Press, Boca Raton, 1994.
[11] W.J. Koros, G.K. Fleming, Membrane-based gas separation, J. Membr. Sci. 83 (1993) 1.
[12] B.D. Freeman, I. Pinnau, "Polymeric materials for gas separations", ACS Symp. Ser. 733 (1999) 1.
[13] M. Langsam, "Polyimides for gas separation", Plastics Eng., 36 (1996) 697.
[14] W.J. Koros, R. Mahajan, "Pushing the limits on possibilities for large scale gas separation: which strategies", J. Membr. Sci., 175 (2000) 181.
[15] N.N. Li, A.G. Fane, W.S.W. Ho, T. Matsuura, "Advanced membrane technology and applications", John Wiley & Sons, Inc., 2008.
[16] V. Stannett, "The transport of gases in synthetic polymeric membranes-an historic Perspective", J. Membr. Sci., 3 (1978) 97-115.
[17] M. Smaihi, T. Jermoumi, J. Marignan, R.D. Noble, "Organic-inorganic gas separation membranes: Preparation and characterization", J. Membr. Sci., 116 (1996) 211-220.
[18] G. Dong, H. Li, V. Chen, "Challenges and opportunities for mixed-matrix membranes for gas separation", J. Mater. Chem. A, 1 (2013) 4610-4630.
[19] P. S. Goh, A. F. Ismail, S. M. Sanip, B.C. Ng, M. Aziz, "Recent advances of inorganic fillers in mixed matrix membrane for gas separation, Sep. Purif. Technol., 81 (2011) 243-264.
[20] A. Brunetti, F. Scura, G. Barbieri, E. Drioli, "Membrane technologies for CO_2 Separation", J. Membr. Sci., 359 (2010) 115-125.
[21] R. Mahajan, D.Q. Vu, W.J. Koros, "Mixed matrix membrane materials: An answer to the challenges faced by membrane based gas separations today?", J. Chin. Inst. Chem. Eng., 33 (2002) 77-86.

[22] W.J. Koros, G.K. Fleming, S.M. Jordan, T.H. Kim, H.H. Hoehn, "Polymeric membrane materials for solution-diffusion based permeation separations", Prog. Polym. Sci., 13 (1988) 339-401.
[23] L.M. Robeson, "Polymer membranes for gas separation", Curr. Opin. Solid State Mater. Sci., 4 (1999) 549-552.
[24] Energy information administration, US department of energy, International energy outlook (2013).
[25] S.A. Rackley, "Carbon Capture and Storage", Elsevier, (2010).
[26] E. D. Bates, R. D. Mayton, I. Ntai, J. H. Davis, "CO_2 capture by a task-specific ionic Liquid", J. Am. Chem. Soc., 124 (2002) 926-927.
[27] S. Ma'mun, V.Y. Dindore, H.F. Svendsen, "Kinetics of the reaction of carbon dioxide with aqueous solutions of 2-((2-Aminoethyl)amino)ethanol", Ind. Eng. Chem. Prod. Res. Dev., 46 (2006) 385-394.
[28] R.W. Baker, "Future directions of membrane gas separation technology", Ind. Eng. Chem. Prod. Res. Dev., 41 (2002) 1393-1411.
[29] K. Ghosal, B. D. Freeman, "Gas separation using polymer membranes: An overview", Polym. Adv. Technol., 5 (1994) 673-697.
[30] R.J. Gardner, R.A. Crane, J.F. Hannan, "Hollow fiber permeator for separating gases", Chem. Eng. Prog. 73 (1977) 76-78.
[31] W.J. Koros, G.K. Fleming, "Membrane-based gas separation", J. Membr. Sci., 83 (1993) 1.
[32] M. Mulder, "Basic principles of membrane technology", Dordrecht: Kluwer Academic Publishers, 1996.
[33] A. Mushtaq , H. Bin Mukhtar, A. M. Shariff, H. Abdul Mannan , "A Review: Development of Polymeric Blend Membrane for Removal of CO_2 from Natural Gas", IJET-IJENS., 13 (2013) 53-60.
[34] K. Scott, "Membrane separation technology", Scientific & Technical Information, Oxford, 1990.
[35] H. Strathmann, "Membrane separation processes: Current relevance and future opportunities", AIChE J., 47 (2001) 1077.
[36] R.W. Spillman, M.B. Sherwin, "Gas separation membranes: The first decade", Chemtech., 20 (1990) 378.
[37] W.J. Koros, "Gas separation in membrane separation systems: Recent developments and future directions", ed. by R.W. Baker, E. L. Cussler, W. Eykamp W. J. Koros, R.L. Riley and H. Strathmann, Noyes Data Corporation, United States of America, (1991) pp. 189-241.
[38] J.-M. Duvala, B. Folkersa, M.H.V. Muldera, G. Desgrandchamps, C.A. Smolders, "Adsorbent filled membranes for gas separation. Part 1. Improvement of the gas separation properties of polymeric membranes by incorporation of microporous adsorbents", J. Member. Sci., 80 (1993) 189-198 .
[39] R. Abedini, A. Nezhadmoghadam, "APPLICATION OF MEMBRANE IN GAS SEPARATION PROCESSES: ITS SUITABILITY AND MECHANISMS.", Pet. Coal., 52 (2010) 69-80.
[40] A. F. Ismail, P. S. Goh, S. M. Sanip, M. Aziz "Transport and separation properties of carbon nanotube-mixed matrix membrane.", Sep. Purif. Technol., 70 (2009)12-26.

[41] J. S. Chiou, D.R. Paul, “Effects of CO_2 exposure on gas transport properties of glassy Polymers", J. Membr. Sci., 32 (1987) 195-205.
[42] S. Kulprathipanja, R.W. Neuzil, N.N. Li, “Separation of gases by means of mixed matrix membranes”, US patent 5127925, (1992).
[43] A. F. Ismail, I. R. Dunkin, S. L. Gallivan, S. J. Shilton, “Production of super selective polysulfone hollow fiber membranes for gas separation”, Polymer, 40 (1999) 6499-6506.
[44] Y. Zhang, J. Sunarso, S. Liu, R. Wang, “Current status and development of membranes for CO_2/CH_4 separation: A review”, Int. J. Greenhouse Gas Control., 12 (2013) 84-107.
[45] Y. Xiao, B.T. Low, S.S. Hosseini, T.S. Chung, D.R. Paul, “The strategies of molecular architecture and modification of polyimide-based membranes for CO_2 removal from natural gas-A review", Prog. Polym. Sci., 34 (2009) 561-580.
[46] R.W. Baker, “Future directions of membrane gas separation technology”, Ind. Eng. Chem. Res., 41 (2002) 1393-1411.
[47] G. Dong, H. Li, V. Chen, “Challenges and opportunities for mixed-matrix membranes for gas separation”, J. Mater. Chem. A, 1 (2013) 4610-4630.
[48] L.M. Robeson, “Correlation of separation factor versus permeability for polymeric Membranes”, J. Membr. Sci., 62 (1991) 165-185.
[49] L. M. Robeson, “The upper bound revisited”, J. Membr. Sci., 320 (2008) 390-400.
[50] H.B. Park, C.H. Jung, Y.M. Lee, A.J. Hill, S.J. Pas, S.T. Mudie, E. Van Wagner, B.D. Freeman, D.J. Cookson, “Polymers with cavities tuned for fast selective transport of small molecules and ions”, Science, 318 (2007) 254-258.
[51] A. Brunetti, F. Scura, G. Barbieri, E. Drioli, “Membrane technologies for CO_2 Separation”, J. Membr. Sci., 359 (2010) 115-125.
[52] A. Bos, I. G. M. Pünt, M. Wessling, H. Strathmann, “Plasticization-resistant glassy polyimide membranes for CO_2/CO_4 separations”, Sep. Purif. Technol., 14 (1998) 27-39.
[53] A.Y. Houde, B. Krishnakumar, S. G. Charati, S. A. Stern, “Permeability of dense (homogeneous) cellulose acetate membranes to methane, carbon dioxide, and their mixtures at elevated pressures”, J. Appl. Polym. Sci., 62 (1996) 2181-2192.
[54] M. D. Donohue, B.S. Minhas, S.Y. Lee, “Permeation behavior of carbon dioxide-methane mixtures in cellulose acetate membranes”, J. Membr. Sci.,42 (1989)197-214.
[55] W. J. Schell, C. D. Houston, W.L. Hopper, Gas Cond. Conf, Norman, University of Oklahoma, 1983.
[56] A. F. Ismail, W. Lorna, “Penetrant-induced plasticization phenomenon in glassy polymers for gas separation membrane”, Sep. Purif. Technol., 27 (2002) 173-194.
[57] C. Zhou, T.-S. Chung, R. Wang, Y. Liu, S.H. Goh, “The accelerated CO_2 plasticization of ultra-thin polyimide films and the effect of surface chemical cross-linking on plasticization and physical aging", J. Membr. Sci., 225 (2003) 125-134.
[58] C. Cao, T.-S. Chung, Y. Liu, R. Wang, K. P. Pramoda, “Chemical cross-linking modification of 6FDA-2,6-DAT hollow fiber membranes for natural gas separation”, J. Membr. Sci., 216 (2003) 257-268.

[59] A.M.W. Hillock, W.J. Koros, "Cross-Linkable Polyimide Membrane for Natural Gas Purification and Carbon Dioxide Plasticization Reduction", Macromolecules, 40 (2007) 583-587.
[60] J. Fang, H. Kita, K.I. Okamoto, "Gas permeation properties of hyperbranched polyimide membranes", J. Membr. Sci., 182 (2001) 245-256.
[61] H. Kita, T. Inada, K. Tanaka, K.-I. Okamoto, "Effect of photocrosslinking on permeability and selectivity of gases through benzophenone- containing polyimide", J. Membr. Sci., 87 (1994) 139-147.
[62] G.C. Kapantaidakis, S.P. Kaldis, X.S. Dabou, G.P. Sakellaropoulos,"Gas permeation through PSF-PI miscible blend membranes", J. Membr. Sci., 110 (1996) 239-247.
[63] A. Bos, I. Punt, H. Strathmann, M. Wessling, "Suppression of gas separation membrane plasticization by homogeneous polymer blending", AlChE J., 47 (2001) 1088-1093.
[64] T.S. Chung, L.Y. Jiang, Y. Li, S. Kulprathipanja, "Mixed matrix membranes (MMMs) comprising organic polymers with dispersed inorganic fillers for gas separation", Prog. Polym. Sci. (Oxford)., 32 (2007) 483-507.
[65] L. A. Neves, J. G. Crespo, I.M. Coelhoso, "Gas permeation studies in supported ionic liquid membranes", J. Membr. Sci., 357 (2010) 160–170.
[66] L. A. Neves, C. Afonso, I. M. Coelhoso, J. G. Crespo, "Integrated CO_2 capture and enzymatic bioconversion in supported ionic liquid membranes", Sep. Purif. Technol., 97 (2012) 34-41
[67] E. L. Cussler, "Diffusion, Mass Transfer in Fluid Systems", third ed., Press Syndicate of the University of Cambridge, Cambridge, 2009.
[68] B. W. Rowe, L. M. Robeson, B. D. Freeman, D. R. Paul, J. Membr. Sci., 360 (2010) 58–69

6. Appendix

6.1. Appendix: FTIR measurements

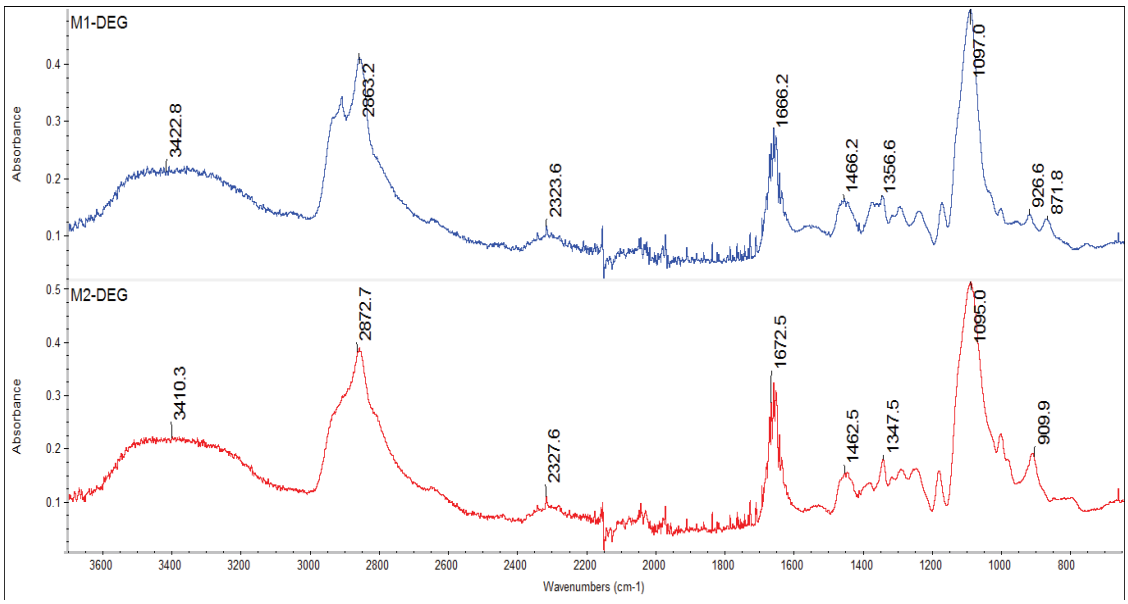

Fig.17: FTIR spectra for the prepared polymeric membranes (M1-DEG) and (M2-DEG).

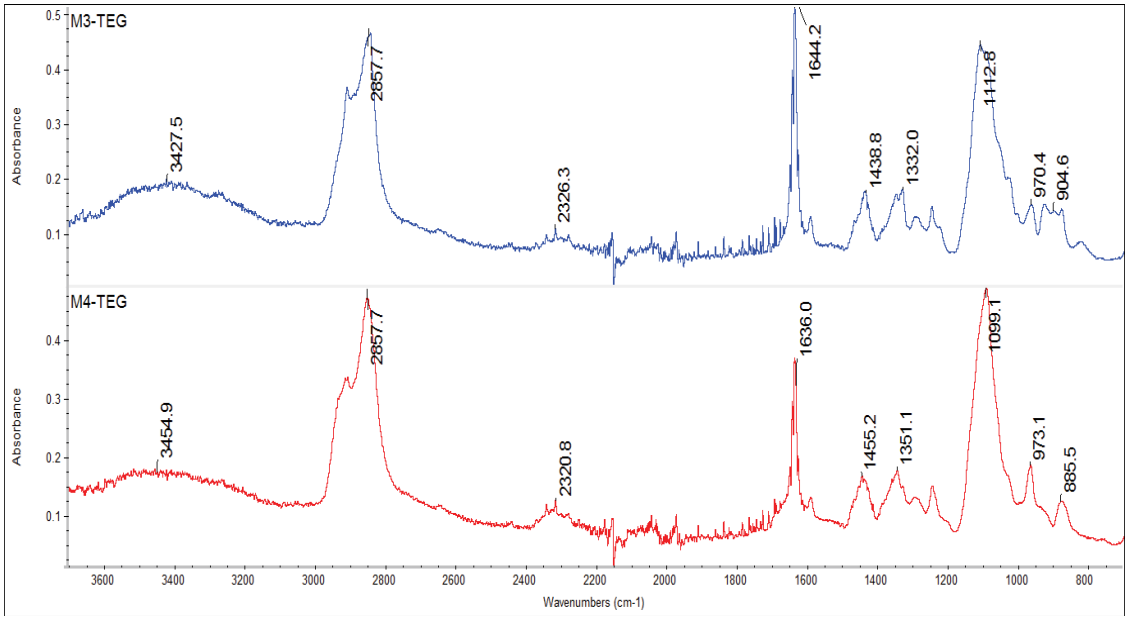

Fig.18: FTIR spectra for the prepared polymeric membranes (M3-TEG) and (M4-TEG).

6.2. Appendix: [1]HNMR measurements

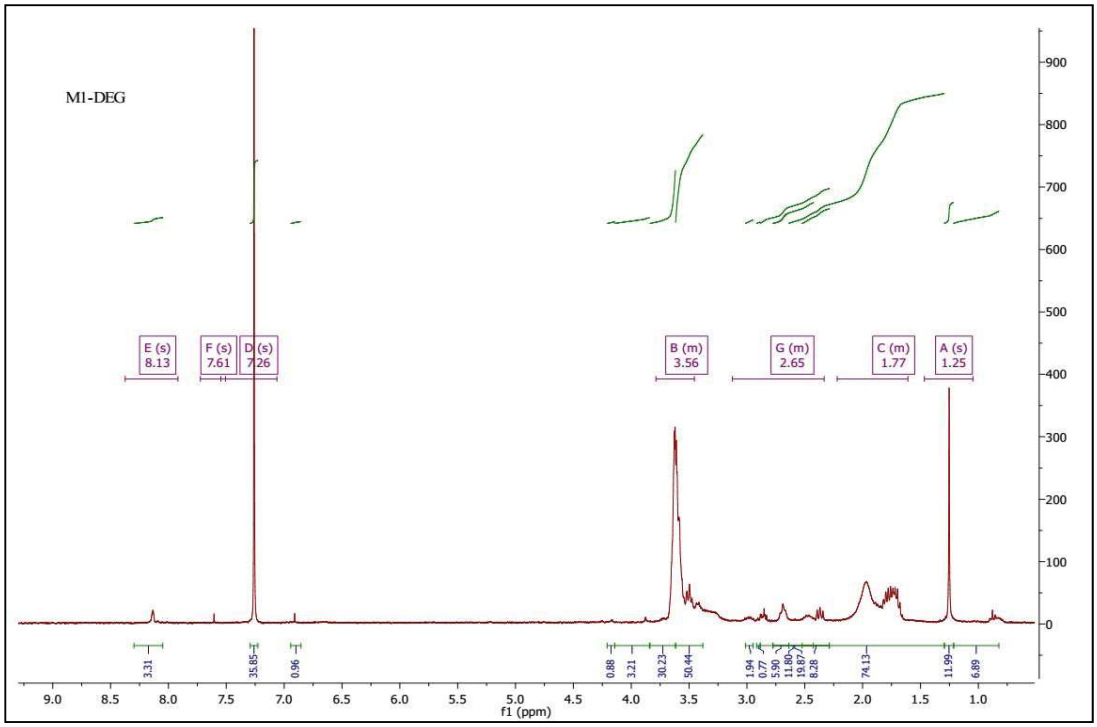

Fig.19: The [1]HNMR spectra for the (M1-DEG) polymeric membrane for gas separation.

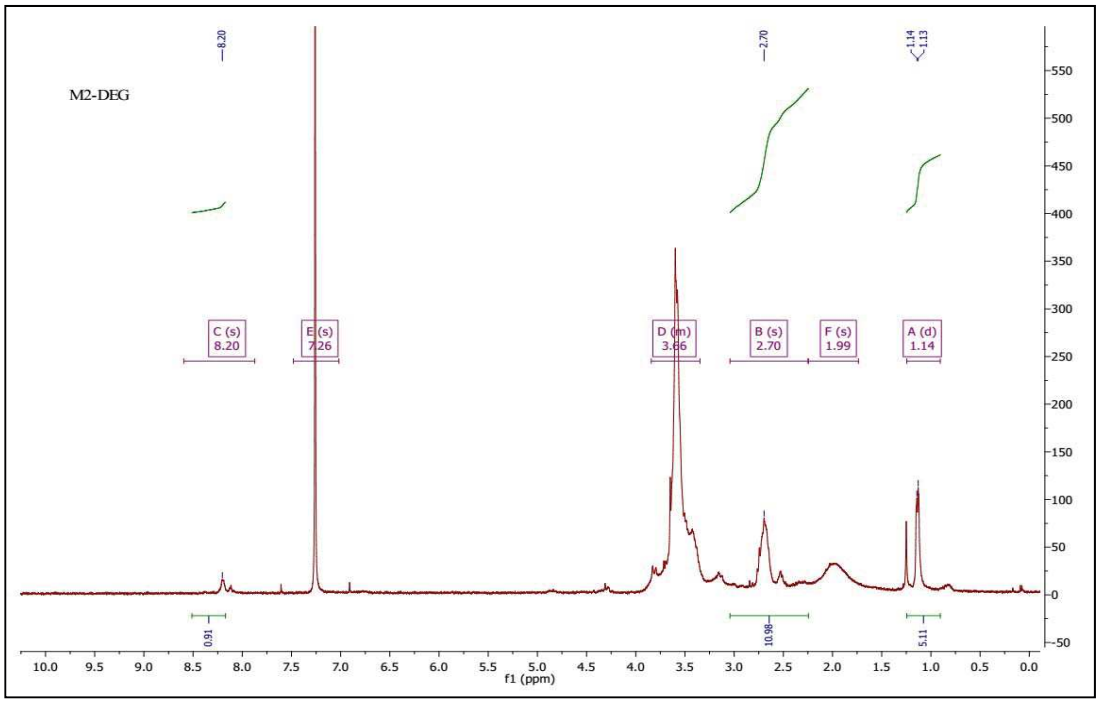

Fig.20: The [1]HNMR spectra for the (M2-DEG) polymeric membrane for gas separation.

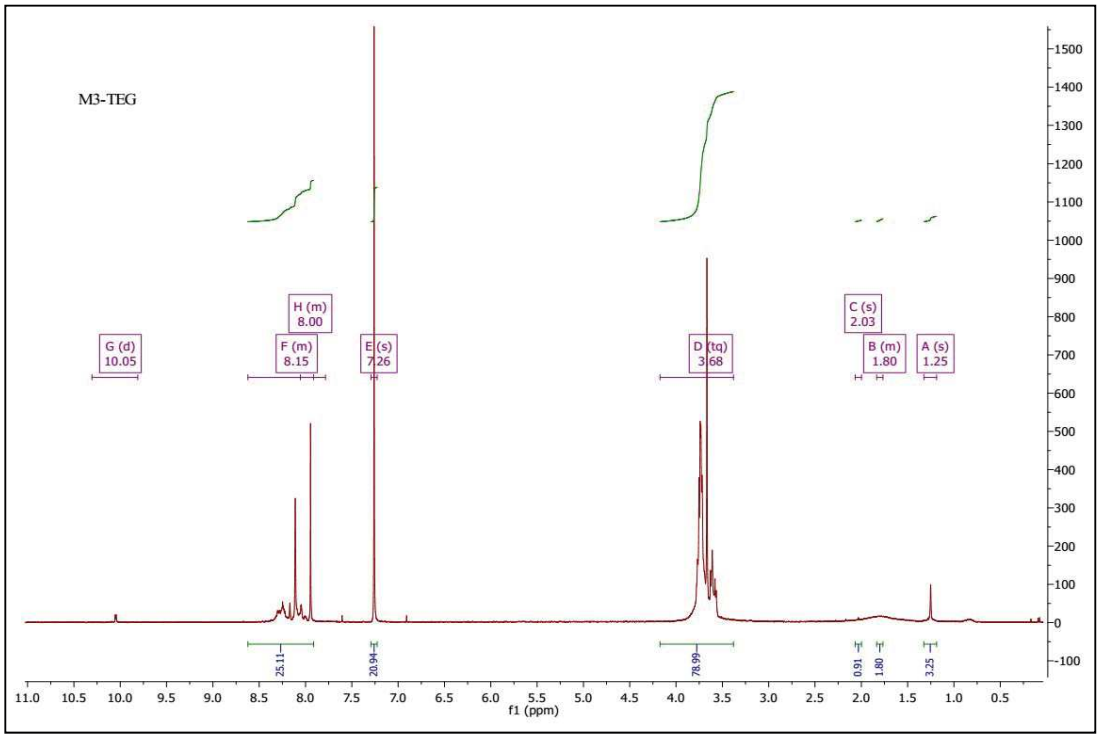

Fig.21: The [1]HNMR spectra for the (M3-TEG) polymeric membrane for gas separation.

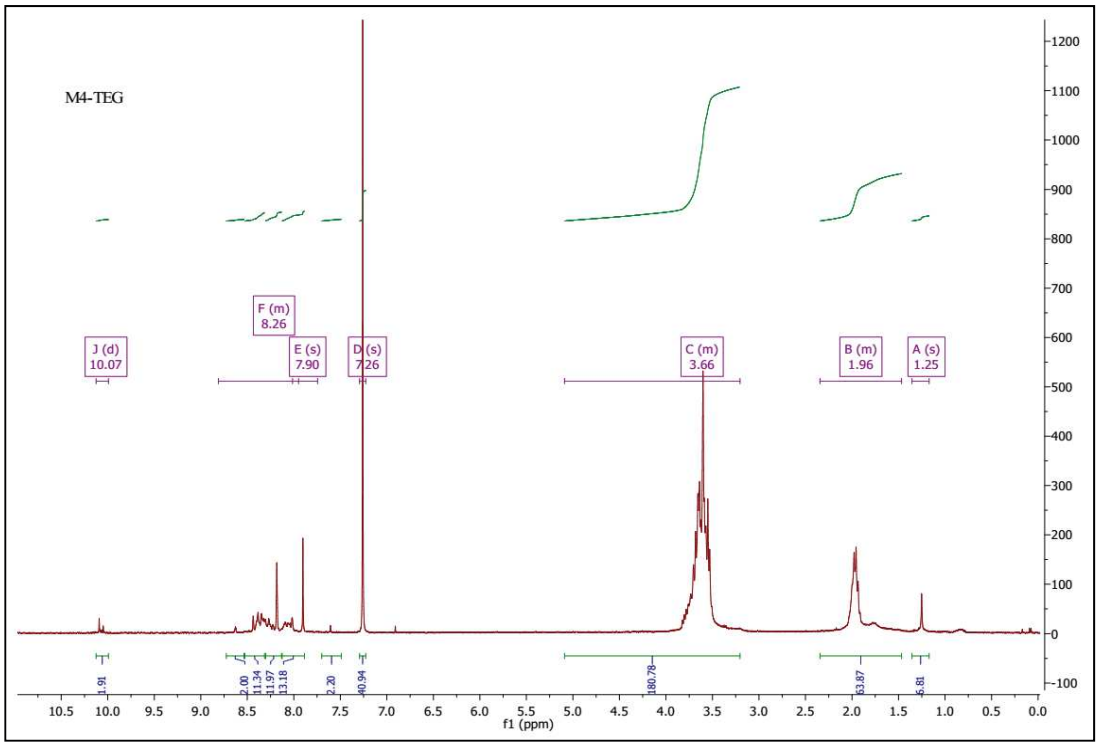

Fig.22: The [1]HNMR spectra for the (M4-TEG) polymeric membrane for gas separation.

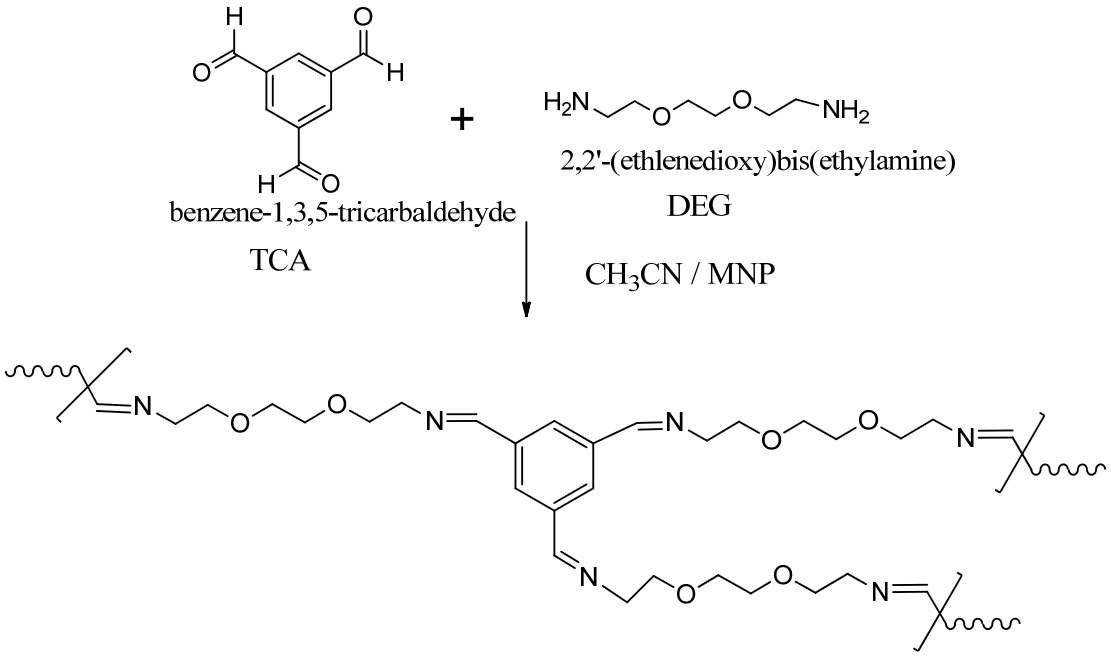

Expected Structure (M1-DEG) / (M2-DEG)

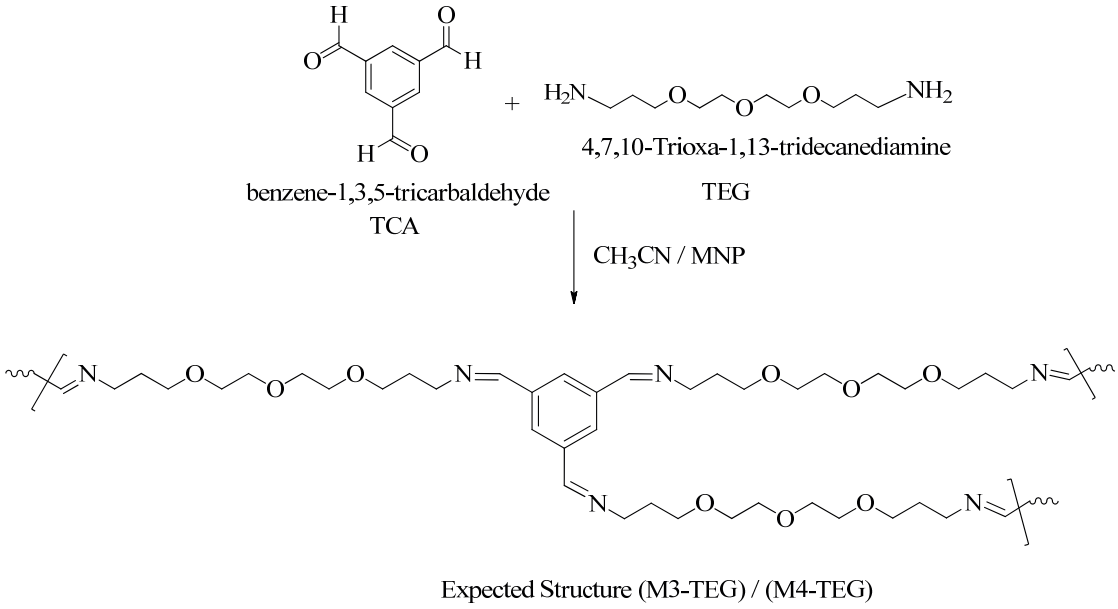

Expected Structure (M3-TEG) / (M4-TEG)

6.3. Appendix: TGA measurements

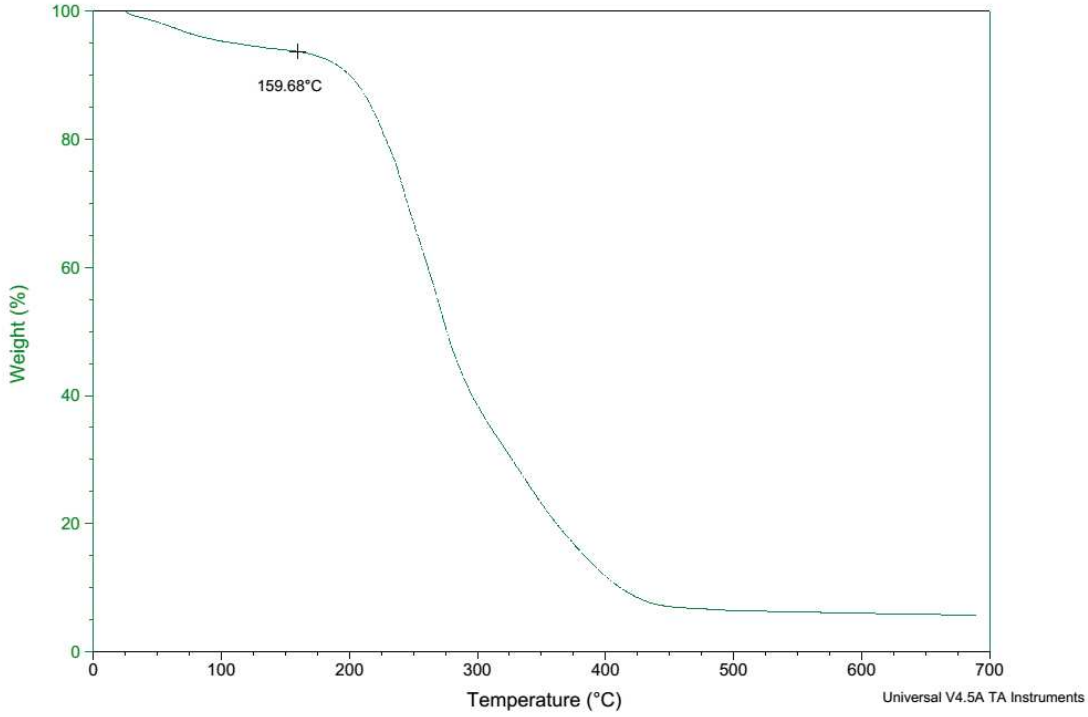

Fig.23: TGA measurements of the (M1-DEG) membrane.

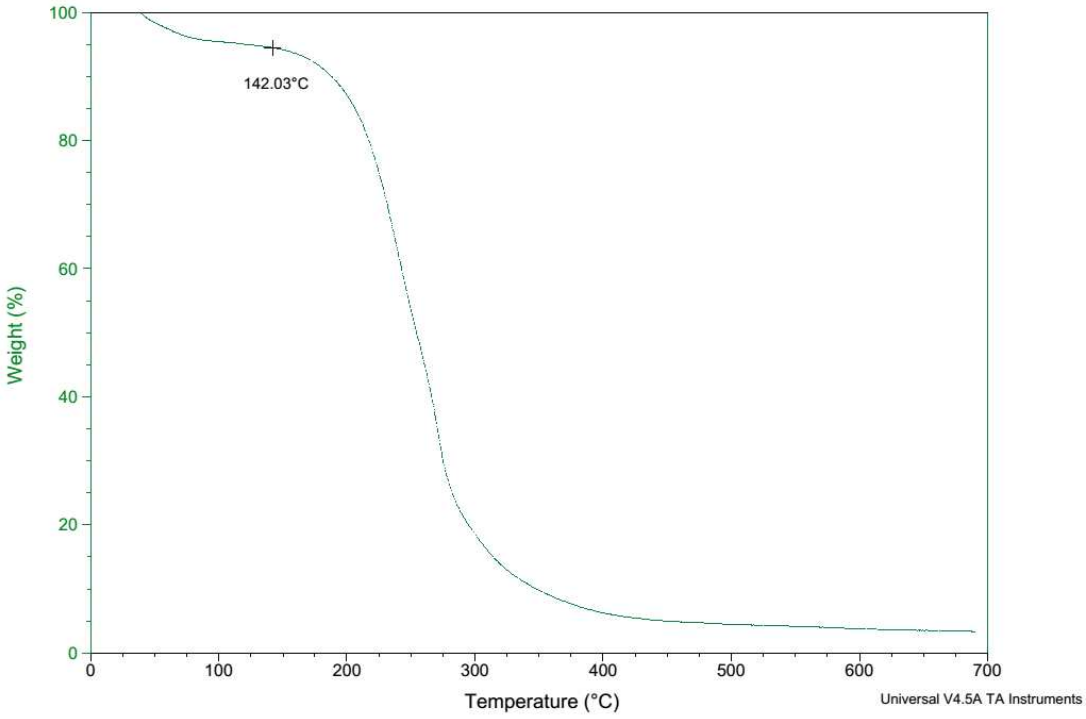

Fig.24: TGA measurements of the (M2-DEG) membrane.

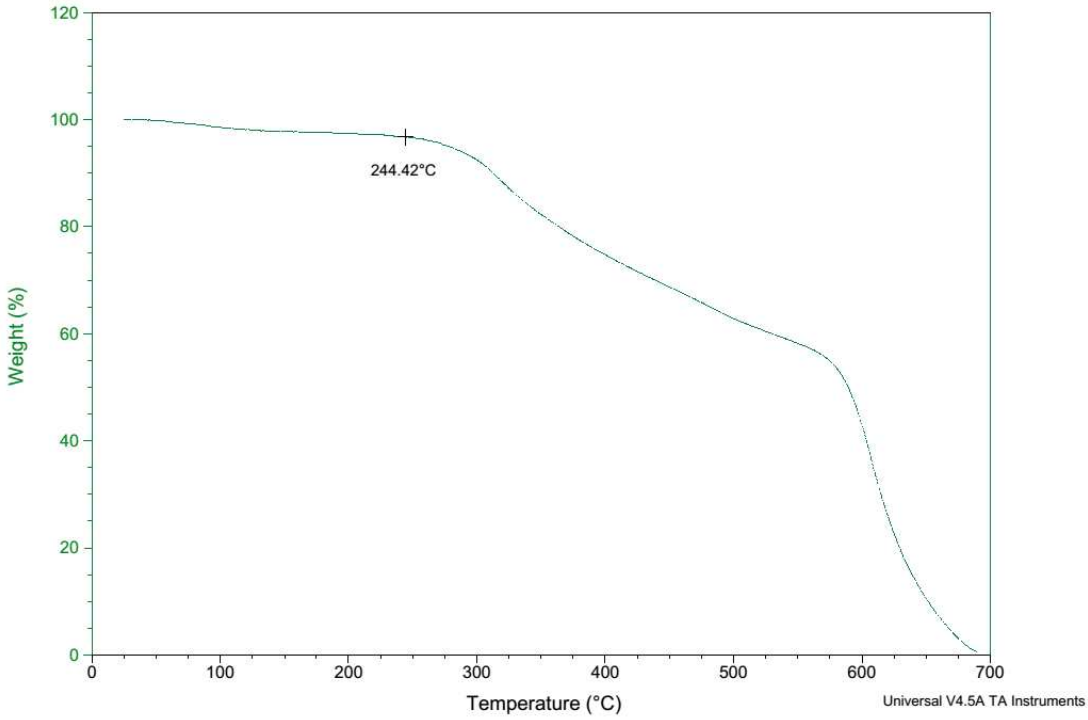

Fig.25: TGA measurements of the (M3-TEG) membrane.

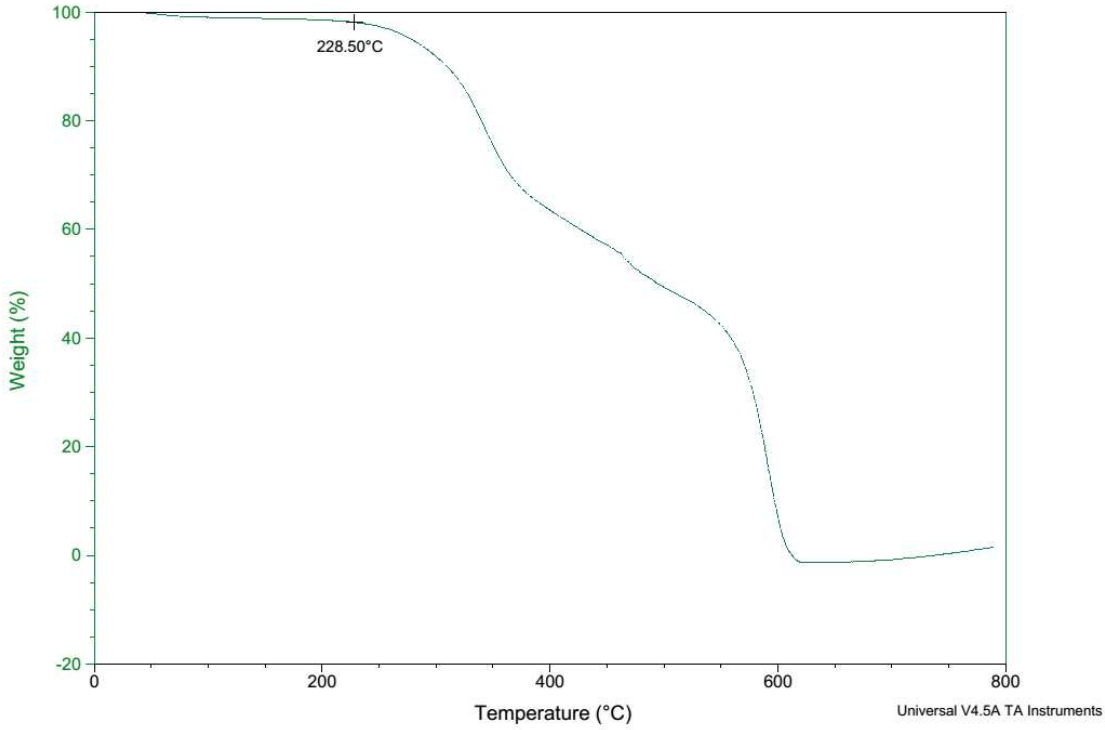

Fig.26: TGA measurements of the (M4-TEG) membrane.

6.4. Appendix: DSC measurements

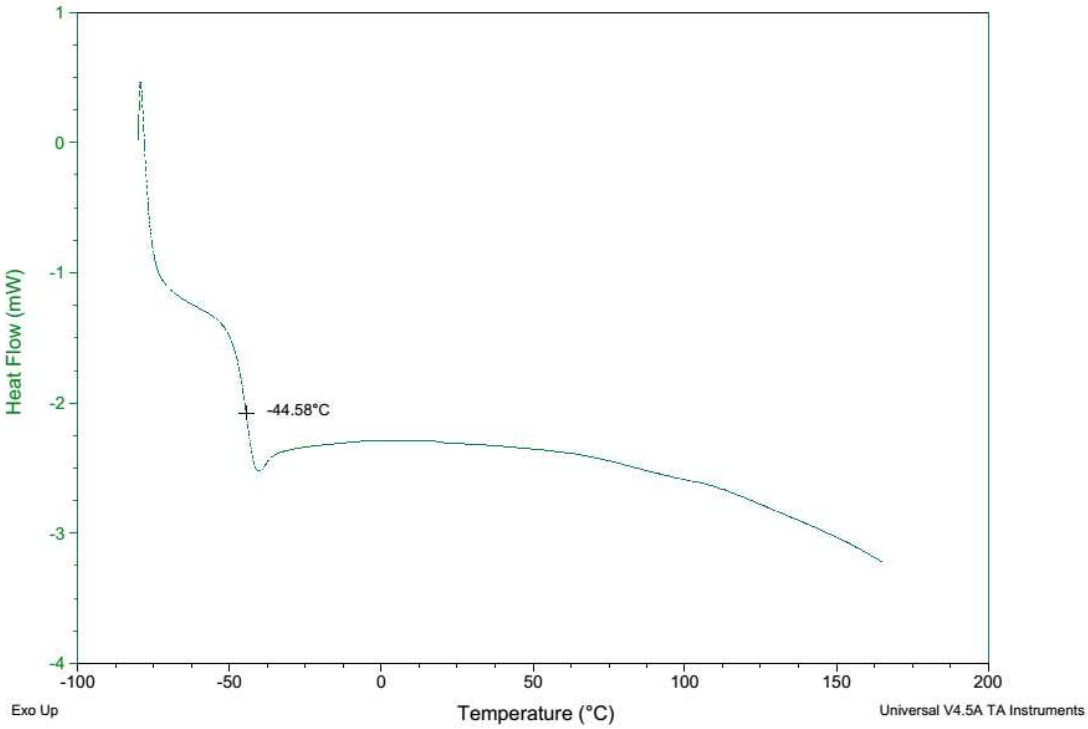

Fig.27: DSC measurements of the (M1-DEG) membrane.

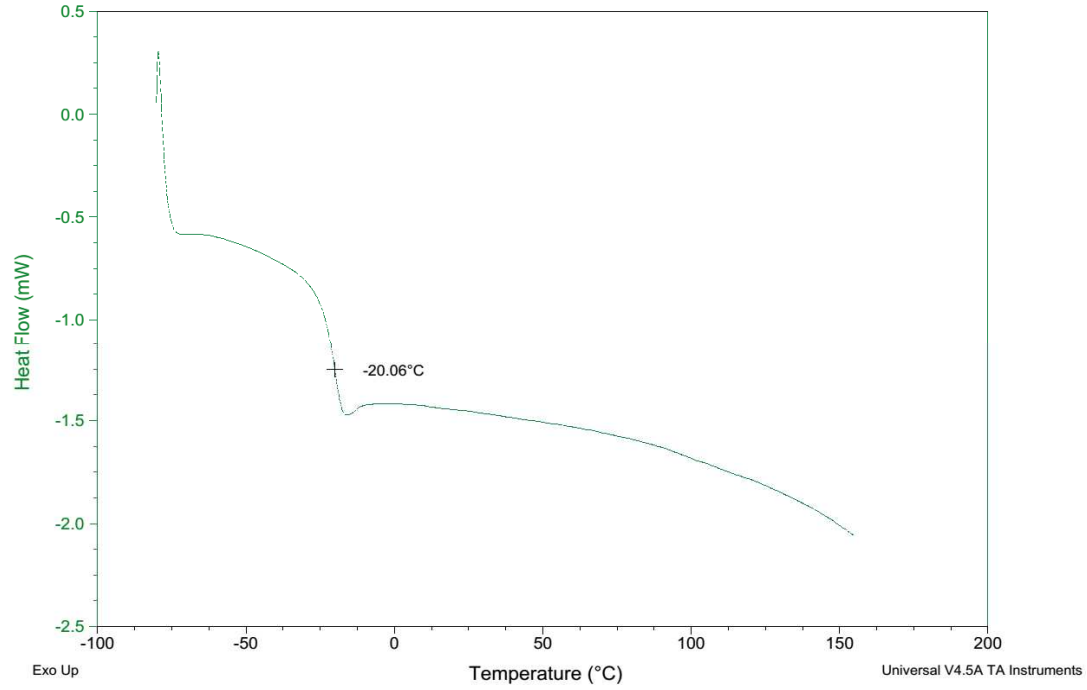

Fig.28: DSC measurements of the (M2-DEG) membrane.

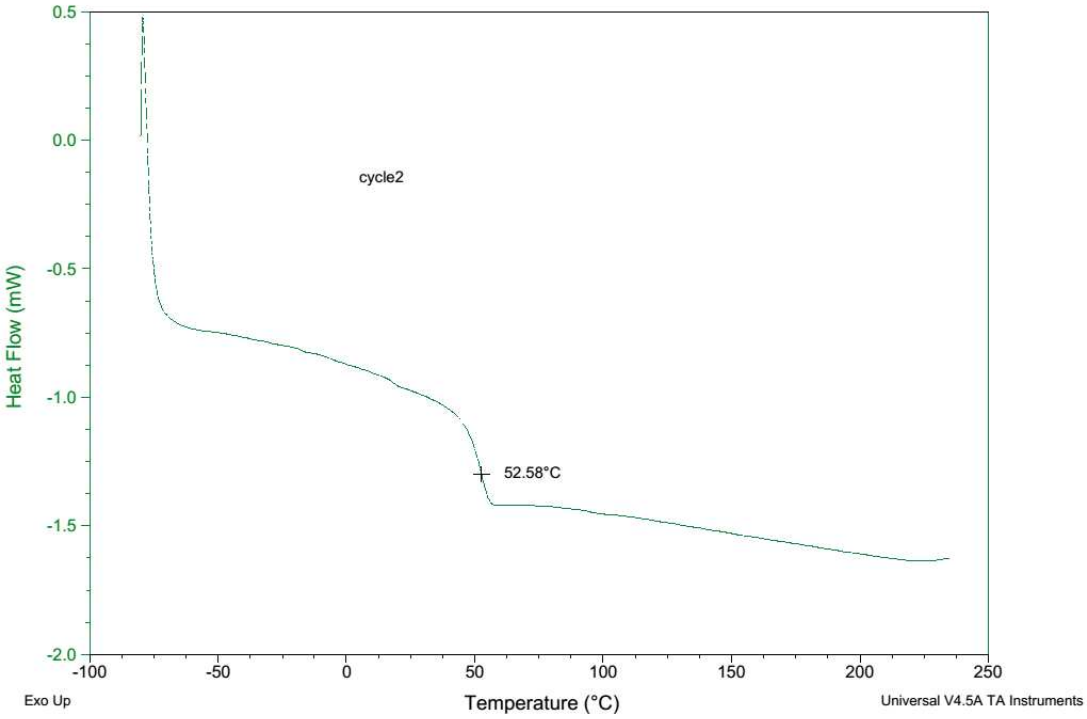

Fig.29: DSC measurements of the (M3-TEG) membrane.

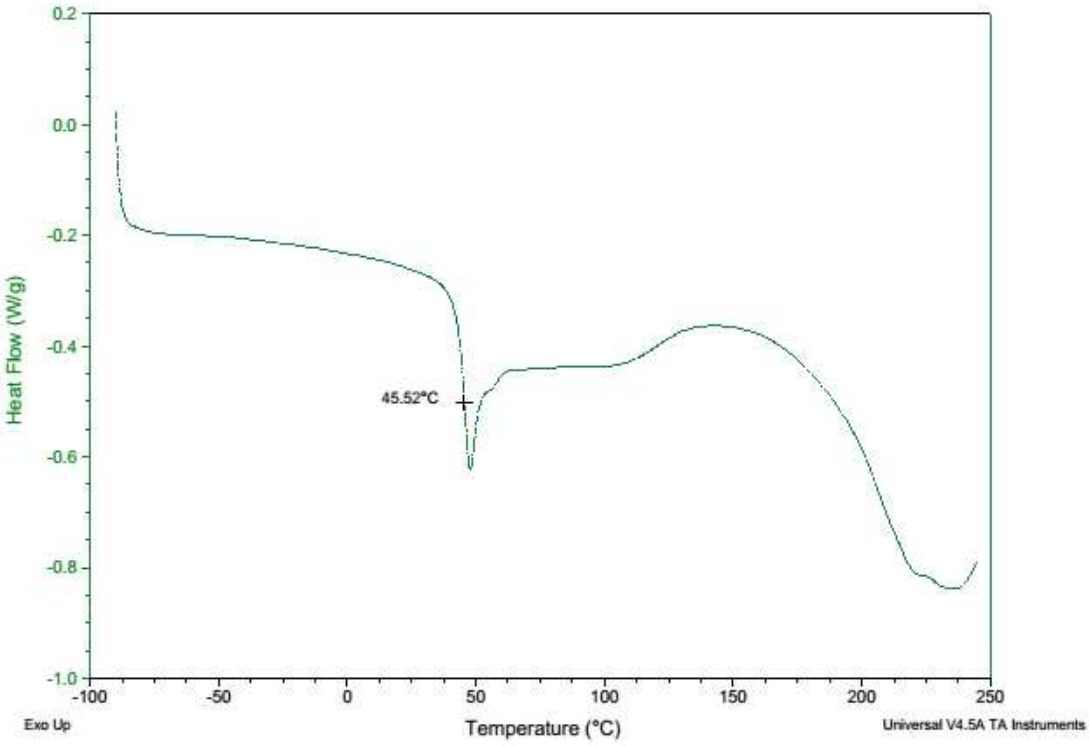

Fig.30: DSC measurements of the (M4-TEG) membrane

6.5. Appendix: Contact angle measurements

The contact angles measurements (The left and right contact angles) for the used polymeric membrane before the permeability of gases through the polymeric membranes have been summarized in table (6).

Table (6): Summary of the average contact angles measurements.

M1-DEG		M2-DEG		M3-TEG		M4-TEG	
LCA	RCA	LCA	RCA	LCA	RCA	LCA	RCA
86.75	83.37	93.32	92.25	101.42	99.15	105.07	104.71
86.42	84.55	92.57	91.33	99.76	98.82	104.88	104.05
87.22	84.36	92.15	91.74	100.51	98.92	104.78	103.94
86.57	84.18	92.77	91.52	100.72	99.89	105.11	104.24
86.74	84.12	92.7	91.71	100.6	99.2	104.96	104.24

*(Left contact angle: LCA) & (Right contact angle: RCA)

Chapter (5)

Membrane functionalized with enzyme for selective conversion and separation.

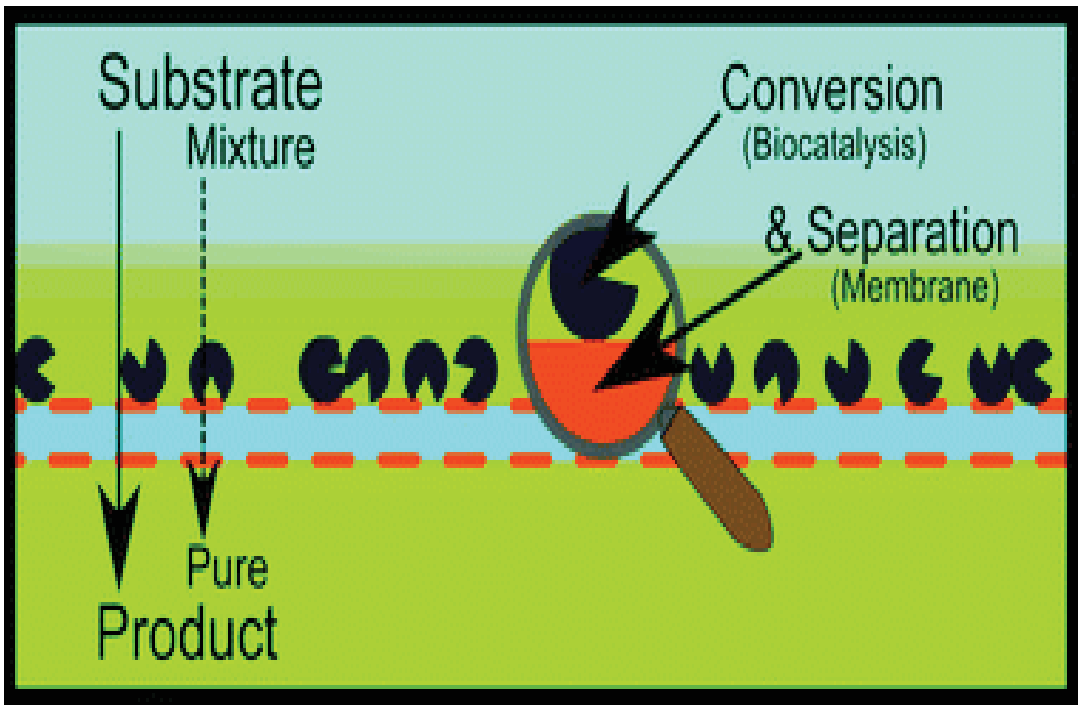

Abstract

The approach proposed in this work consists on the development of two different methods of PVDF membrane functionalization with a phosphotriesterase (PTE) enzyme to construct biocatalytic membrane reactor (BMR) for bioconversion of paraoxon to p-nitrophenol as a product. The first method employs reversible dispersion of magnetic nanoparticle immobilized with PTE using an external magnetic field on the surface of native PVDF membrane. On the contrary, the second method comprises chemical grafting of the PTE enzyme, after surface modification of the native PVDF membrane with DAMP-GA-Enzyme. Both methods of enzyme immobilization showed good efficiency and sensitivity towards the bioconversion of paraoxon substrate at different conditions applied in the biocatalytic membrane reactor (BMR). The immobilized process induced a negative effect on the enzyme activity since both methods of immobilization revealed loss in the enzyme activity. In case of PVDF-MNPs-Enzyme there was an order of magnitude activity loss after immobilization (0.91 U/mg) compared to free enzyme activity (9.164 U/mg), while in case of PVDF-DAMP-GA-Enz there was two order of magnitude activity loss after immobilization (0.06 U/mg) lower than the activity obtained for the free enzyme (9.164 U/mg). Moreover, the modified PVDF-MNPs-Enzyme membrane showed higher enzyme activity when comparing with PVDF-DAMP-GA-Enzyme membrane inside biocatalytic membrane (BMR) reactor. Furthermore, the results showed that the efficiency and performance of the developed polymeric membranes with PTE enzyme are influenced by the enzyme concentration, the substrate concentration, the transmembrane pressure, and the enzyme residence. Overall, the concept developed in this research work will help bring new track on the development of polymeric membrane with biomolecular materials to create biocatalytic membrane reactor (BMR) for different application. Indeed, it is quite possible to transfer these principles to other traditional membrane systems to improve their properties and make them more efficient and selective towards biological applications.

Keywords:

Biocatalytic membrane reactor (BMR); Polymeric membranes; Functionalization; Biomolecular materials; Phosphotriesterase (PTE) enzyme; Paraoxon.

1. Introduction

Numerous polymeric membranes that have excellent physical and chemical bulk properties do not possess the appropriate surface properties required for particular applications. For this reason, surface modification of polymeric membranes has been of prime importance in various applications from the advent of membrane-involving industries. Incorporation of novel functionalities is a versatile means for surface modification of polymeric membranes. Functionalized membranes are used for immobilization of enzymes [1], for improvement of biocompatibility [2], preparation of biosensors [3] and application in membrane bioreactors [4] due to their interesting properties of high specific surface area and the possibility to combine separation with chemical reaction [5].

1.1. Functionalization and properties of PVDF membrane

Polyvinylidene fluoride (PVDF) is a hydrophobic polymer that because of its outstanding properties (high mechanical strength, chemical resistance, thermal stability, ultraviolet weathering resistance), has received great attention as a membrane material compared to other commercialized polymeric materials. For this reason, PVDF has been largely applied in microfiltration (MF) and ultra filtration (UF) membranes processes [6]. Owing to the well-known low reactivity of PVDF, biomolecules are unable to couple with its surface in a covalent manner, so for this aim the grafting of functional groups is required. Different surface modifications of PVDF membranes have been proposed in literature. The functionalization is usually carried out by high energy radiation techniques like plasma, ozonation and UV [7]. Only few examples of PVDF modification by wet chemistry are reported principally in harsh basic or acid environment [8–10]. In this contest one of the main issues to be addressed is the control of the PVDF degradation with loss of mechanical properties. Also in the case of PVDF modification for biomolecule attachment few examples are reported in which wet chemical approach was used [8,11]. Surface grafting is one of the most promising methods to modify the membrane surface through covalent bonding interaction between the grafted chains and the membrane [12]. The grafting method proposed by Kuo et al. [13] which consists of an introduction of amino groups on PVDF is one of the most interesting because it is

economically sound with no expensive equipment requirement. Starting from this method, the functionalization of PVDF membrane under basic condition was investigated. In the literature, it is reported that when PVDF is treated with an alkaline solution an elimination reaction occurs so fluorine and hydrogen are eliminated and double bond is created in the PVDF chains [14]; subsequent attack of nucleophilic molecules can lead to their grafting into PVDF chains.

1.2. Biocatalytic membrane reactors

Biocatalytic membrane reactors combine selective mass transport with chemical reactions, The selective removal of products from the reaction site increases the bioconversion of product-inhibited or thermodynamically unfavourable reactions. Membrane reactors using biological catalysts can be used in production, processing and treatment operations. The recent trend towards environmentally friendly technologies makes these membrane reactors particularly attractive because they do not require additives, are able to function at moderate temperature and pressure, and reduce the formation of by-products. The catalytic action of enzymes is extremely efficient and selective compared with chemical catalysts; Enzymes demonstrate higher reaction rates, milder reaction conditions and greater stereo specificity. Their potential applications have lead to a series of developments in several technology sectors: (1) the induction of microorganisms to produce specific enzymes; (2) the development of techniques to purify enzymes; (3) the development of bioengineering techniques for enzyme immobilization; and (4) the design of efficient productive processes.

Since the 1950s, when protease was first immobilized on diazotized polystyrene, many enzymes and microorganisms have been used in membrane reactors to catalyse bioconversions. The use of biocatalysts for large-scale production is an important application because it enables bio-transformations to be integrated into productive reaction cycles. Biocatalysts (e.g. enzymes, microorganisms and antibodies) can be used: (1) suspended in solution and compartmentalized by a membrane in a reaction vessel or (2) immobilized within the membrane matrix itself. In the first method, the system might consist of a traditional stirred tank reactor combined with a membrane-separation unit.

In the second method, the membrane acts as a support for the catalyst and as a separation unit (Fig. 1). The membrane can have a flat-sheet shape, assembled in a plate-and-frame module (Fig. 2a) or a spiral wound module (Fig. 2b), or tubular-like, assembled in tube-and-shell modules (Fig. 2c); it can also have a symmetric (Fig. 2d) or an asymmetric (Fig. 2e) structure.

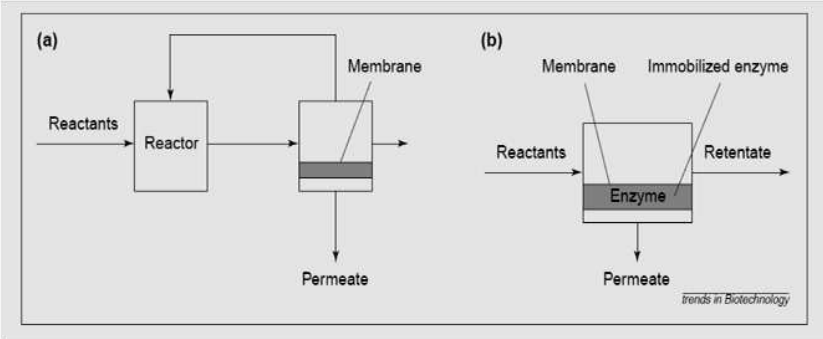

Fig.1. Main configuration types of membrane reactors: (a) a reactor combined with a membrane operation unit, (b) a reactor with the membrane active as a catalytic and separation unit [4].

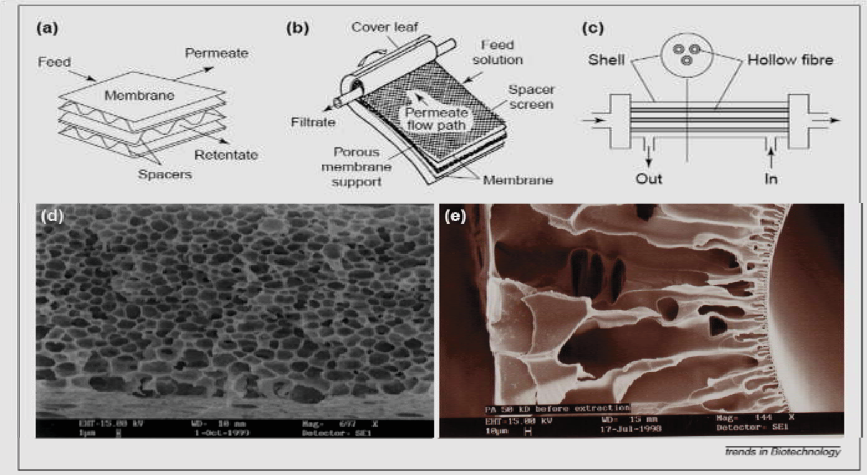

Fig. 2. The different types of membrane and membrane modules: flat-sheet membranes assembled in (a) plate and frame, and (b) spiral wound modules; (c) a hollow fibre membrane assembled in a tube-and-shell module; (d) a symmetric membrane: a cross section of a flat membrane made of polyetheretherketone (PEEK-WC); and (e) an asymmetric membrane: a cross section of a capillary membrane made of polyamide [4].

The biocatalyst can be flushed along a membrane module, segregated within a membrane module, or immobilized in or on the membrane by entrapment, gelification, physical adsorption, ionic binding, covalent binding or cross-linking (Fig. 3) [4].

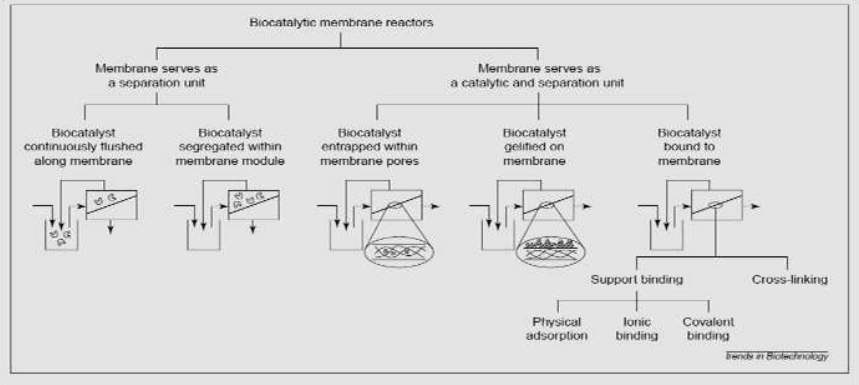

Fig.3. Examples of biocatalytic membrane reactors with enzymes immobilized using different methods [4].

1.3. Organophosphate compounds (Paraoxon)

Organophosphate triesters have been employed in the agricultural industry as pesticides and insecticides for several decades. Approximately 40,000 tons of various organophosphates are applied annually to agriculture crops in the US. The most toxic organophosphorus compounds known are the lethal nerve agents, tabun (GA), sarin (GB), soman (GD), and VX as shown in Scheme 1 [15]. The toxicity of these compounds is due primarily to the practically irreversible inhibition of acetylcholine esterase (AChE), the enzyme responsible for hydrolysis of the neurotransmitter acetylcholine [16]. Enzymes that are capable of hydrolyzing and detoxifying such agents are of significant utility.

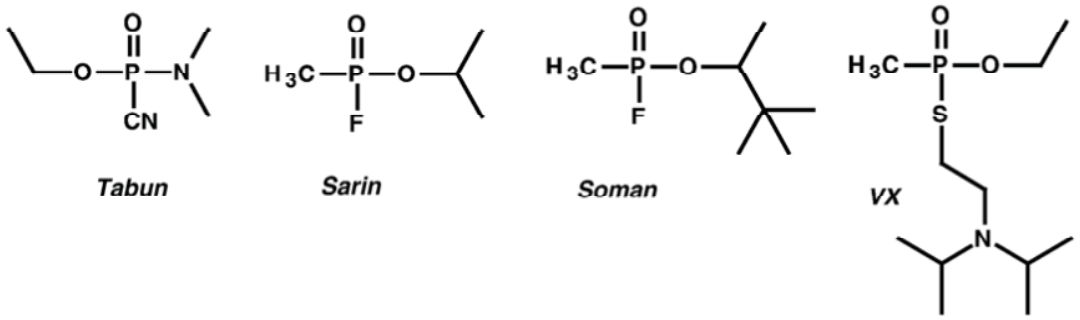

Scheme (1): The most toxic organophosphorus compounds known are the lethal nerve agents [15].

Several organophosphate degrading enzymes have been isolated and characterized. The best characterized among them is the phosphotriesterase (PTE) that was initially isolated from the soil bacterium Flavobacterium sp. Strain ATCC 27551 identified in Philippines [17]. The opd (organophosphate degrading) gene encoding the active hydrolase was located on an extra chromosomal plasmid. The gene for the bacterial phosphotriesterase was subcloned into several expression systems, including Escherichia coli [18], insect cells [19], and in vitro compartmentalization [20]. The natural substrate for PTE remains unknown. However, the purified enzyme is capable of hydrolyzing the insecticide paraoxon at a rate that approaches the diffusion-controlled limit as presented in Scheme 2. The turnover number of the zinc-substituted PTE for Paraoxon hydrolysis is 2100 s^{-1}, while the corresponding value for kcat/Km is 4 × 107 M^{-1} s^{-1}. Since the synthesis of paraoxon was first reported in 1950 [21], it is remarkable that PTE could have evolved to such a catalytic efficiency over a relatively short period of time. PTE also possesses the ability to catalyze the hydrolysis of a wide spectrum of organophosphate insecticides including parathion, methyl parathion, fensulfothion, among others [18]. In addition, PTE is capable of hydrolyzing the nerve agents sarin, soman, and VX, but the catalytic efficiencies for these substrates are significantly lower than the less toxic insecticides [22,23].

1.4.Three-dimensional structure of phosphotriesterase

Phosphotriesterase is a member of the amidohydrolase superfamily [24], which also includes urease [25] and dihydro-orotase [26] among others. Members of this superfamily utilize one or two divalent metal ions to activate a hydrolytic water molecule for a nucleophilic attack at tetrahedral phosphorus or trigonal carbon centers. PTE is a homodimeric metalloprotein with a molecular weight of ~36 kDa/monomer [27]. A high resolution X-ray structure has been solved for the bacterial PTE [28]. The active site of the native enzyme contains two zinc ions per monomer. Incubation of PTE with various metal chelators such as EDTA and 1,10- phenanthroline renders the enzyme inactive [29]. The enzyme retains catalytic activity when the native Zn^{2+} is replaced by Co^{2+}, Cd^{2+}, Ni^{2+}, or Mn^{2+}. The cobalt-substituted enzyme is the most active form [29].

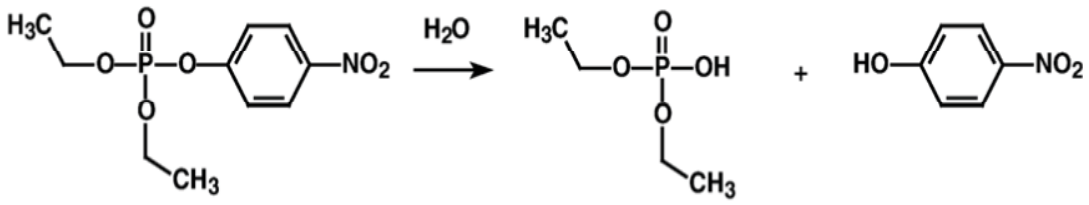

Scheme 2: The hydrolysis of paraoxon to p-nitrophenol [15].

Like other members of the amidohydrolase superfamily, PTE adopts a TIM-barrel $(\alpha\beta)_8$ fold where the binuclear metal center is located at the C-terminal end of the β barrel (Fig.4). The more buried metal ion in the active site, also known as the α-metal, is ligated to His-55, His- 57, and Asp-301. The more solvent exposed metal ion (β-metal) is coordinated by His-201, His-230, and a water molecule. The two metal ions are bridged by the carboxylated Lys-169 and a water/hydroxide molecule, which is the apparent nucleophilic species during the hydrolysis reaction (Fig.5). The X-ray structure of phosphotriesterase bound with the prochiral substrate analog, diethyl 4-methylbenzylphosphonate, revealed the presence of three subsites for substrate binding: the small, large, and leaving group pockets accommodate the three substituents attached to the phosphorus center [30].

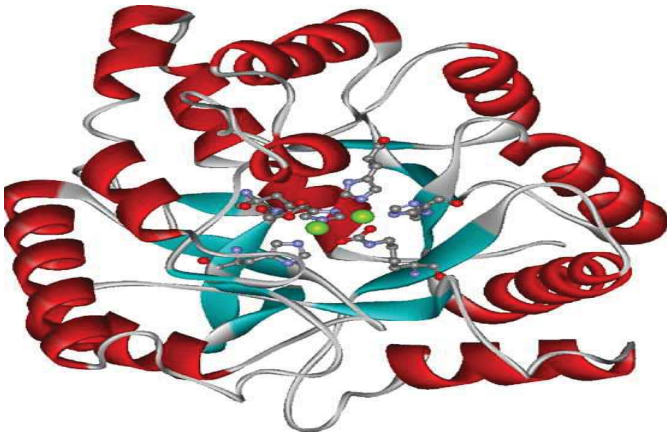

Fig. 4: Crystal structure of phosphotriesterase featuring a TIM barrel fold. Coordinates taken from PDB file 1 HZY [30].

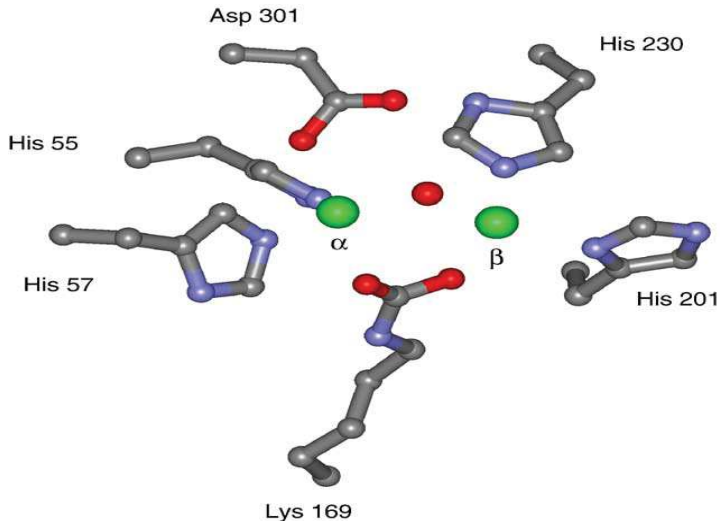

Fig. 5: Binuclear metal center of phosphotriesterase representing the (a) and (h) metals bridged by the catalytic solvent molecule. Coordinates taken from PDB file 1 HZY [30].

1.5. Novel magnetic-responsive biocatalytic membrane reactor

Super paramagnetic ferric oxide based nanoparticles (MNPs) represent a versatile biocompatible nano-platform. Hence, colloidal dispersions of MNPs surrounded by biocompatible coatings have attracted much interest for use in smart devices, sensors, catalysis, bio-separation, magnetic guidance, and targeted drug delivery [31–34]. When used for bio-magnetic separation after functionalization with for instance enzymes, they are often associated with long-term stability over multiple cycles and during storage, in addition to easy recovery from reaction mixtures [35]. The research on hybrid membranes, consisting of a polymeric matrix within corporate MNPs, holds many unexplored interesting avenues [36]. Their incorporation leads to stimuli-responsive "smart" polymeric membrane with magnetic properties that can be modulated in a reversible manner. The MNPs serves a dual purpose in the biocatalytic membrane (micro) reactors (BMRs) where superparamagnetism is employed to tailor physical confinement of enzymes at the membrane surface, thus combining biocatalysis, super paramagnetic nanoparticles and super paramagnetic membranes during reaction. Immobilization of enzymes on membranes to form BMRs is a typical example of process intensification which aims at hybridizing two or more traditional operations to make industrial production more efficient [37], since the coupling lowers chemicals and energy consumption, while increasing reaction yields and minimizing waste [5, 38–40].

BMRs have been applied in different sectors, e.g., in the pharmaceutical industry [41,42], in the production of bio-renewables [43] and in waste valorization [44].

However, membrane fouling and enzyme activity loss demand chemical cleaning of the membrane and enzyme replenishment, respectively. Since enzymes are loaded in conventional BMRs either by simple adsorption on the membrane or by covalent binding to the membrane, they are highly sensitive to chemical cleanings. In addition, when membrane immobilized enzymes get denatured or over saturated, it is very difficult (if not impossible) to replenish with fresh enzymes. Consequently, the ultimate fate of biocatalytic membranes is only disposal. Hence, a novel immobilization technique that fulfils the conditions of the BMRs, but still facilitates membrane chemical cleaning and enzyme renewal is urgently needed. The aforementioned combination of enzyme functionalized superparamagnetic nanoparticles (Bio/nanocomposites) and stimuli-responsive "smart" polymeric membrane is now suggested as the key to solve this bottle neck issue. Particularly, the appearance of the magnetic properties of the MNPs only in presence of an external magnetic field gives a high degree of freedom for reversible enzyme immobilization [45]. They can first be dispersed easily in a reactor in the absence of the magnetic field and readily moved to a desired location by switching the magnetic field on, while being removed later by switching it off again [46,47]. MNPs are used as (1) support material for enzyme immobilization to form an enzyme immobilized super paramagnetic particles (MNPs-Enz) [48–50].

The relatively stronger magnetic force exerted by the external magnetic field situated below the membrane surface creates magnetic field gradient that helps in relocating the MNPs in the liquid to the surface of the membrane. Since the north and south poles of the MNPs attract each other, they align the MNPs and form chains. On the contrary, particles coming close to each other with the magnetization direction parallel will repel each other, thus leaving spaces between the aligned nano biocatalysts [51]. The dynamic layer of MNPs-Enz can thus be considered as a specific reactor resulting from an array of micro reactors formed by the voids between the MNPs connected by magnetic forces. Their superparamagnetic properties can again be employed later on to recover the MNPs-Enz

from the membrane surface whenever the membrane has for instance been severely fouled and needs chemical cleaning, or when the MNPs-Enz has been denatured, by simply switching off the external magnetic field and a subsequent mechanical stirring. This novel approach, further referred as a superparamagnetic BMR (BMR^{SP}), offers a paradigm shift in addressing two of the most critical bottle necks of BMRs currently hindering their wide spread use: easy recycling of the enzyme and extending the membrane working lifecycle beyond the enzyme's active period. Similar to direct on to membrane immobilization, the enzyme immobilized on MNPs will indeed be denaturized in time. The novelty of the current system however is the ease to remove the denatured MNPs-Enz and re-supply with fresh MNPs-Enz, while direct onto membrane immobilization forces one to dispose a full membrane module [51].

2. Material and Methods

2.1. Materials

A phosphotriesterase (PTE) enzyme (Sso-3M), glutaraldehyde (GA) and 1,5-dia-mino-2-methyl pentane (DAMP) were purchased from (Sigma Aldrich, Italy). Flat sheet polyvinylidene fluoride (PVDF) membrane with an average pore size of 0.2 μm, 47 mm, diameter and 200 μm thickness, which were kindly supplied by GVS Spa, Italy was used as support for biomolecule immobilization. . The membrane has hydrophobic properties and composite structure consisting of a selective PVDF layer on a nonwoven polyester (PE) support. Magnetic nanoparticles (MNPs) (Amino-Adembeads) were purchased from Ademtech. They are monodispersed and super-paramagnetic beads composed of magnetic core encapsulated by a hydrophilic polymer shell. The surface was activated with amine functionality. Amino-Adembeads are produced under aseptic conditions and are sold in an aqueous suspension containing 0.09% NaN_3. EGDE (Ethylene Glycol Diglycidyl Ether) and EDC (1-ethyl-3-(3-dimethylamino propyl) carbodiimide hydrochloride), supplied together with the MNPs, were used as activators for the MNPs. As a substrate, paraoxon-ethyl (90%, Sigma Aldrich) was used.

2.2. Enzyme immobilization

2.2.1. Enzyme immobilization on the PVDF membrane

The PVDF membrane was functionalized as described in G.Vitola et al., 2015 [52]. A piece of PVDF membrane with 47 mm diameter was soaked in 20 mL of DAMP solution (1M carbonate buffer, pH 11, 50ºC) in order to graft the DAMP onto the membrane surface. Subsequently, the membrane was washed with ultrapure water. The PVDF–DAMP membrane was then treated for 2 h with glutaraldehyde (GA) solution (20% v/v) at 25ºC to graft the GA onto the PVDF–DAMP membrane (PVDF–DAMP–GA). The membrane was thoroughly washed with distilled water until the entire residual GA was removed. The PVDF–DAMP–GA membrane were then immersed in PTE enzyme (1g/L) solution (25 mL; in 50 mM buffer pH (8.5) at 25ºC for 24 h under gentle stirring (50 rpm). Intense rinsing with buffer and distilled water were followed in order to remove

biomolecules not stably linked on the surface, after that the membrane with immobilized PTE (PVDF–DAMP–GA–PTE) was obtained.

As reported in G. Vitola et.al [52], in order to graft amino groups on the surface of PVDF membrane, DAMP was used in basic environment. The PVDF polymer consists of ($–CH_2CF_2–$) groups, but when it is treated with DAMP at very high pH (>10) (–CH=CF–) groups are formed due to HF elimination. Based on the surface modification mechanism of PVDF in aqueous alkaline medium that is proposed by Ross et.al [53].

2.3. Enzyme immobilization on magnetic nanoparticles

2.3.1. Activation of magnetic nanoparticles

The MNPs used for PTE immobilization have the following physical properties [diameter: 200 nm (CV max 20%), magnetic susceptibility: approximately 40 emu/g, specific surface area: 15 m^2/g, iron oxide content: approximately 70%, surface charge: positive at pH ~2-10, solid content: 10 mg/ml (1%)].

The protocol for activating the MNPs prior to enzyme immobilization is summarized as:

1. Take 1 mL from MNPs sample, and then remove the storage buffer solution by applying magnetic field with magnet.
2. Prepare 20x diluted activation buffer by dissolving 1 mL of activation buffer up-to 20 mL with ultrapure water. The activation buffer is a mixture of EGDE (Ethylene Glycol Diglycidyl Ether) and EDC (1-ethyl-3-(3-dimethylamino propyl) carbodiimide hydrochloride) buffer solutions.
3. Re-suspense the MNPs up to concentration of 1%: For example, 1mL of MNPs taken from the stock, use 1mL of 20x diluted activation buffer.
4. Dilute the washed MNPs in a (1/10) 20x diluted activation buffer: Example, dissolve 1 mL of MNP in 9 mL of activation buffer.
5. Add 100 µL of EGDE per mg of MNPs. In this case 1 mL of MNP contains 10 mg of MNP. Hence add 1 mL of EDGE for 1mL of MNPs containing 10 mg of MNPs.
6. Homogenize and incubate while mechanically stirring the suspension at 200 rpm for 2h, at room temperature.

2.3.2. Magnetic nanoparticles biofuncationalization

The protocol followed to immobilize PTE enzyme on the surface of the MNPs is:

1. Wash the activate beads with 20x diluted amino activation buffer twice to eliminate the excess EDGE buffer solution.
2. Remove the washing solution and add 1 mg of enzyme dissolved in HEPES buffer solution (20 mM, pH 8.5, 25ºC) with 10 mg of MNPs to form a superparamagnetic biocatalytic particle (MNPs-Enz)
3. After vortex mixing, incubate the mixture for 2 h with stirring at 200 rpm at room temperature.
4. Wash the beads well to remove none-systematically attached enzyme. The MNPs-Enz nanoparticles were then decanted using a permanent magnet to separate them from unreacted enzyme solution, before storing them on HEPES buffer (pH=8.5).

In order to determine the enzyme loading efficiency of the MNPs, both post-coupling supernatant and pre-coupling enzyme solutions were kept in a refrigerator at 4ºC. The amount of immobilized enzyme was determined through mass balance by measuring the amount of enzyme according to the BCA protein quantification kit method (Sigma-Aldrich) using BSA as standard. Furthermore, direct quantification of the immobilized enzyme was carried out by injecting a known amount of (MNPs-Enz) into the BCA reagent instead of the magnetically isolated supernatant.

2.4. The enzyme activity measurements

The activity of free PTE enzyme, immobilized enzyme on PVDF membranes, and immobilized on the surface of MNP were measured by following the product formation as a function of time using UV-Visible spectrophotometer. The concentration of the product was calculated from the absorbance value using an extinction coefficient of (19920 $M^{-1}cm^{-1}$). The substrate contained a mixture of 850 µL H_2O, 50 µL tris buffer (pH 8.5) and 100 µL paraoxon (10 mM) to keep the final concentration of paraoxon in the tank solution 1mM. The obtained values of the absorbance are recorded over time; the concentration was then plotted against time. The slope of the p-nitrophenol concentration

as a product against time represents the reaction rate and the slope of mass of p-nitrophenol versus time represents the enzyme activity.

2.5. Experimental set-up

To measure both free and immobilized enzyme activity, known amount of free enzyme or known area of membrane with immobilized enzyme was kept in contact with the reaction mixture. In the first case, the reaction took place in a tank with 30 mL total volume of reaction mixture (Tris buffer, paraoxon, and distilled water) to obtain a final concentration of (1mM) paraoxon substrate at 25ºC. Samples were taken as function of time to measure the amount of paraoxon converted and corresponding p-nitrophenol produced. In the second case (Fig.6a), the chemically grafted (PVDF-DAMP-GA-Enzyme) membrane (4.5 cm diameter) was mounted in a dead-end filtration module. The system was then filled with 30 mL of the reaction mixture with concentration ranging from (0.0625 to 1mM) (Tris buffer, Paraoxon, and distilled water). A N_2 source was used to supply the system with constant pressure. The system, named here biocatalytic membrane reactor (BMR) was then operated under constant pressure mode. The performance of the BMR was assayed through analysis of the flux trough the biocatalytic layer and amount of product in the permeate side of the membrane.

For the enzyme immobilized on the surface of the spherical MNPs, the activity was measured in two different forms. In one case, a known amount of MNP loaded with the maximal amount of enzyme was kept in suspension with the reaction mixture (Tris buffer, paraoxon, and distilled water) to obtain a final concentration of 1 mM. Sample probes were withdrawn from the reaction mixture to analyze the amount of p-nitrophenol formation over time. MNPs that leaked into the sample were magnetically separated and returned back to the reaction mixture. In the other case (Fig.6b) known amount of MNP-Enz were magnetically dispersed on the surface of native PVDF membrane using an external magnetic field. The membrane (4.5 cm diameter) was mounted in a filtration cell and the activity was monitored as mentioned before for case in (Fig.6a).

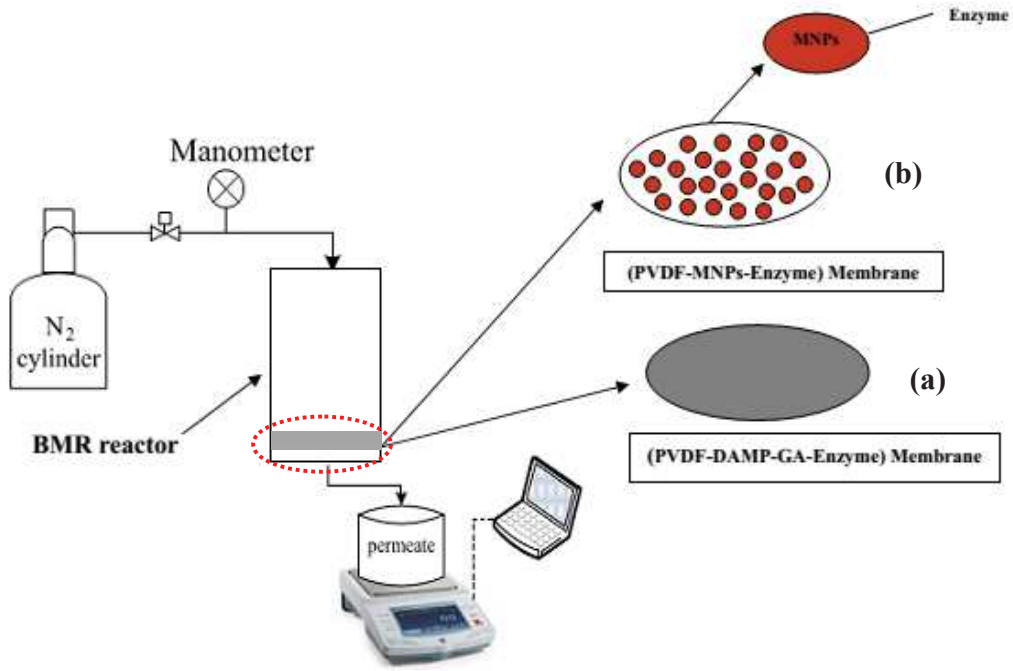

Fig.6: Schematic representation of the biocatalytic membrane reactor (BMR) setup.

3. Results and Discussion

3.1. Amount and activity of immobilized enzyme

3.1.1. Activity of enzyme immobilized on PVDF membrane

The optimal amount of PTE enzyme immobilized on the PVDF membrane was 1 mg corresponding to 0.05 mg/cm^2. The activity of PTE enzyme that is chemically grafted on the surface of modified PVDF membrane (PVDF-DAMP-GA-Enzyme) under static condition was determined by measuring the p-nitrophenol produced. The results were compared with the activity of free enzyme measured under the same condition. Results showed that the activity of the immobilized enzyme was (0.06 U/mg). This result was two orders of magnitude lower than the activity obtained for the free enzyme (9.164 U/mg).

3.1.2. PVDF functionalized with MNPs-Enzyme.

Alternatively, MNPs were used as a support material for enzyme immobilization to form an enzyme immobilized superparamagnetic particles (MNPs-Enz). The MNPs exhibit superparamagnetism which allows the MNPs-Enz initially homogeneously dispersed in the bulk reaction mixture to be deposited onto the PVDF surface by applying an external magnetic field parallel to the surface of the PVDF membrane. The MNPs-Enz layer on the membrane surface will help on reversibly immobilizing the enzyme over the membrane surface to build the biocatalytic membrane (BMR) reactor shown in (Fig.6).

3.1.3 Activity of enzyme immobilized on MNPs

Fig.7 represents the amount of enzyme loaded on MNPs to form enzyme immobilized superparamagnetic nanoparticles (MNPs-Enz). The amount of immobilized enzyme, measured by directly injecting the MNP-Enz into the BCA reagent, increased linearly with the amount of MNPs giving a maximal loading capacity of 41.4 $\mu g_{Enz}/mg_{MNP}$. This result was equivalent to the amount of immobilized enzyme obtained from mass balance between the initial and post coupling solution (48.9 $\mu g_{Enz}/mg_{MNP}$).

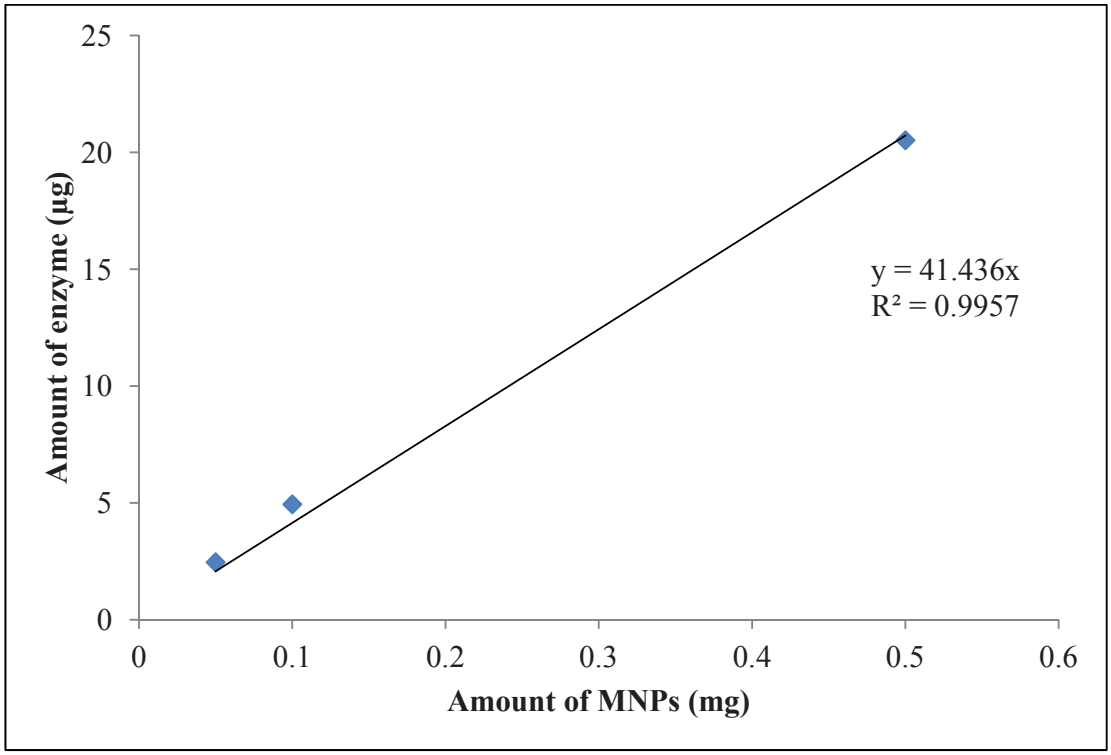

Fig. 7: Behavior of enzyme amount as a function of (MNPs) amount.

The activity of free PTE enzyme and PTE enzyme covalently attached on the surface of MNP (MNPs-Enz) was measured in the tank reactor. The obtained results showed that compared to free enzyme activity (9.164 U/mg), there was an order of magnitude activity loss after immobilization (0.91 U/mg).

3.1.4. Activity comparison for the modified membranes

Compared to free enzyme activity, enzyme immobilized direct on the surface of the PVDF membrane (PVDF-DAMP-GA-Enzyme) resulted in two orders of magnitude activity loss while immobilization on the MNP (MNPs-Enz) gave only an order of magnitude reduction. From these results we can conclude that the immobilized enzyme activity in case of MNPs-Enz was higher than in case of direct immobilization/chemical attachment to the PVDF membrane with covalent bonds to form (PVDF-DAMP-GA-Enzyme).

3.2. Flux measurements through the biocatalytic membrane reactors

3.2.1. Flux measurements for PVDF-DAMP-GA-Enzyme

Fig.8 represents the flux through the native PVDF membrane and modified DAMP-GA-Enzyme. Each experiment was conducted at 25ºC, 0.5 bar transmembrane pressure and 30 mL of 1mM paraoxon in a continuous flow mode in the BMR. Moreover, for each experiment a new set of PVDF-DAMP-GA-Enzyme membrane was used. The flux through the membranes was in the order of: Tris Buffer > Tris Buffer+DAMP-GA> Tris buffer-DAMP-GA-Enzyme > Tris +DAMP-GA-Enzyme+Paraoxon.

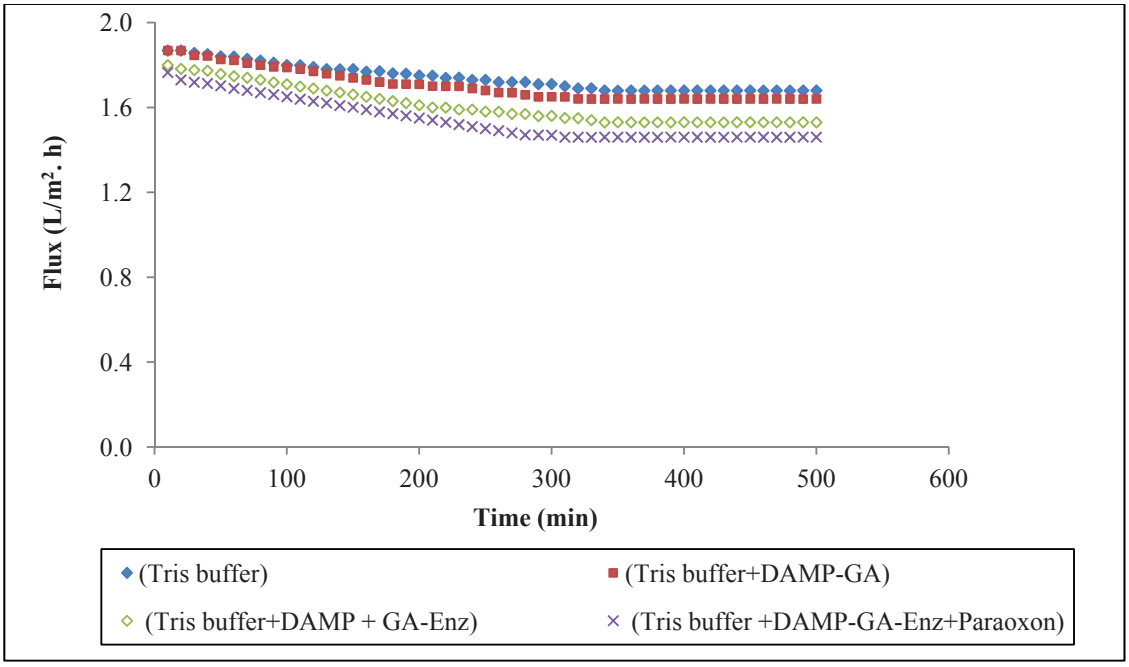

Fig.8: Flux through PVDF-DAMP-GA-Enzyme membrane at 0.5 bar and 25ºC.

3.2.2. Flux measurements for PVDF-MNPs-Enz membrane

Fig.9 represents the flux through the native and membrane containing dynamic layer of MNP-Enz. The orders of the flux value through the various membranes were: Tris Buffer > Tris Buffer+ MNPs > Tris buffer + MNPs-Enz > tris + MNPs-Enz + Paraoxon. The experiments were carried out at 25ºC, 0.5 bar and 30 mL of 1mM paraoxon concentration in a continuous flow mode in BMR. These experimental conditions were similar to the

experimental condition used in the PVDF-DAMP-GA-Enz membrane to provide fair basis for comparison. Moreover, for each experiment a new PVDF membrane and new batch of enzyme activated MNPs-Enzyme were used to keep the same conditions.

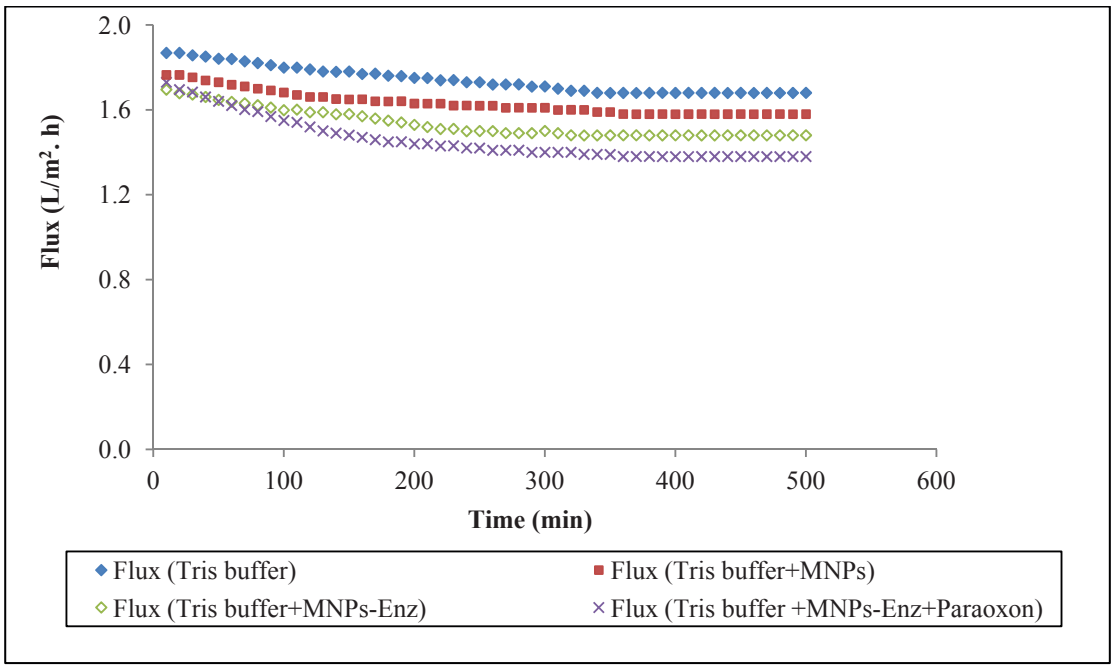

Fig.9: Flux through the immobilized PVDF-MNPs-Enz membrane at 0.5 bar and 25ºC.

3.2.3. Flux comparison for PVDF-GA-DAMP-Enz and PVDF-MNPs-Enz membranes

By comparing the paraoxon flux through the modified PVDF membranes, it's clear that the flux obtained from PVDF-MNPs-Enz membranes was slightly lower than PVDF-DAMP-GA-Enzyme. This might related to the presence of MNPs on the top surface of PVDF membrane that created an additional thickness that slightly reduced the flux.

3.3. Effect of operating conditions on the reactors performance

In this section, detailed investigation of the effect of various operating parameters (enzyme concentration, paraoxon concentration, transmembrane pressure) on the performance of the BMR while using both PVDF-MNPs-Enz and PVDF-DAMP-GA-Enzyme was carried out.

3.3.1. Effect of immobilized enzyme

The effect of MNPs-Enz loaded on native PVDF membrane surface to form PVDF-MNPs-Enz is represented in (Fig.10). The concentration of p-nitrophenol as a product values due to the bioconversion of paraoxon increased with increasing the amount of MPNs-Enz loaded over the surface of the membrane. This might be related to the increment in the amount of MNPs-Enz particles over the membrane surface creating thicker layer of MNP-Enz which led to slightly decreased flux through the bioctalaytic layer as shown in (Fig.11). The decrease in flux might increase the residence time between the MNPs-Enz particles and paraoxon substrate, which helped in accelerating the amount of product formation. In addition to increased flow resistance, the increased bioactivity could be attributed to the presence of higher amounts of immobilized enzyme that eventually increased the rate of reaction occurring at the membrane interface. Moreover, it was observed that the bioconversion of paraoxon substrate to p-nitrophenol inside BMR loaded with the lowest amount of MNPs-Enz containing 10.25 to 20.5 µg PET enzyme have the most stable and controllable product formation compared with other membranes which have higher amount of MNPs-Enz. As a result, membrane with MNPs-Enz particles containing 20.5 µg PTE enzyme was selected to study the effect of other parameters in order to have a better control on the reaction rate.

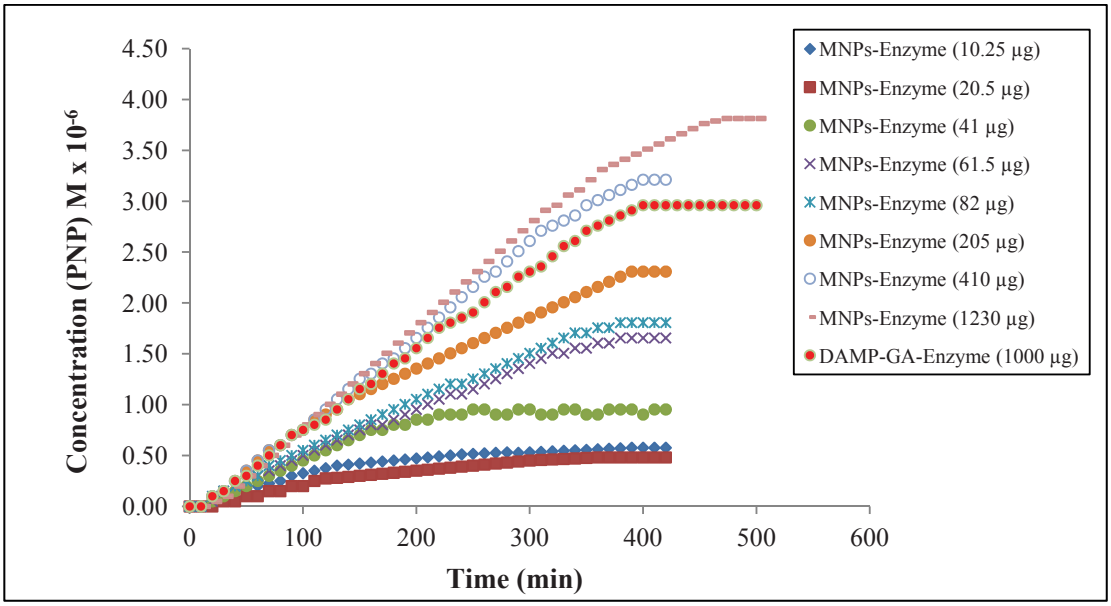

Fig.10: p-Nitrophenol concentration as a function of time with different amount of MNPs-Enz.

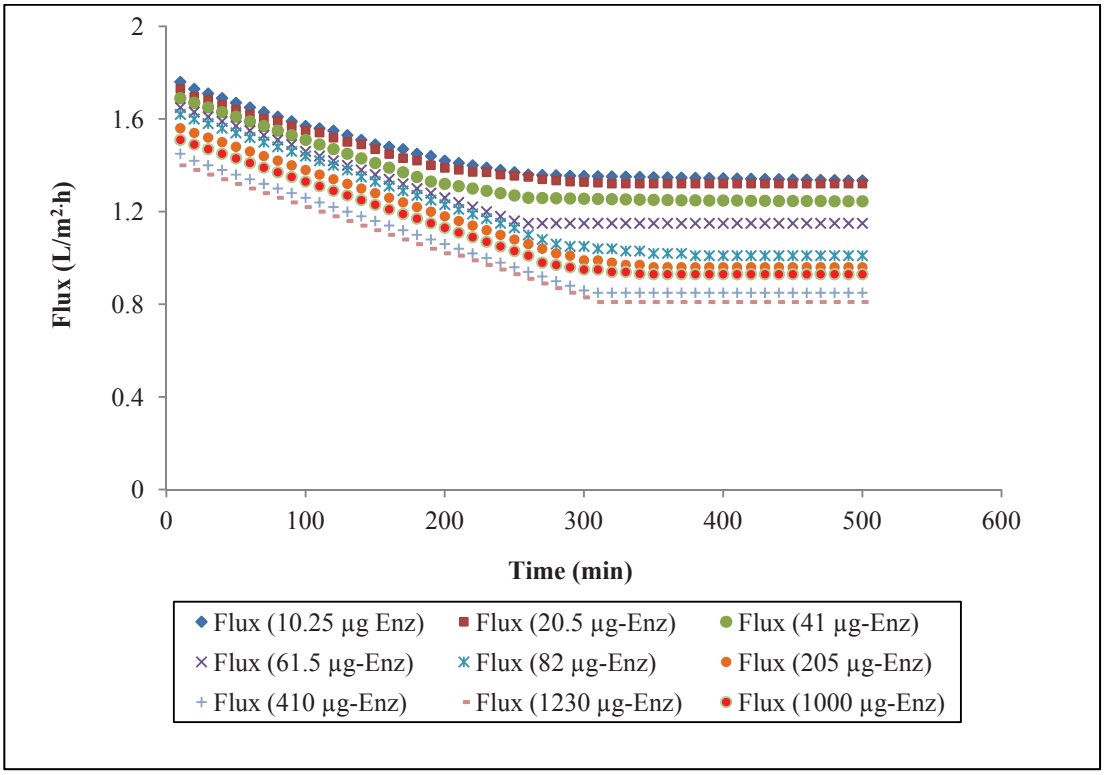

Fig.11: The flux through the membranes as a function of time with different amount of MNPs-Enz

Fig.12 showed that there was no change in the absorbance values obtained when neutral MNPs (without enzyme) were deposited on the surface of the native PVDF membrane while filtering a 1mM paraoxon. The curve exhibit an almost zero slope, hence there was no interference of the MNP on the enzyme activity or the subsequently developed color of the p-nitrophenol. This further proves that the increased p-nitrophenol concentration with increased amount of MNP-Enz deposited on the surface of the membrane was solely due to the immobilized enzyme.

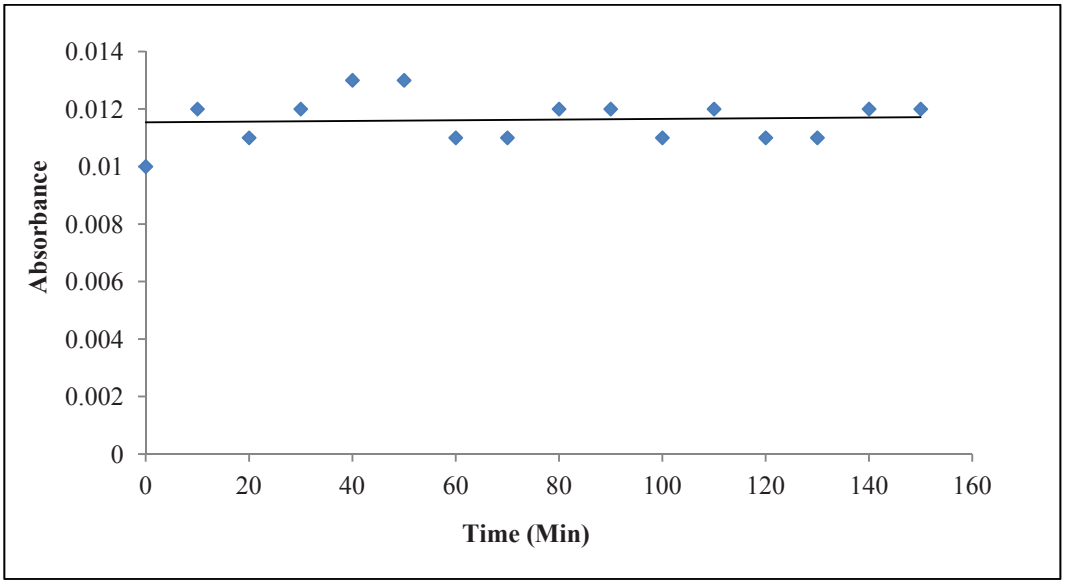

Fig.12: Absorbance measurement of neutral MNPs without enzyme.

Fig.13 represents the PTE enzyme activity in the BMR containing PVDF-MNPs-Enz and PVDF-DAMP-GA-Enz membranes. The specific activity of enzyme attached to the PVDF-DMAP-GA-Enz was 0.0031 µmol/min.mg. Moreover, the figure showed that, for the same amount of immobilized enzyme, the activity of the BMR with PVDF-MNPs-Enz membrane was higher than the BMR containing PVDF-DAMP-GA-Enz membrane. Therefore, carrier mediated enzyme immobilization using MNPs overweighed the covalent immobilization of the enzyme on the native PVDF membrane. This better performance could be attributed to the suitable microenvironment created by the hydrophilic MNPs as compared to the hydrophobic PVDF membrane. Furthermore, the figure showed that with increasing the amount of MNPs-Enz, the amount of enzyme per membrane area increases. This eventually increased the enzyme activity as shown in Fig.13 up to certain point, for example after magnetically depositing 0.41 mg of enzyme, the activity decreased dramatically. The dramatic redaction could be attributed to the formation of bigger MNPs-Enz aggregates that can cause lose in the useful biocatalytically active side.

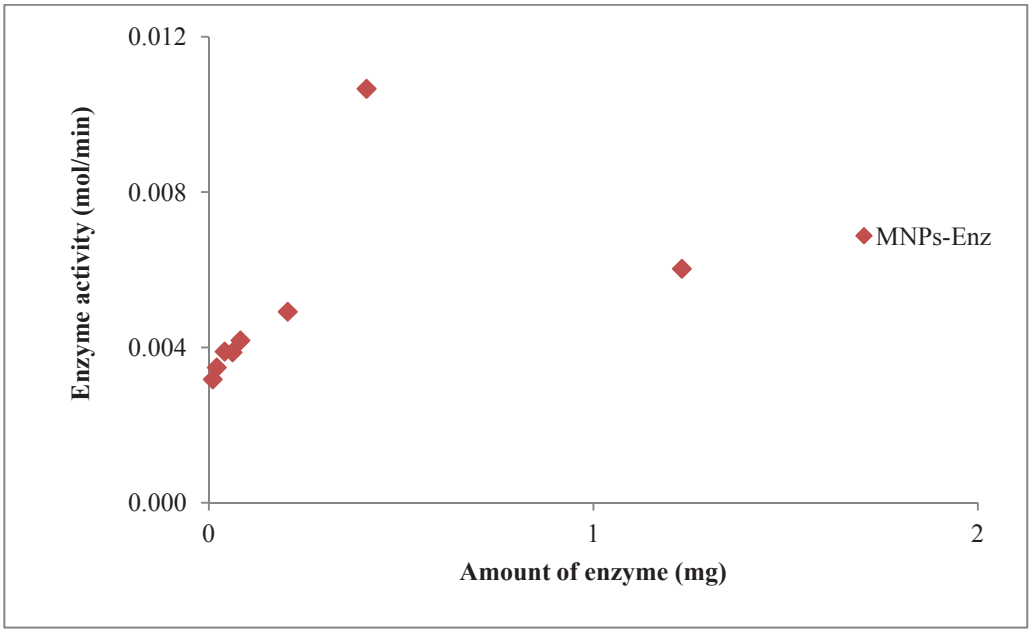

Fig.13: Effect of amount of enzyme increased by increased the amount of MNPs-Enz on the surface of the membrane in the BMR system on the enzyme activity at 0.5 bar and 1 mM substrate concentration.

3.3.2. Effect of paraoxon substrate concentration

In order to study the effect of the paraoxon concentration on the enzyme activity for the modified membranes, the flux for each concentration was studied. Fig.14 and Fig.15 represent the flux as a function of time through PVDF-MNPs-Enz and PVDF-DAMP-GA-Enz membranes respectively. The flux values at 0.5 bar for the BMR containing 20.5 µg and 1000 µg of immobilized enzyme in the PVDF-MNPs-Enz and PVDF-DAMP-GA-Enz membranes respectively were approximately the same for the five different concentration of paraoxon used (0.0625, 0.125, 0.25, 0.5, 1mM). Moreover, at the beginning of each experiment, there is continues flux decline over time until steady state values was achieved.

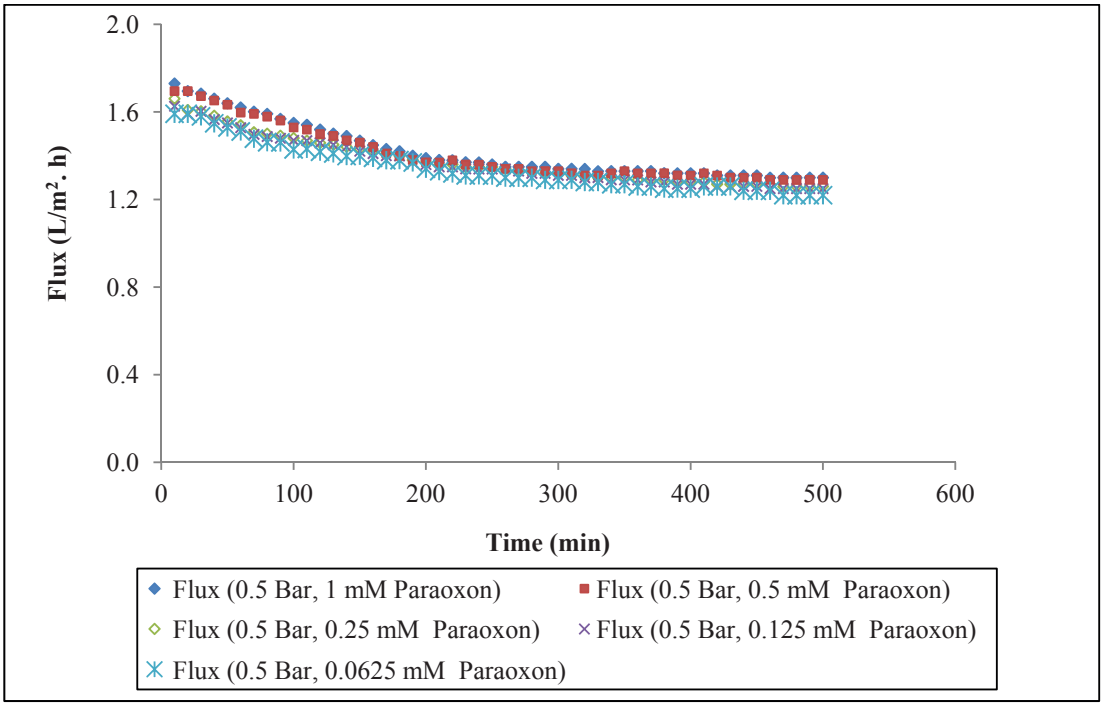

Fig.14: Flux through PVDF-MNPs-Enz membrane at different concentration of paraoxon substrate.

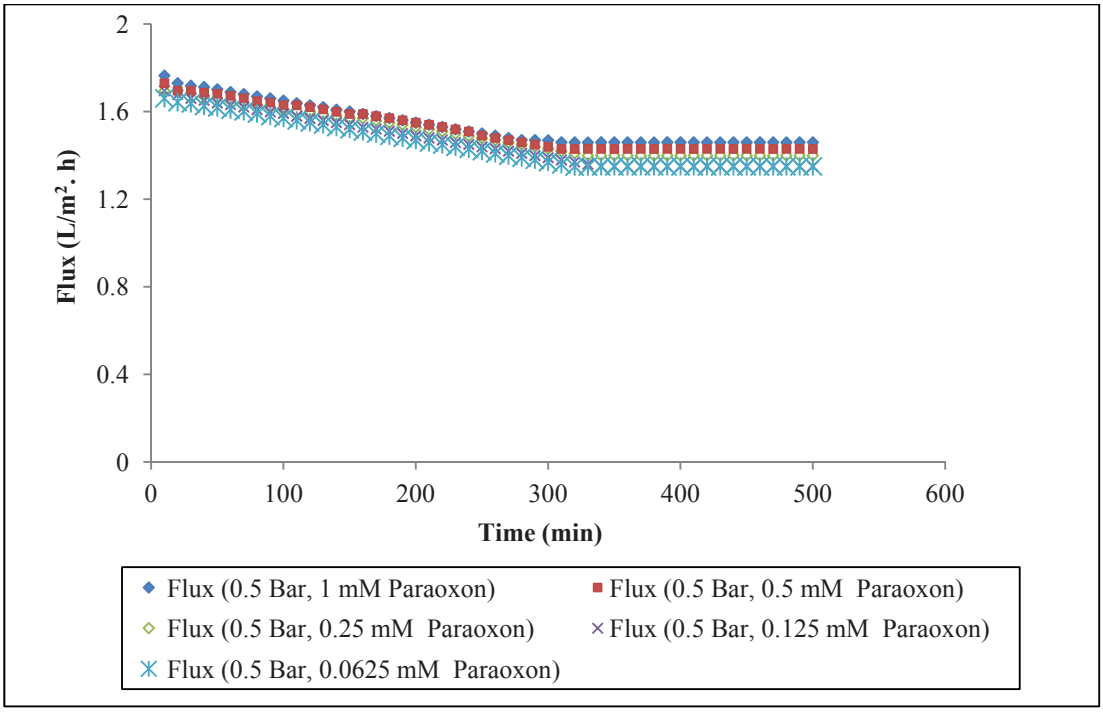

Fig.15: Flux through the modified PVDF-DAMP-GA-Enz membrane at different concentration of paraoxon substrate.

Fig.16 showed that the specific enzyme activity increased with increasing the paraoxon concentration in case of MNPs-Enz. Moreover, MNPs-Enz showed better specific activity compared to DAMP-GA-Enz in the BMR under the same experimental conditions. This could be attributed by the hydrophilic property of MNPs that provided a suitable micro-environment for the PTE enzyme. Furthermore, the specific enzyme activity in case of PVDF membrane containing MNPs-Enz is higher than DAMP-GA-Enz, this might be related to the presence of MNPs on the top surface of PVDF membrane that created an additional filtration resistance. Nevertheless, a decrease in flux through the membrane enhanced the contact time between the enzyme and the substrate, which led to increased activity. Moreover, higher substrate concentration helps to accelerate the reaction rate between the substrate and the immobilized enzyme at the membrane-solution interface.

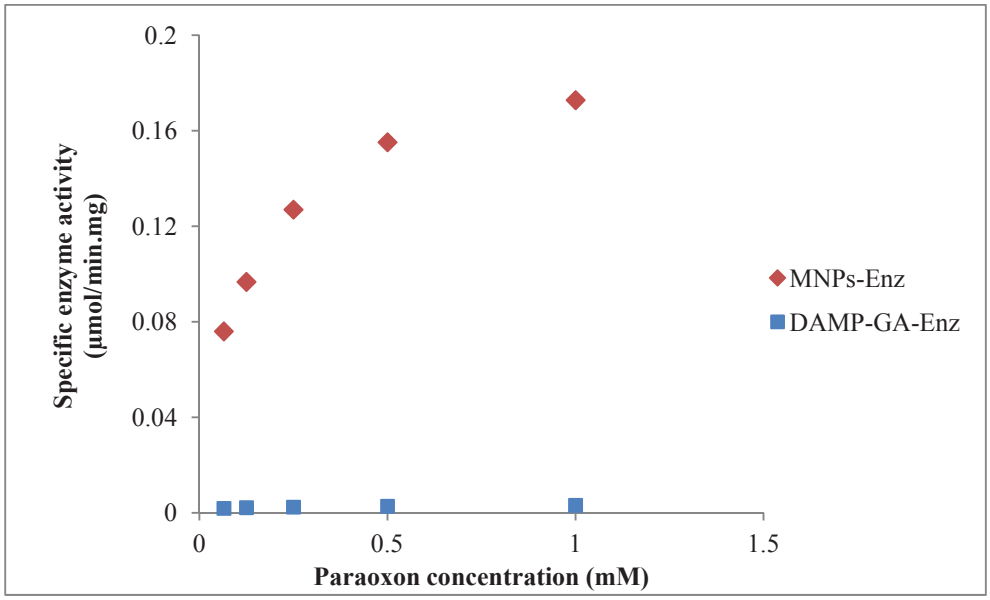

Fig 16: Effect of paraoxon concentration on the MNPs-Enz and DAMP-GA-Enz BMR system at 0.02 mg and 1 mg immobilized PTE respectively at 0.5 bar.

3.3.3. Effect of pressure

Fig.17 and Fig.18 represent the effect of transmembrane pressure on the flux through PVDF-MNPs-Enz and PVDF-DAMP-GA-Enz membranes respectively when a 1mM paraoxon was filtered. It is clear from the figures that by increasing the pressure, the flux through the membranes was increasing. For instance, when the transmembrane pressure was raised from 0.5 bar to 2.5 bar, there was a two fold increase in the flux.

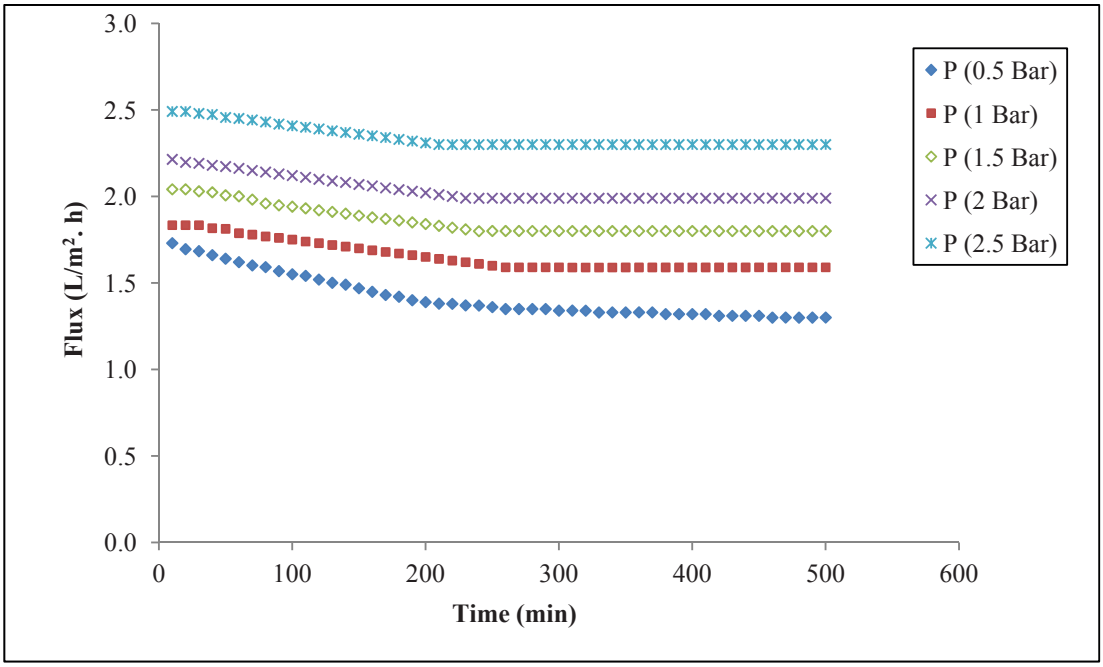

Fig.17: Effect of pressure on the flux through the PVDF-MNPs-Enz membrane.

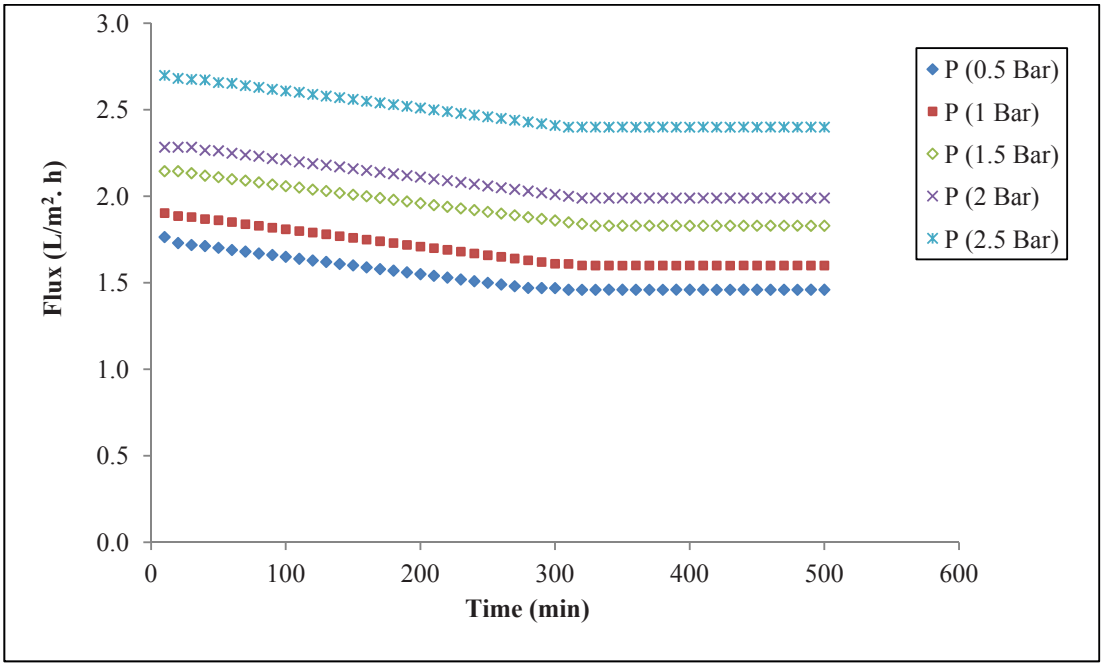

Fig.18: Effect of pressure on the flux through the PVDF-DAMP-GA-Enz membrane.

Fig.19 represents the immobilized enzyme activity as a function of pressure. From the figures, it is clear that the enzyme activity was decreasing with increasing the applied pressure for both modified membranes. This might be related to the increment in the applied pressure leading to increase in the flux through the membranes, which eventually reduce the substrate residence time. Moreover, the figures showed that the enzyme activity in case of PVDF-MNPs-Enz membrane was significantly higher than in case of PVDF-DAMP-GA-Enz membrane. This could be attributed to the presence of MNPs-Enz layer on the membrane surface acting as a resistance layer for the flux through the PVDF-MNPs-Enz membrane. This has thus increased the contact time between the paraoxon and enzyme that also increased the degree of bioconversion. Moreover the amount of enzyme in case of PVDF-MNPs-Enz was higher than the amount of enzyme in PVDF-DAMP-GA-Enz, which might have helped in the increment of bioconversion process in the BMR containing PVDF-MNPs-Enz compared to BMR with PVDF-DAMP-GA-Enz.

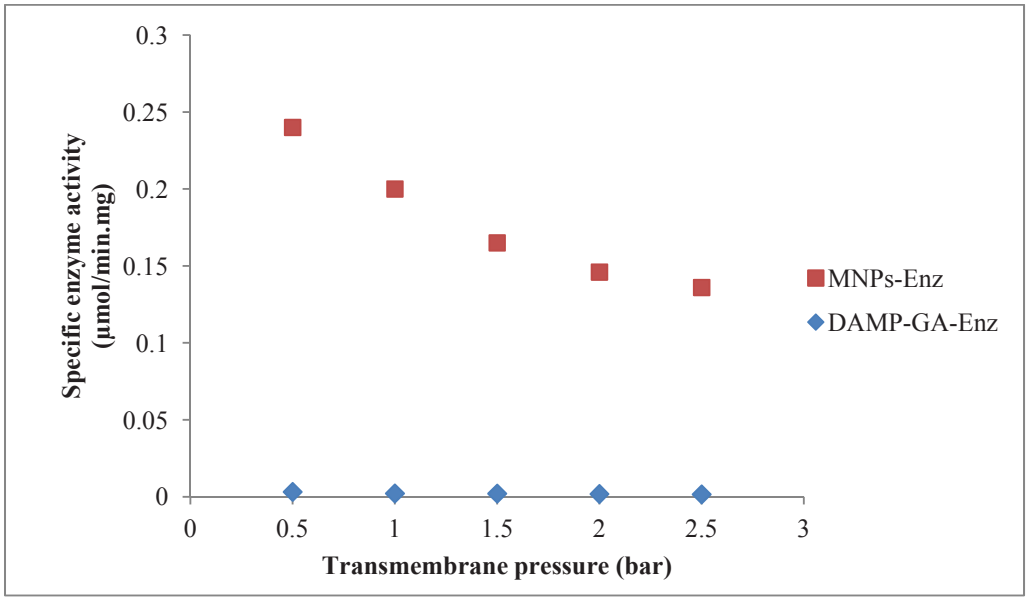

Fig.19: Effect of pressure on the MNPs-Enz and DAMP-GA-Enzyme BMR system at 0.02 mg 1 mg immobilized PTE respectively, 1mM paraoxon and at 0.5 bar.

4. Conclusion

The conclusion from this research work can be summarized as:

1. Two different kind of modified membranes with a phosphotriesterase (PTE) enzyme have been developed for bioconversion of paraoxon to p-nitrophenol. One of these membranes was modified with MNPs-Enzyme, while the other one was modified with DAMP-GA-Enzyme. Both of these two membranes showed good efficiency and sensitivity towards the bioconversion of paraoxon at different conditions applied to the biocatalytic membrane reactor (BMR).

2. The immobilized process induced a negative effect on the enzyme activity since both methods of immobilization revealed loss in the enzyme activity. For example, in case of PVDF-MNPs-Enzyme there was an order of magnitude activity loss after immobilization (0.91 U/mg) compared to free enzyme activity (9.164 U/mg), but in case of PVDF-DAMP-GA-Enz there was two order of magnitude activity loss after immobilization (0.06 U/mg) lower than the activity obtained for the free enzyme (9.164 U/mg).

3. The modified PVDF-MNPs-Enzyme membrane showed higher enzyme activity comparing with PVDF-DAMP-GA-Enzyme when applying different operating parameters (pressure, paraoxon concentration, and enzyme residence time) in the developed BMR.

4. There various parameters that had significant effect on the efficiency and performance of the developed polymeric membranes with immobilized PTE enzyme are summarized as:

- **The amount of enzyme:** The results showed that for the same amount of immobilized enzyme, the activity of the BMR with PVDF-MNPs-Enz membrane was higher than the BMR containing PVDF-DAMP-GA-Enz membrane. This better performance could be attributed to the suitable microenvironment created by the hydrophilic MNPs as compared to the hydrophobic PVDF membrane.

Furthermore, the results showed that with increasing the amount of MNPs-Enz, the amount of enzyme per membrane area increases. This eventually increased the enzyme activity up to certain point, for example after magnetically depositing 0.41 mg of enzyme, the activity decreased dramatically. The dramatic redaction could be attributed to the formation of bigger MNPs-Enz aggregates that can cause lose in the useful biocatalytically active side.

- **The applied pressure:** By increasing the pressure, the bioconversion of paraoxon was decreasing due to limited contact time between the substrate and the MNPs-Enz. This means by increasing the pressure applied to the BMR, the activity of MNPs-Enz were decreasing under the same flux, containing 20.5µg immobilized PTE and 1mM paraoxon.

- **Paraoxon concentration:** By increasing the paraoxon concentration inside the BMR, the enzyme activity of immobilized enzyme was increasing under the same pressure and immobilized enzyme inside the BMR.

- **Residence/Contact time:** When the residence time between the paraoxon substrate and enzyme loaded over the membranes increased; the reaction time between the enzyme and the substrate increased. This parameter was controlled by controlling the flux through the biocatalytic layer using the transmembrane pressure. This has further modulated the enzyme activity as the residence time can be considered as the average time that substrates keep reacting in the BMR.

Overall, the concept developed in this research work will help bring new track on the way to the development of polymeric membrane with biomolecular materials to create biocatalytic membrane reactor (BMR) for different application. Indeed, it is quite possible to transfer these principles to other traditional membrane systems to improve their properties and make them more efficient and selective towards biological applications.

5. References

[1] K.K. Sirkar, P.V. Shanbhag, A.S. Kovvali, "Membrane in a reactor: a functional perspective", Ind. Eng.Chem.Res., 38(1999) 3715–3737.

[2] J. Yuan, J. Zhang, X. Zang, J. Shen, S. Lin, "Improvement of blood compatibility on cellulose membrane surface by grafting betaines", Colloids Surf. B., 30(2003)147–155.

[3] V.G. Gavalas, N.A. Chaniotakis, "Lactate bio sensor based on the adsorption of polyelectrolyte stabilized lactate oxidase in to porous conductive carbon", Mikrochim. Acta., 136(2001)211–215.

[4] L. Giorno, E. Drioli, "Biocatalytic membrane reactors: applications and perspectives", Trends Biotechnol., 18(2000)339–349.

[5] V.C. Gekas, "Artificial membranes as carriers for the immobilization of biocatalysts", Enzym.Microb.Technol., 8(1986) 450–460.

[6] N. Fu Liu, H. Awanis, L. Yutie, M. R. MogharehAbed, K. Li, Progress in the production and modification of PVDF membranes, J.Membr.Sci., 375(2011) 1–27.

[7] F. Liu, N. Awanis Hashim, Y. Liu, M. R. Moghareh Abed, K. Li, "Progress in the production and modification of PVDF membranes", J.Membr.Sci., 375(2011) 1–27.

[8] P. Jochems, Y. Satyawali, L. Diels, W. Dejonghe, "Enzyme immobilization on/in polymeric membranes: status, challenges and perspectives in biocatalytic membrane reactors (BMRs)", GreenChem., 13(2011)1609.

[9] G-d. Kang,Y-m. Cao, "Application and modification of poly(vinylidene fluoride) (PVDF) membranes- a review", J. Membr. Sci., 463(2014)145–165.

[10] G.J. Chen, C.H. Kuo, C.I. Chen, C.C. Yu, C.J. Shieh, Y.C. Liu, "Effect of membranes with various hydrophobic/hydrophilic properties on lipase immobilizer activity andstability", J. Biosci. Bioeng., 113(2012)166–172.

[11] S. Gupta, A. Bhattacharya, C. N. Murthy, "Tune to immobilized lipases on polymer membranes: techniques, factors and prospects", Biocatal. Agric. Biotechnol., 2(2013)171–190.

[12] L.P. Zhu, J.Z. Yu, Y.Y. Xu, Z.Y. Xi, B.K. Zhu, "Surface modification of PVDF porous membranes viapoly (DOPA) coating and heparin immobilization", Colloid Surf. B., 69(2009)152–155.

[13] C.H. Kuo, G.J. Chen, Y.K. Twu, Y.C. Liu, C.J. Shieh, "Optimum Lipase immobilized on diamine-grafted PVDF membrane and its characterization", Ind. Eng. Chem. Res., 51(2012)5141–5147.

[14] G.J. Ross, J.F. Watts, M.P. Hill, P. Morrissey, "Surface modification of poly (vinylidene fluoride) by alkaline treatment1.The degradation mechanism", Polymer, 41(2000)1685–1696.

[15] E. Ghanem, F. M. Raushel, "Detoxification of organophosphate nerve agents by bacterial phosphotriesterase", Toxicol. Appl. Pharmacol. Review, 207 (2005) 459-470

[16] D.J. Ecobichon, "Toxic effects of pesticides. In: Klaassen, C.D. (Ed.), Casarett and Doull's Toxicology: The Basic Science of Poisons, 6th ed. R McGraw-Hill", New York, pp. (2001), 763-810.

[17] F.M. Raushel, H. M. Holden, "Phosphotriesterase: an enzyme in search for its natural substrate", Adv. Enzymol. Relat. Areas Mol. Biol., 74 (2000) 51-93.

[18] D. P. Dumas, S. R. Caldwell, J. R. Wild, F. M. Raushel, "Purification and properties of the phosphotriesterase from Pseudomonas diminuta", J. Biol. Chem., 264 (1989) 19659-19665.

[19] D.P. Dumas, J.R. Wild, F.M. Raushel, "Expression of Pseudomonas phosphotriesterase activity in the Fall Armyworm confers resistance to insecticides", Experientia., 46 (1990) 729-731.

[20] A.D. Griffiths, D.S. Tawfik, "Directed evolution of an extremely fast phosphotriesterase by in vitro compartmentalization", EMBO J., 22 (2003) 24-35.

[21] G. Schrader, "Organische phosphor-verbindungen als neuartige insektizide (auszug)", Angew. Chem., 62 (1950) 471-473.

[22] D.P. Dumas, H.D. Durst, W.G. Landis, F.M. Raushel, J.R. Wild, "Inactivation of organophosphorus nerve agents by the phosphotriesterase from Pseudomonas diminuta", Arch. Biochem. Biophys., 277 (1990)155-159.

[23] J.E. Kolakowski, J.J. DeFrank, S.P. Harvey, L.L. Szafraniec, W.T. Beaudry, K. Lai, J.R. Wild, "Enzymatic hydrolysis of the chemical warfare agent VX and its neurotoxic analogues by organophosphorus hydrolase", Biocatal. Biotransform., 15 (1997) 297-312.

[24] L. Holm, C. Sander, "An evolutionary treasure: unification of a broad set of amidohydrolases related to urease", Proteins, 28 (1997) 72-78.

[25] E. Jabri, M.B. Carr, R.P. Hausinger, P.A. Karplus, “The crystal structure of urease from Klibsiella aerogenes, Science, 268 (1995) 998-1004.

[26] J.B. Thoden, G.N. Phillips, T.M. Neal, F.M. Raushel, H.M. Holden, “Molecular structure of dihydroorotase: a paradigm for catalysis through the use of a binuclear metal center”, Biochemistry, 40 (2001) 6989-6997.

[27] M.M. Benning, J.M. Kuo, F.M. Raushel, H.M. Holden, “Three dimensional structure of phosphotriesterase: an enzyme capable of detoxifying organophosphate nerve agents”, Biochemistry, 33 (1994) 15001-15007.

[28] M.M Benning, H. Shim, F.M. Raushel, H.M. Holden, “High resolution X-ray structures of different metal-substituted forms of phosphotriesterase from Pseudomonas diminuta”, Biochemistry, 40 (2001) 2712-2722.

[29] G.A. Omburo, J.M. Kuo, L.S. Mullins, F.M. Raushel, “Characterization of the zinc binding site of bacterial phosphotriesterase”, J. Biol. Chem., 267 (1992) 13278-13283.

[30] J.L. Vanhooke, M.M. Benning, F.M. Raushel, H.M. Holden, “Three-dimensional structure of the zinc-containing phosphotriesterase with the bound substrate analog diethyl 4-methylbenzylphosphonate”, Biochemistry, 35 (1996) 6020-6025.

[31] L. Cao, “Immobilised enzymes: science or art?”, Curr. Opin. Chem. Biol., 9(2005) 217-226.

[32] C.G.C.M. Netto, H.E. Toma, L.H. Andrade, “Superparamagnetic nanoparticles as versatile carriers and supporting materials for enzymes”, J. Mol. Catal.B: Enzym., 85-86 (2013)71-92.

[33] E. Duguet, S. Vasseur, S. Mornet, J.-M. Devoisselle, Magnetic nanoparticles and their applications in medicine”, Nanomedicine (Lond), 1-2 (2006)157–168.

[34] M. H. Kumar, N. Mathews, P. P. Boix, K. Nonomura, S. Powar, L.Y. Ming, M. Graetzel, S. G. Mhaisalkar, “Decoupling light absorption and charge transport properties in near IR-sensitized Fe_2O_3 regenerative cells”, Energy Environ. Sci., 6 (2013) 3280-3285.

[35] J. Lee, Y. Lee, J.K. Youn, H.B. Na, T. Yu, H. Kim, S.-M. Lee, Y.-M. Koo, J. H. Kwak, H. G. Park, H.N. Chang, M. Hwang, J.-G. Park, J. Kim, T. Hyeon, “Simple synthesis of functionalized superparamagnetic magnetite/silicacore/shell nanoparticles

and their application as magnetically separable high-performance biocatalysts", Small, 4 (2008)143-152.

[36] T. Hoare, J. Santamaria, G.F. Goya, S. Irusta, D. Lin, S. Lau, R. Padera, R. Langer, D.S. Kohane, "Amagnetically triggered composite membrane for on-demand drug delivery", Nano Lett., 9 (2009) 3651-3657.

[37] K. Boodhoo, A. Harvey, "Process intensification: an overview of principles and practice, in: K. Boodhoo, A. Harvey (Eds.), Process Intensification For Green Chemistry, John Wiley& Sons.Ltd., The Atruim, Southern Gate, Chichester, WestSussex.UK, 2013.

[38] E. Drioli, L. Giorno, "Catalytic membrane reactors for retention and recycling of coenzyme", Biocatalytic Membrane Reactors, 1999 (139–152), Taylor & Francis.

[39] M.C.R. Franssen, P. Steunenberg, E.L. Scott, H. Zuilhof, J.P.M. Sanders, "Immobilized enzymes in bio renewable production", Chem. Soc. Rev., 42 (2013) 6491-6533.

[40] P. Lutze, D. K. Babi, J. M. Woodley, R. Gani, "Phenomena based methodology for process synthesis incorporating process intensification", Ind. Eng. Chem. Res., 52 (2013)7127-7144.

[41] Z. Xiao-Ming, I.W. Wainer, "On-line determination of lipase activity and enantioselectivity using an immobilized enzyme reactor coupled to a chiral stationary phase", Tetrahedron Lett., 34 (1993) 4731-4734.

[42] K. Abe, M. Goto, F. Nakashio, "Novel optical resolution of phenylalanine race mate utilizing enzyme reaction and membrane extraction", Sep. Sci. Technol., 32 (1997) 1921-1935.

[43] A. Machsun, M. Gozan, M. Nasikin, S. Setyahadi, Y. Yoo, "Membrane micro-reactor in biocatalytic trans esterification of triolein for biodiesel production", Biotechnol. Bioprocess Eng., 15 (2010) 911-916.

[44] R. Mazzei, E. Drioli, L. Giorno, "Enzyme membrane reactor with heterogenized β-glucosidase to obtain phytotherapic compound: optimization study", J. Memb. Sci., 390-391(2012)121-129.

[45] D-H. Kim, E.A. Rozhkova, I. V. Ulasov, S. D. Bader, T. Rajh, M. S. Lesniak, V. Novosad, "Biofunctionalized magnetic-vortex micro discs for targeted cancer-cell destruction" , Nat. Mater., 9 (2010)165-171.

[46] P. Daraei, S. S. Madaeni, N. Ghaemi, M. A. Khadivi, B. Astinchap, R. Moradian, "Fouling resistant mixed matrix polyethersulfone membranes blended with magnetic nanoparticles: study of magnetic field induced casting", Sep. Purif. Technol., 109 (2013) 111-121.

[47] T.-H. Bae, J.R. Long, "CO_2/N_2 separations with mixed-matrix membranes containing Mg_2 (dobdc) nanocrystals", Energy Environ. Sci., 6 (2013) 3565-3569.

[48] I.T. Kim, A. Tannenbaum, R. Tannenbaum, Anisotropic conductivity of magnetic carbon nanotubes embedded in epoxy matrices", Carbon, 49 (2011) 54-61.

[49] M.A. Correa-Duarte, M. Grzelczak, V. Salgueiriño-Maceira, M. Giersig, L.M. Liz-Marzán, M. Farle, K. Sierazdki, R. Diaz, "Alignment of carbon nanotubes under low magnetic fields through attachment of magnetic nanoparticles", J. Phys. Chem. B, 109 (2005) 19060-19063.

[50] R. Bouskila, R. McAloney, S. Mack, D. D. Awschalom, M.C .Goh, K.S. Burch, "One-dimensional alignment of nanoparticles via magnetic sorting", Appl. Phys. Lett., 96 (2010) 163103.

[51] A.Y. Gebreyohannes, M. Roil Bilad, T. Verbiest, C. M. Courtin, E. Dornez, L. Giorno, E. Curcio, Ivo. F.J. Vankelecom, "Nanoscale tuning of enzyme localization for enhanced reactor performance in a novel magnetic-responsive biocatalytic membrane reactor.", J. Membr. Sci., 487 (2015) 209-220.

[52] G. Vitola, R. Mazzei, E. Fontananova, L. Giorno, "PVDF membrane biofunctionalization by chemical grafting", J. Membr. Sci., 476 (2015) 483-489.

[53] G. J. Ross, J. F. Watts, M. P. Hill, P. Morrissey, "Surface modification of poly (vinylidene fluoride) by alkaline treatment: The degradation mechanism", Polymer 41(2000)1685-1696

[54] S.W. Sun, Y.C. Lin, Y. C. Weng, M. J. Chen, "Efficiency improvements on ninhydrin method for amino acid quantification", J. Food Compos. Anal., 19 (2006) 112-117.

6. Appendix

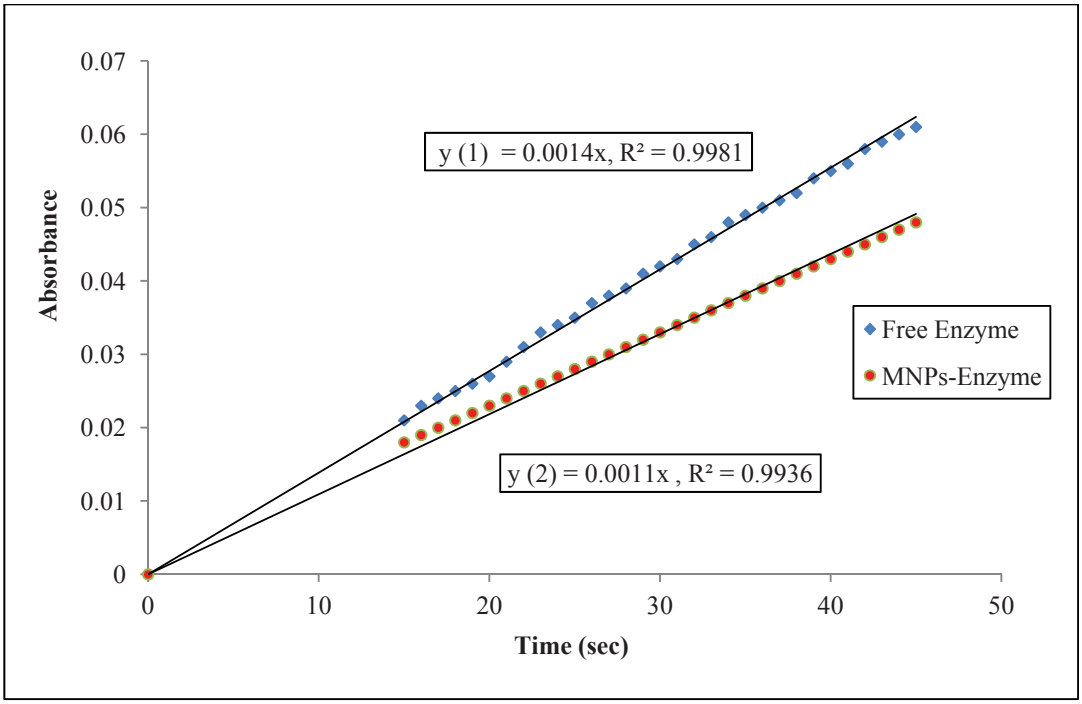

Fig.20: The Absorption measurement for Free Enzyme and (MNPs-Enz).

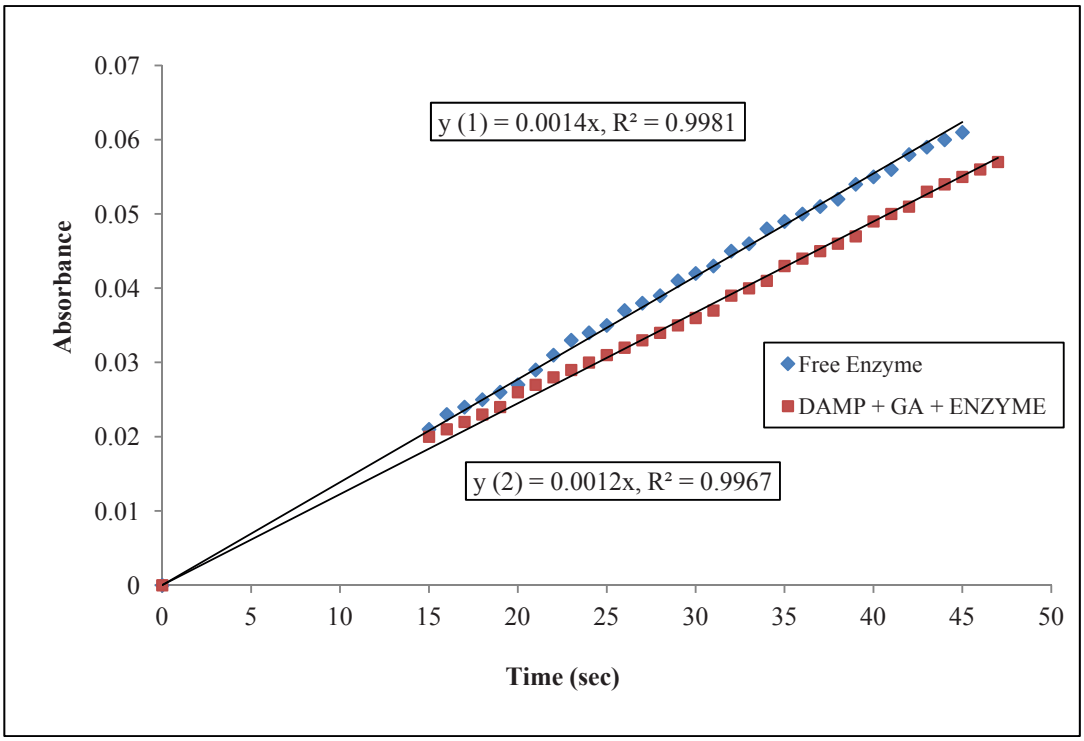

Fig.21: Absorption measurement for free Enzyme and (DAMP-GA-Enzyme).

Thesis Summary

In general, the concepts developed in this thesis research work will help bring new tracks on the way to the development of a polymeric membrane for selective ion and gas separation but also for selective catalytic reaction under bio(molecular) control. In this research thesis, different research works have been described thesis, the conclusions of these research works can be summarized as the following:

Chapter (1): Carbonic anhydrase towards Dynamic Combinatorial Libraries (DCLs):

The goal of the work described in this chapter was the identification of effective potent inhibitors for the human carbonic anhydrase I (hCAI) isozyme. Considering the pharmacological importance to find isoform-selective CA inhibitors (CAIs), human carbonic anhydrase I (hCAI) has been subjected to a parallel screening of various constitutional dynamic libraries (CDL). The use of parallel constitutional screening of CDL chemistry for the discovery of enzyme inhibitors is straightforward and it might provide initial insights toward the generation of efficient classes of selective and high affinity inhibitors. The originality of this work depend on using human isozymes than the studies described in Dynamic Combinatorial Libraries-DCL for bovine isozyme, as human isozyme may have better specificity with respect to certain inhibitors. In this research work our findings show that the DCL-Carbonic Anhydrase story may hold novel surprises, relevant to the general drug design research, especially with enzyme families like CAs with a multitude of members. The present study revealed a new paradigm: if compounds of agonistic inhibitor and activator activities are formed, the Dynamic Deconvolution may lead to the discovery of the inhibitory set of components expressed at the expense of the activator ones. This sheds light on the dominant mechanistic inhibition behaviours. Moreover the simplicity of the Dynamic Deconvolution strategy and of its analysis used in this work can easily lead to valuable simple mechanistic insights into inhibitory–activatory relative synergistic affinities toward the hCAs. This contribution adds several new behaviours to the systematic rationalization and prediction of novel CA active compounds.

Chapter (2): Membrane separation and extraction of lanthanides with constitutional dynamic networks.

The main aims of this research work have been declined as following:

1. Synthesis, characterization, and application of the constitutional dynamic networks as membrane materials.
2. Selective extraction of lanthanides through the prepared membrane materials.
3. Use of the constitutional dynamic networks (Dynamers) in liquid and solid membrane systems as a carrier network for transporting lanthanide metal ions.

In this research work our findings show that Dynamic covalent polymers or dynamers, generated from reversibly interacting monomers, offer the possibility to generate homogeneous molecular networks with addressable domains based on structural relationships different from the former monomers. Constitutional dynamic networks have been used in liquid and solid membrane systems as a carrier network for transporting lanthanides. The transport is based on the complexing ability of lanthanides metals (La^{3+}, Lu^{3+}, and Eu^{3+}) with the functional polyether and amino groups in the membrane materials. Based on corresponding dynamic diffusional domains within the solid and liquid bulk membrane phases, the lanthanides are extracted and selectively transported through the membranes, only in the presence of constitutional networks, while the former monomers did not show any selectivity. This would be explained by the formation of a dynamic self-assembly of low-size and molecularly addressable recognition networks in which the diffusional/selective percolation pathways might exist. The resulting polymeric membranes and their metals complexes have been characterized by (UV-visible, FTIR and ^{1}H NMR), and the thermal stability by (TGA, and DSC). The physico-chemical characterizations gave a good indication about the complexation and selectivity of selected lanthanides metal ions with the prepared dynameric membranes. Additionally, the Jeffamine T-3000 substrate is better than Jeffamine D-2000 in the Lanthanides uptake(%), because Jeffamine T-3000 bears/contains more amino functional groups than Jeffamine D-2000 within the polymeric structure.

Moreover, the results showed that the used dynameric membranes have high selectivity towards (La^{3+} and Lu^{3+}) than Eu^{3+}, this might relate to the stability of the formed complexes in the membrane phase in direct relation with the atomic radius and the hydration behaviors of the used lanthanide metal ions.

In additional too, the results showed that the liquid membrane (LM) is better than solid membrane (SM) for the lanthanides transportation and permeability, this might relate to the free movement of the complexing and carrier functional groups in the dynamic network in case of liquid membranes than solid ones, as the solubility and diffusivity coefficients of the extracted compounds are higher in a liquid medium than in a solid one, so the permeability and transportation of lanthanides metal ions in the liquid membranes are higher than solid ones.

Finally, thanks to the possibility to combine the structural and functional features of different monomers, the heteropolymeric membrane materials can exhibit very different properties from their original homopolymeric components. In the above-developed examples, this strategy revealed itself to be a versatile way for the synthesis of new membranes presenting different permeabilities and preserving their selectivity towards lanthanide metal ions.

Chapter (3): CO_2 capture using supported ionic liquid membranes immobilized with carbonic anhydrase enzyme.

The approach proposed in this research work consisted on using supported ionic liquid membranes (SILMs) comprising two different carbonic anhydrase enzymes, the thermo resistant SspCA enzyme and the Bovine-CA enzyme, which catalyze the reaction of conversion of CO_2 to bicarbonate, enhancing the driving force for CO_2 transport. Membrane stability, CO_2 and N_2 permeability and CO_2/N_2 ideal selectivity were determined. The results showed that the supported ionic liquid membranes prepared by immobilizing a selected ionic liquid [(1-butyl-3-methylimidazolium bis(trifluoromethane sulfonyl)imide] [C_4MIM][Tf_2N] with and without enzyme in a PVDF hydrophobic

polymeric support allowed to obtain stable supported liquid membranes at high temperatures (up to 100ºC), selective towards CO_2 against N_2. Moreover, the selectivity and permeability were affected by different parameters, namely, temperature, water activity and enzyme concentration.

The results showed that, the selectivity and permeability through the supported ionic liquid membranes with and without enzymes were affected by different important factors like temperature, water activity and the presence of enzyme. Temperature had a great effect on the selectivity and permeability, when the temperature was increasing the selectivity was decreasing, this might be related to the increment of the permeability with an increment in temperature, which may be related with a decrease of the ionic liquid viscosity with temperature, also the activity of the enzyme may be influenced by the increasing of the temperature. Also the selectivity and permeability was increasing with increasing the water activity; this might be related to the increasing in the diffusion coefficient increases with an increase in water activity, since with the higher water content the ionic liquid viscosity decreases. This increase was more pronounced for the ionic liquid, for which the diffusion coefficient reaches a higher value for the highest water activity used (a_w= 0.843).

The main important factor was the presence of enzyme, as the presence of carbonic anhydrase enzyme increases the permeability and selectivity of CO_2 through the supported ionic liquid membranes immobilized with [C_4MIM][Tf_2N], when comparing with the supported ionic liquid membrane without enzyme. The permeability was increasing as the following: Supported ionic liquid membrane with (SspCA) enzyme > Supported ionic liquid membrane with (BCA) enzyme > Supported ionic liquid membrane without enzyme.

The results showed that the SILM immobilized with ([C_4MIM][Tf_2N]+SspCA enzyme) at (30ºC) has the highest permeability (3.93 x 10^{-10} m^2/sec) and idea selectivity (CO_2/N_2) (42.44) for CO_2 when comparing with other SILMs immobilized with ([C_4MIM][Tf_2N] +BCA enzyme) (3.70 x 10^{-10} m^2/sec) and [C_4MIM][Tf_2N] (3.40 x 10^{-10} m^2/sec).

Moreover, Two different concentration of enzymes (0.1mg enzyme/g ionic liquid) and (0.25 mg enzyme /g ionic liquid) immobilized with the ionic liquid were also tested.

The results showed that, by increasing the enzyme concentration (2.5 times), the permeability and selectivity of CO_2 were duplicated for both enzymes. The permeability (5.51×10^{-10} m^2/sec) and selectivity (51.02) values obtained at 30ºC in case of SILMs immobilized with ([C_4MIM][Tf_2N]+SspCA enzyme (0.25mg/g IL)) is higher than the values in case of SILM immobilized with ([C_4MIM][Tf_2N]+BCA enzyme (0.25mg/g IL)). In additional too, at higher temperature (100ºC), the highest permeability (6.09×10^{-10} m^2/sec) and selectivity (35.61) values were obtained in case of SILMs immobilized with ([C_4MIM][Tf_2N]+SspCA enzyme (0.25mg/g IL)). Moreover, it could be concluded that, the SILMs immobilized with ([C_4MIM][Tf_2N]+SspCA enzyme) present higher stability at high temperatures (80ºC and 100ºC) than the other used SILMs immobilized with([C_4MIM][Tf_2N]+BCA enzyme) or ([C_4MIM][Tf_2N]).

In order to compare the ideal selectivities obtained in this work with data available in the literature, the (CO_2/N_2) ideal selectivity as a function of the CO_2 permeability at 30ºC is represented in upper bound correlations plot. The results showed that, the data obtained in this work are generally closer to those available in the literature. In case of SILMs immobilized with pure [C_4MIM][Tf_2N] ionic liquid are below the upper bound line, while the results obtained from using SILMs immobilized with pure ionic liquid and low enzyme concentration (0.1mg/1gIL) are little higher and closer to the upper bound line. Moreover, the figure shows that the best results obtained when using the SILMs immobilized with pure ionic liquid and higher enzyme concentration (0.2mg/1gIL), as the results access the upper bound line, this mean the obtained results by using these SILMs may be considered as an improvement over the results published so far. However, In order to improve the selectivity and permeability through the enzyme-solvent system it will be important in further studies to evaluate the behavior of CO_2 task-specific ionic liquids, which combined with the use of higher concentrations of carbonic anhydrase enzymes may lead to efficient and competitive carbon capture systems.

Chapter (4): Synthesis and Characterization of polymeric membranes for gas separation.

The main goals for this research project consisted of three main parts:

- Synthesis of polymeric membranes from low molecular PEG components.
- Characterize the developed membrane in order to find its physico-chemical and thermal properties.
- To evaluate the performance of the developed membrane in terms of selectivity and permeability for the CO_2/N_2 gas separation and to compare the obtained data with the data available in the literature.

The approach proposed in this research work consisted on the synthesis and characterization of dense polymeric membranes for gas separation application. Firstly the different polymeric membranes were synthesized by condensation polymerization between one of main subtracts [(2,2`ethylene dioxide) bis(ethylamine)) / DEG] and [(4,7,10-trioxa-1,13-tridecanediamine) / TEG] with [(Benzene-1,3,5-tricarbaldehyde) / TCA]. The resulting polymer membranes were characterized spectrometry by (FTIR, ^{1}H-NMR), their thermal stability were characterized by (TGA and DSC), and the morphological structure was characterized by (SEM and contact angle). The gas permeability measurements for the tested polymeric membranes showed that the permeability of CO_2 is higher than other used gases (N_2 and CH_4) for the polymeric membranes as shown in table (I). This might related to the polarity behaviour of CO_2 gas comparing with other non-polar gases (N_2, CH_4), this might help to accelerate the diffusion and permeability of CO_2 through the used polymeric membranes. Moreover, the kinetic diffusion diameter of gases effect on the permeability through the dense membranes, as the kinetic diffusion diameter (Å) of used gases are the following (CO_2 = 3.325) < (N_2 = 3.568) < (CH4 = 3.817), this might give an indication about the permeabilities of gases through the used polymeric membranes are arranged as the following (CO_2 gas) > (N_2 gas) > (CH_4 gas).

Table (I): The permeability of (CO_2, N_2, and CH_4) through the tested membranes.

Membranes	Permeability (m^2/sec) x10^{-11}			Permeability (Barrer)		
	P_{CO2}	P_{N2}	P_{CH4}	P_{CO2}	P_{N2}	P_{CH4}
M1-DEG	6.12	0.295	0.221	73.73	3.55	2.66
M2-DEG	6.62	0.245	0.211	79.76	2.95	2.54
M3-TEG	2.95	0.231	0.191	35.54	2.78	2.30
M4-TEG	3.72	0.262	0.218	44.82	3.16	2.63

Additionally, it is observed that the CO_2 permeability and the ideal selectivity through the tested polymeric membranes that contain (DEG) substrate material within the membrane polymeric structures are higher than other polymeric membranes that have (TEG) substrate material. This might relate to the increment in the hydrophilic and rubbery behaviors of the (TCA-DEG) membranes comparing with (TCA-TEG) membranes, which effect on the morphological structure and the permeability of the gases through the polymeric membranes. Moreover, the permeability and ideal selectivity of CO_2 through the used polymeric membranes are arranged as the following [M2-DEG (in NMP solvent) > M1-DEG (in Acetonitrile solvent) > M4-TEG (in NMP solvent) > M3-TEG (in Acetonitrile solvent)] as shown in table (II).

Table (II): (CO_2/N_2) and (CO_2/CH_4) ideal selectivities of the tested membranes.

Membranes	Ideal selectivity α (CO_2/N_2)	Ideal selectivity α (CO_2/CH_4)
M1-DEG	20.75	27.69
M2-DEG	27.02	31.37
M3-TEG	12.77	15.45
M4-TEG	14.20	17.06

Generally, the tested polymeric membranes in this research work are stable at the (30ºC) for a pressure difference of (0.7 bar), and they are selective towards CO_2 when compared with (N_2) and (CH_4) gases, also when compared with other polymeric membrane materials in the literature their selectivity is lower than the common used polymeric membranes for CO_2 permeability. Finally, thanks to the possibility to combine the structural and functional features of different monomers, the heteropolymeric membrane materials can exhibit very different properties from their original homopolymeric components. In the above-developed examples, this strategy revealed itself to be a versatile way for the synthesis of new membranes presenting different permeabilities and preserving their selectivity towards gas separation application.

Chapter (5): Membrane functionalized with enzyme for selective conversion and separation.

The approach proposed in this work consists on the development of two different methods of PVDF membrane functionalization with a phosphotriesterase (PTE) enzyme to construct biocatalytic membrane reactor (BMR) for bioconversion of paraoxon to p-nitrophenol as a product. The first method employs reversible dispersion of magnetic nanoparticle immobilized with PTE using an external magnetic field on the surface of native PVDF membrane. On the contrary, the second method comprises chemical grafting of the PTE enzyme, after surface modification of the native PVDF membrane with DAMP-GA-Enzyme.

The conclusion from this research work can be summarized as:

1. Two different kind of modified membranes with a phosphotriesterase (PTE) enzyme have been developed for bioconversion of Paraoxon to p-nitrophenol. One of these membranes was modified with MNPs-Enzyme, while the other one was modified with DAMP-GA-Enzyme. Both of these two membranes showed good efficiency and sensitivity towards the bioconversion of paraoxon at different conditions applied to the biocatalytic membrane reactor (BMR).

2. The immobilized process induced a negative effect on the enzyme activity since both methods of immobilization revealed loss in the enzyme activity. For example, in case of PVDF-MNPs-Enzyme there was an order of magnitude activity loss after immobilization (0.91 U/mg) compared to free enzyme activity (9.164 U/mg), but in case of PVDF-DAMP-GA-Enz there was two order of magnitude activity loss after immobilization (0.06 U/mg) lower than the activity obtained for the free enzyme (9.164 U/mg).

3. The modified PVDF-MNPs-Enzyme membrane showed higher enzyme activity comparing with PVDF-DAMP-GA-Enzyme when applying different operating parameters (pressure, paraoxon concentration, and enzyme residence time) in the developed biocatalytic membrane reactor (BMR).

4. There various parameters that had significant effect on the efficiency and performance of the developed polymeric membranes with immobilized PTE enzyme are summarized as:

- **The amount of enzyme:** The results showed that for the same amount of immobilized enzyme, the activity of the BMR with PVDF-MNPs-Enz membrane was higher than the BMR containing PVDF-DAMP-GA-Enz membrane. This better performance could be attributed to the suitable microenvironment created by the hydrophilic MNPs as compared to the hydrophobic PVDF membrane. Furthermore, the results showed that with increasing the amount of MNPs-Enz, the amount of enzyme per membrane area increases. This eventually increased the enzyme activity up to certain point, for example after magnetically depositing 0.41 mg of enzyme, the activity decreased dramatically. The dramatic redaction could be attributed to the formation of bigger MNPs-Enz aggregates that can cause lose in the useful biocatalytically active side.

- **The applied pressure:** By increasing the pressure, the bioconversion of paraoxon was decreasing due to limited contact time between the substrate and the MNPs-Enz. This means by increasing the pressure applied to the BMR, the activity of MNPs-Enz were decreasing under the same flux, containing 20.5µg immobilized PTE and 1mM paraoxon.

- **Paraoxon concentration:** By increasing the paraoxon concentration inside the BMR, the enzyme activity of immobilized enzyme was increasing under the same pressure and immobilized enzyme inside the BMR.

- **Residence/Contact time:** When the residence time between the paraoxon substrate and enzyme loaded over the membranes increased; the reaction time between the enzyme and the substrate increased. This parameter was controlled by controlling the flux through the biocatalytic layer using the transmembrane pressure. This has further modulated the enzyme activity as the residence time can be considered as the average time that substrates keep reacting in the BMR.

Overall, the concept developed in this research work will help bring new track on the way to the development of polymeric membrane with biomolecular materials to create biocatalytic membrane reactor (BMR) for different application. Indeed, it is quite possible to transfer these principles to other traditional membrane systems to improve their properties and make them more efficient and selective towards biological applications.

Abstract

Different research works have been described in this thesis. The research works can be summarized as the following. The first chapter deals with the identification of effective potent inhibitors for the human carbonic anhydrase I (hCAI) isozyme. Considering the pharmacological importance to find selective CA inhibitors (CAIs) and CA activators (CAAs), human carbonic anhydrase I (hCAI) has been subjected to a parallel screening of various constitutional dynamic libraries (CDL). In the second chapter, constitutional dynamic networks have been used in liquid and solid membrane systems as a carrier network for transporting lanthanides. The transport is based on the complexing ability of lanthanides metals (La^{+3}, Lu^{+3}, Eu^{+3}) with the functional polyether groups in the membrane materials. In the third chapter, the proposed approach consists in using supported ionic liquid membranes (SILMs) comprising two different carbonic anhydrase enzymes, the thermo-resistant SspCA enzyme and the Bovine-CA enzyme, which catalyze the reaction of reversible conversion of CO_2 to bicarbonate, enhancing the driving force for CO_2 transport. Membrane stability, CO_2 and N_2 permeability and (CO_2/N_2) ideal selectivity were determined for the membranes developed. In the fourth chapter, the research work consists in the synthesis and characterization of dense polymeric membranes for gas separation application. The gas permeability measurements for the synthesized polymeric membranes showed that the permeability of CO_2 is higher than other used gases (N_2 and CH_4). In the last chapter, two different methods of PVDF membrane functionalization with a phosphotriesterase (PTE) enzyme have been developed to construct biocatalytic membrane reactor (BMR) for bioconversion and selective separation of paraoxon substrate. The first method employs reversible dispersion of magnetic nanoparticle immobilized with PTE using an external magnetic field on the surface of native PVDF membrane. On the contrary, the second method comprises chemical grafting of the PTE enzyme after surface modification of the native PVDF membrane (DAMP-GA-Enzyme). Both methods of enzyme immobilization showed good efficiency and sensitivity towards the bioconversion of paraoxon substrate at different conditions applied in a biocatalytic membrane reactor (BMR).

In general, the concepts developed in this thesis research work will help bring new tracks on the way to the development of a polymeric membrane for selective ion and gas separation but also for selective catalytic reaction under bio(molecular) control.

Keywords:

Polymeric membrane; Functionalized; Gas separation; Bio-molecular control; Enzymatic catalytic reactions; Selective ion transport; Bioconversion of paraoxon; Supported ionic liquid membranes (SILMs); Carbonic anhydrase (CA) enzyme; Phosphotriesterase (PTE) enzyme; Biocatalytic membrane reactor (BMR).